NEW METHODS OF EVALUATING BREAST MOTION IN BRALESS AND SPORTS BRA CONDITIONS

ZHOU JIE

Ph.D

The Hong Kong Polytechnic University

2011

THE HONG KONG POLYTECHNIC UNIVERSITY

INSTITUTE OF TEXTILES AND CLOTHING

NEW METHODS OF EVALUATING BREAST MOTION IN BRALESS AND SPORTS BRA CONDITIONS

ZHOU JIE

A Thesis Submitted

in Partial Fulfillment of the Requirements

for the degree of Doctor of Philosophy

August 2010

CERTIFICATE OF ORIGINALITY

I hereby declare that this thesis is my own work and that, to the best of my knowledge and belief, it reproduces no material previously published or written, nor material that has been accepted for the award of any other degree or diploma, except where due acknowledgement has been made in the text.

_________________ (Signed)

ZHOU Jie (Name of student)

DEDICATION

This thesis is dedicated to my family

ABSTRACT

Sports bras are designed to reduce breast movement during exercises, but previous studies on breast movement were based on various, unclear and unreliable reference systems. Heretofore, there is no standardised, valid and reliable method to evaluate relative three-dimensional (3D) breast movement affected by different design features of sports bras; and there is no literature to predict the 3D force acting on the breasts during activities. Both empirical and theoretical studies on this unexplored area are needed to provide a scientific basis for the functional design of supportive sports bras.

The aim of this study was therefore to establish a reliable method to evaluate 3D breast movement and to determine the effective design features of supportive sports bras. The specific objectives were to derive and validate a new Breast Coordinate System (BCS) for investigating 3D breast movement, so as to identify the most effective bra features and to analyse the effects of breast volume and bra strap properties on breast movement, then to develop theoretical models of breast force generated during jogging in braless and sports bra conditions.

To achieve the objectives, the research framework contains five principal parts, including (i) deriving a new BCS; (ii) evaluating the 3D breast displacement and trajectories of six breast points on four subjects; (iii) identifying the effective bra features of seven different sports bras; (iv) analysing the effects of 11 breast volumes and 10 different shoulder straps on breast displacement; and (v) building theoretical models of 3D breast force.

A new BCS was derived and validated based on a reliable reference on the thoracic cage and a local breast origin. The relative 3D breast displacement and trajectories were

evaluated and compared among different breast points, bras, and activities.

Paired *t*-tests showed that the displacement at the nipple was significantly different from other breast points. The relative 3D nipple displacement during jogging was reasonably smaller than previous results for D-cup women. For the subjects in this study, the most effective bra features were identified. Shoulder strap elongation was significantly correlated with the Reduction percentage of Breast Displacement (RBD). The vertical breast movement significantly increased with breast volume.

3D mechanical models have been developed based on a system comprising a mass, springs and dampers. The orthogonal force exerted on the breasts during jogging with or without a sports bra was derived. Breast mechanical models with different shoulder straps predicted that wider shoulder straps were more effective in supporting the breast weight, and the force acting on the shoulder straps was related to the shoulder straps' styles and the positions on the shoulders.

This research has developed a new, valid and reliable breast coordinate system and the techniques to evaluate the effectiveness of sports bra in terms of comprehensive 3D relative breast displacement for different breast volumes. The breast mechanical models were developed to estimate the 3D breast force in different wearing conditions. The new methods will contribute to future research on human locomotion and the design of sports bras.

LIST OF PUBLICATIONS AND AWARDS

Major parts of the material presented in this thesis have formed the basis for papers that have been presented and published as follows:

Journal Articles

1. **Zhou J.,** Yu W. and Ng S. P., A review of literature on breast motion and bra pressure, Journal of Xi'an Polytechnic University, 22(2): 55-64. (2009).
2. **Zhou J.**, Yu W., Ng S. P., and Hale J., Evaluation of shock absorbing performance of sports bras, Journal of Fiber Bioengineering and Informatics, 2(2): 108-113. (2009).
3. **Zhou J.**, Yu W. and Ng S. P., Methods of studying breast motion in sports bras: a review, Textile Research Journal, 81 (12), 1234-1248. (2011).
4. **Zhou J.**, Yu W. and Ng S. P., Studies of three-dimensional trajectories of breast movement for better bra design, Textile Research Journal – revised for review.
5. **Zhou J.**, Yu W. and Ng S. P., Effectiveness of sports bra in reducing 3D breast displacement relative to thorax in various activities, International Journal of Clothing Science and Technology - under review.
6. Ng S.P., Chen L.H., Yu W, **Zhou J.** and Wan K.W.F., Dynamical analysis of breast motion using finite element method, Ergonomics - revised for review.

Conference Presentation and Publications

7. **Zhou J.**, Yu W., Ng S. P., and Hale J., Evaluation of shock absorbing performance of sports bras, 1st International Symposium of Textile Bioengineering and Informatics, Hong Kong, Aug 14-15, 2008.

8. Ng S.P., Au A., **Zhou J.** and Yu W., Measuring methods of bra pressure, The 86th Textile Institute World Conference- Fashion and Textiles: Heading towards New Horizon, Hong Kong, 18-21 November, 2008.
9. **Zhou J.**, Yu W. and Ng S.P., A review of literature on breast motion and bra pressure, Advanced International Textile Science and Technology Forum, Xian Polytechnic University, Xian, China, 12 April, 2009.
10. **Zhou J.**, Yu W. and Ng S.P., 3D dynamic analysis of breast without and with a sports bra, The 17th World Congress on Ergonomics, Beijing, China, 9-14 Aug 2009.
11. **Zhou J.**, Yu W. and Ng S.P., Quantitative evaluation of 3D breast velocity during activities, The 10th Asian Textile Conference, G7-O-10, The Society of Fiber Science and Technology, Japan, Ueda, Japan, 7-9 Sep 2009,
12. **Zhou J.**, Yu W. and Ng S.P., Vertical velocity analysis of the whole breast during activities with braless and sports bras, The Fiber Society 2009 Fall Meeting and Technical Conference, Georgia, USA, 28-30 October, 2009.

Awards

1. Outstanding student papers competition, 1st International Symposium of Textile Bioengineering and Informatics, Hong Kong, Aug 14-15, 2008.
2. W.K. Chui Travelling Scholarship, The Hong Kong Polytechnic University, 2009.

ACKNOWLEDGEMENTS

I would like to take this opportunity to deliver my deep and sincere gratitude to my chief Supervisor, Dr. Winnie Yu, for her invaluable academic advice, professional guidance and great support throughout my research work. I greatly thank her for guiding me to learn a scientific research methodology and develop systematic ways of thinking. Her patient guidance and continuous encouragement have given me the confidence to face all of the problems in the past three years, taught me the ways to systematically and logically conduct research work, and inspired me to widen my range of knowledge. These will be helpful to my study and work in the future.

In particular, I would like to acknowledge and express my sincere thanks to my co-supervisor, Dr. Zerance Ng, for his kind guidance, constructive comments, warm help, inspiring encouragement, as well as interesting discussions throughout the course of my PhD study.

I would also like to express my special gratitude to Dr. Simon Harlock for his professional editing and comments for the whole thesis.

I would like to express my special gratitude to Prof. Xin Zhang, Xi'an Polytechnic University, for her suggestions and encouragement during my research progress. Without her help, I would have never had the chance to study at The Hong Kong Polytechnic University.

I would like to acknowledge the Hong Kong Research Grant Council (RGC) for funding this research (PolyU 532306) and also thank the Institute of Textiles and Clothing (ITC) at the Hong Kong Polytechnic University for providing me with excellent research conditions and environment during the few past years.

I am especially grateful to Dr. Ning Du, Shan Dong University, for his guidance on the data transformation from a global coordinate system to a breast coordinate system.

I would like to give deep thanks to Ms. Huang Yan and Ms. Yan Bin for their advices.

I would like to thank all the colleagues at the Hong Kong Polytechnic University; Dr. Li-hua Chen, Mr. Long Wu, Mr. Albert Au, and Dr. Xian-fu Wan, for their technical support and assistance.

I would like also to give my most grateful appreciation to the colleagues at Xi'an Polytechnic University; Prof. Xing Zhang, Dr. Bo-an Ying, Prof. Jing-wei Liu, Prof. Wei Tian, Prof. Xiao-wen Jiang and Prof. Chi Liu, for their encouragement.

I also thank Prof. Daniel Chow for his advice on Chapter 3 and providing me with the facilities at the Human Locomotion Lab, and thank DBApparel for providing the samples of sports bras. Thanks also go to the female subjects who made this research possible.

Finally, I give my special thanks to my husband, Xuan-ping Wang, my son, Ao-si Wang, and my families for their spiritual encouragement, great support, and deep love all along the course of my study.

CONTENTS

page

CHAPTER 1 INTRODUCTION 1

1.1 BACKGROUND 1

1.2 OBJECTIVES 3

1.3 RESEARCH METHODOLOGY 3

1.4 SIGNIFICANCE 6

1.5 LIMITATIONS OF STUDY 7

1.6 OUTLINE OF THE THESIS 8

CHAPTER 2 LITERATURE REVIEW 10

2.1 INTRODUCTION 10

2.2 THE FEMALE ADULT BREAST 10

2.2.1 Breast structure 10

2.2.2 Kinetics of the female breast 13

2.3 Sports bras 14

2.3.1 Types and features of sports bras 14

2.3.2 Fibre content of sports bras 16

2.3.3 Components of sports bras 17

2.3.3.1 Bra cups 17

2.3.3.2 Shoulder straps and back designs 18

2.3.4 Functions of sports bras 18

2.3.5 Criteria of a good sports bra 19

2.4 BREAST MOTION STUDIES 21

2.4.1 Subject and bra characteristics 25

2.4.2 Exercise characteristics 27

2.4.3 Motion capturing methods 27

2.4.3.1 Motion capturing equipment ... 27
2.4.3.2 Study points ... 29
2.4.3.3 Locations of reference points ... 30
2.4.3.4 Number of reference points ... 32
2.4.3.5 Reference systems ... 33
2.4.4 Findings of breast motion studies ... 36
2.4.4.1 Breast movement trajectory ... 37
2.4.4.2 Breast displacement ... 39
2.4.4.3 Breast velocity and acceleration ... 42
2.4.5 Summary and conclusions from the literature review into breast movement ... 43
2.6 Breast model studies ... 46
2.7 Summary ... 50
CHAPTER 3 DEVELOPMENT OF A NEW BREAST COORDINATE SYSTEM ... 52
3.1 Introduction ... 52
3.2 Development of the Breast Coordinate System (BCS) ... 53
3.2.1 Selecting a reference object ... 53
3.2.2 Selecting reference points ... 54
3.2.3 Building a reference system ... 55
3.2.3.1 Locating breast boundary points to define the Breast Coordinate System 56
3.2.3.2 Defining the origin and three axes of the Breast Coordinate System ... 65
3.3 Transformation from the Global Coordinate System (GCS) to the Breast Coordinate System ... 65
3.3.1 Defining the Global Coordinate System ... 66
3.3.2 Locating the Breast Coordinate System ... 66
3.3.3 Recording breast positions ... 66
3.3.4 Transforming coordinates ... 67
3.3.4.1 Coordinate of the origin "*o*" ... 71
3.3.4.2 Coordinates of R_1, R_2 and R_3 in the Breast Coordinate System ... 76
3.4 Validation of the breast coordinate system ... 79

3.4.1 Subjects ... 79
3.4.2 Bra sample ... 79
3.4.3 Motion experiments ... 80
3.4.5 Results of validation ... 81
3.4.6 Results of reliability test ... 85
3.5 CONCLUSIONS ... 87
CHAPTER 4 EVALUATION OF BREAST MOVEMENT ... 88
4.1 INTRODUCTION ... 88
4. 2 METHODS FOR EXPERIMENT 1 ... 90
4.2.1 Bra samples ... 90
4.2.2 Subjects ... 94
4.2.3 Vicon motion analysis system ... 95
4.2.4 Experimental protocol ... 97
4.2.5 Data pre-processing ... 100
4.2.6 Data processing ... 100
4.2.6.1 Breast movement trajectory ... 100
4.2.6.2 Amplitude of breast displacement ... 101
4.2.6.3 Reduced percentage of breast displacement ... 102
4.2.7 Statistical analysis ... 102
4.3 RESULTS AND DISCUSSIONS OF EXPERIMENT 1 ... 103
4.3.1 Breast movement trajectories ... 103
4.3.1.1 Comparing three activities in the Global Coordinate System ... 103
4.3.1.2 Breast movement trajectories of the three activities in the Breast Coordinate System ... 105
4.3.2 Breast displacement ... 109
4.3.2.1 Breast displacement against time ... 109
4.3.2.2 Amplitude of breast/bra displacement ... 112
4.4 CONCLUSIONS FROM EXPERIMENT 1 ... 123
4.5 METHODS FOR EXPERIMENT 2 ... 125

4.5.1 Sample size of human subjects ... *125*

4.5.2 Samples of shoulder straps ... *127*

4.5.3 Experimental ... *131*

4.5.3.1 [TC]^2 body scanner ... 131

4.5.3.2 Vicon motion analysis system ... 133

4.5.4 Statistical methods ... *133*

4.6 Results and discussion of Experiment 2 ... 134

4.6.1 Bra displacement and volume ... *134*

4.6.2 Bra movement and shoulder strap properties ... *137*

4.7 Conclusions from Experiment 2 ... 141

4.8 Conclusions ... 141

CHAPTER 5 DEVELOPMENT OF BREAST MECHANICAL MODEL ... 143

5.1 Introduction ... 143

5.2 Methodology ... 144

5.2.1 Breast mechanical model ... *144*

5.2.2 Data required to build the breast mechanical model ... *147*

5.2.3 Scanning of breast shapes ... *148*

5.2.3.1 Finite Element analysis of human breasts ... 149

5.2.3.2 Scanning of breast prostheses ... 152

5.2.3.3 Coordinates of the CBM and nipple point of the breast prosthesis ... 156

5.2.4 Free vibration of breast ... *159*

5.2.4.1 Data processing ... 160

5.3 Results ... 167

5.3.1 Motion curves of nipple displacement ... *167*

5.3.2 Calculations of breast force during jogging in braless and sports bra conditions ... *175*

5.3.3 Predicted force involved during jogging under a braless condition ... *179*

5.3.4 Predicted force involved during jogging in a sports bra ... *180*

5.4 Breast mechanical model with different shoulder straps ... 180

5.4.1 Different widths of shoulder straps *180*

5.4.2 Different styles of shoulder straps *181*

5.4.3 Different positions of shoulder straps *183*

5.4.3.1 Straps in a natural position on the shoulder 183

5.4.3.2 Straps in other positions on shoulder 186

5.5 Conclusions 190

CHAPTER 6 SUMMARY, CONCLUSIONS AND RECOMMENDATIONS FOR FUTURE WORK 192

6.1 Summary and Conclusions 192

6.1.1 Development of 3D breast coordinate system *194*

6.1.2 3D breast movement under different bra conditions during various activities *194*

6.2 Limitations and future work 198

Appendix 1 201

Appendix 2 202

Appendix 3 203

Appendix 4 204

Appendix 5 205

Appendix 6 206

Appendix 7 207

Appendix 8 208

Appendix 9 209

References 210

LIST OF FIGURES

page

Figure 1.1 Research framework 4
Figure 2.1 Tangential and sectional view of a breast on the chest wall [24] 11
Figure 2.2 Two types of sports bras 15
Figure 2.3 Sports bras with different types of cup seams 17
Figure 2.4 Five back designs of sports bras 18
Figure 2.5 Study attrition diagram 22
Figure 2.6 Reference points identified on the body skin 31
Figure 2.7 Three markers used by Scurr et al. [20] and Haake et al. [19] 35
Figure 2.8 Movement trajectories of the body (solid line) and breast (dotted line) while the participant wore a sports bra in one stride of running in the vertical direction viewed from the medial-lateral direction perspective [50] 37
Figure 2.9 Vertical displacement of both breast size A-B and C-D during different activities [4,6,16,49-50] 41
Figure 2.10 Internal force on a breast in different postures [22] 48
Figure 3.1 Thorax coordinate system [83] 55
Figure 3.2 Four breast boundary points and a BCS 57
Figure 3.3 The most inferior point and most lateral point on the breast 57
Figure 3.4Ten areas of bra fitting assessment 59
Figure 3.5 The difference of marker points before and after adjusting the everyday bra 61
Figure 3.6 Laser body-landmarker 62
Figure 3.7 Three planes that are formed by the three axes 65
Figure 3.8 Three-axis vectors and position of marker *M* defined in the GCS and BCS 67
Figure 3.9 Transverse plane through two bust points in the GCS 71
Figure 3.10 Relationship of the BCS origin and the three reference points 72
Figure 3.11 Transverse plane through two bust points in the GCS and BCS 77

Figure 3.12 Design details of the sports bra sample with size 75B 80
Figure 4.1 Definitions of bra measurements.. 93
Figure 4.2 a) L-Frame for static calibration and b) wand for dynamic calibration ... 96
Figure 4.3 Points of reference and breast boundary markers in the BCS 98
Figure 4.4 Markers on the bra or on the breast skin 99
Figure 4.5 Determination of positive and negative peaks in vertical displacement in every stride.. 101
Figure 4.6 BMTs of Subject 3 in the GCS under braless and sports bra (Style 6) conditions during walking (unit: cm).. 103
Figure 4.7 BMTs of Subject 3 in the GCS under braless and a sports bra (style 6) conditions during jogging (unit: cm) 104
Figure 4.8 BMTs of Subject 3 in the GCS under braless and sports bra (Style 6) conditions during stepping up and down (unit: cm) 104
Figure 4.9 BMTs of six breast points on Subject 3 in the BCS under braless and sports bra conditions during walking (unit: cm).. 106
Figure 4.10 BMTs of six breast points on Subject 3 in the BCS under braless and sports bra conditions during jogging (unit: cm).. 106
Figure 4.11 BMTs of six breast points on Subject 3 in the BCS under braless and sports bra conditions during stepping up and down (unit: cm)....................... 107
Figure 4.12 3D BMTs of M4 and M6 when a sports bra was worn during jogging on a subject (unit: cm).. 108
Figure 4.13 Open loops of BMTs in the GCS under a sports bra condition during a jogging stride 109
Figure 4.14 Breast displacement of a subject with breast size 80B in braless and bra conditions during jogging 111
Figure 4.15 The mean values of the amplitude of breast displacement of four subjects at different marker positions in three directions during three different activities under two breast-supported conditions (unit: cm) 112
Figure 4.16 RBD of different bra styles in different directions 118
Figure 4.17 Relationships between bra measurements and RBD 120
Figure 4.18 Linear relationship between the shoulder strap elongation percentage

and the Reduced percentage of Breast Displacement (RBD) 123
Figure 4.19 Load-extension behaviour of strap 1 in the third cycle of loading and unloading.. 128
Figure 4.20 Bra Style 6 with the shoulder straps not attached................................ 129
Figure 4.21 A 3D point cloud of the body image of a subject with breast size 75C 131
Figure 4.22 Process of extracting breast volume 133
Figure 4.23 Relationships between breast volumes (cm^3) and the mean amplitudes of bra displacement of 11 subjects jogging for 10 strides............................... 135
Figure 4.24 The breast deformation: The solid and dash lines are the points of the breast in static and dynamic conditions respectively...................................... 136
Figure 4.25 Modulus of shoulder strap versus vertical bra displacement................ 137
Figure 5.1 Schematic of the proposed model to evaluate the force on breasts during jogging 145
Figure 5.2 Mass attached to a spring and damper... 146
Figure 5.3 3D photogrammetric body imaging system 151
Figure 5.4 Building of geometric breast model 151
Figure 5.5 3D meshes of the breast section 152
Figure 5.6 NextEngine 3D scanning apparatus... 154
Figure 5.7 Scanned images of a breast prosthesis... 155
Figure 5.8 Transverse plane of BL, BO and BI 157
Figure 5.9 Relationships between the coordinates of the CBMs and nipple points of 11 breast prostheses 158
Figure 5.10 Three waveforms of breast displacement in a vertical direction 161
Figure 5.11 Single waveform of displacement in a vertical direction 162
Figure 5.12 Linear relationship between the strap modulus and spring constant of the breast 164
Figure 5.13 Linear relationship between strap moduli and damping coefficients ... 167
Figure 5.14 Fit graph and residuals of nipple *x*-displacement during Subject A's jogging under a braless condition. 168
Figure 5.15 Fit graph and residuals of nipple *y*-displacement during Subject A's jogging under a braless condition 171

Figure 5.16 Fit graph and residuals of nipple *z*-displacement during Subject A's jogging under a braless condition. 171
Figure 5.17 Fit graph and residuals of nipple *x*-displacement during Subject A's jogging under a sports bra condition.. 174
Figure 5.18 Fit graph and residuals of nipple *y*-displacement during Subject A's jogging under a sports bra condition.. 174
Figure 5.19 Fit graph and residuals of nipple *z*-displacement during Subject A's jogging under a sports bra condition.. 175
Figure 5.20 Force on breasts for a single jogging stride of Subject A under a braless condition 177
Figure 5.21 Force on breasts for a single jogging stride of Subject A under a sports bra condition 178
Figure 5.22 Two shoulder straps with different widths... 181
Figure 5.23 Force *F* that acts on the shoulder strap 184
Figure 5.24 Force analysis of shoulder straps... 187

LIST OF TABLES

page

Table 2.1 Mechanical properties of breast tissue components [22] 13

Table 2.2 Properties of the fibres used in sports bras [42] 16

Table 2.3 Summary of research about breast motion during exercise 23

Table 2.4 Number of articles that have studied various cup sizes 26

Table 2.5 Rotation and translation of the pelvis and thorax during walking and running [69] 33

Table 2.6 Mean and standard deviation (SD) of breast displacement under braless and sports bra conditions in previous studies (unit: cm)................................... 39

Table 2.7 Formulas to calculate the force and the range of the force acting on the breast [22] 49

Table 3.1 Bra fitting checklist [85] 60

Table 3.2 3D coordinates of the GCS for five different breast types in the standing pose (unit: cm) 64

Table 3.3 Coordinates of six markers at a sampling instant in the GCS in different conditions (unit: cm) 82

Table 3.4 Transformed coordinates of six markers from the GCS to BCS (unit: cm) 83

Table 3.5 Distance between any two markers in the GCS and BCS (unit: cm)......... 84

Table 3.6 The coordinates in the BCS of the same marker on the bra in the static state at different standing positions in the GCS (unit: cm) 86

Table 4.1 Inclusion criteria of the selected sports bras 91

Table 4.2 Descriptions of sports bra samples.. 92

Table 4.3 Measurements of seven bra samples for core size 75B (unit: cm)............. 93

Table 4.4 Breast sizes and shapes of the subjects 94

Table 4.5 Calibration procedure [92] 96

Table 4.6 Differences between M4 and other points in breast displacement of 11 subjects...115

Table 4.7 Displacement at each breast point of 11 subjects during activities in the BCS (unit: cm) 116
Table 4.8 ANOVA results of breast/bra displacement in x-, y- and z- directions during different activities 117
Table 4.9 Pearson correlation coefficients among the elongation percentages and the Reduced percentage of Breast Displacement (RBD) 122
Table 4.10 Effect size and power analysis of Experiment 1 126
Table 4.11 Properties and yarn contents of selected shoulder straps 127
Table 4.12 Properties of the 10 shoulder straps 129
Table 4.13 Pre-experiment extension percentages of the shoulder straps.... 130
Table 4.14 Calibration procedures of the body scanner [101] 132
Table 4.15 Regression equations of breast volumes and mean amplitudes of bra displacement 136
Table 5.1 Equations of the force on the breasts during jogging.... 147
Table 5.2 Size specifications of 11 breast prostheses (unit: cm).... 153
Table 5.3 Coordinates of the breast prostheses' nipple point (x_{bp}, y_{bp}, z_{bp}) and the CBM (x_{bw}, y_{bw}, z_{bw}) (unit: cm).... 157
Table 5.4 The oscillation frequencies f_{sb} and the spring constants k_{sb} of the breast with different shoulder straps.... 163
Table 5.5 Coefficients of the curve-fit equation of the x-, y- and z-displacement under a braless condition 169
Table 5.6 Equations of displacement, velocities and accelerations of the CBM of Subject A in a jogging stride under a braless condition 170
Table 5.7 Equations of displacement, velocities and accelerations of the CBM of Subject A in a jogging stride under a sports bra condition 172
Table 5.8 Coefficients of the curve-fit equation of the x-, y- and z- displacement under a sports bra condition.... 173
Table 5.9 Correlation coefficients R^2 s of all fitted equations of the nipple displacement under braless and sports bra conditions 173
Table 5.10 Equations of the force on the breasts during jogging.... 175
Table 5.11 Force and displacement analysis of shoulder straps.... 182

Table 5.12 Displacement of the shoulder straps 183
Table 5.13 Tensile force on the shoulder strap along the three axes........................ 188
Table 5.14 Moments of F on the CBG in the three axes... 189

CONTENTS

ABBREVIATIONS

A

ANOVA	Analysis of variance
AP	Anterior-posterior
ASIS	Anterior superior iliac spines
az	Azimuth

B

BCS	Breast Coordinate System
BI	most medial point on the left breast intersecting with the breast root and the transverse plane through BR and BL
BL	nipple on the left breast
BMT	Breast movement trajectory
BO	most lateral point on the left breast intersecting with the breast root and the transverse plane through BR and BL
BR	nipple on the right breast

C

C7	spinous process of the 7th cervical vertebra
CBM	The centre of the breast's mass
CD	Breast displacement in a bra-controlled condition

E

el	Elevation

G

GCS	Global Coordinate System

I

IJ	Deepest point of the incisura jugularis (Suprasternal notch)
ISB	The International Society of Biomechanics

M

ML	Medial-lateral

O

OD	The original breast displacement in a braless condition

P

PX	Processus Xiphoideus, the most caudal point on the sternum

R

R^2	The correlation coefficients
RBD	The Reduced percentage of Breast Displacement

S

SD	Standard deviation

T

T8	spinous process of the 8th thoracic vertebra
3D	Three-dimensional

Chapter 1 Introduction

1.1 Background

The female breast contains limited anatomical support due to a lack of muscles and bones. Excessive movement during activities produces large force on the breasts and results in stretching of the Cooper's ligaments, discomfort, pain, embarrassment and/or sagging [1]. The excessive movement causes the breasts to lose their natural perkiness, fullness and cleavage after a certain period of time, and can affect health and breast aesthetics [2].

Previous studies have verified that sports bras were more effective in limiting breast motion and reducing breast discomfort, compared to everyday bras [3-7]. The approach used by sports bra designers to minimise excessive breast movement, has been to use stiff fabric materials around the breasts together with tight shoulder straps. These designs have largely been developed through empirical studies [8-9] and there was relatively little published information on the interaction of the components within the sports bra and how to improve the design of sports bras for controlling breast movement.

To improve the functional design of sports bras, it requires a scientific study of three-dimensional (3D) breast movement for different breast sizes and shapes. Previous studies [3-6,10-20] have investigated the effectiveness of different bra samples made from different materials with different styles, but it is not clear if there are any design rules and the scientific methodology to establish the design criteria has yet to be proposed. In this respect, a standard and valid breast coordinate system for measuring the 3D breast movement relative to the thorax is required to enable comparative evaluations to be made. This has been hitherto an unexplored area in respect of sports bra design. Therefore, the aim of the current research was to establish a reliable method to evaluate 3D breast movement and to determine the functional design criteria of more supportive sports bras. The fundamental research question therefore was:

- How the breasts move relatively to the thorax under braless and sports bra conditions during different activities?

- How can the design of sports bras be improved to reduce the breast movement for the wearer when performing activities?

The approach was to conduct both an empirical and theoretical study to systematically investigate the biomechanical and bra factors that affect the breast movement during activities, with the intention of answering the following series of supplementary key questions:

Q.1 How can relative breast movement be measured more accurately and comprehensively?

Q.2 How do the breasts move three-dimensionally during different activities under braless and sports bra conditions?

Q.3 Which features of sports bras are effective in controlling breast movement and which are not?

Q.4 How do breast volume and the properties of shoulder straps affect the breast movement?

Q.5 Using the answers from the previous questions, can a breast model be developed to simulate the breast movement and predict the force acting on breasts during jogging to provide a theoretical basis for the design of sports bras?

Answers to these questions will improve the understanding of the functional requirements of bra design and enhance the ability to improve the design of sports bras.

1.2 Objectives

To answer the research questions, the following research objectives were set:

a. to derive a 3D local coordinate system to evaluate the comprehensive breast displacement and trajectory relative to the thorax;
b. to investigate 3D breast movement in different support conditions during various activities;
c. to evaluate the effectiveness of different bra features on the reduction of breast movement;
d. to analyse the effects of breast volume and material properties of shoulder straps on the breast displacement; and
e. to build breast mechanical models to analyse the breast force during jogging.

1.3 Research methodology

To achieve the objectives outlined above, the project followed the research framework and adopted the research methodologies outlined in Figure 1.1.

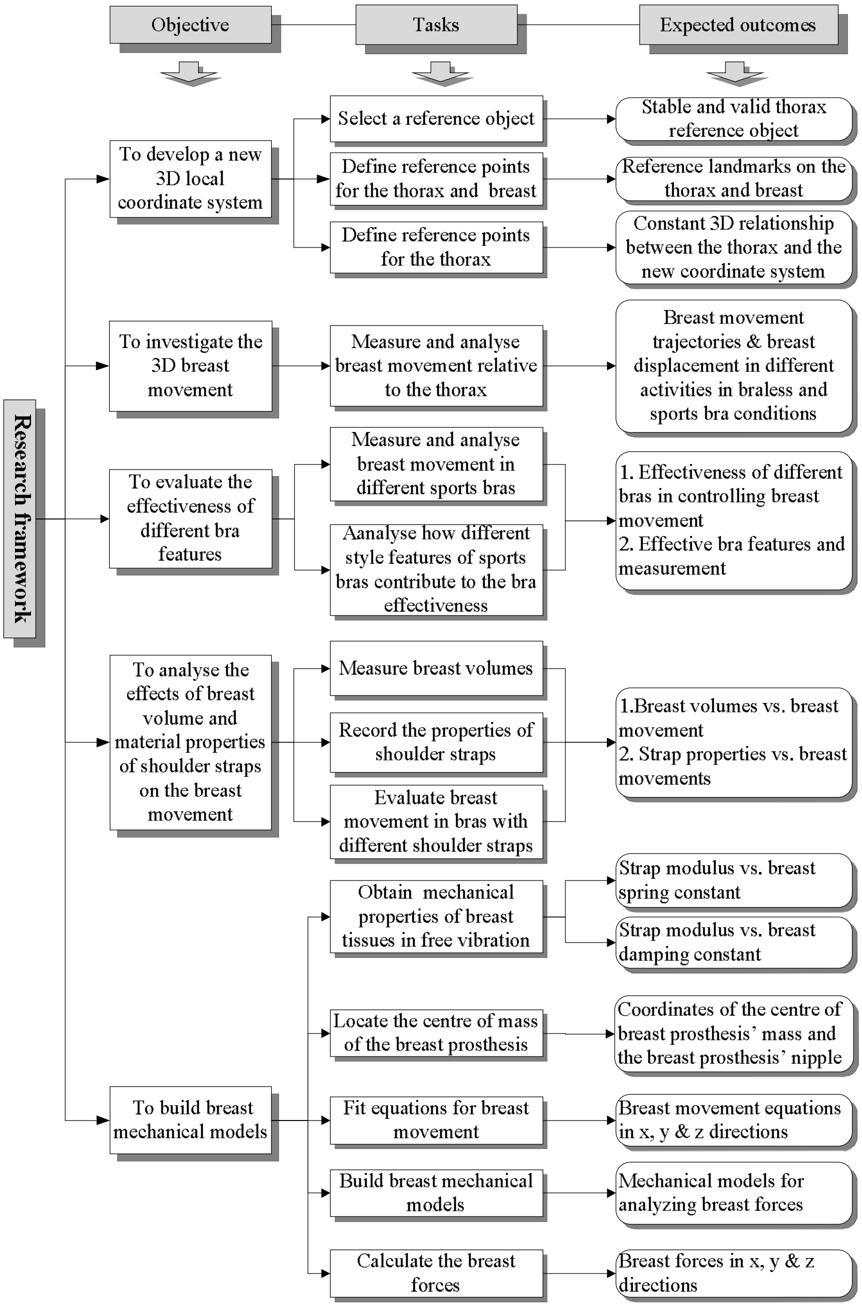

Figure 1.1 Research framework

Using an electronic database and search engines, a systematic review and critical evaluation of literature on previous research into breast movement and breast modelling, was conducted to understand more fully the functionality of sports bras, the behaviour of breast movement with or without sports bras, as well as previous research methods into breast motion studies. The review enabled the knowledge gaps in these research areas to be determined.

With reference to the research framework shown in Figure 1.1, to solve Q.1, the first step was to derive a local coordinate system to measure the 3D breast movement relative to the thorax. This required a consistent definition of a stable reference object and a clear definition of a new origin and axes of the new local coordinate system for the breast itself.

Having established this, to solve Q.2, a pilot motion experiment was carried out with four subjects participating in three activities (walking and jogging on a treadmill, stepping up and down on a platform) under a braless and seven sports bra conditions. A motion analysis system (Vicon 612, Oxford Metrics, Oxford, UK) was used to capture the 3D breast movement for six breast points under different conditions. Using the new coordinate system derived, the 3D breast displacement and trajectories relative to the thorax were determined and compared.

Having determined a methodology to measure breast movement, the effectiveness of seven different styles of sports bras in controlling breast movement was evaluated in terms of the Reduction percentage of Breast Displacement (RBD) to solve Q.3. This afforded some empirically-based initial recommendations for the improvement of future designs of sports bras.

In order to solve Q.4, the breast volumes of 11 subjects were measured by the software of TC^2 3D body scanner (NX-16, Textile/Clothing Technology Corporation, USA). Using the Vicon motion analysis system and the predetermined methodology, a series of experiments were performed whereby ten different shoulder straps were attached to the same sports bra in each motion experiment, and the bra movements were compared. The relationships between the bra movement and the shoulder strap properties for different breast volumes were then derived.

To supplement the empirically derived information and provide further understanding and data for the design of sports bras, theoretical models were developed. To simulate the force of the breast under braless and sports bra conditions, a viscous damping model was derived based on the concept of a mass, spring and dashpot. This required the derivation of the relevant breast mass, spring and damping constants. In order to do this, it was first necessary to determine mechanical and geometric data for the breast. The approach used was to measure the free vibration of a breast to estimate its spring and damping constants. Finite element analysis of 3D scanned human breasts was initially used to calculate the centre of breast mass, but it was too time-consuming. As a simplified approach, 11 breast prostheses were scanned by a 3D laser scanner (Next Engine Inc., Santa Monica, California, America) to find the coordinate relationship between the nipple point and the centre of mass of the prosthesis. Equations that represented the movement of the breast centre were derived that were subsequently used to develop new 3D breast mechanical models to estimate the 3D internal force acting on the simulated breast during jogging. The models laid the foundations for computer modelling of breast and bra mechanics. An example was shown how the models could be used to theoretically explain the force moments on the breasts exerted by different bra straps.

1.4 Significance

These empirical and theoretical 3D breast motion studies provided a standardised, valid and reliable breast coordinate system to assist future analysis of breast kinematics and kinetics, as a scientific basis for the functional design of supportive sports bras and other women's products. The experimental findings and theoretical models can also deepen the understanding of the underlying mechanisms of breast support during activities. It provided a solid foundation for future research into the interactions between human bodies and close-fitting garments.

1.5 Limitations of study

This study has focused on the methods to measure the 3D relative breast movement during activities. Only four subjects participated in the pilot experiment on seven bra samples. Subsequently, based on a power analysis, a sample of 11 women aged below 40 with bra cup sizes ranging from B to D were recruited for the motion experiments, using the same bra style with ten types of shoulder straps.

An acknowledged limitation was that the breast motions whilst wearing the sports bras were recorded by tracking passive markers on the top of the bra, not on the breast surface. Although the bra fit on individual subjects was ensured while they were standing, it was possible that there were some small relative movement between the breast and the bra during the activities. The term "bra movement" was therefore used to present the breast movement in a bra-wearing condition.

The breast mechanical model should refer to the centre of breast mass, not any one point on the breast surface. Magnetic resonance imaging was a reliable, but expensive method to locate the centre of the human breast. However, due to the reluctance of the subjects and the limited budget, finite element analysis of the scanned images of human breasts was initially used preliminarily. As it was a very time-consuming process, commercial breast prostheses were eventually used to simulate various sizes of human breasts as a convenient simplification in constructing the model. It was assumed that the breast was a homogeneous object made of soft matter with elastic damping properties and that the movement of the centre of the breast mass could represent that of the whole breast.

Although the calculated maximum force of the breast was within the range reported by Gefena and Dilmoney [21], experiments will need to be conducted in future work to validate the predicted results more fully.

1.6 Outline of the thesis

This thesis is divided into six distinct chapters. Chapter 1 briefly introduces the background, defines the aims and objectives of the study, and delineates the research framework and methodology

Chapter 2 presents the current literature on breast structure, mechanics and kinetics. Then, there is an analysis of the functions, types and features of existing sports bras. Following this, there is a systematic review of the methods and findings of previous breast motion studies, to determine the knowledge gaps, and identify the research objectives and methodologies to be adopted.

Chapter 3 describes the process of defining the reference of the thorax, and deriving a Breast Coordinate System (BCS). It demonstrates a standardised method of data transformation from a Global Coordinate System (GCS) to the BCS, with tests of validity and reliability.

Chapter 4 reports the 3D displacement of different breast points relative to the thorax in braless and different sports bras conditions during walking, jogging, and stepping up and down. The relative breast displacement is evaluated and compared among different breast points, directions and activities. The Reduced percentages of Bra Displacement are compared among different bra-support conditions. The common features of effective sports bra are identified. The effects of breast volume and shoulder strap properties on the breast displacement are further analysed.

Chapter 5 depicts 3D breast mechanical models based on the estimation of breast material properties by free-vibration tests, and the displacement, velocity and acceleration of the centre of breast mass during jogging, derived from the coordinate relationship between the nipple point and the centre of mass. The force on the breasts caused by a bra with different types of shoulder straps is predicted.

Chapter 6 summarises the research and presents the conclusions in respect of the aims and objectives. Limitations of the study are acknowledged and recommendations are made for future research work.

Chapter 2 Literature review

2.1 Introduction

This chapter presents a critical literature review on the following four main areas related to the research questions as stated in Chapter 1.

a) Essential information about breast structure, its mechanical properties, and kinetics during jogging was reviewed. All these are vital to the scientific understanding of breast motion.

b) The features and claimed functions of sports bras are described and discussed. This information will be used to analyse the effectiveness of different sports bras and to recommend strategies for future bra designs.

c) The research methods and findings of previous breast motion studies are systematically reviewed, so that the knowledge gaps are determined for setting the research objectives and improved research methodologies.

d) The essential data from previous breast modelling are discussed. This helps to build the breast model to simulate breast movement and forces during jogging.

2.2 The female adult breast

2.2.1 Breast structure

A woman's breasts sit over the pectoralis major muscle and usually anteriorly extend from the level of the second rib to the level of the sixth rib [9,22-23]. In the vertical plane, the breast tissue may extend from the clavicle (collarbone) to the middle of the sternum (breastbone). In the lateral portion, breast tissue may continue into the axilla (armpit) and reach as far as the latissimus dorsi muscle, which extends from the lower back to the humerus bone of the upper arm [22]. A schematic diagram of a breast in an adult female human cross section is shown in Figure 2.1.

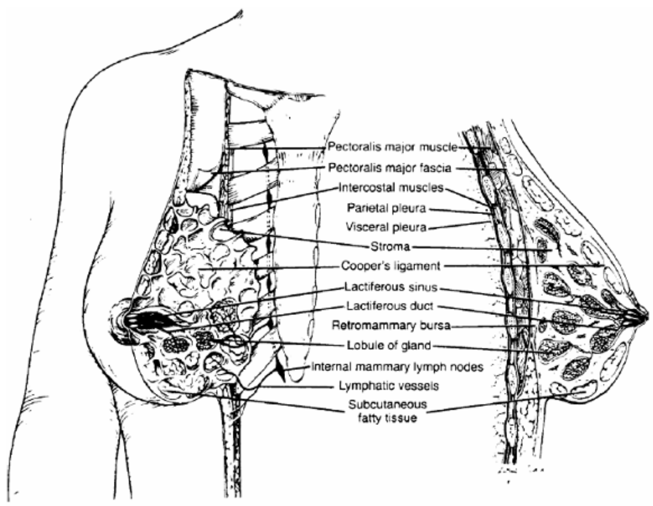

Figure 2.1 Tangential and sectional view of a breast on the chest wall [24]

The size and shape of female breasts can substantially vary between individuals. In general, most breasts are tear shaped [14], 10 to 12 cm in diameter, with a central thickness of 5 to 7 cm [9,24]. Differences in breast size are usually attributed to variations in the amount of adipose tissue. A larger percentage of adipose tissue means less density. If the percentage of adipose tissue is 20, the breast density is about 1.017 g / ml [25].

Each adult breast weighs, on average, approximately 200 to 300 g [9,26] and a large breast can weigh 750 to 1000 g [27] with the left breast often larger than the right breast [28-29]. The size and shape also vary over time in the same woman due to changes during the menstrual cycle, pregnancy, after weaning, and during the menopause [22]. For example, during pregnancy, breasts increase in size and each weigh on average, between 400 to 600 g, which increases to 600 to 800 g during lactation [9].

There are three major structural components within the female breasts: skin, the subcutaneous tissue, and the corpus mammae [9]. The skin of the breasts includes the nipple, areola and the general covering skin. The skin provides a thin, flexible elastic cover for the breasts and lies immediately above a layer of subcutaneous tissue.

The parenchyma of the breast is the glandular tissue responsible for producing and secreting milk. A small percentage of the breast volume is occupied by the parenchyma. The proportion of glandular tissue in young women tends to be higher than that in older women, whereas the proportion of fat in older women tends to be higher [30]. The stroma is made of deep-lying connective and adipose tissues, and supports the nerves, blood vessels, and lymphatic vessels. The shape and size of the breasts are moulded by the elements of the stroma [28]. The composition and distribution of adipose tissue in breasts greatly vary from woman to woman.

Cooper's suspensory ligaments in the upper portion of the breasts extend from the deep fascia over the muscles of the chest wall to the superficial fascia just below the skin. Although suspensory ligaments are not true ligaments, they serve to maintain the breast in position on the thorax with the nipple at the approximate level of the fifth intercostal space [31-32]. As breasts have no muscle tissues or bones to provide support, these weak structures provide the breasts with their primary support [31]. Hence, breast tissue is relatively free to move over the chest wall, especially during motion of the torso [33]. As a result, these ligaments are easily stretched and thus make the breasts sag [29].

For a more scientific understanding of breast mechanics, previous work [22] has published the mechanical properties of different breast tissues in terms of elastic modulus and ultimate strength as shown in Table 2.1.

Table 2.1 Mechanical properties of breast tissue components [22]

Tissue type	Elastic modulus (kPa)	Ultimate strength (kPa)
Ribs	2,000,000-14,000,000	100,000
Pectoralis major and minor muscles	*In the longitudinal direction:* For dynamic loading: ~30 *In the transverse direction:* For dynamic loading: 1.5-6 For static loading: 0.75-3.6	400-700
Pectoralis fascia	100-2000	20,000-100,000
Suspensory ligaments	80,000-400,000	40,000
Glandular tissue	7.5-66	No data available
Adipose	0.5-25	No data available
Skin	200-3000	20,000

2.2.2 Kinetics of the female breast

The human body is exposed to repetitive impact loading during jogging. When the feet hit the ground, impact force (shocks) develop throughout the body [34]. The impact force acting on the feet can be influenced by many factors. They include the inertial properties of the body, masses of various body segments involved in the acceleration and deceleration processes, joint angles between body segments, the coupling between soft and rigid masses, and joint stiffness [35]. With each foot strike during jogging, the shock wave is transmitted throughout the body, ultimately reaching the head. Vance et al. [36] reported that the impact magnitude reduces along the leg to the head, which is known as shock attenuation. Shock attenuation is brought on by the shock absorbers in the human body, such as joint positioning [37], muscle activity [38], synovial fluid, bone, and articular cartilage. When the force is not absorbed by the lower extremity, they will be transmitted up the kinetic chain and exert a force on the pectoralis major [39]. Gravity acting through the breast's centre of mass (CBM) and the force that acts on the pectoralis major largely contribute to initiating breast movement. External support given by a sports bra is necessary to alleviate excessive breast movement. Therefore, it is necessary to study the detailed features and functions of different types of sports bras.

2.3 Sports bras

Although the history of bra design dates back to the early 1900s, the sports bra has been in use for only about 30 years. In 1977, two American women cut two jock straps apart and stitched them together to form a prototype of the first sports bra [9]. It was found that a sports bra could more effectively support breasts than an everyday bra when women were exercising [4,6]. The following will describe the features of sports bras and explain how a sports bra functions.

2.3.1 Types and features of sports bras

Commercially available sports bras are classified into two different types - compression and encapsulation [9,14,40-41] (Figure 2.2). The compression bra is designed to restrict movement of the breasts by compressing and flattening them against the body. The encapsulation bra is similar in appearance to everyday bras. It contains moulded cups that individually separate and support the breasts.

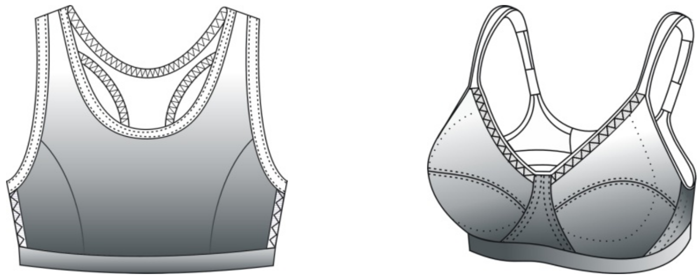

a) Compression bra b) Encapsulation bra

Figure 2.2 Two types of sports bras

The compression bra generally has a higher neckline to restrict upward movement of the breasts [9], and wider shoulder straps to distribute the pressure over the shoulders to larger back panels. The breasts are compressed tightly against the ribcage, so the breasts and the CBM are brought toward the ribcage, which decreases the force moment of breast movement. However, the compression force acting on the breast may cause breast discomfort and/or distort breast shape.

On the other hand, the encapsulation bra has a gore (i.e. a centre piece) and two cups. The gore separates the two breasts and the cups hold the breasts in place, so breast shape is less distorted. The gore cannot be set too high, so it has less control of upward breast movement than the compression bra. However, a sling can be placed at the side of the inner cup in the encapsulation bra, which is perceived to be more effective in limiting the lateral breast movement.

A previous research [9] has claimed that compression bras were more effective for women with smaller breasts (cup sizes A or B), whereas encapsulation bras were more effective for the women with cup size C or above, but this was not confirmed by experimental data. In contrast, White et al. [6] found no significant differences between the two types of sports bras on the effect of controlling breast movement. The limitation of their study was that they only used one compression bra and one encapsulation bra to compare the bra effectiveness in controlling breast movement. These findings need to be further verified by experiments in which a variety of bra types are tested. Many factors such as material, height of neckline, shoulder strap design and properties may influence the effectiveness of sports bras, so a detailed examination of the bra features needs to be considered before discussion. This poses research question Q.3: Which features of sports bras are effective in controlling breast movement and which are not?

2.3.2 Fibre content of sports bras

Page and Steele [9] suggested that the fabrics used in bras largely affected the support quality and effectiveness in controlling breast motion. The fibre content of current commercial sports bras usually contains synthetic fibres such as Coolmax® (Invista) elastanes, polyamide and polyester. They are lightweight with good strength, abrasion-resistant, easy to wash, dimensionally stable, and quick-drying. The properties of these fibres in contrast with cotton are shown in Table 2.2.

Table 2.2 Properties of the fibres used in sports bras [42]

Properties	Fibre				
	Cotton	Coolmax	Spandex (Lycra)	Polyamide (Nylon)	Polyester
Elasticity	Low	High	High	High	High
Stretch ability	Low	High	High	High	High
Recovery	Low	High	High	High	High
Strength	High	High	Low	High	High
Comfort	High	High	High	Low	Low

2.3.3 Components of sports bras

The components of a sports bra include cups, straps, gore, underband, back wing, cradle and fasteners. Commercial designs of sports bras mainly vary in their bra cups, straps and back designs.

2.3.3.1 Bra cups

Most sports bras use a full-cup design with high necklines to prevent upward breast movement. The cups in sports bras can be seamlessly moulded (Figure 2.3 a) or in a cut-and-sewn style (Figure 2.2 b and Figure 2.3 b, c, and d).

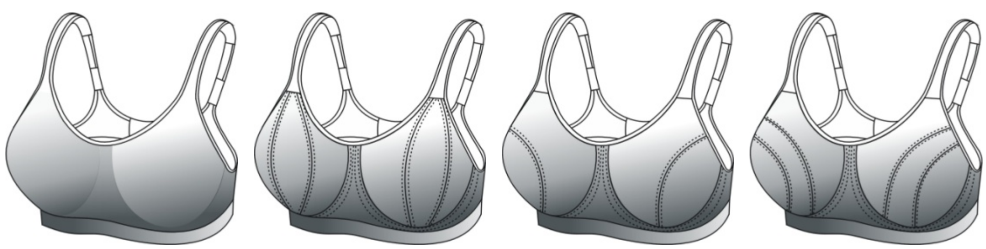

a) moulded b) double vertical seam c) bias seam d) double bias seam

Figure 2.3 Sports bras with different types of cup seams

There are three main types of seam construction in bra cups that include: horizontal (Figure 2.2 b), vertical (Figure 2.3 b) and bias (Figure 2.3 b, c and d). The moulded cups look simple and smooth, but give less control of breast movement because gaps easily appear inside the cup [43]. The cut-and-sewn cups may fit the breasts better and effectively control the medial-lateral breast movement, but scientific evidence to support these claims is unclear.

2.3.3.2 Shoulder straps and back designs

The shoulder straps of bras are essential to support the breast mass and hold the breast in place with limited breast movement. Most shoulder straps of sports bras are wider than those of everyday bras so as to distribute the forces associated with breast motion across a greater area in the back panel and reduce pressure on the shoulders. Current sports bras tend to use padded straps to dissipate the energy produced by the breast mass and velocity during movement.

There are five main back designs of sports bras: cross-over, racer-back, vertical centre [44], straight back and U-back (Figure 2.4). The styles of cross-over, racer-back and vertical centre design can prevent the straps from slipping off the shoulders during activities [44]. The sports bras with straight back or U-back are anticipated to be more effective than the other three types of back designs in reducing vertical breast movement because the force direction acting on these shoulder straps is more aligned with the direction of gravity.

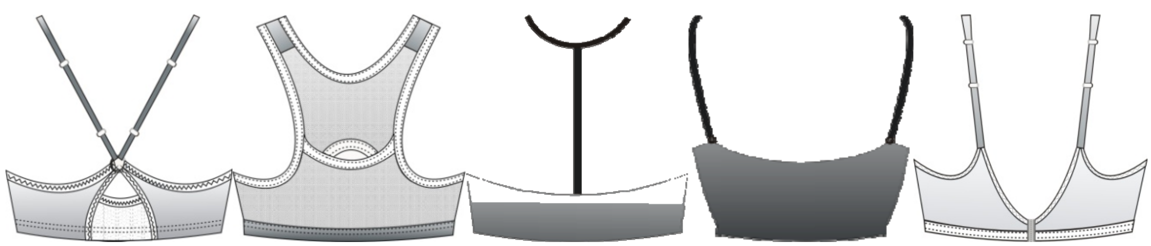

a) cross-over b) racer-back c) vertical centre d) straight back e) U-back

Figure 2.4 Five back designs of sports bras

2.3.4 Functions of sports bras

The sports bra provides firm support for the breasts. It is intended to be worn during vigorous exercising [40] that might cause the breasts to move uncomfortably, thereby preventing discomfort and embarrassment. Sports bras are sturdier than everyday bras and offer greater support for breasts, which allows them to move in unison with the trunk and not separately [45], thus increasing comfort and reducing the chances of damage to the ligaments of the chest during high-impact exercises, such as jogging. A good sports bra can provide adequate support by restricting breast motion [46] and the increased comfort might promote motivation to remain in a fitness program [47].

A well-fitting sports bra might prevent sports-induced breast discomfort, pain, and even injury [48-51]. Some researchers have advocated that younger girls should not use sports bras to allow their breast tissues to become stronger [52]. However, medical research [7] has shown that, if breast discomfort and pain occur, a sports bra could be very helpful in preventing additional pain and in managing acute sports-induced pain.

Hadi [7] studied 200 women with mastalgia in an outpatient surgical department. They were randomly divided into two groups. The first group received treatment with danazole, and the second group was asked to wear sports bras for 12 weeks. It was found that 58 % of the first group gained relief from the symptoms, but 42 % experienced side effects from the drug. In the second group, all participants had some degree of initial discomfort followed by relief of symptoms in 85 % of the cases. The author concluded that good external support provided by sports bras could relieve most of the mastalgia symptoms suffered by patients.

2.3.5 Criteria of a good sports bra

To evaluate the functions of a sports bra, Haycock [31] recommended the following criteria:

- good upward support;
- limited the motion of the breasts relative to the body;
- absorptive, non-allergenic, non-abrasive, and mostly non-elastic materials;
- well covered fasteners on both sides to prevent abrasion to the skin;
- wide and non-elastic straps not slipping off the shoulders;
- no riding up of the bra over the breasts by a wide cradle or underwire; and
- pockets inside the bra to enable the placement of padding, if needed.

A well-designed sports bra evenly distributes the weight of the breasts over the ribcage so that the back carries some of the weight, which relieves the burden commonly placed on the shoulders and the ribcage. Lawson and Lorentzen [49,53] suggested that for sports exercises that require substantial amounts of overhead reaching, bra straps should be stretched so as to prevent the riding of the bra up over the breasts. Large cup sizes should incorporate non-stretching or very high modulus cup fabrics and straps that provide support to the entire breast. Designs for women with small breasts could use less restrictive design features and comfortable fabrics.

McGhee & Steele [54] proposed an inclusion of thick foam pads inside the bra cup to elevate and compress the bras in an encapsulation sports bra in order to reduce vertical breast displacement and exercise-induced bra discomfort. In the industrial practice, inelastic thin bottom cup fabrics and side sling fabric connected with wide shoulder straps were commonly used to elevate the breasts and distribute the gravitational force from the breasts to the back. To reduce the bra moment, a compression style with high neckline was believed to be more effective.

There were contradictory suggestions for the material properties of shoulder straps in previous studies; some recommended that straps should be non-elastic [31] but some preferred stretched ones [49,53]. Hence, it is necessary to confirm which material properties are appropriate for the required functions of sports bras. This brings the research question Q.3: Which features of sports bras are effective? and Q.4: How do the properties of shoulder straps affect the breast movement?

2.4 Breast motion studies

Breasts move in complex 3D motions during exercise. A better understanding of breast motion under braless and sports bra conditions will contribute to the development of women's sports bras, as well as to the future research on functional apparel, sports science and technology. However, various methods of breast motion studies have generated some inconsistent findings. Therefore, a systematic review with a quantitative approach is necessary to guide future research on breast movement in sports bras.

This section presents a critical review of literature (i) to evaluate the methods of studying breast motion; (ii) to compare the previous findings of breast displacement, velocities, accelerations and trajectories under braless and bra conditions; (iii) to determine the efficacy of sports bras; and (iv) to identify the research problems regarding breast movement and recommend future directions for more useful breast motion studies.

Figure 2.5 outlines the systematic review process in a study attrition diagram. The initial electronic database research identified 139 citations for screening. Of these, 90 were rejected in the first scan. After screening the abstracts, 28 citations were excluded. Of the remaining 21 articles, four did not provide sufficient information for further analysis. Therefore, a total of 17 publications satisfied the selection criteria and were selected for detailed review, in which 216 subjects participated in the motion experiments.

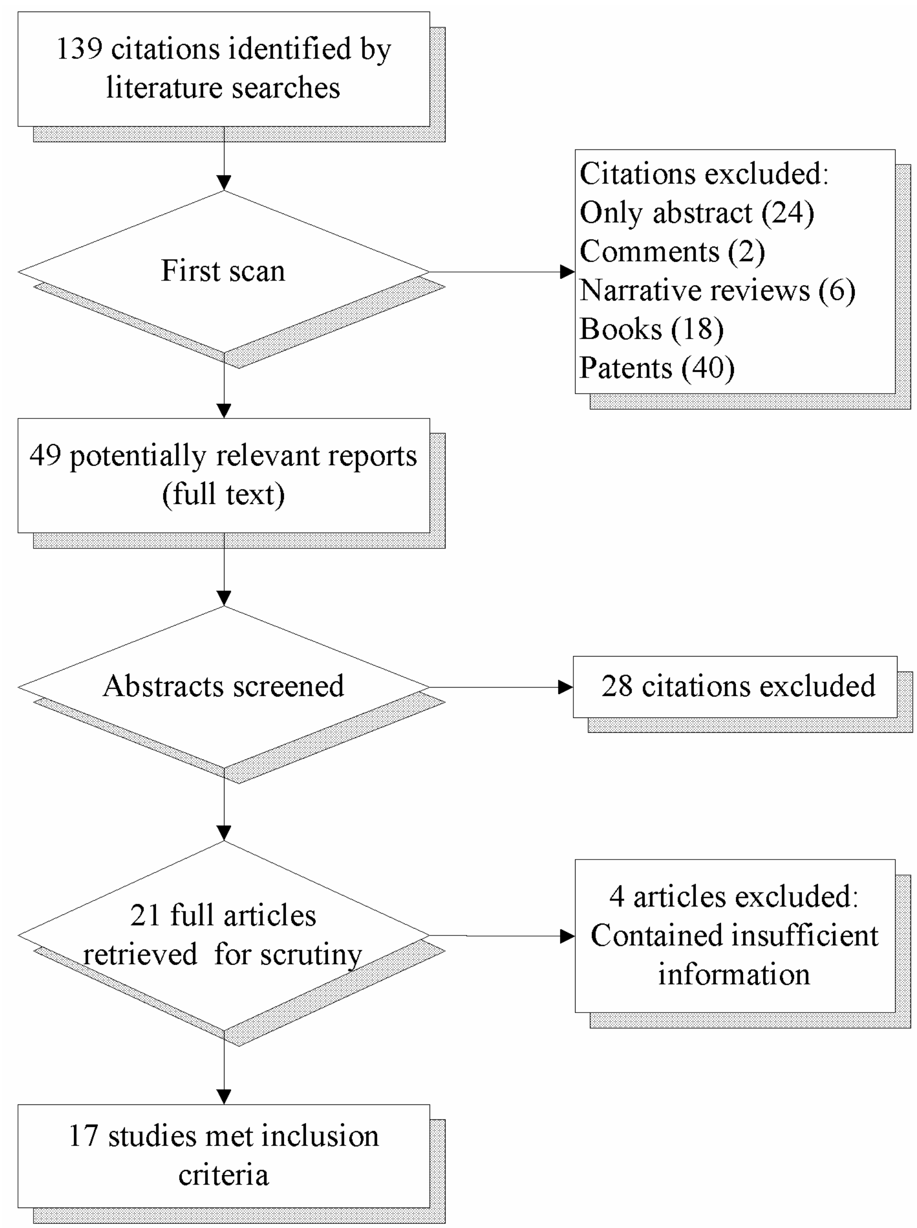

Figure 2.5 Study attrition diagram

Table 2.3 compares the publication year, discipline and methodologies of the breast motion studies in terms of number of subjects, age, breast size, bra types, equipments, exercise types and speed, number of strides, as well as the motion capturing equipment, selected reference points, study points, and type of outcomes.

Table 2.3 Summary of research about breast motion during exercise

Authors, Year [ref]	Subjects	Age	Breast size	Bra styles	Equipments	Activities	Strides & MT	Reference points	Study points	Output
Haycock 1978 [3]	5	NA	B, C & D	Everyday bra Fitted bra	16 mm movie film	W: 4.83 km/h R: 9.66 km/h	1 stride	Not available	nipple	BMT
Gehlsen & Albohm 1980 [55]	40	23.2 ± 4.7	B & D	8 sports bras	Locam camera, Van Guard motion analyser	J: 9.66 km/h & 10.46 km/h	2 strides	Left clavicle centre	nipple	V-D, V-V & BMT
Lorentzn & Lawson 1987 [56]	59	18-60	A, B, C, D	8 sports bras	16 mm Photosonics action master camera Lafayette motion analyser	J: 9.66 km/h	3 strides	Lower sternum	nipple	V-D
Mason et al. 1999 [4]	3	17-21	B, C	Sports bra Fashion bra Crop top	Two photosonics biomechanics 500, 16mm high speed cine cameras filming	W:7 km/h R:13 km/h J:10 km/h	2 strides	Notch of the sternum	nipple	V-D & V-A
Okabe & Kurokawa 2002 [10]	7	22-25	B, C	Sports bra	CCD	W: 2 step/s R: 3 step/s	6 second	Cross point of under bust line with body median	15	V-D, ML-D & BMT
Okabe & Kurokawa 2003 [11]	7	22-25	C	Everyday bra	CCD	W: 2 step/s R: 3 step/s	6 second	Cross point of under bust line with body median	14	V-D & ML-D
Okabe & Kurokawa 2004 [12]	7	22-24	A, B, C, D	Bra with normal wires, Bra with soft wires, Sports bra	CCD	Not available	Not available	Cross point of under bust line with body median	25	V-D, AP-D & ML-D
Okabe & Kurokawa 2005 [5]	11	20-26	B & C	Sports bra, Full-cup bra	CCD	R: 6 km/h	30 second	Cross point of under bust line with body median, jugular notch & front arm point	5	V-D, ML-D & BMT
Okabe & Kurokawa 2006 [13]	11	20-26	151-400 cm^3	Sports bra	CCD	R: 6 km/h	30 second	Cross point of under bust line with body median, jugular notch & front arm point	5	V-D, ML-D & BMT
Starr et al. 2005 [14]	6	23-37	C-DD	3 sports bras	Peak Motus® Movement System	R: velocity not available	3 strides	Lateral points of acromion processes, sternal angle	nipple	V-D
Fuseya & Matsumoto 2006 [15]	2	22	A, C	Sports bra, Adhesive bra, Bra, Strapless bra	Two video cameras	J: velocity not available	1 stride	Foss juglaris point	nipple	V-D, AP-D & ML-D

Table 2.3 Continued

Authors, Year [ref]	Subjects	Age	Breast size	Bra styles	Equipments	Activities	Strides & MT	Reference points	Study points	Output
Campbell et al. 2007 [16]	2	30 & 39	D & E	Everyday bra	OptoTRAK 3020 motion analysis system	W: 7 km/h R: 10 km/h	10 second	Sternal notch	nipple	V-D
McGhee et al. 2007 [17]	16	19-43	C to J	Crop top	Camcorder MV600i digital video camera, Poolcam video camera	R: velocity not available	15 strides	Sternum on the 3rd rib level	nipple	V-D & V-V
White et al. 2009 [6]	8	24.8±6.4	D	Everyday bra 2 sports bras	5 ProReflex infrared cameras	R: 10.8 km/h	2 strides	Clavicles(directly superior to the nipples) and anterior superior iliac spines (ASIS)	nipple	V-D, AP-D, ML-D & R-D
Scurr et al. 2009 [57]	15	24±4.8	D	Everyday bra Sports bra	5 ProReflex infrared cameras	W: 5 km/h R: 10 km/h	5 gait cycles	Left and right clavicles(directly superior to the nipples) and ASIS	nipple	V-D
Scurr et al. 2010 [20]	15	25.1±4.8	D	Everyday bra Sports bra	8 Oqus infrared cameras	R: 10 km/h	10 strides	Suprasternal notch, left and right anteroinferior aspect of the 10th ribs	nipple	V-D,-D,-D, V-V, AP-V, ML-V, V-A, AP-A & ML-A
McGhee et al. 2010 [18]	20	31±8	C-F	Sports bra, Experiment bra, A placebo bra	Two OPTOTRAK 3020 Position Sensors	R: 8.3±1.3 km/h Range: 6.6-12 km/h	30 strides	Sternal notch, Left heel the acromion processes, iliac crests, and spinous process of the 12th thoracic and 5th lumbar vertebra	nipples	V-D, V-V

Note: For activities, W: walking; R: running; J: jumping; A: aerobics. For output, BMT: breast movement trajectory; V-D: Vertical displacement; AP-D: anterior-posterior displacement; ML-D: medial-lateral displacement; R-D: resultant displacement; V-V: vertical velocity; AP-V: anterior-posterior velocity; ML-V: medial-lateral velocity; V-A: vertical acceleration; AP-A: anterior-posterior acceleration; ML-A: medial-lateral acceleration; MT: movement time

2.4.1 Subject and bra characteristics

Eighty eight percents of the studies [3-6,10-20] enrolled 2 to 20 subjects, and only two studies [49-50] recruited 40 and 59 subjects, respectively. It is embarrassing to ask women to participate in bare-breasted or bra motion studies, so a small sample size was often a major limitation of such research.

Excluding the studies with the same subjects in similar work, a total of 216 subjects participated in the breast motion studies. The overall age ranged from 20 to 60. The participant group represented a very small proportion of the population, and the results of these articles may not be extrapolated to all women.

Table 2.4 shows the distributions of articles regarding various cup sizes in different countries of the authors. As Okabe & Kuokawa [13] indicated breast volume rather than the cup size, only 16 studies were counted in Table 2.4 . It shows that the breast motion studies were mainly based in Japan, USA, Australia and England. Subjects with breast sizes from A to J were covered, but the majority has investigated cup sizes B, C and D, probably because the bra cup sizes 75B and 85D in the metric system (i.e. 34B and 38D in the imperial system) were regarded as the core sizes for normal and plus-size women, respectively, in the market.

Table 2.4 Number of articles that have studied various cup sizes

Country	Number of papers	Cup size				
		A	B	C	D	E-J
Japan	5	3	5	4	2	0
		11,15,58	*5,10-11,15,58*	*5,10-11,58*	*11,58*	
USA	4	1	3	3	4	1
		49	3,49-50	*3,14,49*	*3,14,49-50*	*14*
Australia	4	-	1	3	3	3
			4	*4,17-18*	*16-18*	*16-18*
England	3	-	-	-	3	-
					6,20,57	
Total	16	4	9	10	12	4

The italic figures are the reference numbers.

Only three (17.6 %) studies in Japan [11,15,58] and one (5.9 %) in USA [49] have investigated women with cup size A. No Asian studies investigated cup sizes larger than cup size D because these sizes are rare in Asia. As reported by Zheng et al. [59], only 11 out of the 456 Chinese women in their survey had a cup size larger than cup size D, and the most popular Chinese breast sizes were 75B (10.75 %), 75C (7.46 %), 80B (4.82 %) and 80C (4.17 %). Therefore in this study, the subjects in these four sizes were invited to form a pilot sample for breast motion analysis.

Thirteen out of 17 studies (76 %) examined breast movement in more than one kind of bra. The bra types in the investigations included sports bras, everyday bras and crop tops. However, only seven studies (41 %) showed the pictures of the bra samples, and only three studies (18 %) described the material and style characteristics. The discussions on previous findings of breast movement were based on unknown garment parameters and uncontrolled material properties. In this study, detailed data of the construction, material and style features of the tested bra samples will be discussed with a quantitative analysis of their effects on the reduced percentages of breast displacement. The new knowledge will be useful to improve future bra designs for preventing exercise-induced breast discomfort.

2.4.2 Exercise characteristics

The types of exercises reported in the breast motion studies were mainly walking, running, jogging and aerobics. Among the 17 studies, 13 examined running and four studied jogging; whereas five of them also conducted experiments on walking and only one investigated aerobics [4].

The walking speed in the studies ranged from 4.83 to 7 km/h, the running/jogging speed was from 6 to 13 km/h. All these exercises required both arms to swing forward and backward, and the thorax to move upward and downward. The body movement pattern was relatively regular. In future research, more activities should be studied.

2.4.3 Motion capturing methods

The accuracy of breast movement data could be affected by the motion capturing equipment, study points on the breast, location and number of reference points and reference systems. A systematic review of the previous studies that have measured breast movement is provided in the following sections.

2.4.3.1 Motion capturing equipment

The goal of motion capture in previous studies was to record the breast movement of a woman subject in a compact and usable manner. Using standard cameras has been a common method to achieve this goal because of their low cost and simplicity. Haycock [3] used a movie camera to store the images onto 16 mm film and studied breast motion [4] from watching the films. Some other researchers [49,55] used motion analysers to view and record the 2D Cartesian coordinates of several markers on the subjects in every processed film frame by the camera. To acquire the 3D coordinates of markers, Mason [4] used two high speed movie cameras to capture the motion and this experimental setup was calibrated by an array of points with known locations in the filmed volume. In addition to using cameras to acquire 3D coordinates of the surface marks, a 3D digitizer or charge-coupled device (CCD) has also been used [5,10-13]. The subject's surface was scanned with a projected laser light strip and the position of an illuminated surface point relative to the viewpoint was obtained by triangulation.

Due to the advancement in motion capture technology, recent studies have employed video cameras to obtain the subjects' motion characteristics. Starr et al. [14] placed reflective circular markers on the subjects' anatomical landmarks and captured the motion by a video camera. A VHS video recorder was set up to store the images and the motion data was collected and analysed frame-by-frame using a Peak Motus® Motion Measurement System. In the study of McGhee et al. [17], breast kinematics of drawn markers, during deep water running was obtained using a Poolcam video camera. To obtain the 3D breast vibration data, Fuseya & Matsumoto [15] used two unspecified video cameras with 3D motion analysis software to capture the motion of infrared reflective markers attached to subjects' bodies. As the motion capture technology has become well developed, pre-configured and pre-calibrated motion analysis systems (ProReflex, Oqus and Vicon) have prevailed and these enabled convenient uses of the 3D coordinates for motion measurements. The collected 3D raw data was processed using the supplier-provided programs or other software [6,16,18,57,60-61].

Over the years, retro-reflective passive markers were placed on the breast skin or over the bra cup, for infrared cameras to capture the 3D coordinates of the markers [14,19,49-50,61-62]. However, McGhee & Steele [18] used OptoTRAK 3020 position sensors to capture the active markers (infrared light-emitting diodes) directly placed on the nipples under the bra. Both kinds of markers have their pros and cons.

The use of passive markers obviates the need to wear electronic equipment or wires, and allows many markers to be tracked at the same time. The markers are attached on a close-fitting bra, but there is possible relative movement between the breast and the bra if it is does not fit perfectly in all breast regions. Previous studies did not report this possibility because only the nipple point was studied. In contrast, the active markers have illuminating LEDs to shine through the bra, so they can be placed directly on the breast skin under the bra. However, to track multiple points on the breast would require the subject to wear a network of wires that may be uncomfortable for the wearer and could potentially influence the movement of the breast within the bra, as the breasts may be deformed by the markers and the connected wires under the compression bra. The opacity of the bra fabric can also affect the light transmitted and hence the ability of the sensors to detect the lights.

2.4.3.2 Study points

Besides Okabe & Kurokawa [5,10-13] who examined breast movement at 5 to 25 breast points, most studies [3,6,14-17,49-50] have focused only on the nipple or the centre of the breast. As breast tissue is soft and viscoelastic, the nipple movement may be insufficient to describe whole breast movement. Okabe & Kurokawa's studies [5,10-13] showed that the movement of different points on the breast were different, so it is necessary to describe the breast movement at different points on the breast, but the optimal number and locations of the representing points remain unclear. Therefore, this study examined the movement at six breast points to gather more information on breast/bra movement to more comprehensively evaluate and compare the performance of sports bras.

2.4.3.3 Locations of reference points

Breast movement refers to the movement of the breast relative to a reference object. The reference being described should be based on a sufficient number of reference points that can define a stable and valid reference system. Conti et al. [63] recommended that an ideal reference system should be based on the body landmarks that can be easily and repeatedly identified on any human subjects. Anatomical landmarks give the best standardized definitions of reference marks because they are easily identifiable on the skin surface just above the bony ridges [64]. In the 17 studies, the following body landmarks have been used as references (Figure 2.6).

a) Left clavicle centre [55] or clavicle directly superior to the nipple [6,57]),
b) lateral point of acromion processes [14,18],
c) front arm point [5,13],
d) sternum notch [4], jugular notch [5,13], or suprasternal notch [19-20],
e) sternal angle [14], or sternum on the third rib level [17],
f) lower sternum [56], or cross point of underbust line and body median [5,10-13],
g) iliac crests [18],

h) anterior superior iliac spines (ASIS) [6,57],

i) anterior inferior aspect of the 10th rib [20],

j) spinous process of the 12th thoracic [18], and

k) the 5th lumbar vertebra [18]

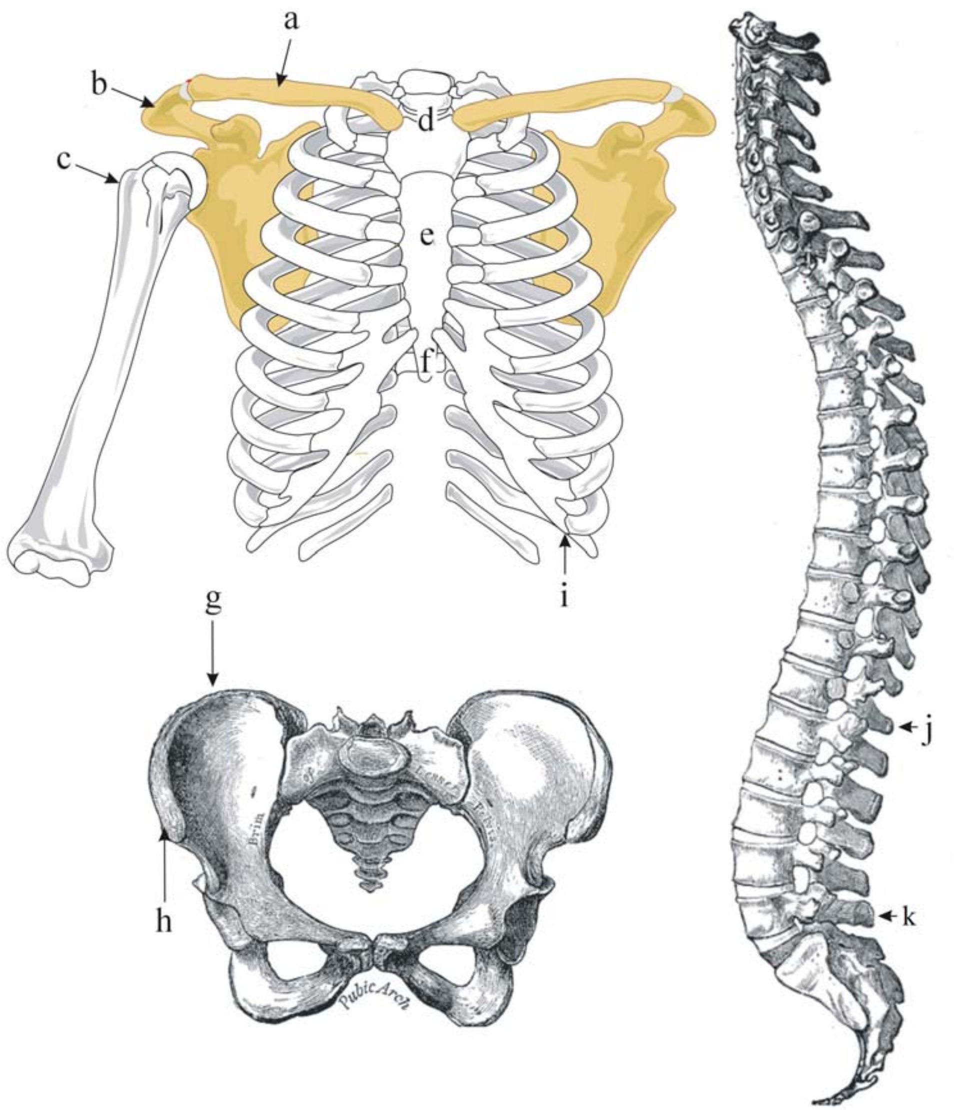

Figure 2.6 Reference points identified on the body skin

However, some of the above-mentioned reference points were actually not anatomical landmarks; for example, the left clavicle centre was directly superior to the nipple, the cross-point of underbust line and body median and front arm point. These positions were hard to locate on the body. Scurr et al. [57] used the clavicle and two ASIS on pelvis to define the thorax. A limitation of their method was that the position of the clavicle would be affected by arm swing, and the pelvis could have rotated in the opposite direction to the thorax during running, so the accuracy of thorax measurements was uncertain. Therefore, this study aimed to develop a valid breast coordinate system based on more stable reference points on the thoracic cage, to address the research question Q1: How can the relative breast movement be measured more accurately and comprehensively?

2.4.3.4 Number of reference points

Fifty-three percents of the studies chose one reference point [4,10-12,15-17,49-50], 17.6 % used three points [5,13-14], and 23.5 % used four points [6,18,20,57] to define the rigid reference system. One article [3] did not even mention the reference points.

It was known that the motion of a rigid body in 3D space can be described by six degrees of freedom [65], namely the ability to move in six directions (forward/backward, up/down, and left/right); combined with the rotations about three perpendicular axes. As the movement along each of the three axes is independent to each other and independent to the rotation about any of these axes, the motion indeed has six degrees of freedom. If one fixed point is used to define a rigid body, other points on the body might move on a sphere centred at that point. If two points are used to defined a rigid body, the body might rotate about the axis joining these two points. Therefore, one reference point is insufficient to describe the 3D movement of a reference object [4,10-12,15-17,49-50]. For motion studies especially in *vivo*, at least three independent non-collinear points should be used to define a body segment's reference system or a reference object [66-67]. Therefore, in this study, four points on the thoracic cage were used to define the thorax reference coordinates.

2.4.3.5 Reference systems

Helm [68] mentioned that because the shapes of bones and joints differ between individuals, a valid and reliable reference system is necessary to compare motion data in similar studies.

White and Scurr et al. [6,57] used the ASIS and two clavicles to define a reference system for analyzing breast movement. In human anatomy, the clavicle is classified as a long bone that makes up the part of pectoral girdle, and the ASIS is an important landmark on the anterior extremity of the iliac crest of the pelvis (Figure 2.6). Obviously, the ASIS and the two clavicles belong to different bone-frames of human body. The ASIS lies on the pelvis whereas the breasts are attached to the thorax. There exists relative movement not only between the pelvis and the thorax, but also between the clavicle and the thorax during activities. Stokes et al. [69] measured the total range of the pelvis and thorax motion of eight subjects. Their summary of the rotations and translations of the pelvis and thorax during walking and running is shown in Table 2.5.

Table 2.5 Rotation and translation of the pelvis and thorax during walking and running [69]

Rotation and Translation	Pelvis	Thorax
Rotation about the anterior-posterior (anterior-posterior) axis (°)	7.2 ± 2.1 to 11.9 ± 3.9	3.9 ± 1.8 to 6.3 ± 2.2
Rotation about the medial-lateral (ML) axis (°)	3.3 ± 0.8 to 7.3 ± 1.4	3.2 ± 0.9 to 4.3 ± 1.6
Rotation about the vertical axis (°)	5.7 ± 0.7 to 20.0 ± 5.8	4.6 ± 1.4 to 4.8 ± 2.4
Translation parallel to the anterior-posterior axis (cm)	3.0 ± 0.7 to 3.5 ± 2.5	2.4 ± 0.5 to 4.3 ± 2.2
Translation parallel to the ML axis (cm)	4.1 ± 1.5 to 7.9 ± 3.1	3.6 ± 1.4 to 5.5 ± 0.9
Translation parallel to the vertical axis (cm)	3.7 ± 1.1 to 7.6 ± 1.7	4.6 ± 2.2 to 6.6 ± 2.0

For clavicle rotation with reference to the thorax, the total range was 15.6° in protraction [70], 26.5° in upward rotation [71], and 22.2° in spinal tilting [70]. Bourne et al. [72] found that during abduction, the scapula posteriorly tipped by 44° ± 11°, rotated upward by 49° ± 7°, and externally by 27° ± 11°; and during reaching, the scapula consistently rotated upwards by 17° ± 3° and internally by 18° ± 6° whereas tipping was generally 5° ± 2° relative to the thorax. Therefore, the three points of the ASIS and two clavicles could hardly be used to define a stable reference system during different activities unless the activities were constrained to particular movement. The three points could not be regarded as standard points to define a reference system for the evaluation of breast movement.

In 2005-2006, Okabe & Kurokawa [5,13] defined a reference system using the front arm point, jugular notch (points c), d) in Figure 2.6), and the cross point of underbust line and body median. However, these three points could not form a reproducible reference system for three reasons. First, the cross point of underbust line and body median is difficult to locate and the authors did not define the underbust and body median lines. Secondly, point d) lies on the thorax, while point c) is on the upper arm, so points d) and c) belong to two different bone frames, and the arms can freely move relative to the thorax during exercise

In 2005, Starr et al. [14] used only two lateral points of the acromion processes and sternum angle (points b) and e) in Figure 2.6) to define a reference system. In 2010, McGhee et al. [18] used four points - acromion processes, iliac crests, the 12th thoracic and the 5th lumbar vertebra b), g), j), k) in Figure 2.6). However, those reference points belong to different bone segments that can have relative movement during activities such as running. Therefore, these three points can hardly construct a valid reference system for the thorax in breast motion studies.

A better method was proposed by Scurr et al. [20] and Haake et al. [19] in 2010. They used the suprasternal notch, and the left and right anteroinferior aspect of the 10th ribs (points d) and i) in Figure 2.6) to define a reference system. These three points belonged to the same thorax segment that could be regarded as a stable reference system. Based on the picture given in Scurr et al. [20] and Haake et al. [19], a schematic diagram was drawn as shown in Figure 2.7. It shows that the origin of the local coordinate system was at the suprasternal notch. The directions of perpendicular axes *u, n* and *v* depended on the thorax reference plane formed by the three points. The direction of *v* was neither perpendicular to the ground, nor parallel to the sagittal plane of the trunk; and *n* was not parallel to the transverse plane of the body when standing. The definitions of axes were not easily understood in any general sense.

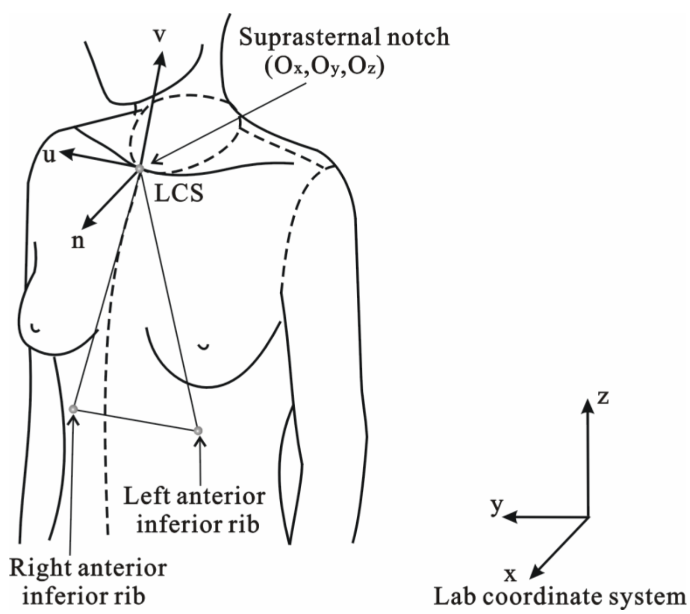

Figure 2.7 Three markers used by Scurr et al. [20] and Haake et al. [19]

As discussed earlier, it is necessary to define a valid, stable and understandable reference system for describing breast movement. This poses the research question Q.1: How can the relative breast movement be measured more accurately and comprehensively?

2.4.4 Findings of breast motion studies

All of the studies recorded breast movement in the vertical direction [3-6,10-20,23,50]. Forty-seven percents of the studies investigated the medial-lateral direction [5-6,10-13,15,20], but only 23.5 % studied the anterior-posterior direction [6,12,15,20]. Fifty-three percents of the studies chose only one reference point to represent a reference object and evaluate breast movement relative to the reference object [4,10-12,15-17,49-50]. However, the breast motion data did not eliminate the errors that were caused by the thoracic rotation, leaning, moving and/or bending during exercises. These errors were greater in the medial-lateral and anterior-posterior directions than the vertical direction. The vertical direction was perpendicular to the ground, while the medial-lateral and anterior-posterior directions were defined relative to the body, i.e. breast movement kept varying with the change of body positions. Previous researchers subtracted the dynamic coordinates from the static coordinates to calculate the vertical breast displacement. This was valid if the subject was on a constant baseline of starting height. However, it was challenging to do the same for *x*- and *z*- directions because the subject's face would be in different orientations at different times of the experiment, so the starting *x*- or *z*- coordinates were not constant every time. This poses the research question Q1: How to measure the relative breast movement more accurately and comprehensively?

Among the 17 publications, only 23.5 % examined the vertical breast velocity [17-18,20,50], and 11.8 % studied the accelerations [4,20], while 29.4 % have shown the breast movement trajectories [3,5,10,13,50].

2.4.4.1 Breast movement trajectory

Limited literature has provided the breast movement trajectory (BMT) to describe breast movement under braless and bra conditions, during walking [3,10] and/or running [3,5,10,13,50]. Haycock et al. [3] in 1978 gave the earliest BMTs in the vertical direction from both anterior-posterior and medial-lateral direction perspectives during walking and running. Each BMT formed a closed route during one stride of activities. In contrast, the BMT in the vertical direction from the medial-lateral direction perspective given by Gehlsen & Albohm [50] were open routes (Figure 2.8). This is more reasonable because the breast consists of nonlinear viscoelastic skin, adipose tissue, glandular tissue, milk ducts, and suspensory ligaments. Both kinds of BMTs showed the pattern of overall 'thoracic and breast' movement. However, the breast movement relative to the thorax is unknown.

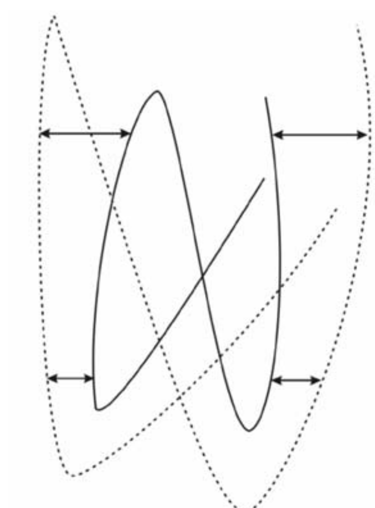

Figure 2.8 Movement trajectories of the body (solid line) and breast (dotted line) while the participant wore a sports bra in one stride of running in the vertical direction viewed from the medial-lateral direction perspective [50]

Figure 2.8 shows that the breast movement relative to the body was larger when the body moved upwards and swings in, rather than downwards and swings out. The differences were visible, but the movement trajectories of the body and breast did not show the axis scales, so the actual displacement of the breasts could not be compared with those of other studies.

Okabe & Kurokawa [5,10,13] provided the following three main findings. Firstly, not surprisingly, the ranges of BMTs were larger in running than walking. Secondly, the sports bra could control the breast movement better in the horizontal direction than in the vertical direction when compared with a full-cup normal bra. Thirdly, the movement of pert breasts were much smaller than the ptotic breasts.

Among the 17 studies, only Okabe & Kurokawa [5,10,13] investigated the BMTs at different breast points other than the nipple. They found that the BMT range of the inner breast was the smallest while the largest movement was at the nipple. The BMTs of the different points were significantly different. Therefore, future studies should examine more points other than the nipple in order to understand the complicated motion characteristics of this kind of nonlinear viscoelastic breast object.

As the BMTs were plotted under unstable systems [5,10,13] or involved the thorax movement [3,50], their characteristics were not yet applicable to improving the design of sports bras. Only recently, Scurr et al. [20] presented the vertical, anterior-posterior and medial-lateral trajectories of relative nipple displacement during walking and running. However, there was no 3D BMTs in 3D space. Therefore, the intention in this study was to investigate 3D BMTs under a valid, reliable breast coordinate system for measuring the breast movement relative to the thorax.

2.4.4.2 Breast displacement

Based on the previous findings [4,6,14,16,18,49-50,57], the mean breast displacement in three directions of an encapsulation bra, a compression bra and everyday bras whilst participants performed different activities, are summarized in Table 2.6.

Table 2.6 Mean and standard deviation (SD) of breast displacement under braless and sports bra conditions in previous studies (unit: cm)

Authors	Encapsulation bra	Compression bra	Everyday bra	Braless	Direction	Activity
Gehlsen & Albohm [55]	1.4 ± 0.4 to 3.3 ± 1.3	2. 9 ± 1.2 to 3.7 ± 1.2			V	jogging
Lorentzn & Lawson [56]	2.1 to 3.3	3.5		5.7 to 8.0	V	jogging
Mason et al. [4]	1.4 to 2.2		2.3 to 2.9	3.2 to 6.2	V	walking
	2.3 to 3.2		3.4 to 3.7	4.6 to 6.9	V	aerobics
	3.3 to 4.6		5.0 to 5.2	6.0 to 9.7	V	jogging
	3.5 to 4.4		4.3 to 7.1	5.7 to 10.5	V	running
Starr et al. [14]	0.05	0.08			V	running
Campbell et al. [16]			1.1 to 2.5		V	walking
			4.3 to 6.8		V	running
White et al. [6]	3 ± 2	3 ± 1	4 ± 2	8 ± 3	V	
	2 ± 1	2 ± 0	3 ± 1	4 ± 1	AP	running
	2 ± 0	2 ± 0	2 ± 1	4 ± 2	ML	
Scurr et al. [57]				8.1 ± 2.4	V	
				2.2	AP	running
				-1.1-4.2	ML	
McGhee et al. [18]	3.9 ± 1.2	3.7 ± 1.4			V	running
Captions: V: vertical; AP: anterior-posterior; ML: medial-lateral						

The vertical breast displacement in the compression bras were larger than those in the encapsulation bras in three studies [14,55], so it was believed that encapsulation bras were more effective than compression bras in reducing breast movement. However, White et al.

[6] and McGhee et al. [18] challenged this claim and found no significant difference between these types of bras. The effect of the sports bras on the reduction of breast movement involves many factors, such as the fabric elasticity, breast stiffness and body characteristics. However in these studies [6,14,55], the above factors were not well controlled, so the findings were compared with reservations.

According to White et al. [6], the mean breast displacement was the largest in a vertical direction because of the breast inertia and vertical reaction force generated when the subject's foot hit the ground. Breast inertia depends on the movement of the thorax (back and forth leaning, left and right swing). As the breast movement in anterior-posterior and medial-lateral directions are caused mainly by breast inertia, the breast displacement was smaller than that in a vertical direction.

According to Starr et al. [14], the vertical breast displacement whilst running wearing a sports bra was 0.08 cm or below. The level of accuracy was uncertain. In contrast, McGhee et al. [6] found that the mean breast displacement was up to 5.1 cm. This large difference might be due to different breast sizes, breast stiffness, running speed and sports bras with different fabrics. Most importantly, it was because different reference points and reference systems were chosen in the two studies.

Table 2.6 shows that the breast displacement is greater in the braless condition than that in sports bra conditions in the same direction and activity. Therefore, women should wear sports bras to limit their breast movement and hence reduce breast pain.

Figure 2.9 summaries the vertical breast displacement of different breast sizes under braless and sports bra conditions. The vertical breast displacement of breast sizes A and B were smaller than those of breast size C and D in both braless and sports bra conditions. The findings show that larger breasts had much more breast displacement during activities. Therefore, larger breasts will need special attention in the future studies. However, the relationship between breast size and displacement is unclear. This leads to research question Q.4: How does breast volume affect the breast movement?

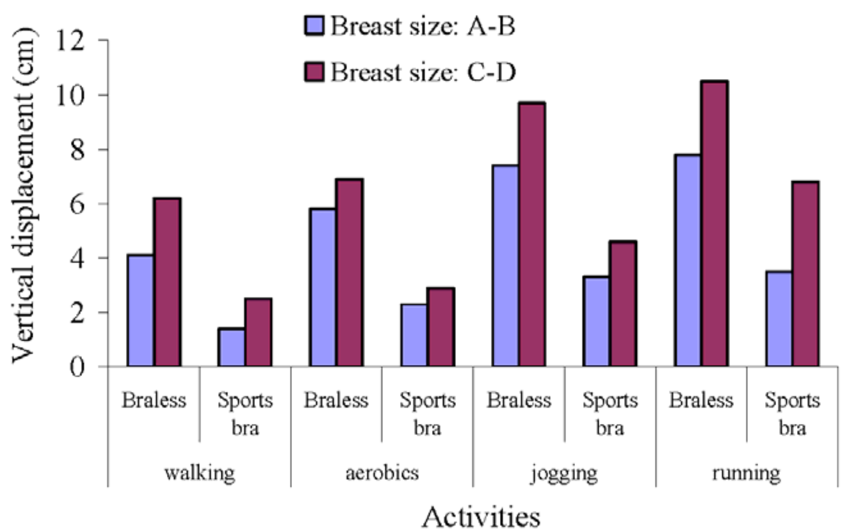

Figure 2.9 Vertical displacement of both breast size A-B and C-D during different activities [4,6,16,49-50]

This summary of vertical breast displacement would be useful as a reference for validating the findings based on the global coordinate system.

Only one 3D breast motion study [61] has recently presented the vertical, anterior-posterior and medial-lateral nipple displacement relative to a local coordinate system. Figure 2.10 shows the mean and standard deviations of nipple displacement relative to the suprasternal notch of 21 D-cup women in braless and compression at different treadmill speeds. The data can be used as a reference for comparison with the findings in this study.

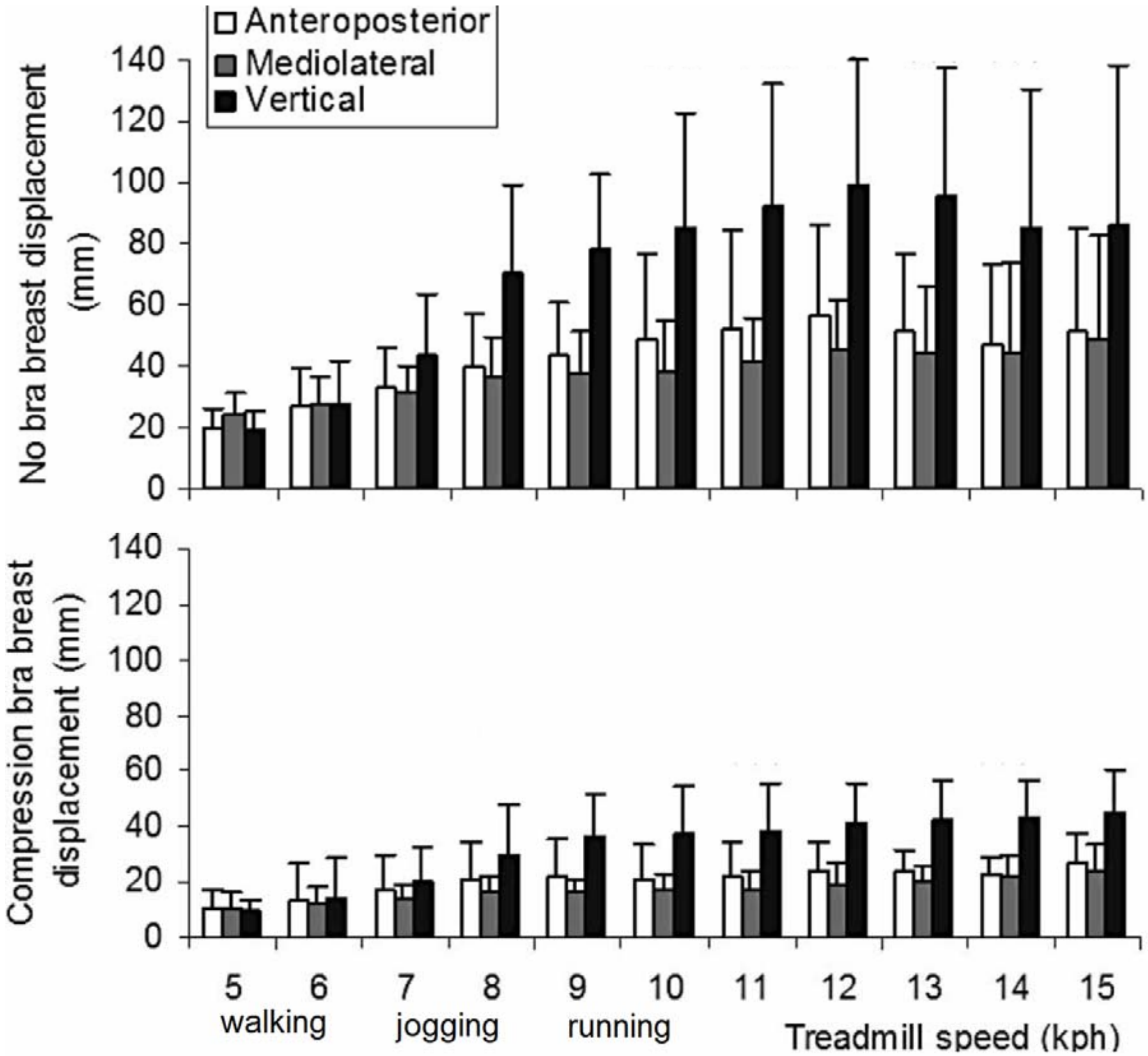

Figure 2.10 Multi-planar nipple displacement of 21 D-cup women in different treadmill speeds [61]

2.4.4.3 Breast velocity and acceleration

Only four studies [17-18,20,50] measured the breast velocities and just two papers [4,20] mentioned breast acceleration. During running the maximum vertical breast velocity was 0.8 m/s upward and 1 m/s downward [17]; while the breast velocity in the medial-lateral direction ranged from - 0.26 m/s to 0.48 m/s [20]. Scurr et al. [20] found that the vertical breast velocity in the anterior-posterior direction was reduced with increased breast support, while breast velocity in the medial-lateral direction was not related to the breast support.

The vertical breast acceleration was up to 2.8 m/s^2 during running [4,20]. Breast acceleration in the medial-lateral direction ranged from 1 to - 0.7 m/s^2 and breast acceleration ranged from - 0.6 to 0.5 m/s^2 [20] in the anterior-posterior direction.

McGhee et al. [4] found that the breast pain was related to the vertical breast displacement rather than acceleration, while another study [17] showed that increased comfort was attributed to the reduced vertical breast velocity rather than the reduction in displacement. Scurr et al. [20] found that breast comfort was highly correlated with breast velocity, but had moderate relationships with breast displacement and acceleration. Based on the findings above, the breast comfort was related to breast displacement, velocity and acceleration. The acceleration affects the external force acting on the breasts during activities. Measuring the force on the breasts is difficult. However, this poses research question Q5: Can a breast model be developed to simulate breast movement to enable the force acting on the breasts to be derived from their accelerations, velocities and displacement during jogging?

2.4.5 Summary and conclusions from the literature review into breast movement

The number of publications on breast motion has increased exponentially during the last decade. This chapter presented a systematic review on the English and Japanese literature about breast movement in sports bra, but there were only 17 articles found to be directly relevant. Eighty-eight percents of the studies enrolled 21 or fewer subjects in the breast motion experiments. Excluding the publications describing the same subjects in similar experiments, totally 216 subjects aged from 20 to 60 have participated. They were mainly in cup sizes B, C and D. Therefore, this study also recruited subjects in this size range for relevant comparisons of the results.

In addition to sports bras, everyday bras and crop tops have also been studied. However, the findings were based on unclear garment and material parameters. Consequently, the intention in this study was to develop an improved research method to facilitate further detailed analysis of the bra parameters that affect breast displacement.

In the previous studies, mainly four activities (running, jogging, walking and aerobics) have been examined, but other sports exercises involving irregular movement have never been investigated. This study aimed to investigate breast movement not only during walking and jogging, but also during stepping.

Recent research commonly used reflective markers and infrared cameras to collect kinematics data that were processed using motion analysis software. These have proven to be accurate methods, which justified the use of the Vicon Motion Analysis System used in this study.

Researchers mainly used the nipple movement to present whole breast movement, but Japanese articles examined multiple breast points. The optimal number and locations of the representing points remain unclear. Therefore, this study examined the movement at six breast points to gather more information on breast/bra movement to more comprehensively evaluate and compare the performance of sports bras.

Fifty-three percents of the studies chose only one body reference point to define a reference system. As human motion has six degrees of freedom, at least three independent non-collinear points should be used. In addition, previous studies have used 10 different body landmarks. Some were difficult to be identified on human skin, and there was no standard method in the choice of reference points and definition of a reference system for evaluating breast movement. Previous researchers have tended to focus on breast displacement in the vertical direction, but only 47 % studied breast displacement the medial-lateral direction and 24 % mentioned the anterior-posterior direction. Therefore, this study aimed to develop a reliable and valid 3D local coordinate system to evaluate 3D breast movement relative to the thorax under braless and sports bra conditions.

Three studies concluded that encapsulation bras gave less breast displacement than compression bras, but two studies found the opposite. The results of vertical breast displacement during running in a sports bra also varied from 0.05 cm to 5.10 cm. Therefore, this study proposed to further investigate the effects of bra style, and shoulder straps on breast displacement.

With a valid local coordinate system for evaluating breast movement relative to the thorax, a more reliable and comprehensive 3D analysis of breast displacement and trajectory at multiple breast points could provide useful information for the future design of sports bras. This is a niche research area that warrants more attention because breasts are viscoelastic in nature, their motion in 3D space is highly complex and appropriate support to the breasts are crucial to women's well-being.

2.6 Breast model studies

The number of models that have been developed to predict the interactions between the body and the bra are quite limited. Li et al. [73] first developed a biomechanical model to study the dynamic pressure distribution between a bra and the breasts during wear. The virtual human model consisted of three layers of materials with different mechanical properties for the skin, soft tissue and bone. A finite element biomechanical model was developed based on the theory of contact mechanics in the time domain for deriving a numerical solution for the dynamic contact model. It was able to generate a quantitative description of garment pressure distributions, human body deformation and inner stress in the skin. However, the model was over-simplified as the body consisted of a rigid thorax and two soft breasts only.

In the medical field, finite element models have been used to predict breast deformations in static conditions. Applications include breast plastic surgery [74], clinical biopsy [75], modelling of breast compression similar to X-ray mammography [76], registering X-ray and MRI mammography, validation of non-rigid registration algorithms [77] and testing of reconstruction algorithms for elastography [78].

To design a bra with effective control of breast motion during physical activity, the kinematics and kinetics of braless breast motion must be quantified in the first instance. However, biomechanical modelling of the breasts using finite element method is still in its infancy [79]. The predominant types of tissues within the breast are fat, glandular tissue and skin that have different mechanical properties that vary according to genetic factors and age [22]. The constitutive material parameters for these tissues are generally obtained from ex *vivo* indentation tests [80]. Current biomechanical static analysis of the breasts has used a non-a linear hyper-elastic neo-Hookean material model for fatty and fibroglandular tissues, and a polynomial model for the skin [74]. The effect of non-linear visco-elastic behaviour of dynamic breast motion has not really been considered in modelling breast displacement.

When breast tissue moves over the chest wall, there is internal force acting on the breast tissues. This internal force acting on the breast may cause breast discomfort or pain, so they need careful investigation. A fabric strain gauge has been used to measure breast biomechanics [16]. However, this is not a practical way to measure this internal force acting on human breasts. It would be less embarrassing to use biomechanical models to simulate the internal force in breast tissues.

Gefen and Dilmony [22] used free body diagrams to analyse the internal force that acted on the breast tissues in static postures; namely, standing, kneeling on all fours, and lying supine, as well as during dynamic activities, including running, stair climbing and jumping (Figure 2.10).

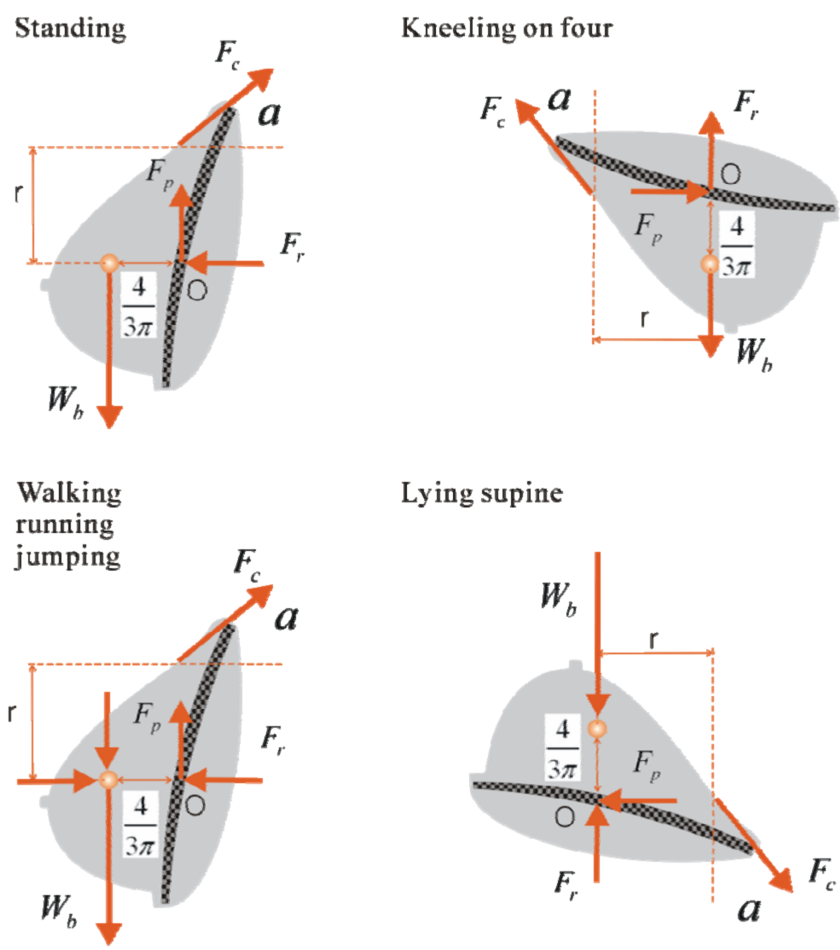

Figure 2.10 Internal force on a breast in different postures [22]

Note: F_c , F_p and F_r are the force transferred through the Cooper's ligaments, the pectoralis fascia and the ribs during static posture and dynamic activities respectively. r is the effective radius of breast curvature; α *is* the dorsal insertion angle of the breast; O is the reference point at the base of the breast.

The equilibrium of force vectors and moments were used to derive analytical solutions for the force transferred through Cooper's ligaments (F_c), the pectoralis fascia (F_p), and the ribs (F_r) during static and dynamic activities. The models used to calculate the force and the range of the force attained and shown in Table 2.7.

Table 2.7 Formulas to calculate the force and the range of the force acting on the breast [22]

Activities		Internal Breast Force		
		F_c(N)	F_p(N)	F_r(N)
Standing	model	$\frac{4W_b}{3\pi\cos\alpha}$	$W_b(1-\frac{4\tan\alpha}{3\pi})$	$\frac{4W_b}{3\pi}$
	range	2.9-8.3	1.3-5.6	2.1-4.2
Lying supine	model	0	0	W_b
	range	0	0	4.9-9.8
Kneeling on all fours	model	0	0	W_b
	range	0	0	4.9-9.8
Walking; running	model	$\frac{4}{3\pi\cos\alpha}(W_b+m_b a_y)$	$(W_b+m_b a_y)(1-\frac{4\tan\alpha}{3\pi})$	$\frac{4}{3\pi}(W_b+m_b a_y)+m_b a_x$
Walking	range	5.3-15	2.3-10.2	5.7-11.4
Running; stair climbing	range	17.7-50	7.8-33.9	24.8-49.5
Vertical jumping	model	$\frac{4}{3\pi\cos\alpha}(W_b+m_b a_y)$	$(W_b+m_b a_y)(1-\frac{4\tan\alpha}{3\pi})$	$\frac{4}{3\pi}(W_b+m_b a_y)$
Free	range	8.8-25	3.9-16.9	6.2-12.5
Trampoline	range	20.6-58.3	9.1-39.5	14.6-29.1

Note: W_b is the weight of the breast; m_b is the mass of the breast; a_x and a_y are the accelerations of breast movement in horizontal and vertical directions; F_c, F_p and F_r are the force transferred through the Cooper's ligaments, the pectoralis fascia and the ribs respectively.

The breast is a 3D viscoelastic material. Its shape varies with different poses of the body, and leads to changing positions of its centre of mass. The internal breast force exists in 3D space; they should not be only evaluated in the sagittal plane. As previously mentioned, the force acting the breast are difficult to measure. This, therefore again poses an original research question Q.5 Can an alternative visco-elastic breast model be developed to simulate the force acting on the breasts derived from the acceleration, velocities and displacement of the breast during jogging? The predicted values from such a model could then be compared with those derived by Gefen and Dilmony[22]. This would help to validate the model and to gain further understanding and insight into the relative magnitude of the force acting on the breasts in different directions.

2.7 Summary

From the literature review performed above, the following knowledge gaps were found.

a) Literature related to the breast movement in sports bras, everyday bra and crop top was examined. However, the findings were often based on uncertain garment and material parameters.

b) Four activities (running, jogging, walking and aerobics) were examined in previous studies, but the exercise of simply stepping up and down has never been researched.

c) Previous studies mainly used nipple displacement to represent the whole breast movement, but Japanese articles examined multiple breast points. The optimal number and locations of the breast-representing points remain unclear.

d) 53 % of the studies chose only one body reference point to define the reference frame. As human motion has six degrees of freedom, at least three independent non-collinear points should be used. In addition, previous studies have used 10 different body landmarks. Some were difficult to identify on human skin, and there was no standard method in the choice of reference points and definition of reference frame for evaluating breast movement.

e) Without a well-defined stable reference frame, the breast motion data usually included the body or thoracic movement.

f) Previous researchers tended to focus on breast displacement in the vertical direction, but only 47 % studied the medial-lateral direction and 24 % mentioned the anterior-posterior direction. Few studies have examined the 3D BMTs.

g) Three studies concluded that encapsulation bras showed smaller breast displacement compared to compression bras, but two studies found the opposite. The amount of vertical breast displacement during running in a sports bra has been reported to vary from 0.05 cm to 5.10 cm. As there were many uncontrolled variables in the previous studies, inconsistent findings occurred.

h) Not surprisingly, sports bras controlled breast movement better than everyday bras during activities. Breast displacement was largest in the vertical direction during running in a braless condition, especially for large breasts. The BMTs showed that the breast movement during running in sports bras were the largest in the vertical direction, especially for the ptotic breasts and nipple point. However, the BMTs did not clearly describe the breast movement relative to the thorax.

i) The effects of non-linear material properties on dynamic breast motion have not been well investigated. When breast tissue moves over the chest wall, there is internal force acting on the breast tissue. Heretofore, no biomechanical model is available to simulate the internal force in breast tissues in 3D space.

Therefore, a valid, stable and understandable coordinate system should be built for evaluating the realistic breast movement relative to the thorax. More comprehensive 3D analysis of breast movement trajectory for multiple breast points in the horizontal direction will provide useful information for the future design of sports bra.

This is a niche research area that warrants more attention because breasts are viscoelastic in nature, its motion in the 3D space is highly complex and appropriate support to the breasts are crucial to women's well-being.

Chapter 3 Development of a new Breast Coordinate System

3.1 Introduction

In the traditional global coordinate system (GCS), body position is measured relative to a fixed point in the motion capturing space. The change of coordinates reflects the movement of the whole body, not the breast relative to the body movement. For example, while a woman is standing still on an escalator, even though her breasts do not move relative to her body, their global coordinates relative to the ground are changing. In terms of breast discomfort, it is important to know the movement of the breasts relative to the body. Therefore, evaluating breast movement cannot rely solely on the GCS.

Breast movement refers to the movement of the breasts relative to a reference object. As mentioned in Chapter 2, previous researchers [3,6,14-17,49-50] chose different body segments as reference objects that were defined by one, two or more points on that segment's skin. Then, the reference points have been used to build reference systems to describe breast movement in different directions. Reference systems should be stable and valid, which means that there is neglectable relative movement between the selected reference points, which should be clearly defined and be palpated [81]. However, human muscles and joints move in complicated patterns. Relative movement among different segments of the body can happen due to rotation, bending, and leaning. Therefore, all selected reference points must be located on the same segment of the body. If reference points are chosen on different body segments, the reference system may be invalid, unstable and unreliable. For a reproducible system, Conti et al. [63] recommended that an ideal reference system should be based on anatomical landmarks that are easily and reproducibly identified in all subjects. Veeger [64] suggested that anatomical landmarks give the best standardized measures of reference because they are easily identifiable on the skin surface just above the bony ridges. To define a universal reference system to evaluate breast movement, the reference object should be consistent. If different reference objects are used to measure breast movement, different results will be obtained. This introduces difficulties in using and comparing the findings from different studies. To quantify the breast movement, a valid, reliable, reproducible and universal reference system should be standardized.

This chapter presents a newly-proposed body reference system for describing breast movement relative to the thorax. There were three steps in the development of the reference system. First, a reference object was selected; second, stable and reproducible positions on the reference object were chosen; and third, the reference system was built.

3.2 Development of the Breast Coordinate System (BCS)

3.2.1 Selecting a reference object

As breast has no bones or muscles, it cannot move without external force. It is necessary to determine the causes of breast movement before selecting a reference object. Breasts are attached onto the pectoralis major, a thick fan-shaped muscle, which is situated on the thorax (anterior) of the body. This means that the breast is closely related to the thorax.

However, the human body has a very complicated organization. There is relative movement among different body parts while the body is in motion, so the reference points in different body segments cannot be regarded as a reference object to evaluate breast movement. The pectoralis major is not only covered by the breasts, but also contracts by itself and produces deformation. Therefore, the pectoralis major cannot be used as a reference object either. The thorax is composed of the sternum, thoracic vertebrae and ribs. A previous investigation [82] showed that the thorax is not deformed during humeral abduction and anteflexion once the effects of inspiration and expiration are considered. Therefore, for the purpose of this study, the thorax was regarded as the best reference object to measure breast movement relative to the body.

3.2.2 Selecting reference points

Wu et al. [83] recommended four anatomical landmarks to define a thorax coordinate system as follows:

C7: spinous process of the 7th cervical vertebra;

T8: spinous process of the 8th thoracic vertebra;

IJ: deepest point of the incisura jugularis (suprasternal notch); and,

PX: processus xiphoideus, the most caudal point on the sternum

These four points were also used to define the thorax in this study for three reasons. First, a cluster made of four markers placed on the body surface with minimum skin movement was a good choice to eliminate errors caused by readily movable body segments [84]. Second, taken from Wu et al.'s [83] recommendation, the four points were used to define the thorax segment [83]. Third, the points were visible for recording purposes. Finally, they had minimum muscle flexing and traction [82], and could be manually identified on the body surface based on the skeletal structure.

3.2.3 Building a reference system

Wu et al. [83] recommended a method to build a thorax coordinate system. The origin and three coordinate axes of the system (Figure 3.1) were defined as follows:

O_t: The origin at IJ;

Y_t: The line that points from the midpoint between PX (processus xiphoideus) and T8 (spinous process of the 8th thoracic vertebra) to the midpoint between IJ (suprasternal notch) and C7 (spinous process of the 7th cervical vertebra);

Z_t: The line perpendicular to the plane containing IJ and line Y_t that points to the right; and

X_t: The line perpendicular to the Z_t- and Y_t-axis, which points forward;

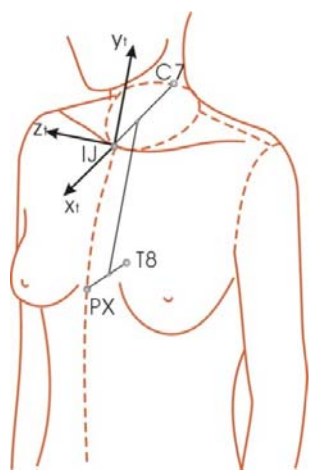

Figure 3.1 Thorax coordinate system [83]

where O_t (IJ) is the origin of the thorax coordinate system; and X_t, Y_t and Z_t are the three coordinate axes of the system.

The four points listed on the previous page were then used to define the thorax coordinate system that could be used to describe thorax movement relative to other segments of the body. However, breast movement was not easily understood based on this coordinate system due to the ambiguous directions of the X_t, Y_t and Z_t axes. The direction of Y_t was neither perpendicular to the ground, nor parallel to the sagittal plane of the trunk; and X_t was not parallel to the transverse plane of the body when standing. Hence, the coordinates of Wu et al.'s [83] recommendation was problematic to be used as a standard reference system for breast motion studies. This project therefore recommends a new BCS to standardize future studies of 3D breast movement.

3.2.3.1 Locating breast boundary points to define the Breast Coordinate System

A new BCS needs a new origin and new orthogonal axes to be defined by a transverse plane. Breast movement is related to the breast mass, so a physically-meaningful origin should be near the centre of mass. To ensure repeatability in a standard procedure, the location of the origin should be based on at least two landmarks on the breast boundary.

There are four landmarks on the breast boundary - namely, the most medial point (BI), the nipple (BL), the most lateral points (BO), and the most inferior point as in Figure 3.2. The most inferior point was not considered because the motion capturing cameras might not "see" the marker at that low point as shown in Figure 3.3. The most medial point (BI) and the most lateral point (BO) could be used to define the origin as the mid-point between them, but sometimes the latter was difficult to be identified, when the side breast boundary was unclear.

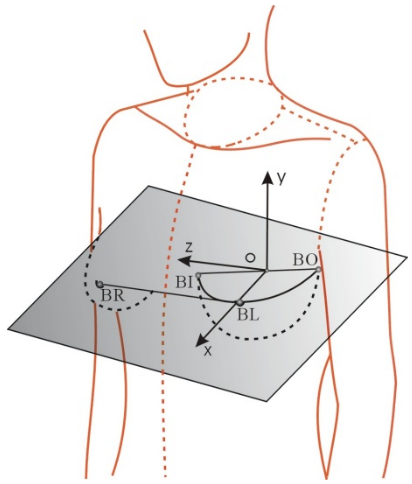

Figure 3.2 Four breast boundary points and a BCS

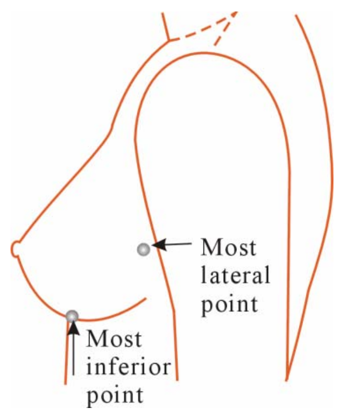

Figure 3.3 The most inferior point and most lateral point on the breast

Therefore, the nipple point was selected to align the most medial point and the most lateral point on a transverse plane. This transverse plane changed orientation with body movement, but the breast landmarks should remain on the same plane regardless of the body postures. As a convenient and standardised procedure for testing the validity and reliability of the BCS, this transverse plane should be horizontal, that means all the landmarks at the same height from the ground, while the subject was standing naturally upright. Although only the left breast was studied, the right nipple was also aligned onto the same plane because an imbalanced height of two breasts would become a variable in the motion measurements.

For the above-mentioned reasons, four points on the breast boundary (Figure 3.2) were chosen to define the origin and three coordinate axes of the BCS, as follows:

BR: nipple on the right breast;

BL: nipple on the left breast;

BI: most medial point on the left breast intersecting with the breast root and the transverse plane through BR and BL; and

BO: most lateral point on the left breast intersecting with the breast root and the transverse plane through BR and BL.

Figure 3.5 explains the concept of the BCS and, in particular, the procedure for locating the BCS using a subject whose breasts sagged downward, spread outward and were asymmetric (Figure 3.5 a). In order to align the reference points on the same line, the subject was asked to wear an everyday bra to uplift the breasts. The same researcher evaluated the bra fit with control of tension according to a bra fitting checklist [85]. A standard procedure was given to each subject for her to adjust the bra underband and shoulder straps with appropriate tension on her ribcage and shoulder, respectively. When the bra underband was set firmly on her chest wall, her breasts were filled inside the cup without any gap, wrinkle or bulging, based on the fitting checklist (Table 3.1) for ten bra areas (Figure 3.4). The tension of the shoulder straps was then adjusted to align (Figure 3.5 b), the four breast boundary points onto the same horizontal plane (Figure 3.5 c and d) when the subject was standing upright. The nipple locations were touched and identified by the subject herself and marked on the bra using a fabric marker.

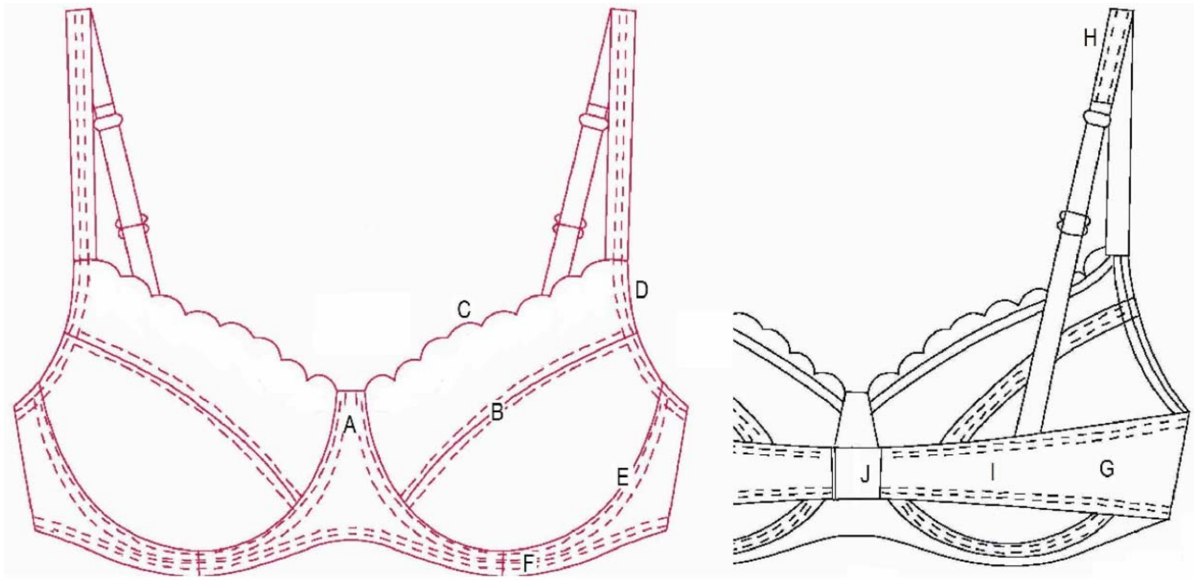

Figure 3.4Ten areas of bra fitting assessment

Table 3.1 Bra fitting checklist [85]

<u>A) Gore</u>	E) <u>Wire</u>
Gore sits against the sternum, and allow comfortable breathing	Wire matches breast root
Gore width fits for the purpose	Correct gauge
Wire tip not dig into the flesh	Not dig into the flesh
	Correct size and width
<u>B) Cup</u>	<u>F) Cradle</u>
Cover the nipples	Keep the breast inside the cups
No gap inside the cup	Does not curl up when the wearer sits down
Cup seam or lining is not itching	
No irritating lace or trims	<u>G) Wing</u>
Cup peak matches the bust point	Leveling around the body
Breast is projected during motion	Appropriate tension to hold the bra in position
Project a nice shape and curve	
Cup capacity is sufficient	<u>H) Strap</u>
	Correct tension for breast support
<u>C) Neckline</u>	Allow enough adjustment, but not too much turnings
No gap	Strap not easy fall off
No bulging	No cutting in the shoulder
Symmetric and balanced	No fatigue
Thin, soft and smooth	
	<u>I) Underband</u>
<u>D) Underarm</u>	Tension allows for comfort breathing
No gap	No riding up during motion
No extra fabric	The bra still sits securely when the wearer raises up the arms
No digging in	
Not too much pressure	<u>J) Fastener</u>
	Hooks and eyes wide enough for the style and size
	Front closure not touching sternum

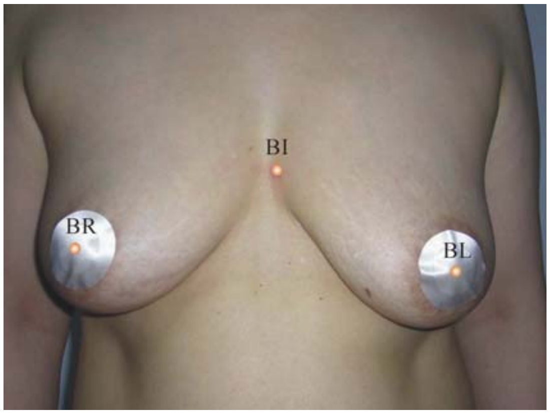

Figure 3.5a Saggy breasts

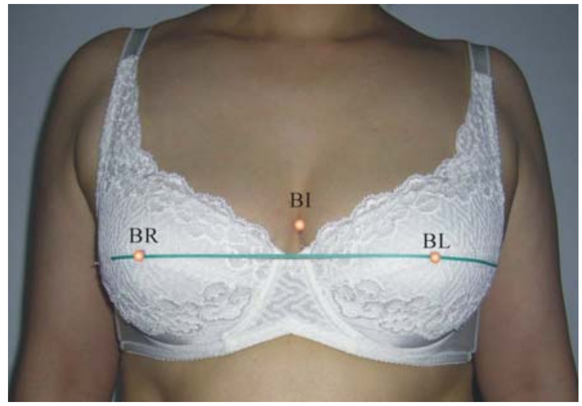

Figure 3.5b Saggy breasts in an everyday bra, before strap adjustment

Figure 3.5c After adjusting the strap tension, breast boundary markers on the same horizontal plane (front view)

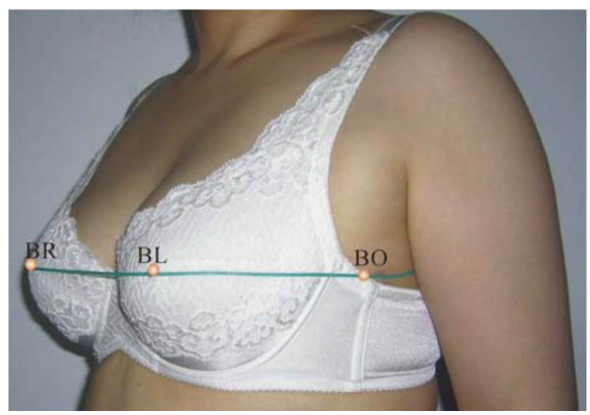

Figure 3.5d After adjusting the strap tension, Breast boundary markers on the same horizontal plane (side view)

Note: BR and BL are nipple on the right and left breasts, respectively; BI and BO are most medial and lateral points on the left breast intersecting with the breast root and the transverse plane through BR and BL, respectively.

Figure 3.5 The difference of marker points before and after adjusting the everyday bra

The horizontal levelling of the four marker points was checked using a laser body-landmarker, mounted on a horizontal frame as shown in Figure 3.6, The square frame could slide up and down until the laser shone onto the centre of the four breast boundary markers, and confirmed that they were at the same horizontal level.

	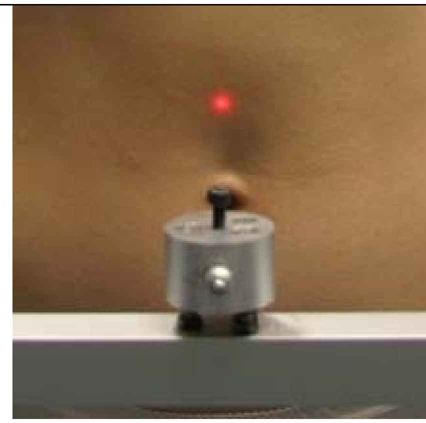
Four laser emitters mounted on a square frame at the same horizontal level	A laser spot emitted onto the skin

Figure 3.6 Laser body-landmarker

The standardized BCS requires that the reference markers lie on the same plane. Therefore, to verify the vertical coordinates of the four breast boundary markers in the GCS, the positions of the markers were captured by the Motion Analysis System (Vicon, Oxford Metrics, UK) and their coordinates were calculated for five subjects with different breast sizes and shapes. To test the reliability of the location of the BCS, the markers were removed and reattached to the same subject and the procedure for aligning the markers was repeated three times for the five subjects with different breast shapes. Table 3.2 confirms the reproducibility and accuracy of the BCS because the positions of the four breast boundary markers were consistently at the same height with very similar (maximum 2 mm difference, Interclass correlation coefficient ICC = 1) *y*-coordinate values with reference to the GCS origin at ground level.

In Table 3.2, the *x*- and *z*- coordinates of the same markers were different among three different experimental repeats in the same condition. This shows that the subject could move position relative to the position she was in, when recording the initial reference coordinates. This would be an issue if the GCS is used because the coordinates change with the subject's body position, posture and orientation, even though the breasts do not move. However, the position of the subject (thorax) within the GCS is not critical in the new breast coordinate system, because the coordinates of the breast during subsequent activities are derived relative to the thorax reference.

Table 3.2 3D coordinates of the GCS for five different breast types in the standing pose (unit: cm)

Breast size & characteristics	Marker coordinates (cm)	Left nipple (BL)			Right nipple (BR)			Inner breast (BI)			Outer breast (BO)		
		x	y	z	x	y	z	x	y	z	x	y	z
75C pert, slightly saggy	repeat 1	72.2	143.0	18.3	58.6	143.1	5.5	67.1	143.2	9.7	82.6	143.2	14.3
	repeat 2	-11.7	142.9	-1.2	-25.3	143.0	-14.0	-16.7	143.1	-9.8	-1.3	143.0	-5.2
	repeat 3	11.9	143.0	41.9	-1.7	142.9	29.0	6.8	143.1	33.2	22.2	143.0	37.8
75B Pert, not saggy	repeat 1	60.9	130.0	-25.7	45.5	130.1	-36.2	69.2	129.9	-29.7	55.0	130.0	-31.1
	repeat 2	-12.3	129.8	54.5	-27.6	129.9	43.9	-3.9	129.9	50.4	-18.1	129.9	49.1
	repeat 3	28.4	129.9	31.1	13.0	130.1	20.6	36.7	130.0	27.0	22.5	129.9	25.7
80B Ptotic, saggy	repeat 1	-26.7	114.6	56.3	-45.5	114.5	54.4	-34.7	114.6	54.2	-20.6	114.5	50.4
	repeat 2	14.8	114.8	102.0	-4.1	114.6	99.8	6.7	114.6	99.7	20.7	114.6	94.9
	repeat 3	-32.2	114.6	45.6	-51.1	114.6	43.4	-40.3	114.7	43.3	-26.3	114.5	38.5
80C pert, slightly saggy	repeat 1	29.9	129.4	56.2	14.6	129.2	42.4	24.3	129.3	47.9	38.8	129.3	53.8
	repeat 2	54.0	129.4	-31.8	38.8	129.3	-45.7	48.4	129.3	-40.1	63.0	129.2	-34.2
	repeat 3	42.6	129.3	22.2	27.5	129.2	8.2	37.0	129.2	13.9	51.5	129.3	19.8
85D Pert, saggy	repeat 1	77.1	118.8	1.9	56.1	118.8	0.9	67.9	118.9	0.3	82.5	118.7	-6.4
	repeat 2	23.0	118.7	26.0	2.0	118.6	25.0	13.8	118.8	24.4	28.4	118.7	17.8
	repeat 3	66.5	118.9	70.3	45.5	118.7	69.3	57.3	118.8	68.7	71.9	118.9	62.1

3.2.3.2 Defining the origin and three axes of the Breast Coordinate System

The origin "*o*" of the BCS (Figure 3.2) was defined by the intersection point of the line BI-BO, and the line perpendicular to BR-BL through the point BL.

The next step was to define the three axes, *x-, y-,* and *z- axes*. The *z*-axis was defined to be parallel to the line BL-BR that pointed to the right and was perpendicular to the *x*-axis that was perpendicular to the *z*-axis on the plane that was formed by four breast boundary points (Figure 3.2). The *y*-axis was defined as the line that was perpendicular to both the *x*- and *z*-axes. These three axes formed a right-handed system of coordinates and three planes as shown in Figure 3.7: the sagittal plane (*x*- and *y*- axes), transverse plane (*x*- and *z*- axes) and frontal plane (*y*- and *z*- axes). The planes intersected each other at the origin of the BCS.

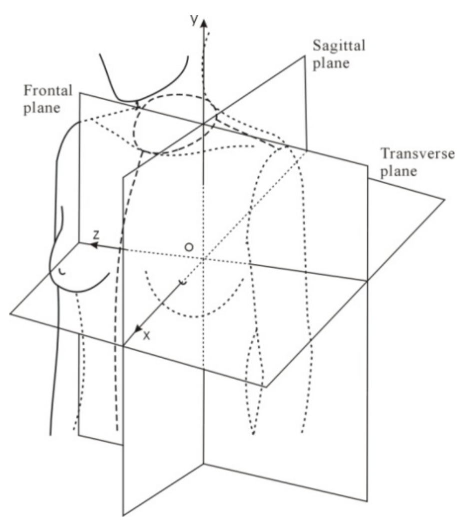

Figure 3.7 Three planes that are formed by the three axes

3.3 Transformation from the Global Coordinate System (GCS) to the Breast Coordinate System

In the past 20 years, body movement studies have mainly used multiple-camera arrangements, which require passive reflective markers, whereas the rest used active infrared emitting diode markers with infrared sensors [66]. Regardless of the systems used, for example, the Vicon motion analysis system and the OPTOTRAK system, the output data was a file of *x-, y-,* and *z-* coordinates for each marker at a sample point in time, assuming the analysis was in 3D. The coordinates were based on the GCS that was an absolute reference frame and fixed in the laboratory or data collection space. The following sub-section explains how the coordinate data was transformed into the BCS to analyse breast movement relative to the thorax.

3.3.1 Defining the Global Coordinate System

For convenience, the directions of the axes in the GCS were defined with a right-hand rule: *X* was the forward/backward direction, *Y* was the vertical (gravitational) axis, and *Z* was the left/right axis. Thus, the *XZ* plane was a horizontal plane and by definition, was orthogonal to the vertical axis.

3.3.2 Locating the Breast Coordinate System

Four breast boundary markers were attached onto BR, BL, BO and BI to define the origin "*o*" and the three coordinate axes of the BCS. At the same time, four reference markers were pasted onto C7, T8, IJ and PX, which represented the thorax segment. The coordinates of these eight markers were recorded in the GCS with the subject standing. It was assumed that the relationships among these eight landmarks were fixed.

3.3.3 Recording breast positions

The four boundary markers were removed before pasting on the experimental breast markers. The breast markers were attached onto the breast skin for the cameras of the Vicon motion analysis system (Vicon, 612, Oxford Metrics, Oxford, UK) to record the breast coordinates. The 3D coordinates of the four reference markers and the breast markers were recorded in the GCS during standing and/or dynamic conditions. The coordinates of all markers were transformed from the GCS to the BCS, so as to exclude the perspective errors caused by thoracic rotation, translation, bending or/and tilting during activities.

3.3.4 Transforming coordinates

The mathematical procedure of transforming the coordinates from the GCS to BCS by the theory of Coordinate Geometry is explained as follows. The three axis-vectors of the GCS and the BCS are expressed as $(\vec{e}_1, \vec{e}_2, \vec{e}_3)$ and $(\vec{e}_1^{'}, \vec{e}_2^{'}, \vec{e}_3^{'})$, respectively, as shown in Figure 3.8. The coordinates of $\vec{e}_1^{'}, \vec{e}_2^{'}, \vec{e}_3^{'}$ are (a_{11}, a_{12}, a_{13}), (a_{21}, a_{22}, a_{23}) and (a_{31}, a_{32}, a_{33}) in the GCS. At time *t*, the coordinate of the BCS "*o*" is (x_{0t}, y_{0t}, z_{0t}) in the GCS.

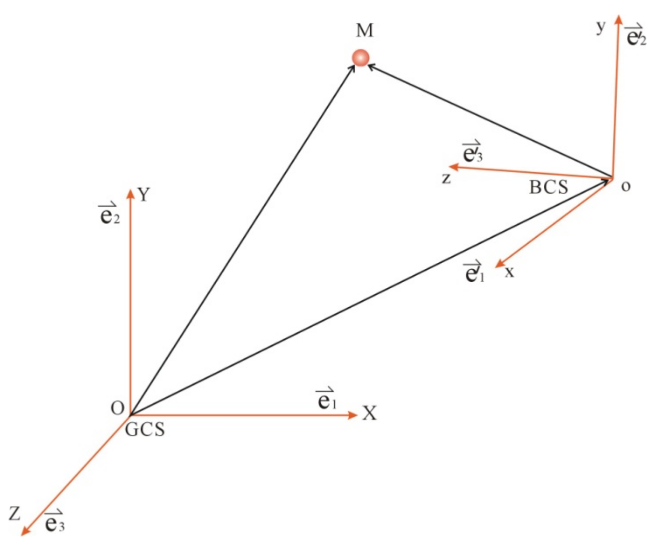

Figure 3.8 Three-axis vectors and position of marker *M* defined in the GCS and BCS

For any point M, the vector OM is the sum of the two vectors $\overrightarrow{Oo}$ and $\overrightarrow{oM}$ (Figure 3.8), as expressed in Equation (3.1)

$$\overrightarrow{OM} = \overrightarrow{O\mathrm{o}} + \overrightarrow{\mathrm{o}M} \tag{3.1}$$

that means

$$x_{mt}\vec{e}_1 + y_{mt}\vec{e}_2 + z_{mt}\vec{e}_3 = \left(x_{0t}\vec{e}_1 + y_{0t}\vec{e}_2 + z_{0t}\vec{e}_3\right) + \left(x_{mt}^{'}\vec{e}_1^{'} + y_{mt}^{'}\vec{e}_2^{'} + z_{mt}^{'}\vec{e}_3^{'}\right) \tag{3.2}$$

where (x_{mt}, y_{mt}, z_{mt}) and $\left(x_{mt}^{'}, y_{mt}^{'}, z_{mt}^{'}\right)$ are the coordinates of point M at time t in the GCS and the BCS, respectively.

Because:

$$\begin{cases} \vec{e}_1^{'} = a_{11}\vec{e}_1 + a_{21}\vec{e}_2 + a_{31}\vec{e}_3 \\ \vec{e}_2^{'} = a_{12}\vec{e}_1 + a_{22}\vec{e}_2 + a_{32}\vec{e}_3 \\ \vec{e}_3^{'} = a_{13}\vec{e}_1 + a_{23}\vec{e}_2 + a_{33}\vec{e}_3 \end{cases} \tag{3.3}$$

By Equations (3.2) and (3.3), we can have:

$$\begin{cases} x_{mt} = a_{11}x_{mt}^{'} + a_{12}y_{mt}^{'} + a_{13}z_{mt}^{'} + x_{0t} \\ y_{mt} = a_{21}x_{mt}^{'} + a_{22}y_{mt}^{'} + a_{23}z_{mt}^{'} + y_{0t} \\ z_{mt} = a_{31}x_{mt}^{'} + a_{32}y_{mt}^{'} + a_{33}z_{mt}^{'} + z_{0t} \end{cases} \tag{3.4}$$

or expressed in a matrix format:

$$\begin{bmatrix} x_{mt} \\ y_{mt} \\ z_{mt} \end{bmatrix} = \begin{bmatrix} a_{11} & a_{12} & a_{13} \\ a_{21} & a_{22} & a_{23} \\ a_{31} & a_{32} & a_{33} \end{bmatrix} \begin{bmatrix} x'_{mt} \\ y'_{mt} \\ z'_{mt} \end{bmatrix} + \begin{bmatrix} x_{0t} \\ y_{0t} \\ z_{0t} \end{bmatrix} \tag{3.5}$$

or rewritten as:

$$\begin{bmatrix} x'_{mt} \\ y'_{mt} \\ z'_{mt} \end{bmatrix} = \begin{bmatrix} a_{11} & a_{12} & a_{13} \\ a_{21} & a_{22} & a_{23} \\ a_{31} & a_{32} & a_{33} \end{bmatrix}^{-1} \begin{bmatrix} x_{mt} - x_{0t} \\ y_{mt} - y_{0t} \\ z_{mt} - z_{0t} \end{bmatrix} \tag{3.6}$$

In Equation (3.6), the coordinates of the BCS "*o*" (x_{0t}, y_{0t}, z_{0t}) and point *M* (x_{mt}, y_{mt}, z_{mt}) can be obtained in the GCS. If $\begin{bmatrix} a_{11} & a_{12} & a_{13} \\ a_{21} & a_{22} & a_{23} \\ a_{31} & a_{32} & a_{33} \end{bmatrix}^{-1}$ is found, the coordinate of point *M* $(x'_{mt}, y'_{mt}, z'_{mt})$ in the BCS can be calculated, i.e. the coordinate of point *M* can be transformed from the GCS to the BCS.

Equation (3.6) is revised as:

$$\begin{bmatrix} a_{11} & a_{12} & a_{13} \\ a_{21} & a_{22} & a_{23} \\ a_{31} & a_{32} & a_{33} \end{bmatrix}^{-1} = \begin{bmatrix} x'_{mt} \\ y'_{mt} \\ z'_{mt} \end{bmatrix} \begin{bmatrix} x_{mt} - x_{0t} \\ y_{mt} - y_{0t} \\ z_{mt} - z_{0t} \end{bmatrix}^{-1} \tag{3.7}$$

Point *M* is an arbitrary point, so we can use the coordinates from any of the three reference points of C7, T8, IJ and PX to calculate $\begin{bmatrix} a_{11} & a_{12} & a_{13} \\ a_{21} & a_{22} & a_{23} \\ a_{31} & a_{32} & a_{33} \end{bmatrix}^{-1}$, because the coordinates of the reference points can be measured in the GCS and calculated in the BCS. The coordinate relationships (distances and directions) of the three points are constant at any time. Points R_1, R_2 and R_3 represent the three selected points.

So, Equation (3.7) can be elaborated as Equation (3.8):

$$\begin{bmatrix} a_{11} & a_{12} & a_{13} \\ a_{21} & a_{22} & a_{23} \\ a_{31} & a_{32} & a_{33} \end{bmatrix}^{-1} = \begin{bmatrix} x'_{10} & x'_{20} & x'_{30} \\ y'_{10} & y'_{20} & y'_{30} \\ z'_{10} & z'_{20} & z'_{30} \end{bmatrix} \begin{bmatrix} x_{1t}-x_{0t} & x_{2t}-x_{0t} & x_{3t}-x_{0t} \\ y_{1t}-y_{0t} & y_{2t}-y_{0t} & y_{3t}-y_{0t} \\ z_{1t}-z_{0t} & z_{2t}-z_{0t} & z_{3t}-z_{0t} \end{bmatrix}^{-1} \tag{3.8}$$

where (x_{1t}, y_{1t}, z_{1t}), (x_{2t}, y_{2t}, z_{2t}) and (x_{3t}, y_{3t}, z_{3t}) are the coordinates of R_1, R_2 and R_3, respectively, at time *t* in the GCS. The coordinates of R_1, R_2 and R_3 are constant in the BCS at any time, so $(x'_{10}, y'_{10}, z'_{10})$, $(x'_{20}, y'_{20}, z'_{20})$ and $(x'_{30}, y'_{30}, z'_{30})$ are used to stand for them, respectively, at standing or dynamic conditions in the BCS.

By combining Equations (3.6) and (3.8),

$$\begin{bmatrix} x'_{mt} \\ y'_{mt} \\ z'_{mt} \end{bmatrix} = \begin{bmatrix} x'_{10} & x'_{20} & x'_{30} \\ y'_{10} & y'_{20} & y'_{30} \\ z'_{10} & z'_{30} & z'_{30} \end{bmatrix} \begin{bmatrix} x_{1t}-x_{0t} & x_{2t}-x_{0t} & x_{3t}-x_{0t} \\ y_{1t}-y_{0t} & y_{2t}-y_{0t} & y_{3t}-y_{0t} \\ z_{1t}-z_{0t} & z_{2t}-z_{0t} & z_{3t}-z_{0t} \end{bmatrix}^{-1} \begin{bmatrix} x_{mt}-x_{0t} \\ y_{mt}-y_{0t} \\ z_{mt}-z_{0t} \end{bmatrix} \tag{3.9}$$

where the coordinates $R_1(x_{1t}, y_{1t}, z_{1t})$, $R_2(x_{2t}, y_{2t}, z_{2t})$, $R_3(x_{3t}, y_{3t}, z_{3t})$ and $M(x_{mt}, y_{mt}, z_{mt})$ can be measured by a motion analysis system in the GCS.

As the distances and directions of the three points (R_1, R_2 and R_3) relative to "*o*" are fixed, "*o*" (x_{0t}, y_{0t}, z_{0t}), R_1 $(x'_{10}, y'_{10}, z'_{10})$, R_2 $(x'_{20}, y'_{20}, z'_{20})$ and R_3 $(x'_{30}, y'_{30}, z'_{30})$ can be calculated, if $R_1(x_{1t}, y_{1t}, z_{1t}), R_2(x_{2t}, y_{2t}, z_{2t})$ and $R_3(x_{3t}, y_{3t}, z_{3t})$ are known.

The methods to calculate (x_{0t}, y_{0t}, z_{0t}) and $R_1(x'_{10}, y'_{10}, z'_{10})$, $R_2(x'_{20}, y'_{20}, z'_{20})$ and $R_3(x'_{30}, y'_{30}, z'_{30})$ are discussed in the following section.

3.3.4.1 Coordinate of the origin *"o"*

There are three steps to calculate the coordinate of "*o*" (x_{0t}, y_{0t}, z_{0t}) in the BCS.

Step 1: The coordinate of "*o*" (x_{00}, y_{00}, z_{00}) is calculated during an initial standing condition.

During an initial standing condition, BR(x_R, y_{00}, z_R), BL(x_L, y_{00}, z_L), BI(x_I, y_{00}, z_I) and BO(x_O, y_{00}, z_O), $R_1(x_{10}, y_{10}, z_{10})$, $R_2(x_{20}, y_{20}, z_{20})$, and $R_3(x_{30}, y_{30}, z_{30})$ can be measured in the GCS.

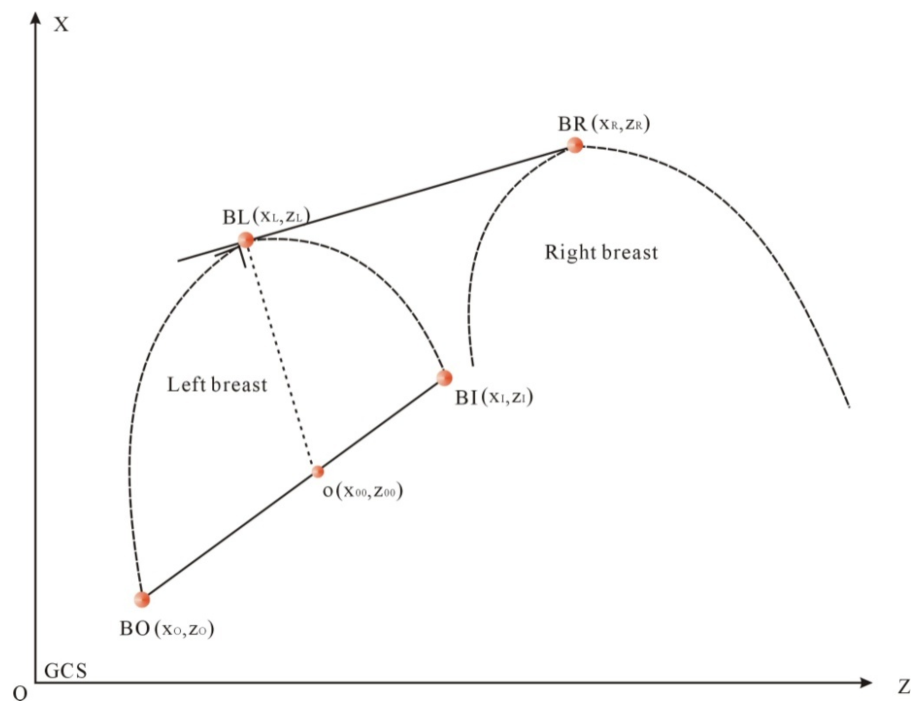

Figure 3.9 Transverse plane through two bust points in the GCS

Since point "*o*"(x_{00}, y_{00}, z_{00}) is the cross point of both the vertical line BR and BL through point BL and line BI and BO as shown in Figure 3.9, Equation (3.10) can be written as:

$$
\begin{cases}
\dfrac{z_O - z_{00}}{z_{00} - z_I} = \dfrac{x_O - x_{00}}{x_{00} - x_I} \\
\dfrac{z_L - z_R}{x_L - x_R} \times \dfrac{z_{00} - z_L}{x_{00} - x_L} = -1
\end{cases}
\tag{3.10}
$$

The value of y_{00} has been recorded during the initial standing condition, and x_{00} and z_{00} can be calculated from Equation (3.10) to attain the coordinate $o(x_{00}, y_{00}, z_{00})$.

Step 2: The coordinates of point *P*, at the foot of the perpendicular point from "*o*" to the plane of R_1 R_2 R_3 (Figure 3.10), are calculated in the GCS during the initial standing condition.

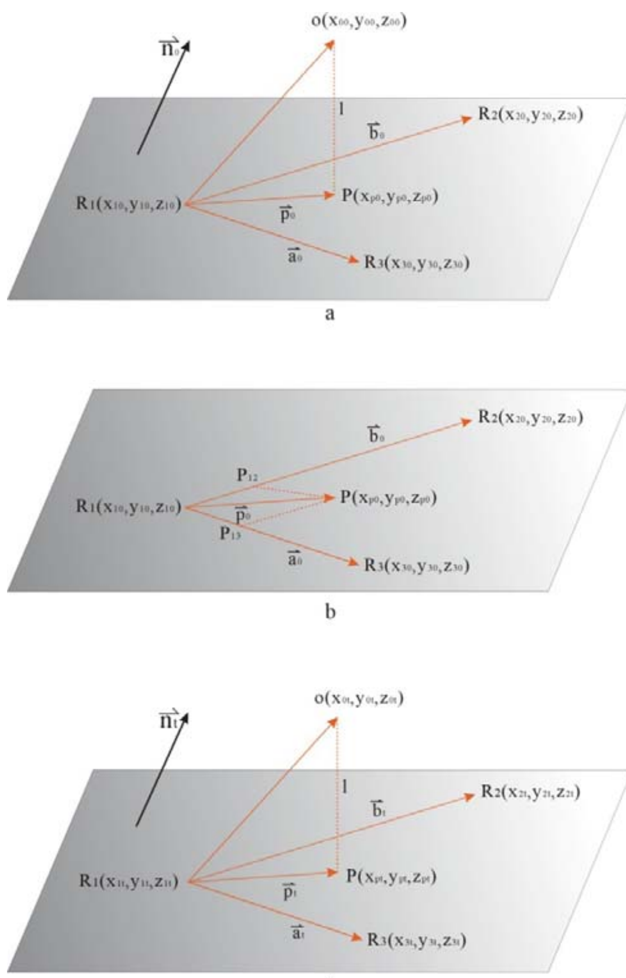

Figure 3.10 Relationship of the BCS origin and the three reference points

In Figure 3.10 (a), $\vec{a}_0$ and $\vec{b}_0$ stand for the vector of R_1R_2 and R_1R_3 in a standing condition. The unit vector $\vec{n}_0$ of the vertical plane of R_1 R_2 R_3 prompts the following equation:

$$\vec{n}_0 = \frac{\vec{b}_0 \times \vec{a}_0}{\left|\vec{b}_0 \times \vec{a}_0\right|} = \left(n_{10}, n_{20}, n_{30}\right)$$

Moreover, the plane equation of R_1 R_2 R_3 can be calculated during the standing condition too:

$$\begin{bmatrix} x - x_{10} & y - y_{10} & z - z_{10} \\ x_{20} - x_{10} & y_{20} - y_{10} & z_{02} - z_{10} \\ x_{30} - x_{10} & y_{30} - y_{10} & z_{03} - z_{10} \end{bmatrix} = 0 \tag{3.11}$$

The shorthand notation for Equation (3.11) may be written as:

$$A'x + B'y + C'z + D' = 0 \tag{3.12}$$

Thus, the length of *l* (*l* is the distance between points "*o*" and *P*) is:

$$l = \frac{\left|A'x_{00} + B'y_{00} + C'z_{00} + D'\right|}{\sqrt{A'^2 + B'^2 + C'^2}}$$

The coordinates for *P* are $\left(x_{p0}, y_{p0}, z_{p0}\right)$ and $\left(x_{pt}, y_{pt}, z_{pt}\right)$ in the GCS during the initial standing condition and at any time *t*, respectively.

By the unit vector $\vec{n}_0$ and the length of *l*, three equations may be written.

$$\frac{x_{p0} - x_{00}}{n_{10}} = \frac{y_{p0} - y_{00}}{n_{20}} = \frac{z_{p0} - z_{00}}{n_{30}} = l \tag{3.13}$$

According to the system of Equation (3.13), the coordinates of $P\left(x_{p0}, y_{p0}, z_{p0}\right)$ can be acquired,

$$\begin{cases} x_{p0} = x_{00} + n_{10}l \\ y_{p0} = y_{00} + n_{20}l \\ z_{p0} = z_{00} + n_{30}l \end{cases}$$

Step 3: The coordinates of "*o*" $\left(x_{0t}, y_{0t}, z_{0t}\right)$ is calculated in the GCS during time *t*.

As shown in Figure 3.10 (b), the line PP_{12} is parallel to the line R_3R_1, and the line PP_{13} is parallel to the line R_2R_1.

If $\lambda_1 = \dfrac{R_1P_{12}}{R_1R_2}, \lambda_2 = \dfrac{R_1P_{13}}{R_1R_3}$ and $\vec{p}_0$ represents the vector of the R_1P, Equation (3.14) can be written as:

$$\vec{p}_0 = \lambda_1\vec{a}_0 + \lambda_2\vec{b}_0 \tag{3.14}$$

From Equation (3.14), we get:

$$\begin{bmatrix} x_{p0} - x_{10} \\ y_{p0} - y_{10} \\ z_{p0} - z_{10} \end{bmatrix} = \lambda_1 \begin{bmatrix} x_{20} - x_{10} \\ y_{20} - y_{10} \\ z_{20} - z_{10} \end{bmatrix} + \lambda_2 \begin{bmatrix} x_{30} - x_{10} \\ y_{30} - y_{10} \\ z_{30} - z_{10} \end{bmatrix} \tag{3.15}$$

According to Equation (3.15), the system of Equation (3.16) can be written as:

$$\begin{cases} x_{p0} - x_{10} = \left(x_{20} - x_{10}\right)\lambda_1 + \left(x_{30} - x_{10}\right)\lambda_2 \\ y_{p0} - y_{10} = \left(y_{20} - y_{10}\right)\lambda_1 + \left(y_{30} - y_{10}\right)\lambda_2 \end{cases} \tag{3.16}$$

λ_1, λ_2 can be calculated by Equation (3.16).

Figure 3.10 (c) indicates time *t*, $\vec{a}_t$ and $\vec{b}_t$ that represent the vectors of R_1R_2 and R_1R_3, and $\vec{p}_t$ represents the vector of R_1P at time *t*.

The coordinate relationships of R_1, R_2, R_3 and "*o*" are constants as mentioned above, $\vec{p}_t$ represents the vector of R_1P at time *t*, and $\vec{p}_t$ can be written as Equation (3.17):

$$\vec{p}_t = \lambda_1 \vec{a}_t + \lambda_2 \vec{b}_t \tag{3.17}$$

By Equation (3.17), we have:

$$\begin{bmatrix} x_{pt} - x_{1t} \\ y_{pt} - y_{1t} \\ z_{pt} - z_{1t} \end{bmatrix} = \lambda_1 \begin{bmatrix} x_{2t} - x_{1t} \\ y_{2t} - y_{1t} \\ z_{2t} - z_{1t} \end{bmatrix} + \lambda_2 \begin{bmatrix} x_{3t} - x_{1t} \\ y_{3t} - y_{1t} \\ z_{3t} - z_{1t} \end{bmatrix} \tag{3.18}$$

Equation (3.18) can also be written as:

$$\begin{cases} x_{pt} - x_{1t} = \left(x_{2t} - x_{1t}\right)\lambda_1 + \left(x_{3t} - x_{1t}\right)\lambda_2 \\ y_{pt} - y_{1t} = \left(y_{2t} - y_{1t}\right)\lambda_1 + \left(y_{3t} - y_{1t}\right)\lambda_2 \\ z_{pt} - z_{1t} = \left(z_{2t} - z_{1t}\right)\lambda_1 + \left(z_{3t} - z_{1t}\right)\lambda_2 \end{cases} \tag{3.19}$$

The system of Equation (3.19) then leads to the coordinate of point $P\left(x_{pt}, y_{pt}, z_{pt}\right)$:

$$\begin{cases} x_{pt} = \left(x_{2t} - x_{1t}\right)\lambda_1 + \left(x_{3t} - x_{1t}\right)\lambda_2 + x_{1t} \\ y_{pt} = \left(y_{2t} - y_{1t}\right)\lambda_1 + \left(y_{3t} - y_{1t}\right)\lambda_2 + y_{1t} \\ z_{pt} = \left(z_{2t} - z_{1t}\right)\lambda_1 + \left(z_{3t} - z_{1t}\right)\lambda_2 + z_{1t} \end{cases}$$

In Figure 3.10 (c), at time *t*, the unit vector $\vec{n}_t$ of the vertical plane R_1 R_2 R_3 can be written as:

$$\vec{n}_t = \frac{\vec{b}_t \times \vec{a}_t}{\left|\vec{b}_t \times \vec{a}_t\right|} = \left(n_{1t}, n_{2t}, n_{3t}\right)$$

As the length from "*o*" to the plane of $R_1R_2R_3$ is a constant, the system of Equation (3.20) can be written as:

$$\frac{x_{pt} - x_{0t}}{n_{1t}} = \frac{y_{pt} - y_{0t}}{n_{2t}} = \frac{z_{pt} - z_{0t}}{n_{3t}} = l \tag{3.20}$$

Equation (3.20) calculates the coordinate of "*o*" $\left(x_{0t}, y_{0t}, z_{0t}\right)$ in the GCS:

$$\begin{cases} x_{0t} = x_{pt} - n_{1t} l \\ y_{0t} = y_{pt} - n_{2t} l \\ z_{0t} = z_{pt} - n_{3t} l \end{cases} \tag{3.21}$$

3.3.4.2 Coordinates of R_1, R_2 and R_3 in the Breast Coordinate System

If the angle between axes z and Z is α during the initial standing condition, the angle of the axis Z and the line of the BR and BL is α too. So, $\sin\alpha$ and $\cos\alpha$ can be obtained as follows.

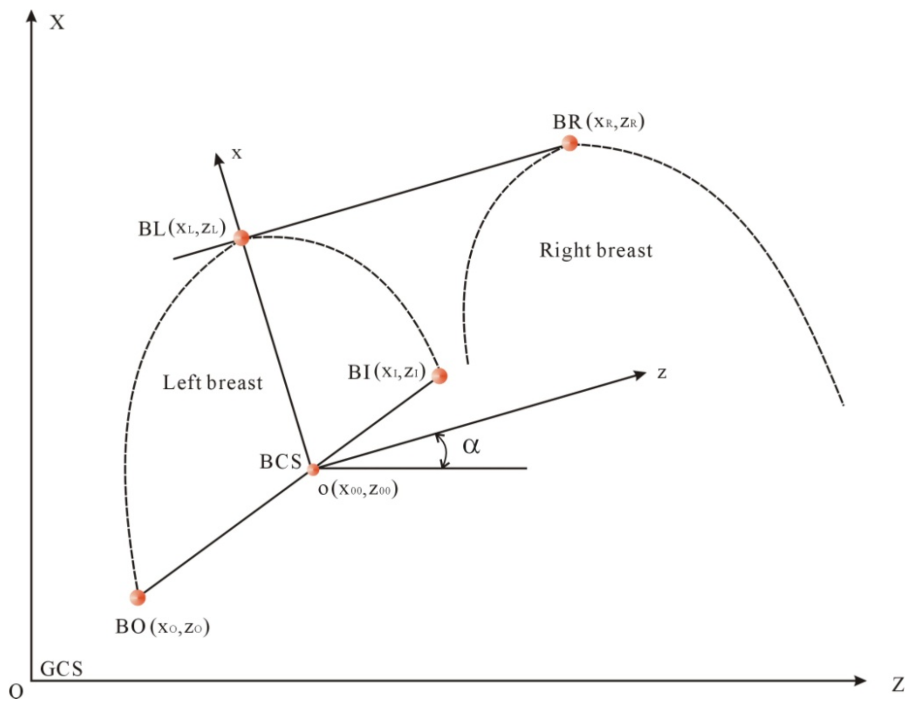

Figure 3.11 Transverse plane through two bust points in the GCS and BCS

$$\sin\alpha = \frac{z_L - z_R}{\sqrt{\left(x_L - x_R\right)^2 + \left(z_L - z_R\right)^2}}$$

$$\cos\alpha = \frac{x_L - x_R}{\sqrt{\left(x_L - x_R\right)^2 + \left(z_L - z_R\right)^2}}$$

By rotating and moving factors, Equation (3.22) becomes:

$$\begin{bmatrix} x \\ z \end{bmatrix} = \begin{bmatrix} \cos\alpha & -\sin\alpha \\ \sin\alpha & \cos\alpha \end{bmatrix} \begin{bmatrix} x' \\ z' \end{bmatrix} + \begin{bmatrix} x_{00} \\ y_{00} \end{bmatrix} \tag{3.22}$$

Equation (3.23) is developed as:

$$\begin{bmatrix} x' \\ z' \end{bmatrix} = \begin{bmatrix} \cos\alpha & \sin\alpha \\ -\sin\alpha & \cos\alpha \end{bmatrix} \begin{bmatrix} x - x_{00} \\ z - z_{00} \end{bmatrix} \tag{3.23}$$

As the plane of the four breast boundary markers parallels the ground during the initial standing condition, the y-axis parallels the Y-axis. Equation (3.23) can be expressed as:

$$\begin{bmatrix} x' \\ y' \\ z' \end{bmatrix} = \begin{bmatrix} \cos\alpha & \sin\alpha & 0 \\ 0 & 0 & 1 \\ -\sin\alpha & \cos\alpha & 0 \end{bmatrix} \begin{bmatrix} x - x_{00} \\ y - y_{00} \\ z - z_{00} \end{bmatrix} \tag{3.24}$$

By Equation (3.24), we can assemble:

$$\begin{bmatrix} x'_{10} \\ y'_{10} \\ z'_{10} \end{bmatrix} = \begin{bmatrix} \cos\alpha & \sin\alpha & 0 \\ 0 & 0 & 1 \\ -\sin\alpha & \cos\alpha & 0 \end{bmatrix} \begin{bmatrix} x_{10} - x_{00} \\ y_{10} - y_{00} \\ z_{10} - z_{00} \end{bmatrix} \tag{3.25}$$

$$\begin{bmatrix} x'_{20} \\ y'_{20} \\ z'_{20} \end{bmatrix} = \begin{bmatrix} \cos\alpha & \sin\alpha & 0 \\ 0 & 0 & 1 \\ -\sin\alpha & \cos\alpha & 0 \end{bmatrix} \begin{bmatrix} x_{20} - x_{00} \\ y_{20} - y_{00} \\ z_{20} - z_{00} \end{bmatrix} \tag{3.26}$$

$$\begin{bmatrix} x'_{30} \\ y'_{30} \\ z'_{30} \end{bmatrix} = \begin{bmatrix} \cos\alpha & \sin\alpha & 0 \\ 0 & 0 & 1 \\ -\sin\alpha & \cos\alpha & 0 \end{bmatrix} \begin{bmatrix} x_{30} - x_{00} \\ y_{30} - y_{00} \\ z_{30} - z_{00} \end{bmatrix} \tag{3.27}$$

The coordinates of $R_1\left(x'_{10}, y'_{10}, z'_{10}\right)$, $R_2\left(x'_{20}, y'_{20}, z'_{20}\right)$ and $R_3\left(x'_{30}, y'_{30}, z'_{30}\right)$ in the BCS are formulated by Equations (3.25), (3.26) and (3.27), as follows:

$$\begin{bmatrix} x'_{10} & x'_{20} & x'_{30} \\ y'_{10} & y'_{20} & y'_{30} \\ z'_{10} & z'_{20} & z'_{30} \end{bmatrix} = \begin{bmatrix} \cos\alpha & \sin\alpha & 0 \\ 0 & 0 & 1 \\ -\sin\alpha & \cos\alpha & 0 \end{bmatrix} \begin{bmatrix} x_{10} - x_{00} & x_{20} - x_{00} & x_{30} - x_{00} \\ y_{10} - y_{00} & y_{20} - y_{00} & y_{30} - y_{00} \\ z_{10} - z_{00} & z_{20} - z_{00} & z_{30} - z_{00} \end{bmatrix} \tag{3.28}$$

The coordinate of point M, which is determined from combining Equations (3.9), (3.21) and (3.28), is transformed from the GCS to the BCS.

3.4 Validation of the breast coordinate system

It was necessary to validate the transformation of the coordinates from the GCS to the BCS and the reliability of the breast coordinate system. The validation of the data transformation method was conducted as follows.

If the process of the transforming coordinates (Section 3.3.4) from the GCS to the BCS is correct, and for the BCS to be considered to be reliable for different breast shapes, then the distance between any two points in the GCS should be equal to that in the BCS under the same condition.

3.4.1 Subjects

To verify this and validate the derived coordinate transformation procedure, 11 subjects aged from 24 to 40 (24.5 ± 6 years) with different breast shapes from 75B to 85D were invited to participate in a standing and jogging motion experiment. Prior ethical approval was obtained from the Human Subjects Ethics Sub-Committee of the University (Approval number: PolyU 532306). The subjects were fully informed of all the procedures and protocols before signing their written consents.

3.4.2 Bra sample

The subjects participated in a series of jogging experiments with no bra and a well-fitted sports bra Shock Absorber™ (DBApparel, UK). It was a full-cup cut-and-sewn encapsulation bra with a single layer one-way elastic fabric in the cup and a supportive sling at the side of each cup with no wire, with high underarm, high gore, and high neckline (near the top of tear-drop shape). Both the bottom band and shoulder straps of the bra were wider than those of normal bras. The details for the size 75B are shown in Figure 3.12.

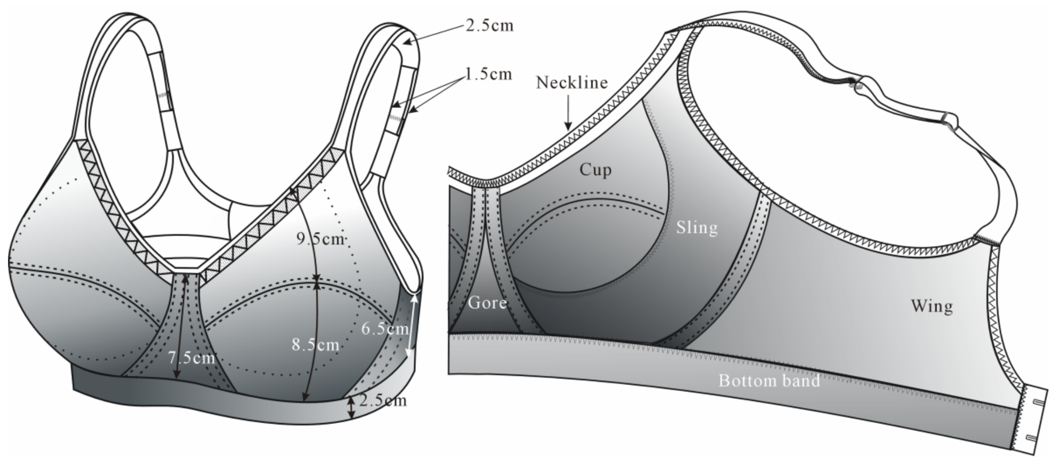

Figure 3.12 Design details of the sports bra sample with size 75B

3.4.3 Motion experiments

The jogging motion experiments at 7 km/h on a treadmill were carried out in a Human Locomotion Laboratory in the University under a controlled condition of room temperature of 23 ± 0.5°C and relative humidity of 65 ± 3 %. A Vicon motion analysis system (Vicon, 612, Oxford Metrics, Oxford, UK) with six infra-red cameras, which were mounted on the ceiling of a 102 m^2 room with a 2.8 m height, was used to record the coordinates of spherical retro-reflective markers (9.5 mm in diameter and 1.81 g in mass) at a 120 Hz sampling frequency in a GCS. The markers were attached to the subject's breast region at the points defined in Section 3.2.3. Prior to data acquisition, standing and dynamic calibrations of the system were performed. The detailed calibration method is described in Chapter 4. The residuals were kept to 1 mm or less [86].

3.4.4 Data processing

The recorded 3D coordinates of the six experimental markers, that were pasted on the left breast or left bra cup over the breast of the 11 subjects standing and jogging, were transformed from the GCS to the BCS using the process mentioned in Section 3.3.4. The distance between any two points from P1 to P6 was calculated in both the GCS and the BCS, in different support and activity conditions. The formulas used for calculating the distances between two points in the GCS and BCS were as follows:

$$G_{P_mP_n} = \sqrt{(x_{Gm} - x_{Gn})^2 + (y_{Gm} - y_{Gn})^2 + (z_{Gm} - z_{Gn})^2} \tag{3.29}$$

$$B_{P_mP_n} = \sqrt{(x_{Bm} - x_{Bn})^2 + (y_{Bm} - y_{Bn})^2 + (z_{Bm} - z_{Bn})^2} \tag{3.30}$$

where $G_{p_mp_n}$ *and* $B_{p_mp_n}$ represent the distances between any two points "*m*" to "*n*" in the GCS and the BCS respectively; $(x_{Gm}, y_{Gm}, z_{Gm}), (x_{Gn}, y_{Gn}, z_{Gn})$ and (x_{Bm}, y_{Bm}, z_{Bm}), (x_{Bn}, y_{Bn}, z_{Bn}) are the coordinates of the points "*m*" and "*n*" in the GCS and the BCS respectively, where "*m*" or "*n*" = 1, 2,…6 but not equal.

3.4.5 Results of validation

Table 3.3 shows the coordinates of six markers when the two subjects were standing and jogging in braless and sports bra conditions at a specific time in the GCS. After transformation, the coordinates in the BCS (Table 3.2) became much smaller than those in the GCS because the new coordinates are relative to the breast origin "*o*".

Table 3.3 Coordinates of six markers at a sampling instant in the GCS in different conditions (unit: cm)

Points		Standing				Jogging			
		Subject 1		Subject 2		Subject 1		Subject 2	
		braless	bra	braless	bra	braless	bra	braless	bra
P1	x_{G1}	84.9	83.1	87.1	-32.4	93.1	-93.8	94.0	-79.0
	y_{G1}	103.4	103.7	110.9	113.9	115.3	114.3	122.0	123.3
	z_{G1}	-83.8	-42.9	-84.5	55.1	-42.2	51.0	-41.7	47.0
P2	x_{G2}	84.4	81.8	86.3	-28.9	91.9	-92.7	92.1	-75.6
	y_{G2}	98.7	99.2	106.3	109.9	110.6	109.4	117.3	120.0
	z_{G2}	-88.7	-46.3	-88.0	53.5	-46.9	47.0	-44.7	43.9
P3	x_{G3}	80.7	79.1	82.0	-24.0	88.0	-90.2	89.4	-71.2
	y_{G3}	102.4	102.7	111.5	113.9	113.1	113.2	121.9	124.8
	z_{G3}	-92.5	-50.0	-92.0	52.2	-51.1	43.5	-50.2	43.3
P4	x_{G4}	84.3	82.4	86.7	-28.0	92.0	-93.1	93.6	-74.7
	y_{G4}	104.0	103.6	112.9	114.8	115.9	113.9	123.5	124.2
	z_{G4}	-88.2	-47.5	-89.4	55.8	-46.9	46.4	-46.8	47.2
P5	x_{G5}	82.6	80.1	84.0	-28.1	90.3	-90.8	91.3	-75.2
	y_{G5}	106.6	107.1	116.8	118.2	117.8	117.5	127.4	128.2
	z_{G5}	-88.1	-47.0	-88.3	53.2	-46.8	46.9	-45.7	45.7
P6	x_{G6}	80.7	78.0	82.2	-27.3	88.7	-88.4	89.9	-74.8
	y_{G6}	109.2	110.1	120.8	121.2	119.9	120.4	131.8	131.8
	z_{G6}	-87.7	-46.9	-88.1	51.1	-46.5	47.0	-45.6	44.2

where $(x_{G1}, y_{G1}, z_{G1}), (x_{G2}, y_{G2}, z_{G2})$, ……, (x_{G6}, y_{G6}, z_{G6}) are the coordinates of P1 to P6 in the GCS, respectively.

Table 3.4 Transformed coordinates of six markers from the GCS to BCS (unit: cm)

Points		Standing				Jogging			
		Subject 1		Subject 2		Subject 1		Subject 2	
		braless	bra	braless	bra	braless	bra	braless	bra
P1	x_{B1}	4.4	4.6	6.6	5.6	4.6	5.3	5.5	5.5
	y_{B1}	1.6	1.3	-6.6	-0.9	2.8	1.9	-6.5	-1.3
	z_{B1}	4.7	3.7	4.0	4.5	4.2	4.4	4.7	4.6
P2	x_{B2}	3.9	3.3	5.8	3.4	3.4	4.2	3.6	3.2
	y_{B2}	-3.0	-3.1	-11.3	-5.1	-2.0	-3.0	-11.2	-5.3
	z_{B2}	-0.2	0.3	0.5	1.4	-0.5	0.4	1.7	1.4
P3	x_{B3}	0.2	0.6	1.5	1.5	-0.5	1.7	0.9	1.7
	y_{B3}	0.7	0.3	-6.0	-1.3	0.6	0.8	-6.6	-1.0
	z_{B3}	-4.0	-3.4	-3.5	-3.4	-4.7	-3.1	-3.7	-3.2
P4	x_{B4}	3.8	3.9	6.2	5.6	3.5	4.6	5.1	5.6
	y_{B4}	2.3	1.2	-4.7	-0.2	3.3	1.6	-5.1	-0.6
	z_{B4}	0.3	-0.8	-0.9	0.0	-0.4	-0.2	-0.3	0.3
P5	x_{B5}	2.1	1.6	3.5	3.0	1.8	2.3	2.8	3.3
	y_{B5}	4.9	4.7	-0.8	3.1	5.3	5.1	-1.1	3.1
	z_{B5}	0.4	-0.4	0.2	0.2	-0.3	0.3	0.7	0.5
P6	x_{B6}	0.2	-0.5	1.7	0.8	0.2	-0.1	1.4	1.0
	y_{B6}	7.5	7.7	3.2	6.0	7.4	8.1	3.3	6.2
	z_{B6}	0.8	-0.3	0.4	-0.4	0.0	0.3	0.8	-0.1

where $(x_{B1}, y_{B1}, z_{B1}), \left(x_{B2}, y_{B2}, z_{B2}\right)$, …… , (x_{B6}, y_{B6}, z_{B6}) are the coordinates of P1 to P6 in the BCS, respectively.

Based on the coordinates in Tables 3.3 and 3.4 and the Equations (3.29) and (3.30) in the

GCS and BCS, the distances of any two markers were calculated, as shown in Table 3.5.

Table 3.5 Distance between any two markers in the GCS and BCS (unit: cm)

GCS Distance between	Standing				Jogging			
	Subject 1		Subject 2		Subject 1		Subject 2	
	braless	bra	braless	bra	braless	bra	braless	bra
P1-P2	6.8	5.7	5.9	5.6	6.8	6.4	5.9	5.7
P1-P3	9.7	8.2	9.1	8.9	10.5	8.4	9.6	8.7
P1-P4	4.5	4.6	5.3	4.5	4.8	4.7	5.3	4.4
P1-P5	5.9	6.1	7.6	6.4	5.9	6	7.2	6.3
P1-P6	8.2	9.1	11.6	9.7	7.7	9.2	11.3	9.9
P2-P3	6.5	5.7	7.9	6.4	6.3	5.8	7.6	6.5
P2-P4	5.3	4.6	6.7	5.5	5.3	4.6	6.6	5.5
P2-P5	8.1	8	10.8	8.3	7.5	8.3	10.2	8.4
P2-P6	11.2	11.6	15.1	11.6	10	11.9	14.7	11.8
P3-P4	5.9	4.2	5.6	5.5	6.5	4.2	5.6	5.3
P3-P5	6.4	5.4	6.7	5.9	6.8	5.5	7.3	5.8
P3-P6	8.3	8.1	10	8	8.3	8.2	10.9	7.9
P4-P5	3.1	4.1	4.9	4.2	2.7	4.2	4.7	4.3
P4-P6	6.3	7.9	9.2	7.9	5.3	8	9.3	8.2
P5-P6	3.2	3.8	4.4	3.7	2.7	3.8	4.6	3.9

BCS Distance between	Standing				Jogging			
	Subject 1		Subject 2		Subject 1		Subject 2	
	braless	bra	braless	bra	braless	bra	braless	bra
P1-P2	6.8	5.7	5.9	5.6	6.8	6.4	5.9	5.7
P1-P3	9.7	8.2	9.1	8.9	10.5	8.4	9.6	8.7
P1-P4	4.5	4.6	5.3	4.5	4.8	4.7	5.3	4.4
P1-P5	5.9	6.1	7.6	6.4	5.9	6	7.2	6.3
P1-P6	8.2	9.1	11.6	9.7	7.7	9.2	11.3	9.9
P2-P3	6.5	5.7	7.9	6.4	6.3	5.8	7.6	6.5
P2-P4	5.3	4.6	6.7	5.5	5.3	4.6	6.6	5.5
P2-P5	8.1	8	10.8	8.3	7.5	8.3	10.2	8.4
P2-P6	11.2	11.6	15.1	11.6	10	11.9	14.7	11.8
P3-P4	5.9	4.2	5.6	5.5	6.5	4.2	5.6	5.3
P3-P5	6.4	5.4	6.7	5.9	6.8	5.5	7.3	5.8
P3-P6	8.3	8.1	10	8	8.3	8.2	10.9	7.9
P4-P5	3.1	4.1	4.9	4.2	2.7	4.2	4.7	4.3
P4-P6	6.3	7.9	9.2	7.9	5.3	8	9.3	8.2
P5-P6	3.2	3.8	4.4	3.7	2.7	3.8	4.6	3.9

Table 3.5 shows that the distances between any two markers in the GCS and BCS were the same, regardless of the marker positions, bra condition and activities. These findings have revealed that the process of transforming coordinates from the GCS to BCS is valid for different breast sizes, bra conditions and activities.

3.4.6 Results of reliability test

The test for consistency and reproducibility of the breast coordinate system was conducted by examining 11 subjects standing in three different positions, in both braless and sports bra conditions, in the GCS in a static state. Table 3.6 shows the coordinates in the BCS of the same marker on the bra in the static state at different standing positions.

The coordinates of the same marker on the bra in the BCS in the same condition had impressive consistency/reproducibility (Interclass correlation coefficient ICC = 1.00) for both the braless and sports bra conditions, based on the results obtained from the Statistical Package for the Social Sciences (Version 15.0; SPSS Inc., Chicago, IL). This shows that the BCS has very high consistency, reproducibility and reliability, as a basis for breast motion studies.

Table 3.6 The coordinates in the BCS of the same marker on the bra in the static state at different standing positions in the GCS (unit: cm)

Subject	Coordinates in the BCS	Position 1	Position 2	Position 3
Subject 1	x	5.51	5.52	5.54
	y	-0.13	-0.13	-0.14
	z	-0.05	-0.04	-0.04
Subject 2	x	5.85	5.82	5.78
	y	-0.04	-0.05	-0.07
	z	-0.04	-0.03	-0.02
Subject 3	x	5.16	5.14	5.13
	y	0.84	0.84	0.84
	z	-2.27	-2.27	-2.28
Subject 5	x	5.70	5.71	5.72
	y	0.20	0.20	0.20
	z	0.51	0.51	0.51
Subject 6	x	5.60	5.60	5.59
	y	-0.06	-0.06	-0.07
	z	0.33	0.32	0.32
Subject 8	x	3.86	3.86	3.86
	y	1.23	1.23	1.23
	z	-0.85	-0.83	-0.82
Subject 9	x	6.55	6.56	6.57
	y	3.30	3.31	3.31
	z	-1.10	-1.10	-1.10
Subject 10	x	7.11	7.11	7.10
	y	1.23	1.24	1.24
	z	-1.12	-1.12	-1.13
Subject 11	x	6.55	6.60	6.65
	y	-0.88	-0.83	-0.78
	z	2.24	2.20	2.15
Subject 12	x	5.71	5.72	5.74
	y	2.34	2.36	2.38
	z	0.06	0.04	0.03
subject 13	x	6.04	6.05	6.06
	y	2.62	2.63	2.64
	z	0.28	0.31	0.34

3.5 Conclusions

In this chapter, a new procedure to develop a new BCS was presented. A method of transforming the 3D coordinates from the GCS to BCS was developed. The reliability of the process for defining the breast boundary points to form the axes of the BCS as an initial reference was verified for two different breast shapes in three repeats of experiments. The transformation of 3D coordinates from the GCS to BCS was verified by static and jogging experiments for the same five subjects and by comparing the distances between any two markers in the GCS and BCS under different wearing and activity conditions. The BCS was proven to have a very high reliability (ICC =1.00) for 11 subjects standing at three different positions, in both braless and sports bra conditions, in a static state.

Chapter 4 Evaluation of breast movement

4.1 Introduction

Studies of breast motion started in the 1970's. A systematic review of literature has been reported in Chapter 2. Previous research has shown that sports bras could control breast movement during activities [3-4,6,11,43] and manage acute sports-induced pain and discomfort [7]. However, there were significant differences in breast movement between different bra designs and breast sizes [12,87] and different shoulder straps with different properties may affect the breast/bra movement. As a consequence this posed the following research questions:

Q.3: which features of sports bras are effective and which are not, in terms of their effectiveness in controlling the 3D breast movement, at different breast points and different activities?

and

Q.4: how do breast volume and the properties of shoulder straps affect the breast movement?

The answers to these questions will fill in the following knowledge gaps and limitations of previous studies.

- Most studies only focused on the vertical movement of the breast [3-4,13-14,50,53,62];
- researchers tended to use the movement of the nipple only to represent that of the whole breast [4,13-14,49-50,53,62,88]. The movement of other breast quadrants that were supposed to be controlled by a bra have been neglected;

- there was a lack of valid and reliable coordinate system to describe the breast movement. The previous findings of breast movement mostly contained unknown thoracic rotation, translation, bending and tilting [89], so the true breast movement relative to the thorax remained unclear;
- previous work focused on running, jogging and walking experiments; other types of exercises such as stepping up and down, which was believed to be more challenging to the bra support, has not been studied;
- the relationships between breast volume and breast movement were unknown; and
- no studies have been published to investigate the effects of shoulder strap properties on the effectiveness of sports bras in controlling breast movement.

In this study, two experiments were performed to answer research questions Q3 and Q4. In Experiment 1, the 3D breast movement relative to the thorax, using the validated Breast Coordinate System (BCS), was measured in *vivo* for six marker positions on four woman subjects wearing seven different sports bras or no bra, during three different activities (walking, jogging, and stepping up and down). Based on the results, the most important design features of each bra sample were determined for the future development of ideally effective sports bras.

In Experiment 1, the breast movement trajectories (BMTs) in the newly developed BCS were presented to compare the ranges and patterns of breast movement at different breast points, in different directions, under different bra-supported conditions, during different activities. The significances of differences among different conditions were examined by paired *t*-test. From this experiment, the mean and variance of the results were used to calculate the power and required sample size for Experiment 2 with a larger sample size to investigate the significant factors such as breast volume and shoulder straps.

4. 2 Methods for Experiment 1

4.2.1 Bra samples

Seven types of sports bras comprising two compression bras and five encapsulation bras were tested in this study. The bra samples were manufactured by a brand Shock Absorber™ (DBApparel, UK). The subjects' breast sizes were measured by a trained bra fitter, and the most appropriate bra size was provided for her to try on, according to the standard procedure mentioned in Chapter 3. The bra fit was assessed and confirmed by the same bra fitter, according to a bra fitting checklist (Table 3.1) [85] for 10 bra areas (Figure 3.4).

This study focused on the evaluation of the different bras' functional performances in terms of reducing breast displacement. The aesthetic, tactile, thermal, moisture and convenience comfort were well confirmed by the subjects. The bras were professionally produced and well accepted by customers in the market, and the motion experiment was carried out in an air-conditioned laboratory. It was assumed that the thermophysiological and skin sensorial comfort were kept consistent. Bra comfort is important and has been well researched so there was no need to duplicate the previous work. The sports bras with various fibre contents and design features were selected for the 3D breast motion analysis. The criteria for selecting the bra samples are shown in Table 4.1.

Table 4.1 Inclusion criteria of the selected sports bras

Bra item	Included features
Types	1. Compression bras & encapsulation bras
Cup	2. Single layer & double layer 3. Full cup & short vest 4. Horizontal & bias seam & moulded cups 5. Different materials
Shoulder strap	6. Different width 7. Different elongation 8. Adjustable length & fixed length
Back designs	9. Cross-over, Racer-back & U-back
Inner lining	10. With & without inner lining
Gore	11. With & without gore
Wire	12. With & without wire

The detailed characteristics of the bra samples are shown in Table 4.2.

Table 4.2 Descriptions of sports bra samples

Bra style		1	2	3	4	5	6	7
Product sketches	Front							
	Back				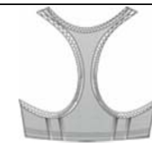		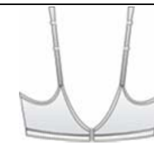	
Design features	cup layers	2	2	1	1	2	1	1
	front cup	full cup	short vest	short vest	full cup	short vest	full cup	full cup
	cup seam elongation %	30	40	5	mould	30	8	mould
	inner lining	mould	mould	no	no	mould	no	no
	sling	yes	no	yes	yes	no	yes	yes
	neckline elongation %	35	34	14	14	5	20	30
	gore	yes	no	no	no	no	yes	yes
	wire	no	no	no	yes	no	no	yes
	cradle	yes	no	no	yes	no	yes	yes
	back design	Racer-back	Racer-back	Racer-back	Racer-back	Racer-back	U-back	Cross-over
	closure	side	back	side	front	side	back	side
	shoulder strap elongation %	35	50	28	35	30	10	10
Fiber contents	Polyamide %	42	55		18	67	5	56
	Polyester %	53	16	91	72	28	85	27
	Elastane %	5		9	10	10	10	15
	Cotton %		29			5		2

The core bra size 75B was expected to fit a wearer of 75 ± 2.5 cm underbust and 87.5 ± 2.5 cm full bust girth, with 12.5 ± 1.25 cm difference between these two measurements. The bra samples in the core size were carefully measured by the same professionally-trained researcher using a calibrated tape measure. The definitions of measurements relative to bra support are shown in Figure 4.1, and the bra measurements are shown in Table 4.3.

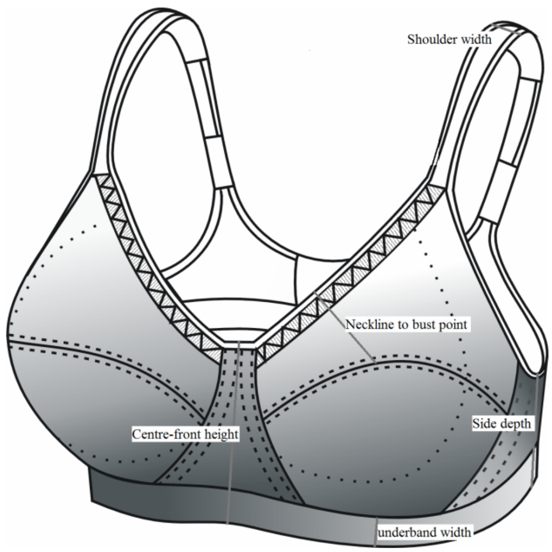

Figure 4.1 Definitions of bra measurements

Table 4.3 Measurements of seven bra samples for core size 75B (unit: cm)

Bra style	Neckline to Bust point	Shoulder width	Underband width	Side depth	Centre front height
1	6	3	2.5	9	6
2	6.5	3	2.5	8.5	11.5
3	8.5	2.5	2.5	9.5	17
4	6	2.5	2.5	7.5	0
5	5.5	2.8	2.5	8.5	7
6	7.5	2	2.5	10	7.5
7	7	1.2	2.5	10	5.5

Various sizes from 75B to 80C were provided for the subjects to ensure the best fit on their breasts, before motion experiments, according to Yu's bra fitting guidelines [90].

First, correct tension was ensured along the underband wrapping around on the ribcage, and comfortable pressure was exerted by the shoulder strap on the shoulder. Once the bra underband formed a firm frame on the body, the breasts were filled nicely in the cup to ensure there was no gap or bulging problem.

4.2.2 Subjects

For the pilot experiment to test the effectiveness of different sports bras using the newly validated BCS for breast motion analysis, four unpaid volunteered Chinese women aged 32 ± 8.12 years with 161.25 ± 0.96 cm height, 56.50 ± 5.45 kg mass, and 21.7 ± 2.2 kg/m^2 body mass index were recruited, with informed consent. They had the most prevalent breast sizes 75B, 75C, 80B and 80C in China, according to a breast sizing survey of 456 Chinese women conducted by Zheng [91]. The measurements and shapes of their breasts are given in the following table.

Table 4.4 Breast sizes and shapes of the subjects

Subject no.	Breast size	Bust girth (cm)	Underbust girth (cm)	Breast shape
1	75B	86	74	hemisphere
2	80B	93.5	80.5	tear
3	75C	91.5	76	conical
4	80C	94	79	tear

Convenience sampling was used because Hong Kong women were usually not willing to participate in research that requires them to take off their clothes. The inclusion criteria were that the participants must be healthy, premenopausal women of the most popular four Chinese breast sizes 75B, 80B, 75C and 80C in the Metric Bra Sizing system [91]. To avoid the influence of abnormal hormonal conditions on the connective breast tissues [17], subjects were excluded if they were currently breast feeding or pregnant. Those with a history of previous breast surgery or any musculoskeletal disorder or pain were also excluded because that would inhibit their activities [17].

4.2.3 Vicon motion analysis system

The breast movement of each subject was captured using a six-camera Vicon motion analysis system (Vicon, 612, Oxford Metrics, Oxford, UK). Each camera was positioned 6 m apart from each other, on a 2.8 m high ceiling. With a 120 Hz sampling frequency, the Vicon motion analysis system recorded the static and dynamic 3D coordinates of predetermined spherical retro-reflective positions (9.5 mm in diameter, 1.81 g in mass), which were well attached to the skin or a well-fitted bra by using double-sided adhesive tape.

In this study, passive markers were selected because wireless markers were preferred to avoid breast deformation under the bra. Accurate bra fit was ensured before the motion experiments. In case there was relative breast movement within the bra during activities, the term “bra displacement” was used in this thesis to represent the breast movement with bra.

Prior to data acquisition, a static calibration was performed by using an L-Frame (Figure 4.2a), which was made from two metal rods fixed at 90° with one arm that had three reflective spheres attached and the other arm with one reflective sphere, according to the Vicon operation manual [92]. This calibration defined the centre of the capture volume, and determines the orientation of the 3D workspace. The residuals were kept at less than 1 mm, which was regarded as acceptable [86].

In the dynamic calibration, a 500 mm calibration wand (Figure 4.2 b) was used. This was a metal rod with two 50 mm reflective spheres that were attached 500 mm apart. It was moved throughout the whole volume, which allowed the Vicon system to calculate the relative positions and orientations of the spheres from the cameras. The calibration procedure is listed in Table 4.5.

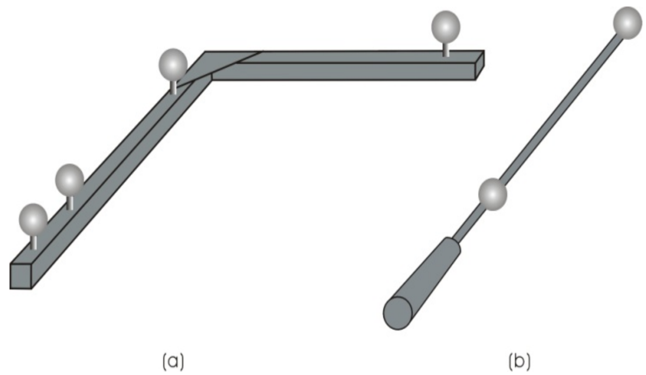

Figure 4.2 a) L-Frame for static calibration and b) wand for dynamic calibration

Table 4.5 Calibration procedure [92]

Step	Procedure
1	Place the L-Frame on the floor in the centre of the capture volume
2	Select system/live monitors
3	Check that each camera is viewing only the four markers on the L-Frame
4	Remove the L-Frame from the capture volume and ensure that it is not visible to any of the cameras
5	Have an assistant stand in the capture volume with the wand
6	Click on “Start” to start collecting data
7	Wave the wand and cover all positions in the capture volume and all orientations
8	Collect sufficient data and click on “Stop”
9	If the calibration residuals are less than 1, click on “Accept”

4.2.4 Experimental protocol

Most of the previous breast motion studies [3,6,14-17,49-50] focused on the movement of the nipple or the so called “centre of the breast”. For consistency and easy comparison with previous studies, the nipple was included in this work. In this study, six points were chosen to describe breast movement because breast movement followed a very complex pattern and the movement of only one single breast point may not represent the entire breast motion.

When the breast is divided into four quadrants, it can be seen that each quadrant varies in shape and volume, depending on the spatial distribution of fat tissues, and skin thickness [93]. Their movement may be also different. For example, the upper part of the breast is thinner than that in the adjacent chest wall and axilla region [94]. An investigation suggested that the skin in the lower breast region is the thickest (1.94 ± 0.36 mm), and the upper region is the thinnest (1.32 ± 0.27 mm), whereas the outer region is 1.62 ± 0.26 mm and the inner region is 1.41 ± 0.24 mm [95]. The upper breast has a larger parenchyma ratio over fat tissue. It possesses the Cooper's suspensory ligaments, which help to support the breast weight and prevent sagging [96]. Therefore, it is anticipated that movement at different breast points may be different. In this study, only the left breast was studied because a previous study had shown that there was no significant difference in the vertical displacement between the left and right breasts [17].

The experimental process involved the following three steps.

Step 1: Pasting reference and breast boundary points

The subject was asked to wear a well-fit everyday bra and stand straight. The method of confirming BL, BR, BI and BO was shown in Section 3.2.3.1.

Four spherical retro-reflective markers with a diameter of 9.5 mm and a mass of 1.81 g were attached to the skin at the four reference points (IJ, PX, C7, and T8 defined in Section 3.2.2) and four breast boundary points (BL, BR, BI and BO defined in Section 3.2.3) or the well-fitted everyday bra as shown in Figure 4.3. The 3D coordinates of the eight markers were recorded in the standing condition by the Vicon motion analysis system in the GCS.

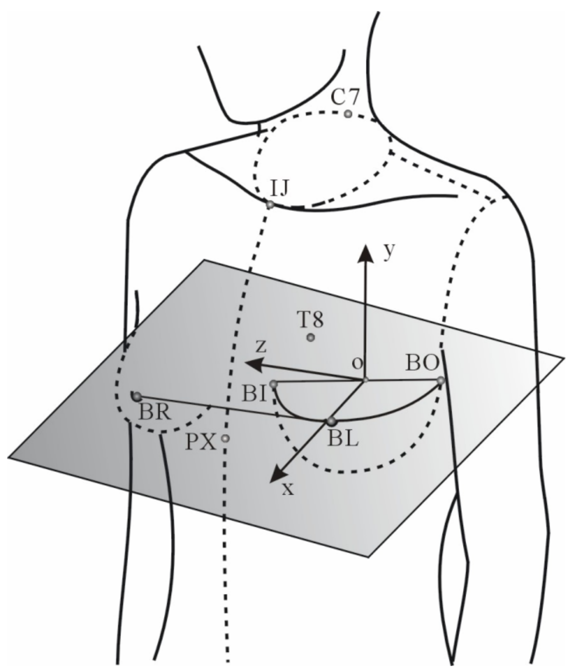

Figure 4.3 Points of reference and breast boundary markers in the BCS

Step 2: Attaching markers on the breast or bra

The four breast boundary markers and the everyday bra were then removed. Six experimental markers were attached onto the left breast (or over a well-fitted sports bra in a standing condition). The first marker M4 was placed on a nipple. The markers M1, M2, M3, M5 and M6 were 4 cm apart from M4 along the horizontal and vertical directions (Figure

4.4). The 3D coordinates of these four reference markers and six experimental markers were recorded under the static condition in the GCS. The movement of the markers on the bra was presented as “bra movement”.

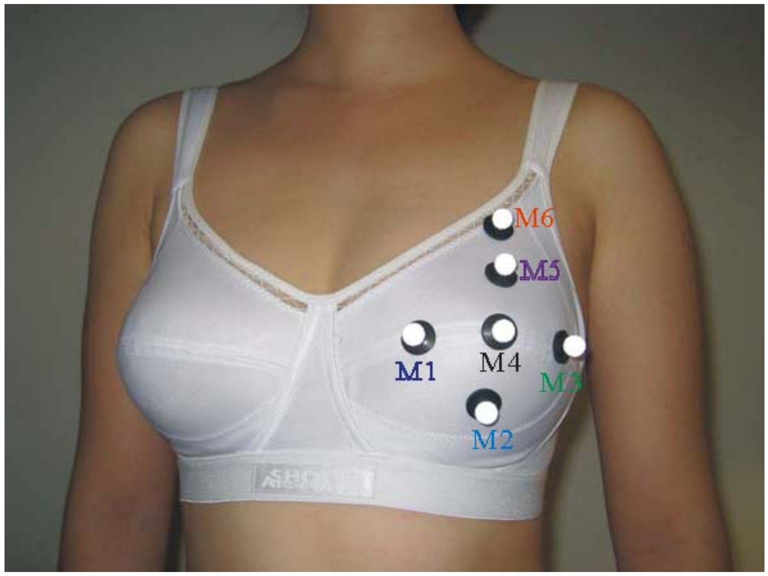

Figure 4.4 Markers on the bra or on the breast skin

Step 3: Performing three activities

Each subject performed three different activities in a random order, including walking at 3 km/h and jogging at 7 km/h on a treadmill, and stepping up and down on a platform that was 24 cm high. These speed settings were slower than that in Scurr et al. [61] who defined 5 to 6 km/h as walking speed, 7 to 8 km/h as jogging, and 8 to 15 km/h as running. This difference is probably due to the shorter stature of Chinese than Caucasian women, so they walk with a shorter stride length and, in turn, slower speed. As the stride rate was known to influence breast motion [97], each subject was required to keep the pre-determined velocity during each activity, for at least 100 seconds to achieve a steady condition.

The dynamic coordinates of the markers during the activities were captured by the Vicon motion analysis system (as explained in Section 4.2.3) in the GCS. Steps 2 and 3 were repeated under different supported conditions in a randomized order, to avoid any order effects. The subjects had a 5-minute break in between the two experimental conditions, to allow them to relax and to prevent fatigue.

4.2.5 Data pre-processing

To remove the background noise signals during motion capturing [66], the motion data of the six markers in the GCS was first smoothed out by using a low pass filter with a cut off frequency of 8 Hz after performing the analysis of breast movement frequencies in three directions and in three activities. To avoid the effects of thoracic movement, the recorded 3D coordinates were transformed from the GCS to the BCS for a new presentation of breast movement relative to the thorax. The transforming method has already been explained in Section 3.3 of Chapter 3.

4.2.6 Data processing

4.2.6.1 Breast movement trajectory

MATLAB version 7 (The MathWorks, Inc.) was used to plot the breast movement trajectories (BMTs). The matrices of the coordinates of the breast markers were imported into the MATLAB version 7 software system. Then, the custom programs were run to plot the BMTs.

4.2.6.2 Amplitude of breast displacement

The breast displacement was defined as the change of the coordinates in the BCS from a static condition to a dynamic condition under the same supported condition. Figure 4.5 shows an example of the vertical breast displacement against time when a subject with breast size 75B was jogging in a sports bra. The example was given to illustrate how to determine the positive and negative peaks in the vertical directions in the BCS. The peak-to-peak amplitude (henceforth, simply called the amplitude) was computed by subtracting the negative peak value from the positive peak value.

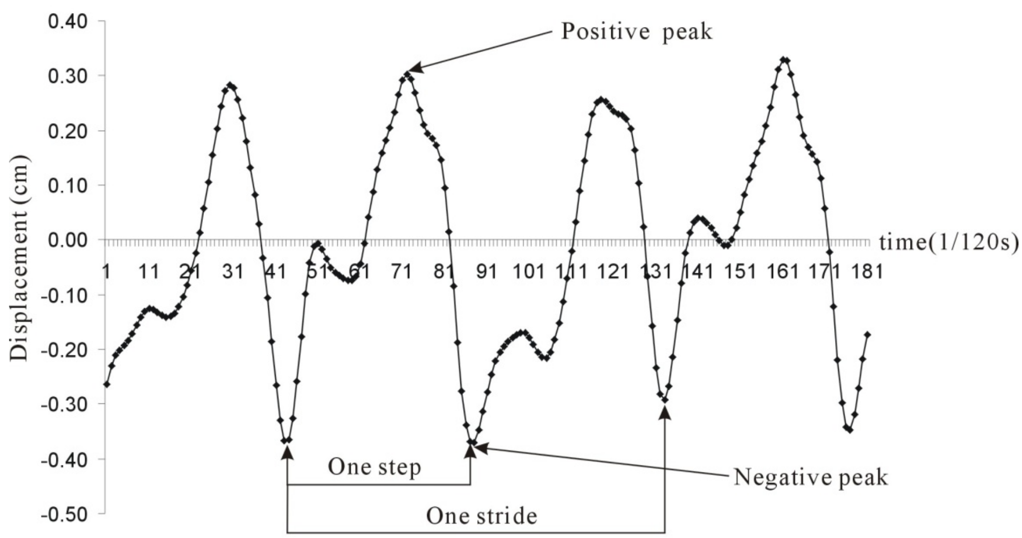

Figure 4.5 Determination of positive and negative peaks in vertical displacement in every stride

Three strides of activities were taken for each extraction of the peak amplitude of displacement, for four different subjects, six breast points, eight experimental conditions, three activities and three directions.

4.2.6.3 Reduced percentage of breast displacement

The Reduced percentage of Breast Displacement was labelled as ‘RBD’, which was calculated as follows:

$$RB\mathrm{D} = \frac{O\mathrm{D} - C\mathrm{D}}{O\mathrm{D}} \times 100\%$$

where OD was the original breast displacement in a braless condition, and CD was the breast displacement controlled by a bra. A sports bra with a larger RBD implied that the bra was better at reducing breast movement than that with a lower RBD.

4.2.7 Statistical analysis

The mean and standard deviation of the breast displacement was calculated for each subject in the same condition. Paired *t*-tests were used to test the significance of differences ($p < 0.05$) in the mean breast displacement between the nipple and other breast points in *x*-, *y*- and *z*- directions during different activities. The differences of breast displacement in different activities were compared using Analysis of Variance (ANOVA). The mean of RBD of seven different bra styles were also compared by using Pearson correlation coefficients. All statistical procedures were conducted using the Statistical Package for the Social Sciences (Version 15.0; SPSS Inc., Chicago, IL).

4.3 Results and discussions of Experiment 1

4.3.1 Breast movement trajectories

4.3.1.1 Comparing three activities in the Global Coordinate System

In the GCS, the breast movement trajectories (BMTs) showed the overall 'thorax and breast' movement. The thorax moved up and down, leaned back and forth, and the breasts swung left and right to various extents in different activities. The following figures show the BMTs of the six points, M1 to M6, on the breast skin and a sports bra when Subject 3 walked (Figure 4.6), jogged (Figure 4.7) and stepped up and down (Figure 4.8) in one stride. To clearly present the appearance of BMTs from different viewing directions in one graph, the axes were not in the same scale.

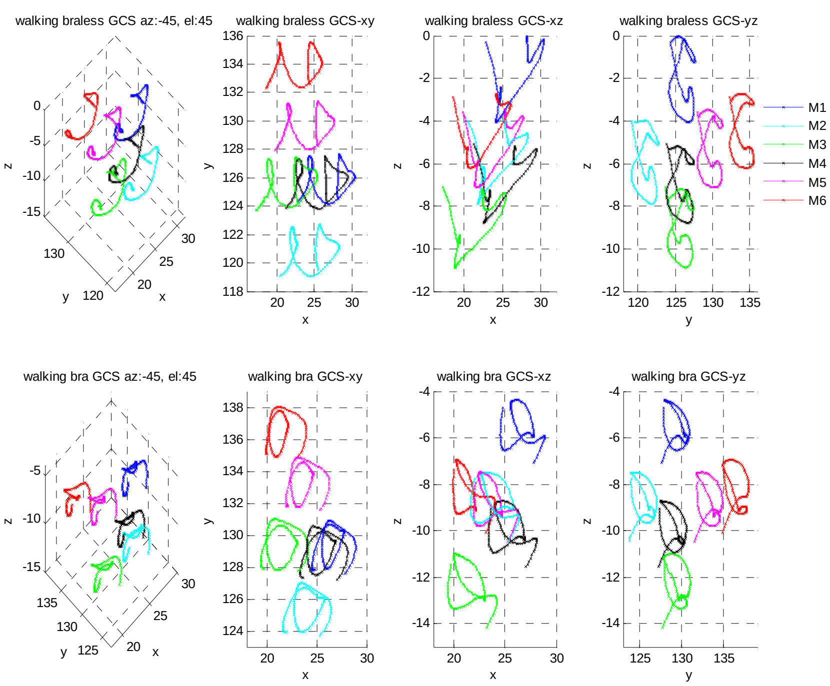

Figure 4.6 BMTs of Subject 3 in the GCS under braless and sports bra (Style 6) conditions during walking (unit: cm)

(az: azimuth, el: elevation; xy: side view, xz: top view, yz: front view)

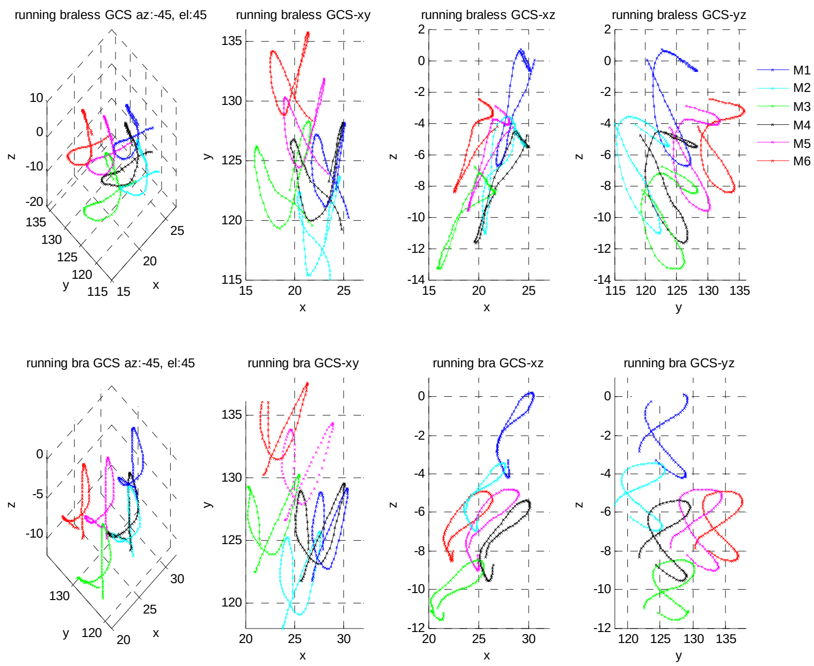

Figure 4.7 BMTs of Subject 3 in the GCS under braless and a sports bra (style 6) conditions during jogging (unit: cm)
(az: azimuth, el: elevation; xy: side view, xz: top view, yz: front view)

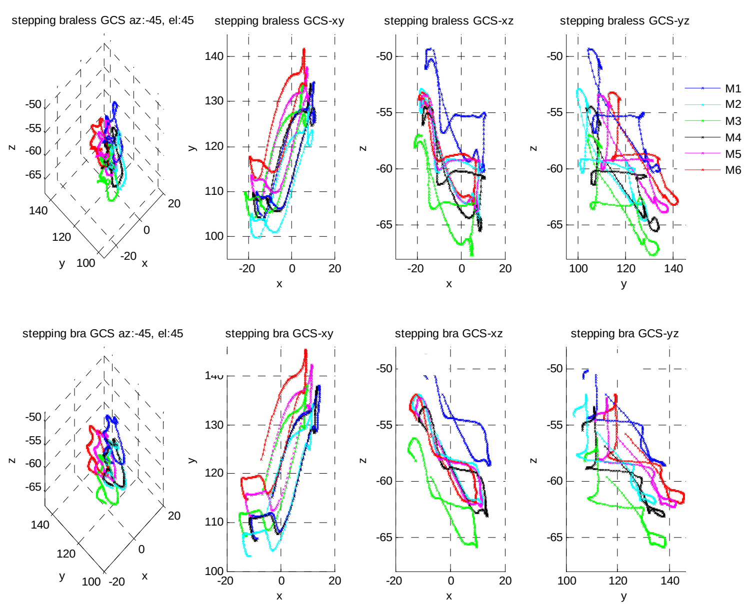

Figure 4.8 BMTs of Subject 3 in the GCS under braless and sports bra (Style 6) conditions during stepping up and down (unit: cm)
(az: azimuth, el: elevation; xy: side view, xz: top view, yz: front view)

The BMTs in the GCS were relative to the ground. They actually contain a) the thoracic movement relative to the ground, and b) the breast movement relative to the thorax. However, they did not show the real breast movement relative to the thorax.

The BMTs of the six points in the GCS appeared to be similar for the same direction and same viewing directions in the same activity. This was because the differences in the movement of different marker positions relative to the thorax were insignificant, when movement of the thorax was involved.

The BMTs varied among different viewing directions for the same activity. This implied that it was necessary to indicate the ‘viewing direction’ when comparing the BMTs in different studies.

Figures 4.6 to 4.8 show that the BMTs are different among three different activities. For example, the swing of the thorax from side to side during jogging was larger than that during walking; and the superior height during stepping was higher than that during walking and jogging.

4.3.1.2 Breast movement trajectories of the three activities in the Breast Coordinate System

After transforming the 3D raw data from the GCS to the BCS, the breast/bra movement relative to the thorax can be analysed. As this was the first time that the BCS was used, the following figures present the BMTs of six marker positions when Subject 3 was walking (Figure 4.9), jogging (Figure 4.10) and stepping up and down (Figure 4.11) in which a bra was not worn and a sports bra was worn, respectively.

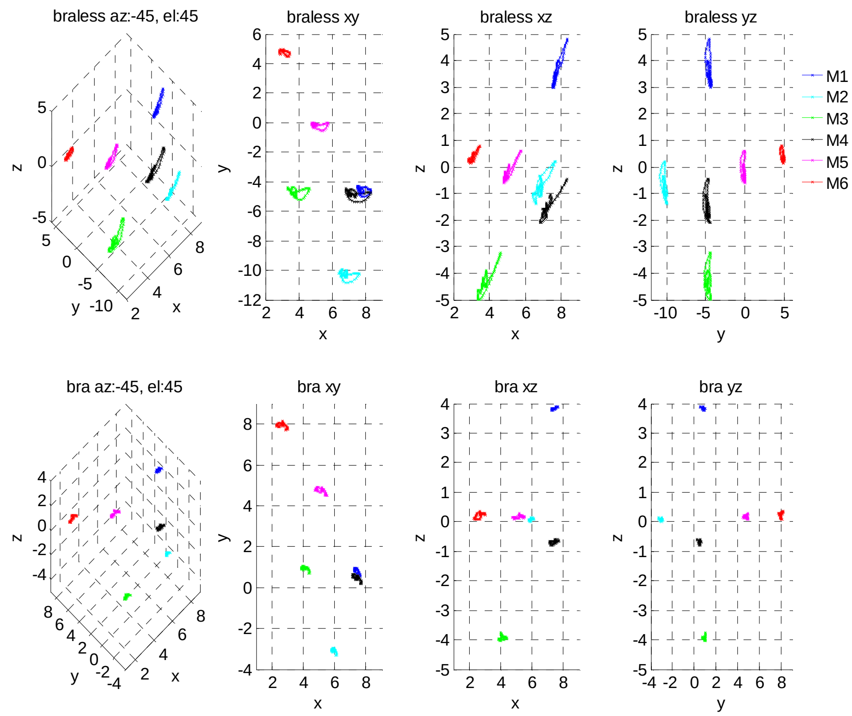

Figure 4.9 BMTs of six breast points on Subject 3 in the BCS under braless and sports bra conditions during walking (unit: cm)
(az: azimuth, el: elevation; xy: side view, xz: top view, yz: front view)

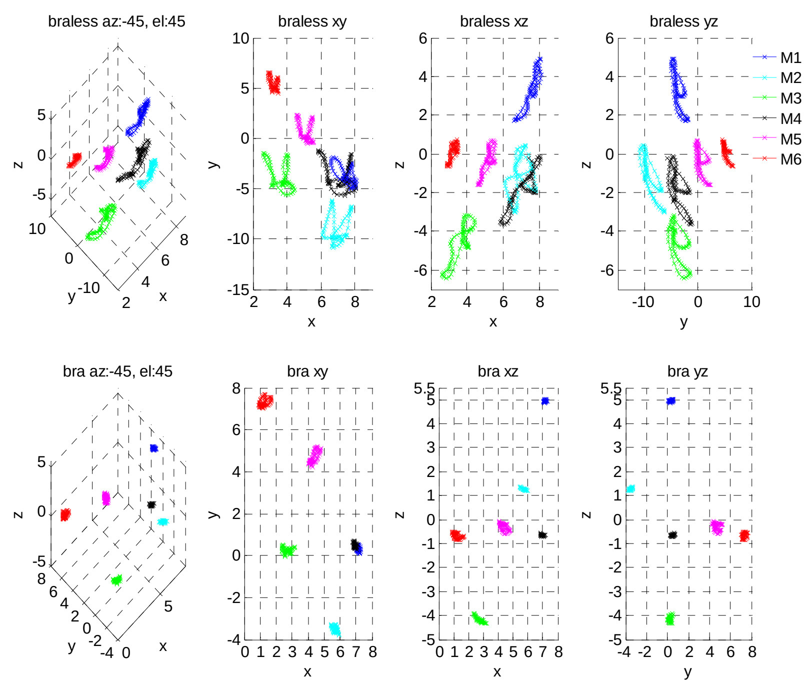

Figure 4.10 BMTs of six breast points on Subject 3 in the BCS under braless and sports bra conditions during jogging (unit: cm)
(az: azimuth, el: elevation; xy: side view, xz: top view, yz: front view)

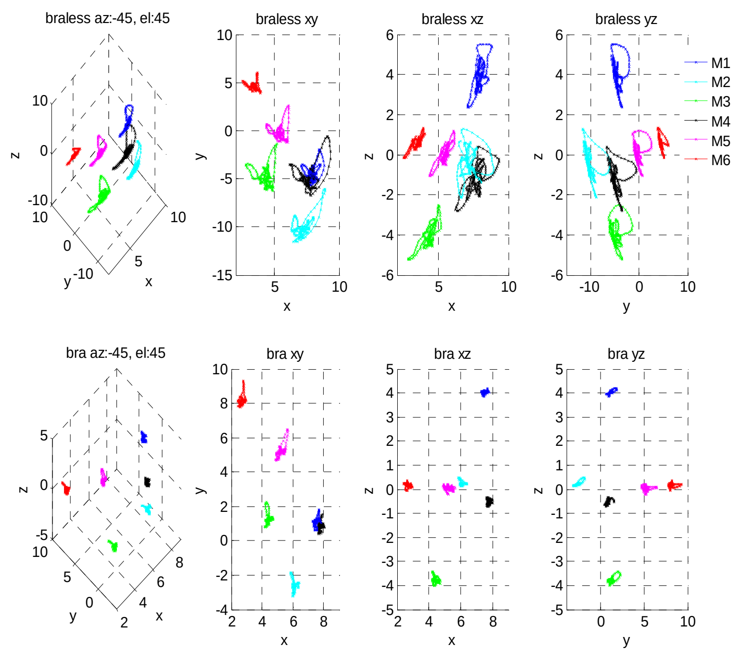

Figure 4.11 BMTs of six breast points on Subject 3 in the BCS under braless and sports bra conditions during stepping up and down (unit: cm)
(az: azimuth, el: elevation; xy: side view, xz: top view, yz: front view)

When comparing the BMTs of Figures 4.9 to 4.11, the ranges of the six marker movement for different directions were larger in braless than in the sports bra condition. This finding confirmed that the sports bra can control breast movement along different directions [4,6,53].

From visual observation, the movement ranges of the six markers during walking were smaller than those during jogging and stepping up and down for the same viewing direction and the same breast-supported condition. This implied that the ranges of breast movement were related to the intensity of body movement [4,6,10].

The movement ranges of the marker M6 were smaller than those of other marker positions for the same viewing direction and the same activity in the braless condition. This inferred that less breast movement occurred on the superior part of breast when a bra was not worn.

Figure 4.12 shows a closer look at the BMTs of two typical marker positions on the bra, M4 and M6, for a sports bra during jogging, from a viewing direction of - 45° azimuth and + 45° elevation. The precise BMT of the M4 appeared to be chaotic, but the M6 and other markers uniformly resemble a “butterfly” shape. M4 was situated over the very soft nipple area on the bra, and readily moves in an irregular pattern during jogging. In contrast, M6 was near the upper breast boundary had thinner soft tissues, so its dynamic behaviours were more regular.

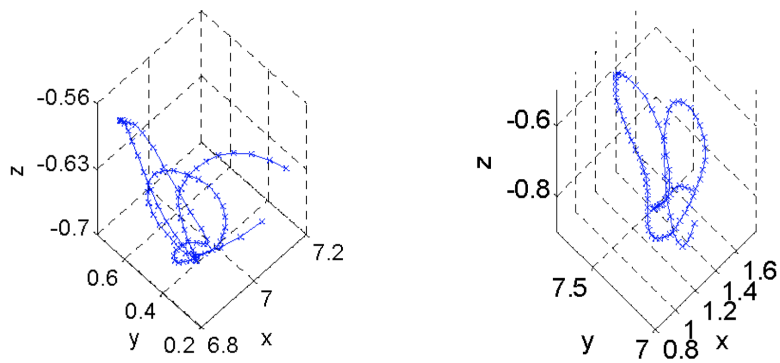

a) M4 (nipple) b) M6 (superior aspect of the breast)

Figure 4.12 3D BMTs of M4 and M6 when a sports bra was worn during jogging on a subject (unit: cm)

To be exact, the BMTs of the six marker positions were somewhat different from each other because the breast is a hyper-elastic body with various internal stresses. Any breast movement at one point influenced the others to a different extent. This showed that previous studies [3-4,16-17,23,50,53,87] that used only one position to represent the whole breast movement were insufficient for the research that aims to improve the design of different parts of sports bras.

All the BMTs in the new BCS presented above were in open loops. In the GCS, the BMTs of the six markers were also in open loops, as shown in Figure 4.13. The patterns of the

BMTs formed a frontal view uniformly resemble a "∞" shape because it largely reflected the thorax (including breasts) movement during bare-breasted jogging. The BMTs were in open loops, which showed that the movement were non-periodic. This was because the soft tissues (skin, adipose tissue, glandular tissue, milk ducts, Cooper's ligaments) in breasts have nonlinear mechanical characteristics.

This raised the question as to why Haycock [3] reported closed loops in the BMTs in the GCS. We found that a closed loop could occasionally occur in the following conditions: i) when the BMT of a particular gait cycle was chosen, ii) when the time was considered a bit longer than one stride, and iii) when only a particular viewing direction was selected.

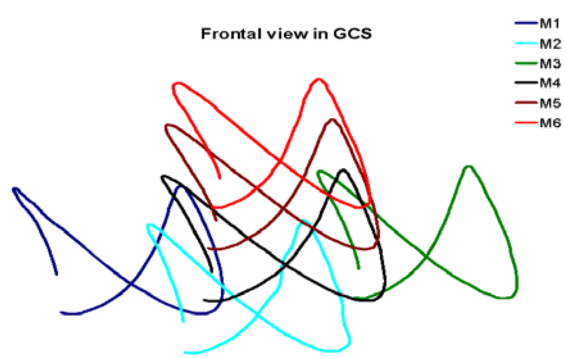

Figure 4.13 Open loops of BMTs in the GCS under a sports bra condition during a jogging stride

4.3.2 Breast displacement

4.3.2.1 Breast displacement against time

After understanding the BMTs, it is necessary to study the patterns of breast displacement against time because they show the exact time when the breasts change positions in each direction during the gait cycle. Figure 4.14 shows the displacement of six markers in one jogging stride, under braless and sports bra conditions, in the *x*-, *y*- and *z*- directions.

It was found that breasts had two substantial anterior-posterior movements, and up-down movements, in every jogging stride. During treadmill jogging, the body segments rotate about the joints and bring the feet onto the ground while the contralateral leg was swinging, followed by an airborne moment where both feet were off the ground. To counterbalance leg rotation, the shoulders and the arms moved opposite to the motion of the pelvis and legs. As soon as the right leg came up, the left arm and shoulder moved forward. In the jogging cycle, the arms swung and the shoulders extended forward and backward. This action led to the anterior-posterior movement of the breast twice within one stride. When the left and right foot hits the ground one after the other, the breasts went up and down twice in the *y*-direction. Similar description of breast movement in relation to gait cycle has been reported by Scurr et al. [20].

In the braless condition as shown in Figure 4.14, the superior displacement (4 cm) of the breasts was much larger than the inferior one (1 cm), whereas the anterior movement (1 cm) was slightly less than the posterior (1.5 cm), and the lateral displacement (1.2 cm) was a bit smaller than the medial (2.6 cm). The largest displacement occurred at M4 (black line) and the smallest at M6 (red line).

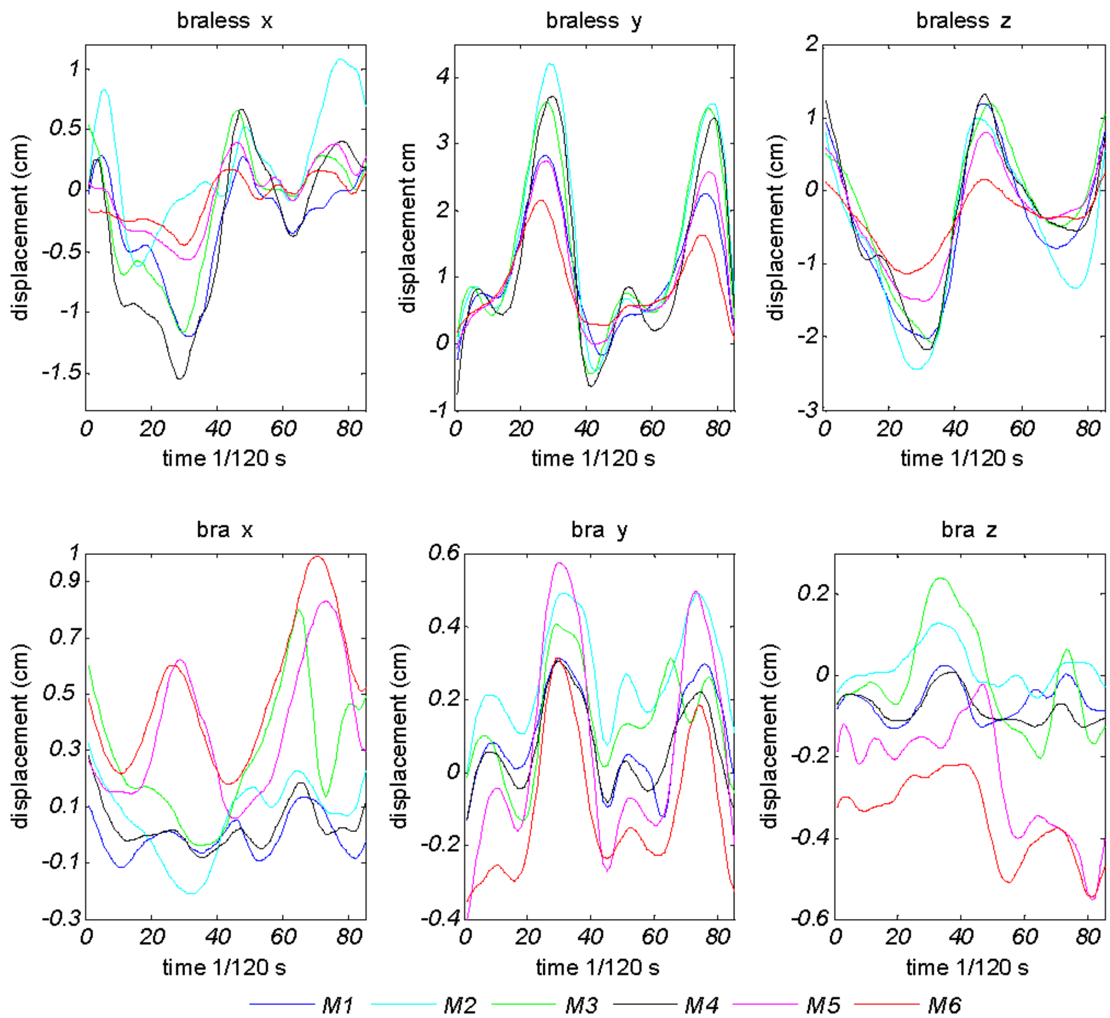

Figure 4.14 Breast displacement of a subject with breast size 80B in braless and bra conditions during jogging

With the sports bra, as shown in Figure 4.14, the displacement was mostly controlled within a range of ± 0.3 cm in all directions. The finding was similar to a previous study [10]. The less controlled regions at M5 and M6 did little to avoid breast bouncing, which was perceived as embarrassing in Chinese society [98]. The displacement at M5 (pink line) and M6 (red line) needed further reduction in anterior, superior and medial directions, by better designed sports bras.

4.3.2.2 Amplitude of breast/bra displacement

Comparing different marker positions

An examination of individual marker positions (Figure 4.15 a) in the braless condition reveals that there was the least amount of breast displacement (0.38 ± 0.11 cm) at M6 in the *y*-direction during walking. This finding was consistent with previous studies [10-11]. The nude breast displacement at M6 (upper chest) was the smallest because it had the least amount of fat tissue near the rib bones. It also had the largest distance from the CBM so its skin extension during activities was less affected by breast weight [2].

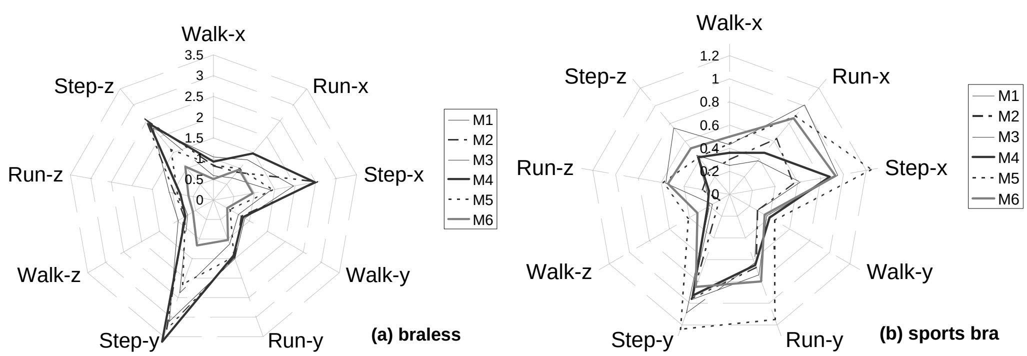

Figure 4.15 The mean values of the amplitude of breast displacement of four subjects at different marker positions in three directions during three different activities under two breast-supported conditions (unit: cm)

The maximum nude breast displacement was mostly found at M3 (outer breast) or M4 (nipple), especially during stepping up and down in the *y*-direction (3.6 ± 0.3 cm).

M4 (bust point) was located where the breast tissues were fullest. The body movement produces the greatest torque at M4 because it was located at the greatest distance from the thorax. The breast tissues are the thickest at the nipple point, and the breast mass tends to shift laterally in the braless condition. Therefore, the breast skin extended the greatest amount in these two positions.

With support from a sports bra (Figure 4.15 b), the maximum and minimum breast displacement occurred in different points on the bra. The minimum was at M1 (inner breast) or M2 (lower breast), especially in the *z*-direction during walking (0.1 ± 0.02 cm). This was because the rigid material of the centre gore and lower cup produces the force of the bouncing in the breasts and reduces their movement.

The maximum displacement (1.2 ± 0.2 cm) was found at M5 (upper breast) when a sports bra was worn. It is worth-noting that the upper cup of the bra did not perfectly fit the upper breasts when the body jumped upward. In such cases, a gap between the body and the neckline of the bra could allow the breasts to move forward during activities.

The sports bra fitted well on the subject's body when she was standing. However, a gap appeared between the upper breast and the bra cup when the breasts moved upward. To remove these gaps, there are two suggestions for the designers of sports bras as follows.

Firstly, the sports bra neckline should be positioned near the superior borderline of the breast. If the neckline is higher, gaps can easily form in between the breasts and sports bra cups, and the gaps cause the inability of the cups to control superior breast movement. If the neckline is lower, the upper breast cannot or can only minimally be controlled by the sports bra. A method to define the neckline is as follows: Step 1 is to define the borderline of the breast [99], which can be found by pushing in a vertical direction the bulk of the breast hard and form a folding line. The borderline is marked and forms a region. This region is also a breast movement region. Step 2 is to choose the neckline position according to the design of the sports bra. The neckline should lie on or close to the borderline of the breast.

These borderlines may vary between individuals. By now, little literature has reported about the differences in breast borderlines among individuals. So, in future studies, it is necessary to investigate the breast borderlines and find useful information for improving the neckline design of sports bras.

Secondly, the sports bra straps should have appropriate elasticity. Page and Steele [9] suggested that the fabrics of bra straps should contain minimal elastic in a vertical plane to assist in limiting breast movement. In our study, we observed that if the bra straps had minimal or no elasticity in the vertical plane, a gap might be formed between the straps and the shoulders. In this case, the sports bras with low elasticity straps did not control the upper breast movement well. However, if the bra straps had maximal elasticity, gaps did not easily form, but the sports bra was less effective in reducing the breast movement. The relationship between the elongation of shoulder straps and the reduction of breast displacement (RBD) during jogging was therefore investigated and the results are reported in the last part of Section 4.3.2.2.

Most previous breast motion studies [3,6,14-17,49-50] only captured the displacement of nipples (M4). However, additional points may be required to record the 3D movement of the whole breast. In this study, markers were attached at six points either to the subject's breast skin or the bra's surface. The 3D displacement of the additional five markers was compared with that of the nipple point. The significance of the difference in mean displacement between M4 (nipple) and each marker was determined by paired *t*-tests in *x*-, *y*- and *z*- directions. There were 96 data sets comprising four subjects, three activities, and eight bra wearing conditions (seven sports bras and one braless). The mean differences and the values of significance are shown in Table 4.6.

In 11 out of 15 cases, the displacement of the additional five markers was different from those of M4 (nipple) at a significance level of 95 %. Particularly, M1 (inner breast) and M2 (bottom breast) had significant differences (p<0.05) in breast displacement with M4 in all three directions. M6 (top breast) had the largest and significant (p<0.05) mean difference of breast displacement up to 0.3 cm with M4 in the x- and y- directions.

Table 4.6 Differences between M4 and other points in breast displacement of 11 subjects

Direction	Markers in comparison	Mean difference (cm)	Significance (p-value)
x	M4 – M1	0.2	<0.001*
	M4 – M2	0.1	<0.001*
	M4 – M3	0.2	<0.001*
	M4 – M5	0.2	0.104
	M4 – M6	0.3	0.018*
y	M4 – M1	0.2	<0.001*
	M4 – M2	0.1	0.002*
	M4 – M3	0.1	0.657
	M4 – M5	0.1	0.007*
	M4 – M6	0.2	0.001*
z	M4 – M1	0.2	<0.001*
	M4 – M2	0.2	<0.001*
	M4 – M3	0.1	<0.001*
	M4 – M5	0.1	0.615
	M4 – M6	0.2	0.154

M1: inner breast, M2: bottom breast, M3: outer breast, M4: nipple, M5: upper breast, M6: top breast

* p-value < 0.05

Comparing different activities

Table 4.7 shows the mean and SD values of the amplitude of bare-breasted displacement of six breast points for the four subjects in three directions during three different activities. The amplitude of breast displacement during stepping up and down was generally the largest among the three activities, in all directions for six breast points.

Table 4.7 Displacement at each breast point of 11 subjects during activities in the BCS (unit: cm)

	Breast point	*Anterior-posterior displacement*			*Vertical displacement*			*Medial-lateral displacement*		
		Walk-*x*	Jog-*x*	Step-*x*	Walk-*y*	Jog-*y*	Step-*y*	Walk-*z*	Jog-*z*	Step-*z*
		Mean(SD)	Mean(SD)	Mean(SD)	Mean(SD)	Mean(SD)	Mean(SD)	Mean(SD)	Mean(SD)	Mean(SD)
braless	M1	0.6(0.2)	*0.7(0.2)*	1.4(0.2)	0.7(0.2)	1.1(0.3)	2.4(0.2)	0.7(0.1)	0.8(0.3)	2.5(0.4)
	M2	0.8(0.2)	0.9(0.1)	2.5(0.1)	0.8(0.2)	1.5(0.4)	3.3(0.3)	0.8 (0.2)	1.0(0.4)	2.6(0.5)
	M3	1.0(0.2)	1.3(0.1)	2.0(0.4)	0.9(0.1)	1.5(0.4)	3.1(0.3)	1.0(0.3)	1.1(0.3)	2.3(0.4)
	M4	0.9(0.4)	1.5(0.2)	2.5(0.3)	0.8(0.2)	1.4(0.4)	3.6(0.6)	0.8(0.5)	0.8(0.3)	2.4 (0.4)
	M5	0.8(0.2)	1.0 (0.1)	1.4(0.3)	0.5(0.1)	1.4(0.2)	2.2(0.1)	0.8(0.4)	0.9(0.2)	1.6 (0.4)
	M6	*0.5(0.1)*	1.0(0.1)	*1.0(0.3)*	*0.4(0.1)*	*1.0(0.2)*	*1.2(0.1)*	*0.6(0.2)*	*0.6(0.1)*	*1.16(0.3)*
sports bra	M1	*0.3(0.1)*	*0.4(0.2)*	0.6(0.1)	*0.3(0.0)*	*0.6(0.1)*	1.1(0.2)	0.2(0.0)	0.2(0.1)	0.4(0.1)
	M2	0.3(0.1)	0.6(0.0)	*0.6(0.2)*	*0.3(0.1)*	0.7(0.1)	*1.0(0.2)*	*0.1(0.0)*	0.2(0.1)	*0.3(0.4)*
	M3	0.4(0.1)	1.0(0.1)	1.0(0.2)	0.4(0.1)	0.7(0.1)	1.0(0.2)	0.8(0.0)	0.6(0.1)	0.8(0.2)
	M4	0.4(0.1)	0.5(0.1)	0.9(0.3)	0.4(0.1)	0.7(0.2)	0.9(0.2)	0.2(0.0)	*0.2(0.1)*	0.4(0.2)
	M5	0.4(0.1)	0.9(0.1)	1.2(0.2)	0.5(0.0)	1.2(0.2)	1.2(0.2)	0.4(0.0)	0.9(0.1)	0.4(0.1)
	M6	0.5(0.0)	0.9(0.2)	0.9(0.3)	0.4(0.0)	0.8(0.2)	0.9(0.2)	0.3(0.0)	0.5(0.1)	0.5(0.1)

Note: Numbers in bold are the maximum among the six points in the same activity, same direction and bra-supported condition.

During braless jogging at 7 km/h, the mean displacement of the nipple (M4) was 1.5 cm anterior-posterior, 1.4 cm vertical, and 0.8 cm medial-lateral. Corresponding values reported by Scurr et al. [61] were much bigger for D-cup women's nipple displacement relative to the clavicle (3.7 cm anterior-posterior, 4 cm vertical, and 3.4 cm medial-lateral) in the same jogging conditions. In the sports bra conditions, the mean nipple displacement during jogging was 0.2 cm - 0.7 cm in three different directions, which were also smaller than Scurr et al.'s [61] findings of a mean of 1.4 cm in an encapsulation bra and 2.0 cm in a compression bra. The difference is considered reasonable because smaller-breasted B-cup and C-cup Chinese women were participating in this study.

The differences of breast displacement in different activities were compared using analysis of variance (ANOVA) at 95 % significance level. There were 32 sets of data including the breast/bra displacement from all four subjects in all eight bra-supported conditions. Table

4.8 shows the *p*-values obtained and the brackets show the mean breast/bra displacement in *x*-, *y*- and *z*- directions.

Table 4.8 ANOVA results of breast/bra displacement in *x*-, *y*- and *z*- directions during different activities

Direction	Activity	Activity in comparison	Significance (*p*-value)
x	Walking (0.5 cm)	Jogging (0.9 cm)	0.004*
		Stepping (0.8 cm)	0.005*
	Jogging (0.9 cm)	Stepping (0.8 cm)	0.904
y	Walking (0.4cm)	Jogging (0.9 cm)	0.021*
		Stepping (1.0 cm)	0.004*
	Jogging (0.9 cm)	Stepping (1.0 cm)	0.577
z	Stepping (0.8 cm)	Walking (0.5 cm)	0.074
		Jogging (1.1 cm)	0.091
	Walking (0.5 cm)	Jogging (1.1 cm)	0.001*

In the anterior-posterior (*x*) direction, the mean breast/bra displacement during walking (0.5 cm) was significantly smaller than those during jogging (0.9 cm, $p = 0.004 < 0.05$) and stepping (0.8 cm, $p = 0.005 < 0.05$). The same trend happened in the vertical (*y*) direction, the mean breast/bra displacement during walking (0.5 cm) was significantly smaller than those during jogging (0.9 cm, $p = 0.021 < 0.05$) and stepping (1.0 cm, $p = 0.004 < 0.05$). However, in the medial-lateral (*z*) direction, the mean breast/bra displacement during stepping (0.8 cm) had no significant difference when compared to walking (0.5 cm, $p = 0.074 > 0.05$) and jogging (1.0 cm, $p = 0.091 > 0.05$).

Comparing different directions

The amplitude of breast displacement was the greatest in the *y*-direction during stepping up and down, and jogging. This finding was consistent with the result reported by White et al.

[6]. During bare-breasted walking, the amplitude of breast displacement was the greatest in the *x*-direction for M2, M3, M4 and M5, but the largest in the *z*-direction for M1 and M6. With a sports bra, the amplitudes were much more reduced. Therefore, a good bra should limit breast motion mainly in the vertical direction for sports activities. To prevent embarrassing bouncing, the bra should focus on the control of vertical movement, and the medial-lateral movement of the inner and upper breasts.

Comparing different types of bras

By averaging the RBD for four subjects, six points and three activities, Figure 4.16 shows the mean RBDs for seven different bra styles (n = 72) in three different directions. The bras with different design features exhibited different levels of control.

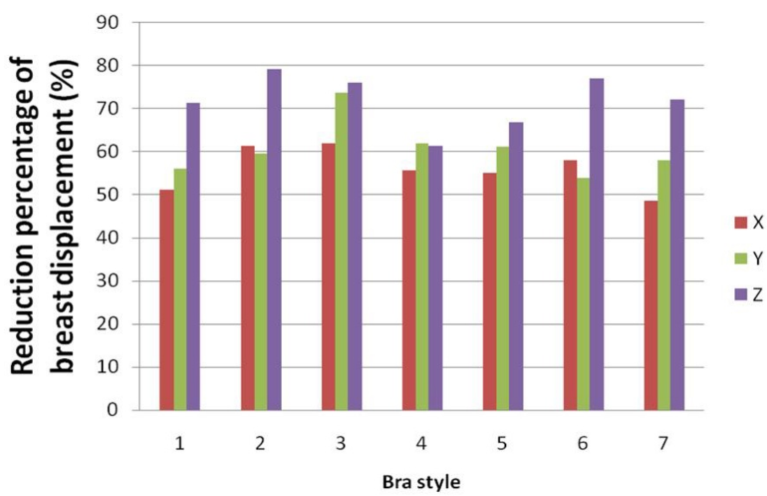

Figure 4.16 RBD of different bra styles in different directions

As shown in Figure 4.16, Style 3 was most effective in reducing breast displacement in all directions (61.90 %, 73.80 %, 76.00 % in the *x-, y-* and *z-* directions respectively), followed by Style 2 (61.31 %, 59.64 %, 79.14 % in the *x-, y-* and *z-* directions respectively). In the *x*-direction only, Style 7 gave the smallest RBD. In the *y*-direction only, Styles 1 and 6 provided the poorer RBDs (56.04 % and 53.99 % respectively). In the *z*-direction only, Styles 2 and 6 showed strong RBDs (79.14 % and 77.03 %) whereas Style 4 was the weakest (61.38 %). Referring to Table 4.2 the common design features of the effective bra samples of Styles 2 and 3 can be listed as follows.

- compression type to limit breast movement in all directions
- short vest style with high neckline to maximize the coverage
- rigid cup seam to fit the breasts and prevent movement
- side slings to restrict the medial-lateral breast movement
- racer-back panel to distribute the tension to the back.
- slightly elastic bound neckline to fit the upper breast boundary for stabilization
- no centre gore, no cradle, no wire, no pad
- wide strap adjustment with good recovery, but with no adjustment.

The RBDs were also affected by the bra measurements, as shown in Figure 4.17. In general, a higher centre-front gave a larger anterior-posterior RBD; wider shoulder straps provided larger vertical RBD; higher neckline or deeper side seam also gave a larger medial-lateral RBD.

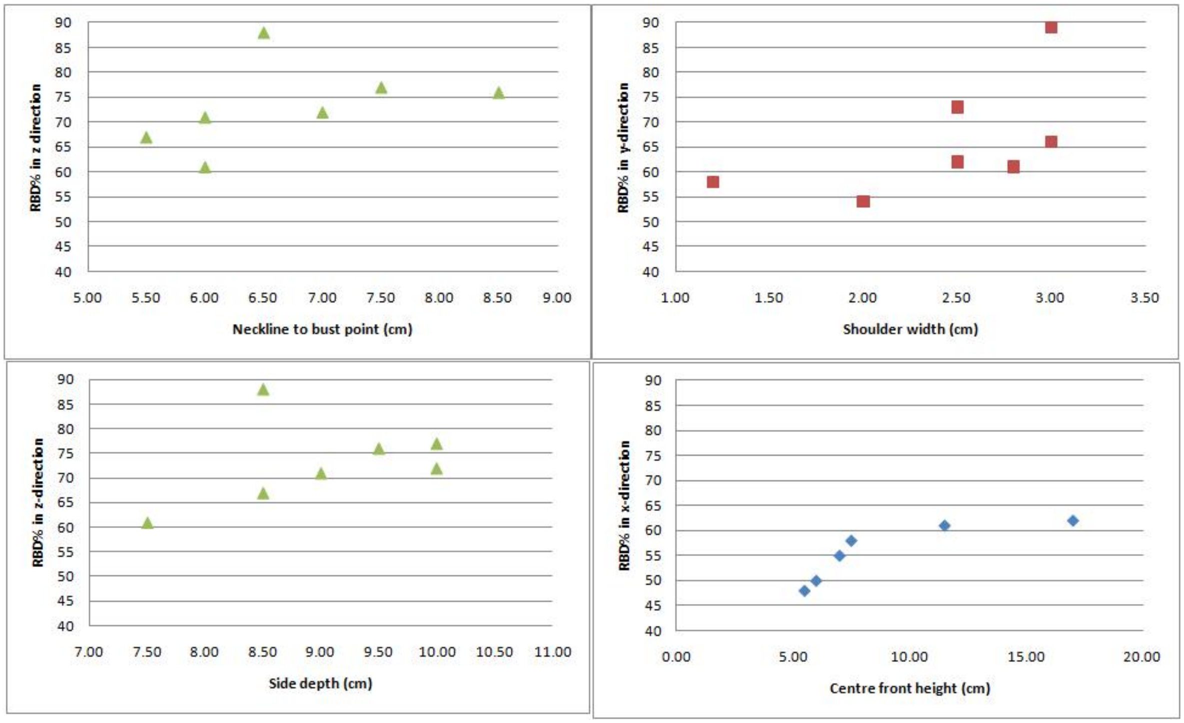

Figure 4.17 Relationships between bra measurements and RBD

Based on Figures 4.16 and 4.17, the bra measurements of size 75B for the most effective control of breast movement were suggested in the following.

- Centre front height = 11.5 cm
- Shoulder width = 3 cm
- Neckline to bust point = 6.5 cm
- Side depth = 6.5 cm
- Underband width = 2.5 cm

It was also note-worthy that a higher support level of sports bra claimed by the manufacturer/retailer may not guarantee a more effective control of breast movement. In this study, Style 1 was labelled as giving a high level support, whereas Style 2 was labelled as a medium level. However, the experimental results showed that Style 2 provided much higher RBD than Style 1, which was inconsistent with the manufacturer's categorization of support levels.

Style 3 was the most effective bra. It was a firm-control short vest that had a unique inverted-U shape bounded seam over the upper and side boundaries of the cups. It strongly restricted the vertical and medial-lateral (z-direction) breast movement, and held the breast tissues firmly around the chest, underarm and underbust with wide racer-back design. The inelastic top front panel had high neckline, so the cups fully encaged the whole breasts. The cup panel used double bias cup seams to create the required volume and shape. A narrow-width fabric panel with a straight grainline passing through the nipple area guranteed rigidity from the inner bottom breast to the outer top breast areas. Therefore, breast movement in all directions was much reduced by this bra.

Style 7 was ineffective in controlling breast movement, in the anterior-posterior direction (x-direction), due to its narrow shoulder strap (1.2 cm) and the absence of shoulder-to-back fabric panel. Wide shoulder straps can definitely help to distribute breast weight to the wearer's shoulders, and the back panel can transmit the tension to the wearer's back. Moreover, the shoulder straps of Style 7 were so rigid that a gap easily occurred when the breasts moved upward. It was not a perfect fit to the body, thus control of movement became ineffective. It also had elastic seamless cup fabric and a low centre-front, so it allowed larger breast movement, in the x-direction.

In the y-direction, Styles 1 and 6 were less effective because Styles 1 and 6 had a low neckline (6 cm from the cup peak) with elastic fabrics, so the upper parts of the breasts moved upward easily.

In the z-direction, Style 2 reduced the medial-lateral (z-direction) breast displacement most effectively because it was a compression bra with 11.5 cm high and rigid centre-front. It firmly stabilized the two breasts. Style 6 gave the second strongest RBD in the z-direction, because the large side depth and the slings in the side cups functioned well in limiting lateral movement. In contrast, Style 4 gave the weakest RBD because it used front closure. The two cups were separated and had low neckline. The bra cups did not firmly hold the breasts, so the medial-lateral breast movement was not well controlled.

Comparing the elongations of different bra components

The correlation coefficients among the elongation percentage of cup seam, neckline and shoulder straps and the RBD are shown in Table 4.9.

Table 4.9 Pearson correlation coefficients among the elongation percentages and the Reduced percentage of Breast Displacement (RBD)

direction	RBD-x	RBD-y	RBD-z
cup seam elongation %	-0.33	0.51	0.19
neckline elongation %	-0.32	0.37	0.53
shoulder strap elongation %	0.39	0.82	0.23

Only the shoulder strap elongation percentage was significantly and positively correlated with the RBD ($r = 0.82$, $n = 7$, $p<0.05$). The relationship was established using a regression equation $y = 0.6711x + 47.161$, $r^2 = 0.6718$, as shown in Figure 4.18..

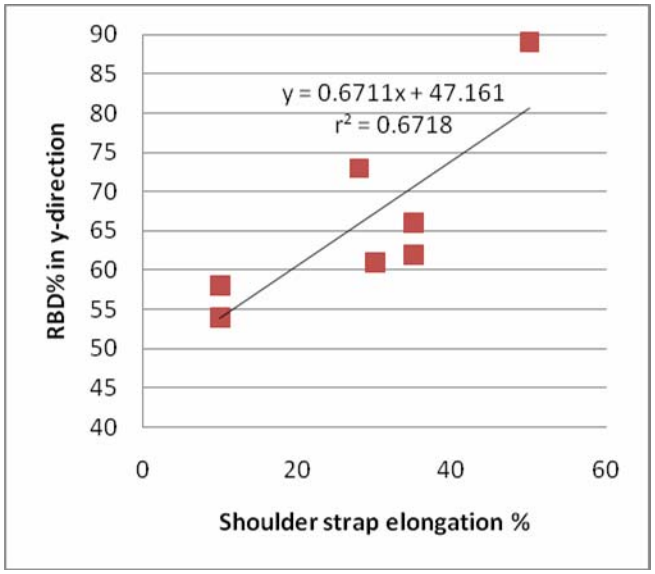

Figure 4.18 Linear relationship between the shoulder strap elongation percentage and the Reduced percentage of Breast Displacement (RBD)

4.4 Conclusions from Experiment 1

The relative 3D breast/bra displacement was analysed using the BCS (Breast Coordinate System). The effectiveness of the sports bra was measured by RBD (Reduced percentage of Breast Displacement). The results showed that there were significant differences in displacement between the nipple, inner breast and bottom breast, so using only the nipple displacement was insufficient for a scientific analysis of detailed breast movement related to bra design. The bra samples were most effective in controlling the breast movement in the medial-lateral direction, but less effective in the anterior-posterior direction, so more attention should be given to the centre front, the plasticity of the cup fabric and the location of the cup seam and neckline to address this. For some bra styles, the poor control at the top part of the breast was attributed to a gap between the bra and the breast inside the top cup during activity, so it should be ensured that the neckline height should fit the upper breast boundary not just while standing but also during exercise. It was anticipated that the shoulder straps made of extensible elastic should be helpful to control the breast movement. This posed the research question Q.4: how do the properties of shoulder straps affect the breast movement? The answer to this question was reported in Section 4.2.6.

The more effective bras had common features such as compression type, short vest style, high neckline, rigid cup seams, side slings, racer-back panel, bound neckline with slight elasticity, no centre gore, no cradle, no wire, no pad, and non-adjustable wide strap with good recovery. This recommendation was consistent with McGhee & Steele's study [54] that found significantly less vertical breast displacement and less exercise-induced bra discomfort in a combination of breast elevation and compression. In the industrial practice, the sports bra designers often used inelastic thin bottom cup fabrics and side sling fabric connected with wide shoulder straps to distribute the gravitational force from the breasts to the back. To reduce the bra moment, compression bras with high neckline were believed to be effective.

The most effective bra had a unique inverted-U shape bounded seam over the upper and side boundaries of the cups with wide racer-back design. The inelastic top front panel was so high that the cups fully encased the whole breasts. The cup panel used a narrow-width fabric panel with straight grainline passing through nipple area to gurantee the rigidity from the inner bottom breast to the outer top breast areas. Therefore, the bra and breast movement in all directions was much reduced.

To date, there was no international standard for the evaluation of sports bras in reducing breast movement. The methodology that has been devised based on the BCS enables the performance to be more completely and reliably compared. The bra measurements related to effective bra support was also determined for the core size.

4.5 Methods for Experiment 2

The results of Experiment 1 showed that shoulder straps with different elasticity had significantly different effectiveness in controlling breast movement. Therefore, it was necessary to study the effects of shoulder strap properties on the bra movement in more detail. As larger breasts moved more rigorously than smaller breasts during activities, it was also interesting to study the relationship between breast volume and bra displacement.

Based on the variations in Experiment 1, the sample size for Experiment 2 was determined as 14. Therefore, 14 subjects were recruited to wear a well-fitted consistent style of sports bra attached with changeable 10 types of shoulder straps. The experimental procedures were presented as follows.

4.5.1 Sample size of human subjects

The G*Power software (Erdfelder, Faul, & Buchner, 1996) was used to calculate the sample size of human subjects for Experiment 2 based on the mean and standard deviation of the breast displacement for four subjects in Experiment 1 as reported. Two-tailed paired *t*-test and both type I and type II errors were considered.

The aim of this study was to investigate whether there was any relationship between the bra movement and the properties of shoulder straps for different breast volumes during jogging. The breast sizes from Experiment 1 were divided into two groups: Cup B and Cup C. The shoulder straps were divided into two groups according to the elongations as shown in

Table 4.2. Group 1 included the bra styles 1 to 5 with shoulder strap elongations of more than 20 %, whereas Group 2 included the bra styles 6 and 7 with shoulder strap elongations of 20 % or below.

Table 4.10 Effect size and power analysis of Experiment 1

Direction	Group	Breast displacement (Mean and SD) (cm)	Effect size dz	Minimum sample size	Actual power
Different breast sizes					
x	1	0.61 ± 0.18	1.596	6	0.873
	2	0.99 ± 0.27			
y	1	0.52 ± 0.12	2.260	4	0.840
	2	1.17 ± 0.18			
z	1	0.53 ± 0.15	1.594	6	0.873
	2	0.99 ± 0.27			
Different shoulder straps					
x	1	0.62 ± 0.09	1.134	9	0.864
	2	0.71 ± 0.03			
y	1	0.55 ± 0.03	1.143	9	0.850
	2	0.63 ± 0.08			
z	1	0.61 ± 0.07	1.761	6	0.833
	2	0.72 ± 0.02			

The mean and SD of the breast displacement of the six marker positions in Experiment 1 was calculated for the two groups of breast sizes as shown in Table 4.10. The data was used to estimate the effect size (dz), total sample size and actual power (Table 4.10) using G*Power software.

The actual powers were all larger than 0.833 as shown in Table 4.10, so the total sample sizes can be accepted [100], meaning that the required sample size of human subjects should be nine or above for further studies. Therefore, in this study, a convenient sample of 14 volunteers (age: 24.5 ± 6 years old, height: 160.0 ± 6.9 cm, mass: 60.2 ± 6.6 kg, body mass index: 23.6 ± 2.7 kg/m^2) was recruited. Their breast sizes ranged from 75B to 85D in the Metric system, which were the most prevalent Chinese breast sizes [91]. Before data collection, the participants received a thorough explanation of the procedures and risks involved and provided written consent. The inclusion criteria were healthy, premenopausal women.

4.5.2 Samples of shoulder straps

Ten different shoulder straps with a constant width of 1.6 cm but with different designs and material properties were selected from 38 commercial shoulder straps, so that they covered a wide range of various densities, elongations and moduli, according to the data provided by the same supplier. The strap SS10 was very strong and inextensible, so its modulus was not applicable. The fibre contents and material properties of the selected shoulder straps are listed in Table 4.11 for reference only.

Table 4.11 Properties and yarn contents of selected shoulder straps

Shoulder strap code		SS1	SS2	SS3	SS4	SS5	SS6	SS7	SS8	SS9	SS10
Properties	Density (kg/100m)	1.06	0.82	1.18	1.13	1.18	1.06	1.23	0.95	1.11	0.85
	Elongation (%) at 5kgf	133	82	80	91	72	105	96	74	81	0
	Load at 40% strain (kg)	0.553	1.036	1.458	1.785	2.062	0.82	1.348	1.462	1.57	n/a
	Recovery (%)	85	85	85	85	85	85	85	85	85	100
	Shrinkage (%)	5	5	5	5	6	6	6	5	5	6
Yarn Content (%)	Nylon filament	64.47	40.66	27.1	40.67	51.95	53.06	56.07	39.66	48.28	37.35
	Nylon twisted thread			3.65	3.55						
	Spandex yarn	10.79	13.71	16.53	18.12	18.31	9.77	17.83	20.67	25.22	
	Stretch nylon yarn	24.74	45.63	52.72	35.34	29.74	37.17	26.1	39.67	26.5	57.99
	Thermo-fusible yarn				2.32						4.66

To obtain more detailed strap properties for establishing the relationships with the breast displacement to answer the research question Q.4, the 10 straps were tested according to the ASTM standard D 4964–96: Standard Test Method for Tension and Elongation of Elastic Fabrics. A calibrated constant rate of extension type tensile testing machine (Instron 4411, Instron, U.K.) in a standard laboratory condition in 20°C and 65 % relative humidity was used. Five specimens from each strap were cut into 35 cm lengths, and sewn into a loop of 25 cm circumference and tensile tested at a constant rate (30 cm/min) of traverse up to 50 % extension, by loading and unloading them for three continuous cycles. Figure 4.19 shows the load-extension behaviour of strap 1 in the third cycle as an example of the load extension graphs obtained. The load-extension curves of other straps are attached in the Appendix 1.

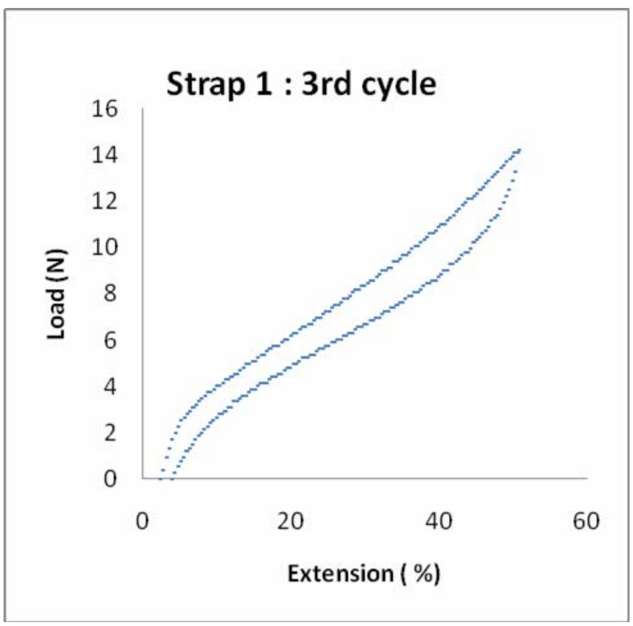

Figure 4.19 Load-extension behaviour of strap 1 in the third cycle of loading and unloading

The thicknesses of the straps were measured to an accuracy of 0.0001 cm by the deep throat dial thickness gauge (BNS-0110, GEI International, USA). The masses were recorded to an accuracy of 0.0001 g by the analytical balance (Ohaus Explorer Pro EP214, Phantom

Scales, USA). According to the laboratory tests, the properties of the 10 straps are summarised in Table 4.12.

Table 4.12 Properties of the 10 shoulder straps

Strap	Density (kg/100m)	Modulus MPa at 25%	Thickness (mm)
SS1	1.0756	3.81	1.36
SS2	0.8265	6.79	1.05
SS3	1.1604	9.79	1.42
SS4	1.1009	13.22	1.29
SS5	1.2596	13.41	1.33
SS6	1.0038	3.18	1.35
SS7	1.2526	9.85	1.49
SS8	0.9174	15.85	1.21
SS9	1.0096	12.59	1.17
SS10	0.8313	Not available	0.9

To test the effectiveness of these straps on the same bra, 10 pairs of different straps of 40 cm long were sewn into 30 cm long lengths with 1.5 cm seam allowance at both ends and an initial turning of 7 cm that was adjustable by a slider to fit on the shoulders of different subjects.

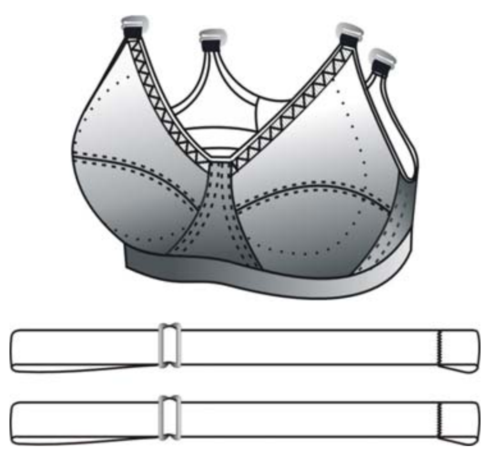

Figure 4.20 Bra Style 6 with the shoulder straps not attached

The bra sizes were chosen to fit the subjects' sizes ranged from 75B to 85D. The 10 different shoulder straps were attached to or detached from the same bra, which was chosen as a controlled variable, using a modular design with four "figure 9" hooks as shown in Figure 4.20. This allowed easy attachment and detachment of shoulder straps.

The bras were accurately fitted to each subject by adjusting the tension of the bra underband and shoulder straps, according to the procedures mentioned in Section 3.2.3.1. Table 4.13 shows the extension percentage of nine shoulder straps (SS10 was inextensible) that fit individual subjects before the motion experiments. For example, the mean percentage of the pre-extension of strap 1 was 10.1 ± 4.2 %. The strap was working over the pre-tension, and the load during jogging would be affected by the strap modulus characterised by the slope of the linear portion of the third loading curve, as plotted in Figure 4.19.

Table 4.13 Pre-experiment extension percentages of the shoulder straps

	Extension % of shoulder strap to fit the subjects								
Subject	SS1	SS2	SS3	SS4	SS5	SS6	SS7	SS8	SS9
S1	14.4	8.4	5.7	3.8	5.4	17.5	7.2	8.8	11.6
S2	4.4	3.8	3.8	3.4	3.8	13.4	5	5	7
S3	9.3	6.9	4.6	5.7	6.5	10.5	6.7	5.2	9.8
S5	3.9	3	2.5	4.3	5.2	7.5	3.3	4.4	4.5
S6	11.7	1.6	4.5	2.3	3.8	16.5	1.9	4.2	4.8
S8	14.5	4.1	5.4	4.1	6.1	14.3	5.5	5.4	7.1
S9	12.3	4.5	2.6	3.8	5.8	18.4	3.9	3.9	8.3
S10	10.9	2.7	7.1	3.8	3.8	10.1	6.7	5.1	8.8
S11	16	6.6	3.8	3.6	7.1	12.3	4.5	5.7	9.6
S12	8.1	3.8	3	1.8	3.8	7.7	5.3	4.9	5.3
S13	5.9	5.1	3.2	1.7	6.4	13.8	6.1	4.7	6.1
mean	10.1	4.6	4.2	3.5	5.3	12.9	5.1	5.2	7.6
SD	4.2	2.0	1.4	1.2	1.3	3.7	1.6	1.3	2.3

4.5.3 Experimental

To study the relationship between breast volume and bra displacement, the breast volume was measured by a TC^2 NX-16 3D full-body non-contact body scanner (Textile/Clothing Technology Corporation, America). To record the 3D breast movement, a Vicon motion analysis system (Vicon, 612, Oxford Metrics, Oxford, UK) as described in Section 4.2.3 was used.

4.5.3.1 [TC]^2 body scanner

The [TC]^2 NX-16 3D full-body non-contact body scanner used 16 independent cameras to capture a series of images of the body surface. These images containing over 600,000 data points formed a 3D point cloud. Then, the 3D body was reconstructed as shown in Figure 4.21 and the measurements were extracted automatically from the scanning software.

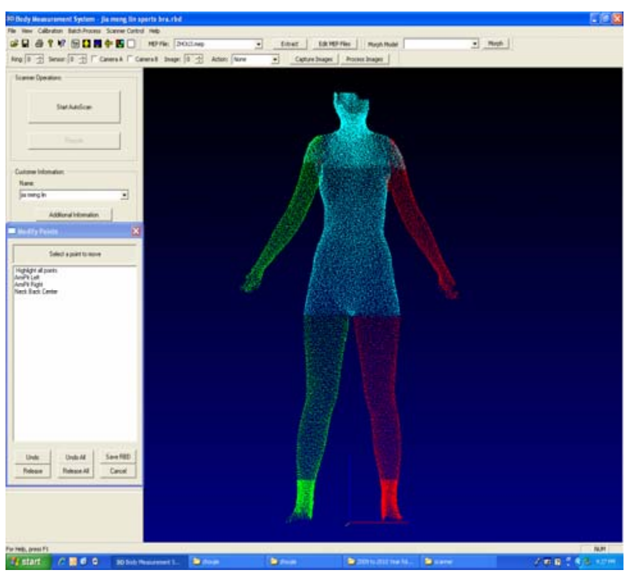

Figure 4.21 A 3D point cloud of the body image of a subject with breast size 75C

Prior to data acquisition, calibration was performed. The procedure of calibration is listed in Table 4.14.

Table 4.14 Calibration procedures of the body scanner [101]

Step	Procedure
1	Place the white cylinder in the centre of the scan chamber
2	Make sure that the scanner entrance curtains are closed
3	Select "calibration" on the menu bar
4	Signify the cylinder in the scanner and then "scan cylinder to verify calibration"

Each subject was asked to stand on the foot prints at the centre of the scanning booth. During scanning, the subject wore no bra, stood still and looked straight, with both hands on handholds, and breathed naturally according to the standardised procedure [101].

In the TC^2 body measurement extraction program, the yellow dotted lines on the body model signify the measurement-related body landmarks, as shown in Figure 4.22 a). For example, the boundary line of the lower-breast side-quadrant was highlighted for the measurement "breast volume lower outside left" as in Figure 4.22 b). The boundary line was checked using the surface data of the 3D display as in Figure 4.22 c). If the boundary line did not sit on the breast root, the dots Figure 4.22 b) could be moved manually until they were all on the breast root. After all the boundary lines of the four quadrants of breast volume were checked and manually fixed, the total breast volume was extracted from the software. The mean of breast volumes was 320 ± 54 cm^3 that was similar to the mean value (325 ± 13 cm^3) of a previous study on 125 Chinese women [102].

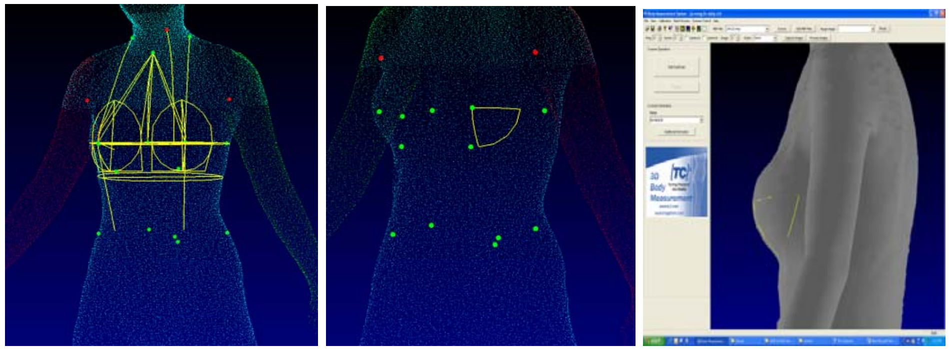

a) b) c)

Figure 4.22 Process of extracting breast volume

4.5.3.2 Vicon motion analysis system

After attaching the markers on the subject, as mentioned in Steps 1 and 2 in Section 4.2.4, the subjects were asked to remain in a standing pose and then jog on the treadmill at 7 km/h to record the coordinates of the markers positioned on the thorax or sports bra with different shoulder straps in a random order. The experiment was repeated three times in both static and jogging conditions for each type of shoulder strap. The subjects had a 2-minute break in between the two jogging cycles with the same strap, and a 5-minute break in between each test with different shoulder straps in order to prevent fatigue.

Then the origin "*o*" and three axes of the BCS were defined and the motion data were transferred from the GCS to the BCS (see Section 3.3.4 of Chapter 3) and the noise was filtered. Ten values of the positive and negative peak displacement for each jogging stride was determined for each condition. The method for extracting the peak values has been explained earlier in Section 4.2.6.

4.5.4 Statistical methods

The bra displacement during the 10 jogging strides with 10 different shoulder straps was averaged for 11 subjects (Three subjects have been excluded because the sports bras did not fit perfectly well on their breasts.). Repeated-measure two-way ANOVA ($p < 0.05$) with one within-factor (bra strap condition) was used to compare the data across different breast volumes and different shoulder straps, with a Bonferroni *post-hoc* analysis, using the Statistical Package for the Social Sciences (Version 15.0; SPSS Inc., Chicago, IL). A linear regression analysis was also applied to establish the relationships between the breast displacement and breast volume.

4.6 Results and discussion of Experiment 2

4.6.1 Bra displacement and volume

The breast volumes of the subjects ranged from 250 cm^3 to 396 cm^3. There were significant differences in the mean amplitude of bra displacement for the different breast volumes (all $p > 0.05$) with 10 different bra straps in all three directions, while 11 subjects were jogging for 10 strides.

Figure 4.23 shows the relationship between breast volume and mean amplitude of bra displacement. Unsurprisingly, the breast volume had a consistently positive effect on the bra displacement, but with different correlation coefficients R^2 in *x-, y-* and *z-* directions, as shown in Table 4.15

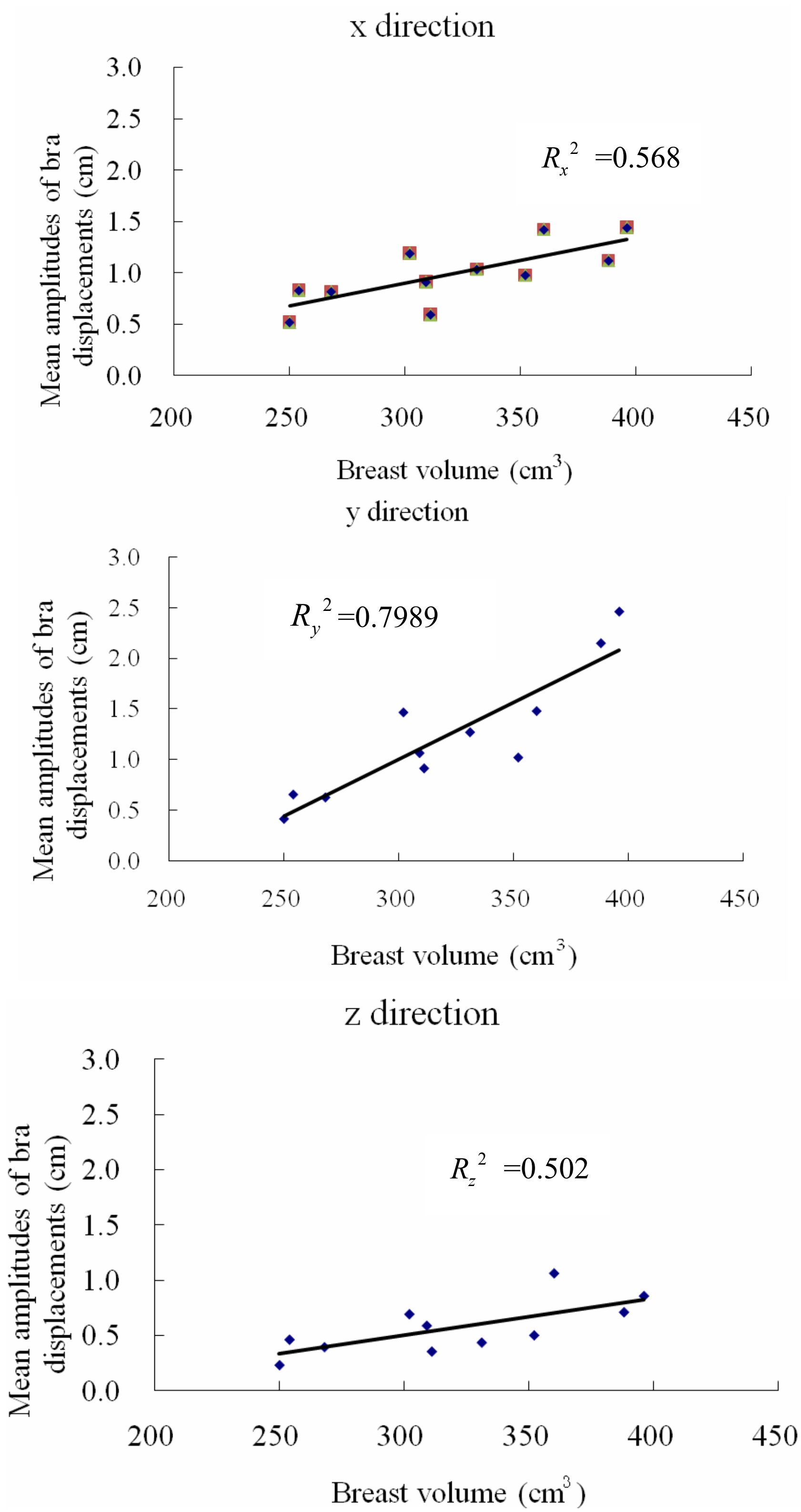

Figure 4.23 Relationships between breast volumes (cm^3) and the mean amplitudes of bra displacement of 11 subjects jogging for 10 strides

Table 4.15 shows that the correlation between breast volumes and bra displacement was significant and strong in the *y*-direction (R^2 = 0.7989, n = 11), but weak in the *x*- and *z*-directions (R^2 = 0.5021 & 0.5685 respectively). The larger breast had greater gravitational force to decelerate and accelerate the breast movement when the subject jumped up and down, respectively. The larger breast might have moved more superiorly and posteriorly, as shown in Figure 4.24. Therefore, the breast volumes were more strongly correlated with the bra displacement especially in the *y*-direction.

Table 4.15 Regression equations of breast volumes and mean amplitudes of bra displacement

Direction	Regression equation	R^2
x	$D_x = 0.0044V - 0.4353$	R_x^2=0.5685
y	$D_y = 0.0112V - 2.349$	R_y^2=0.7989
z	$D_z = 0.0034V - 0.515$	R_z^2=0.5021

D_x, D_y *and* D_z are the mean amplitudes of bra displacement of 11 subjects in *x*-, *y*- and *z*- directions respectively, V is the breast volume, R_x^2, R_y^2, R_z^2 are the correlation coefficients of three equations in *x*-, *y*- and *z*- directions respectively. The critical value of the Pearson Product-Moment Correlation Coefficient is 0.576 at a significance level of 0.05 for two-tailed test.

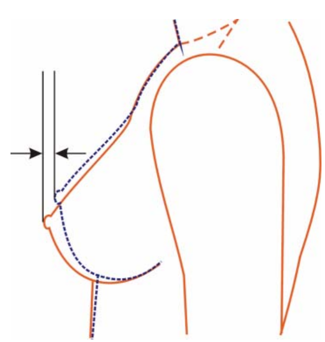

Figure 4.24 The breast deformation: The solid and dash lines are the points of the breast in static and dynamic conditions respectively

4.6.2 Bra movement and shoulder strap properties

To answer Q.4 if the shoulder strap properties affect the breast displacement, the modulus of shoulder strap at 25 % extension were plotted against the vertical bra displacement, for individual subjects, with different breast volumes presented in an decreasing order (Figure 4.25).

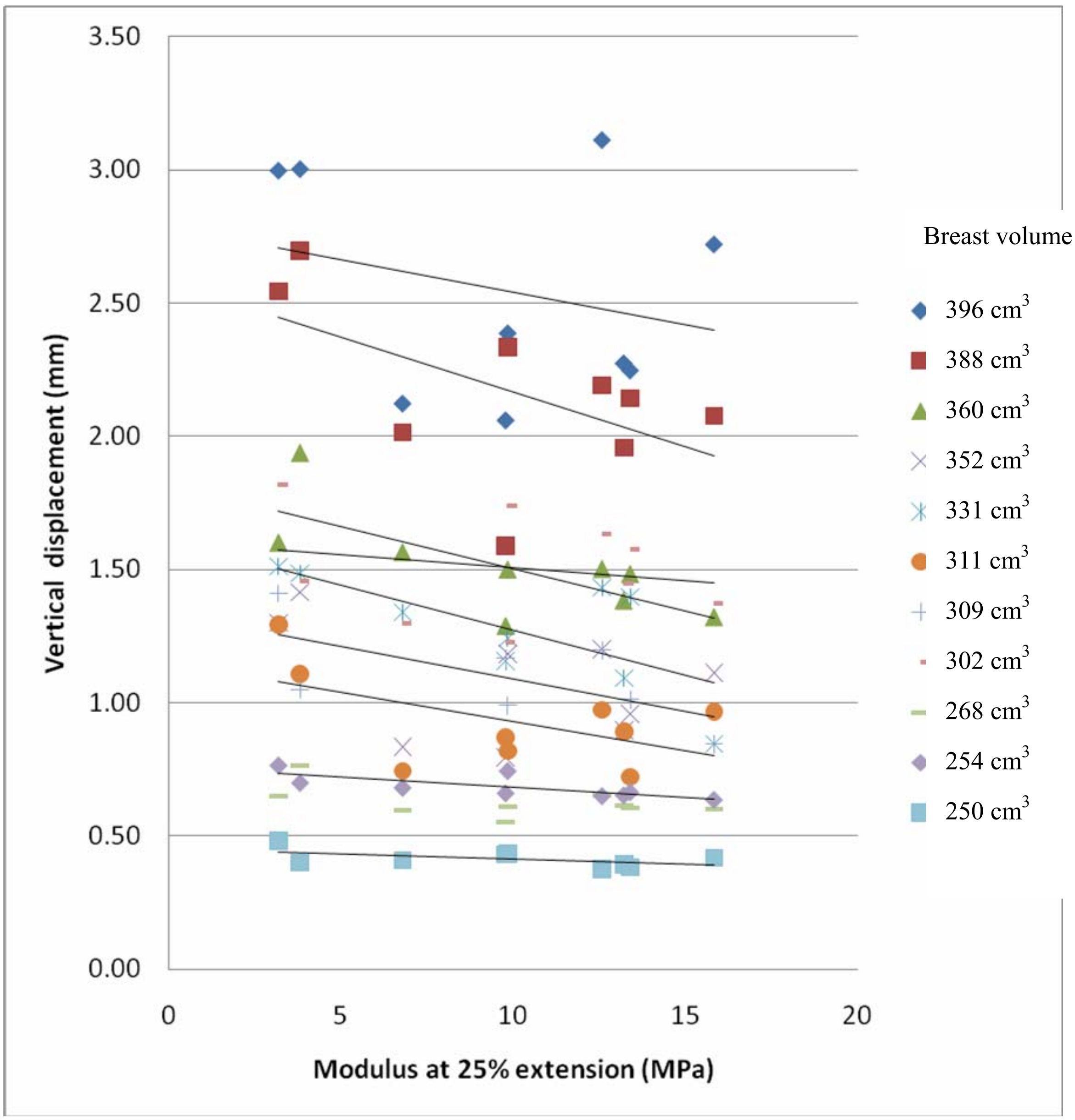

Figure 4.25 Modulus of shoulder strap versus vertical bra displacement

As shown in Figure 4.25, the modulus of the shoulder straps at 25% extension had an inverse relationship with the vertical bra displacement, for large breast volumes over 309 cm^3. However, the displacement for smaller breasts did not show any significant change with different shoulder straps. This finding could not be confirmed as no relevant literature has been published.

As mentioned in Table 4.13 there was pre-extension for the straps to fit the subjects' shoulders. The strap was working over 6.5 ± 3.7% extension during jogging, so the load at that point of extension in the third cycle of loading was used to plot against the vertical displacement and RBD for individual breast volume, as shown in Figure 4.19.

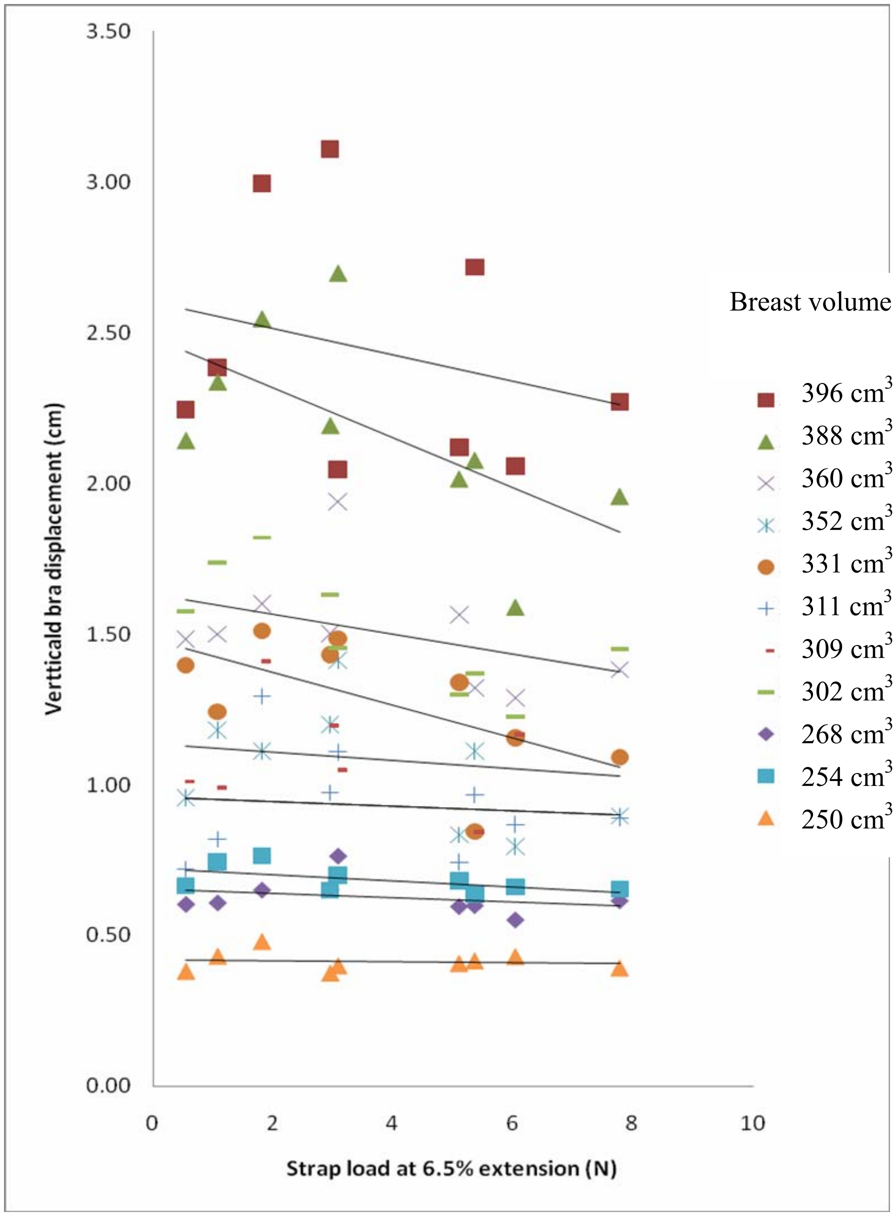

Figure 4.26 Strap load at 6.5% extension versus vertical bra displacement

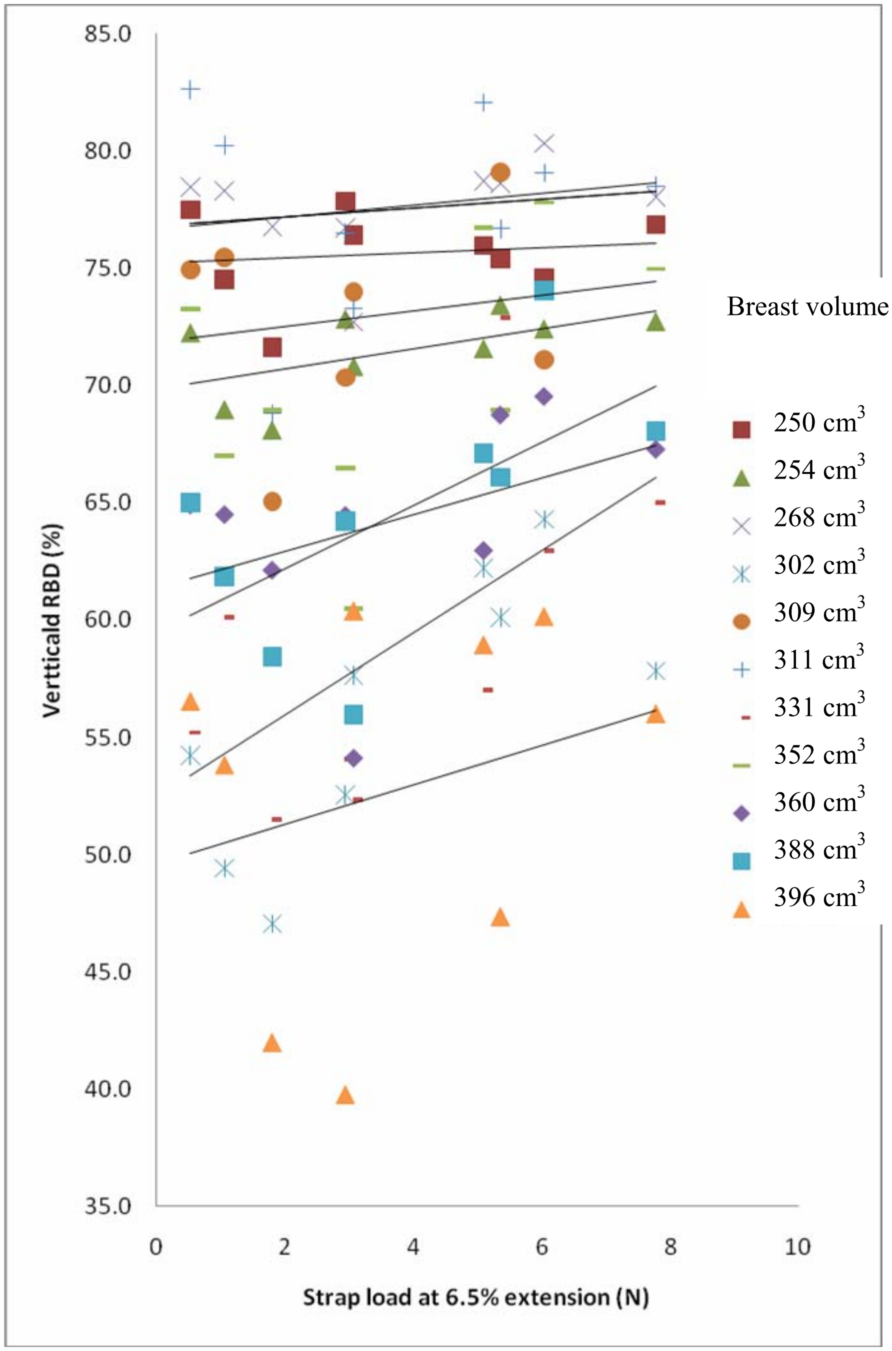

Figure 4.27 Strap load at 6.5% extension versus vertical RBD

As shown in Figures 4.26 and 4.27, the load of the shoulder straps at 6.5% extension also had an inverse relationship with the vertical bra displacement, and had a positive relationship with the vertical RBD for large breasts rather than smaller breasts.

In the light of this, it was proposed to derive mechanical models to analyse the mechanics of different combinations of shoulder straps. This will be presented in Chapter 5.

4.7 Conclusions from Experiment 2

To conclude, the vertical bra movement significantly increased with increasing breast volume, but less significantly in the *x*- and *z*- directions. There was inverse relationship between bra displacement and the shoulder strap modulus at 25 %, more obviously for larger breast volumes in excess of 309 cm^3.

4.8 Conclusions

In Experiment 1 as a pilot study applying the BCS, the 3D relative displacement of six breast points of four women was evaluated in both braless and sports bra conditions during walking, jogging and stepping. When comparing the previous studies regarding the nipple displacement during braless jogging, the mean displacement in this study (1.5 cm anterior-posterior, 1.4 cm vertical, and 0.8 cm medial-lateral) was smaller than that reported for D-cup women (3.7 cm anterior-posterior, 4 cm vertical, and 3.4 cm medial-lateral). In the sports bra condition, the mean nipple displacement in this study was reduced to 0.2 cm - 0.7 cm in three different directions, which were also smaller than a previous study (1.4 cm in encapsulation bra and 2.0 cm in compression bra). The difference was considered reasonable because smaller-breasted women would have smaller nipple displacement during jogging.

The maximum displacement among six breast points was found at nipple during braless activities, so it confirmed that the trajectory of nipple movement can be used as indicative data for deriving the trajectory for the centre of breast mass in a breast mechanical model, based on the coordinate relationship between the nipple and the centre of breast mass, in Chapter 5.

The paired *t*-tests showed that displacement at the nipple was significantly different from other breast points. It confirmed the advantages of using multiple breast points to provide important information on the comprehensive breast movement corresponding to different aspects of bra design to ensure adequate support for the whole breast.

The bra samples were the most effective in controlling the breast movement in the medial-lateral direction, but less effective in the anterior-posterior direction, so more attention will be required in designing the bra's centre front, the plasticity of cup fabric and the location of cup seam and neckline. To improve the effectiveness of sports bras at the top part of the breast, the neckline height should fit the upper breast boundary even during exercise.

The more effective bras for the four subjects who were tested had common features such as compression type, short vest style, high neckline, rigid cup seams, side slings, racer-back panel, bound neckline with slight elasticity, no centre gore, no cradle, no wire, no pad, and non-adjustable wide strap.

The vertical bra movement significantly increased with increasing breast volume, but less significantly in the *x*- and *z*- directions. Smaller vertical bra displacement was observed for higher modulus of shoulder straps. Therefore, designers of sports bras were recommended to use wider shoulder straps for larger-breasted women.

Chapter 5 Development of breast mechanical model

5.1 Introduction

As reviewed in Section 2.6, when breast tissue moves relative to the thorax, there is internal force acting on the breast tissue. This internal force may cause breast discomfort and sag. It is also therefore important to evaluate the effects of sports bras on the mechanical support of the wearer's breasts. Force that acts on the body has been directly measured using a strain gauge [66]. However, the device would have to be attached onto the human skin, and matched for extensibility (strain gauges are more commonly used for low strain applications and calibration in situ is difficult) so this is not really a practical way to measure the force on women's breasts in *vivo*. To date, no finite element model has been published to compute the internal force of the breast tissues. Gefen and Dilmony [21] first used free body diagrams to analyse the internal breast force supported by the Cooper's ligaments, the pectoralis fascia and the ribs, in static postures (standing, kneeling on all fours, and lying supine) and during dynamic activities (walking, running, jogging, stair climbing and jumping in a vertical direction). However, the internal force within the breasts in the medial-lateral and anterior-posterior directions during activities remain unknown. Therefore, it was aimed in this study to apply the experimental results of breast motion analysis in Chapter 4, to develop a new 3D breast mechanical model to evaluate the 3D internal force of the whole breast involved during jogging exercises, based on the following assumptions.

- The breast was considered as a homogeneous object made of soft matter with elastic damping properties.
- The movement of the centre of the breast's mass (CBM) could represent those of the whole breast.
- The coordinates of the CBM have a constant relationship with those of the nipple in both static and dynamic conditions.
- All the forces acting on the breast can be decomposed and/or synthesized into component force acting on the breast in three orthogonal directions.

5.2 Methodology

5.2.1 Breast mechanical model

A breast is an elastic and viscously soft object. Therefore, an alternative approach to finite element modelling for the development of a 3D model to simulate the breast is to consider it to be analogous to a system comprising a mass, springs and dampers. An advantage of such a model is that it also affords a better theoretical understanding of the physical behaviour of the breast during exercise.

To develop the breast mechanical model, the force acting on the breasts was considered in the *x-, y-* and *z-* directions. The CBM, defined as the mean location of all the masses in the breast was assumed to represent the whole breast. In this study, the breast was assumed to be homogeneous visco-elastic object. Based on the measured breast displacement, velocities and acceleration, a model based on the Kelvin-Voigt model [103] comprising a mass, six springs and six viscous dampers was developed to describe the force on the breasts under braless and sports bra conditions during jogging, as shown in Figure 5.1.

The Kelvin-Voigt model needs an input of viscous constant damping ratio ζ. The logarithmic decrement method [104] in the time domain was used in this study. It means the natural logarithmic value of the ratio of two adjacent peak values of vibration displacement in free decay. A free vibration experiment of the Subject A's breast was performed in a standing position, which will be described in Section 5.2.4.

For this theoretical study, the breast was assumed to be represented by a single point mass with pairs of springs and dashpots attached to the mass in three orthogonal directions.

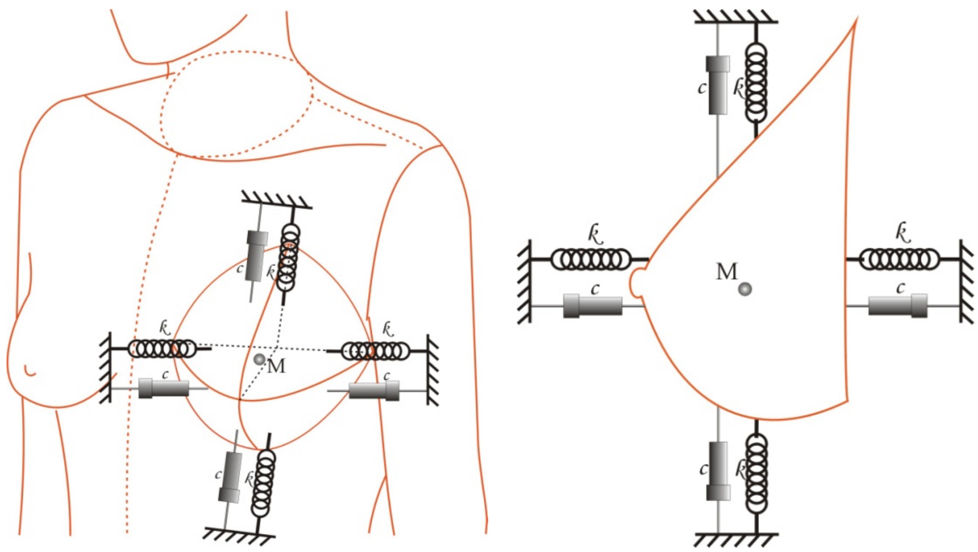

Figure 5.1 Schematic of the proposed model to evaluate the force on breasts during jogging (M is the CBM, *k* is the spring constant and *c* is the viscous damper of damping coefficient)

Each mass spring dashpot component was considered to be an ideal spring-damper system with mass *m* (in kg), spring constant *k* (in N/m) and viscous damper of damping coefficient *c* (in N/s or kg/s) that is subjected to an oscillatory force (F_S) where:

$$F_S = -kx$$

and the damping force (F_D): $F_D = -c\dot{x}$

where x is the amount of the stretched spring; and $\dot{x}$ is the velocity of the whole breast.

An external force $f\left(t\right)$ acts on the breast mass as shown in Figure 5.2.

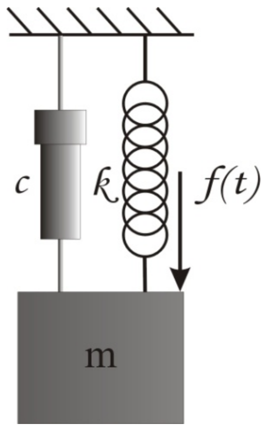

Figure 5.2 Mass attached to a spring and damper

Treating the breast mass as a free body and applying Newton's second law, the total force F_{tot} on the breast is:

$$F_{tot} = ma = m\frac{d^2x}{dt^2} = m\ddot{x}$$

where a is the acceleration (in m/s^2) of the breast mass.

Since $F_{tot} = f(t) + F_S + F_D$,

$$m\ddot{x} = f(t) - kx - c\dot{x} \tag{5.1}$$

This differential equation (5.1) may be rearranged into Equation 5.2 as:

$$f\left(t\right) = m\ddot{x} + c\dot{x} + kx \tag{5.2}$$

Based on Equation (5.2), the equations of the force on the breasts can be written as follows:

$$F_x = m_b \ddot{x}_x + c_b \dot{x}_x + k_b x_x \tag{5.3}$$

$$F_y = m_b \ddot{x}_y + c_b \dot{x}_y + k_b x_y \tag{5.4}$$

$$F_z = m_b \ddot{x}_z + c_b \dot{x}_z + k_b x_z \tag{5.5}$$

where F_x, F_y, F_z is the force, $\ddot{x}_x, \ddot{x}_y, \ddot{x}_z$ are the accelerations, $\dot{x}_x, \dot{x}_y, \dot{x}_z$ are the velocities and x_x, x_y, x_z is the displacement of the CBM along the *x*-, *y*- and *z*- axes, respectively.

The equations of the force on the breasts under braless and sports bra conditions can be written as shown in Table 5.1.

Table 5.1 Equations of the force on the breasts during jogging

Direction	Braless condition	Sports bra condition
x	$F_1 = m_b \ddot{x}_1 + c_b \dot{x}_1 + k_b x_1$ (5.6)	$F_4 = m_b \ddot{x}_4 + c_{sb} \dot{x}_4 + k_{sb} x_4$ (5.7)
y	$F_2 = m_b \ddot{x}_2 + c_b \dot{x}_2 + k_b x_2$ (5.8)	$F_5 = m_b \ddot{x}_5 + c_{sb} \dot{x}_5 + k_{sb} x_5$ (5.9)
z	$F_3 = m_b \ddot{x}_3 + c_b \dot{x}_3 + k_b x_3$ (5.10)	$F_6 = m_6 \ddot{x}_6 + c_{sb} \dot{x}_6 + k_{sb} x_6$ (5.11)

where F_1, F_2, F_3 is the force in the *x*-, *y*- and *z*- directions, respectively, under the braless condition. F_4, F_5 *and* F_6 is the force in the *x*-, *y*- and *z*- directions, respectively, under the sports bra condition.

5.2.2 Data required to build the breast mechanical model

To construct a 3D mechanical model based on the analogy, and to derive the force acting on the breast, the following tasks and data were needed.

a) scanning of breast shapes to determine the CBM and its 3D relationship with the nipple;

b) free vibration of a breast to estimate the values of spring constants and damping coefficients of the breast; and

c) motion analysis to determine the nipple displacement against time during jogging.

The concepts to be tested were that

- the breast mechanics referred to the CBM of the human subjects, not the breast surface points;

- the centre of breast mass moved with the nipple in a known relationship, to confirm that the breast force under supported and braless conditions during jogging was nonlinear like the nipple displacement; and

- the breast force could be estimated by the mechanical model, with given spring constant, viscous damping coefficients and the CBM-nipple relationship.

It was assumed that the breast was a homogeneous object made of soft matter and that the movement of the centre of the breast mass could represent those of the whole breast. A method needed to be devised to determine the CBM and its 3D motion relationship with the nipple.

5.2.3 Scanning of breast shapes

Magnetic resonance imaging is a reliable, but expensive method to locate the centre of the human breast. However, such a facility was not available. Furthermore, due to the reluctance of the subjects to undergo such imaging and the limited budget, alternative methods were considered to obtain data on various sizes of human breasts.

Therefore, the following methods to characterise the human breast shapes were investigated in order to construct the breast model.

- Finite element analysis of human breasts; and
- Laser scanning of breast prostheses.

5.2.3.1 Finite Element analysis of human breasts

To characterise real breast shape, finite element methods were first considered. Modelling of the breasts using finite element methods is still in its infancy [79]. The breast is an inhomogeneous structure containing different tissue layers of different mechanical properties [21]. Accurate identification of the body parameters such as boundary conditions and material properties is very important for finite element models [105].

In our previous study, individual-specific biomechanical models of the human breasts were constructed. The procedure involved the following nine steps.

i. Captured the nude breasts of subjects by the 3D Photogrammetric imaging system (Industrial Centre, The Hong Kong Polytechnic University);
ii. Built the 3D geometric breast model;
iii. Determined the breast boundary based on the breast surface measurements from the nipple to the landmarks on the breast boundary;
iv. Imported the geometric breast model to the finite element software (ANSYS 12.0, ANSYS Inc., USA);

v. Created the 3D meshes for the finite element model of the breast by applying solid 8-node (hexahedral) tri-linear parametric elements;

vi. Calculated every hexahedral volume automatically by the ANSYS software;

vii. Calculated the total breast volume by summing up all the hexahedral volumes;

viii. Calculated the CBM automatically by the ANSYS software;

ix. Calculated the breast mass as the product of the breast volume and density.

The detailed descriptions of the subjects, Photogrammetric imaging system and research procedures are described below.

Subjects

In the study, two healthy Chinese women subjects of the most common breast sizes volunteered with informed consent to participate in this study. Subject A was 40 years old female with tear-shaped asymmetric dropping breasts in size 80B, married and had breast-fed one child 10 years ago. She had a body mass index of 22.6 kg/m^2. Subject B was aged 21 with round-shape breasts in size 75C. She was not married and had a body mass index of 21.8 kg/m^2. Both of them had no previous breast surgery.

3D photogrammetric breast imaging

The subjects were scanned by a 3D photogrammetric body imaging system (Figure 5.3) recently developed by the Industrial Centre of the Hong Kong Polytechnic University.

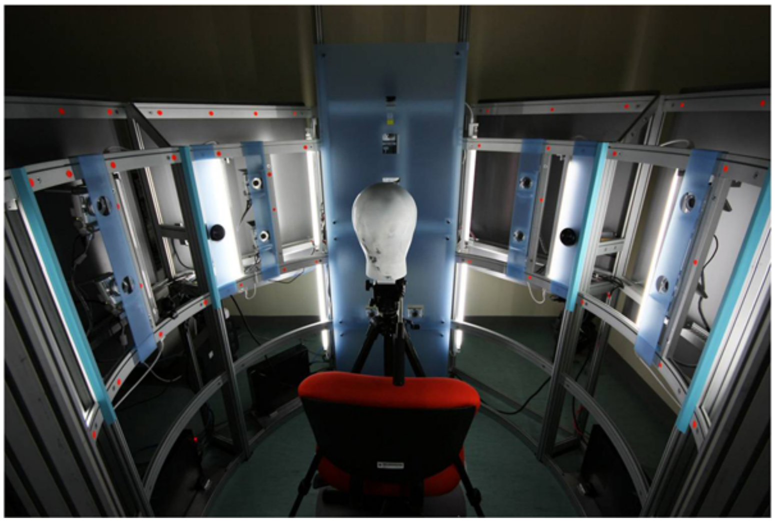

Figure 5.3 3D photogrammetric body imaging system

This optical system acquired high-definition data in terms of geometric and textural information. It generated 3D high-resolution point clouds with an average point-to-point distance of less than 1 mm. This allowed very fine surface features to be captured. The geometric breast model (Figure 5.4 b) was developed.

	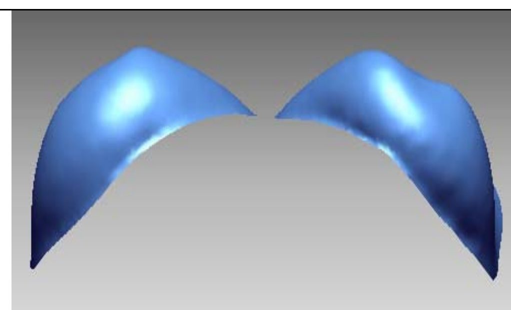
a) Geometric breast model from front view	b) Geometric breast model from bottom view

Figure 5.4 Building of geometric breast model

Determination of breast boundaries

The upper breast boundary was defined based on breast surface measurements from the superior end to the nipples. Other parts of the boundary were identified by observing the breast root. The 3D meshes of the arbitrary breast section are shown in Figure 5.5.

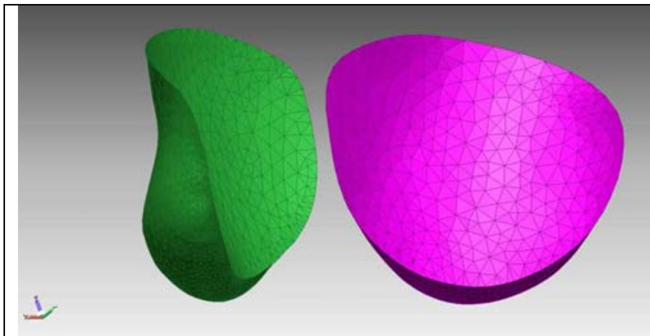

Figure 5.5 3D meshes of the breast section

Calculation of breast volume and centre of mass

Every hexahedral volume was calculated using the ANSYS software. For Subject A, the total breast volume was ($V_b = 3.112 \times 10^{-4} m^3$) by summing up all hexahedral volume. Then the centre of mass was calculated automatically by the software. The breast mass was $m_b = V_b \times D_b$ where D_b was breast density (D_b=1017 kg/m^3 [25]), so, m_b=0.31649 kg.

Limitation of the FEM method

The experience showed that it was feasible to use finite element methods to determine the CBM. However, it was very time-consuming because it required substantial effort in the building of the geometric model and mesh creation for the finite element model. Within the limited time, it was unrealistic for this study to continue using this method to find the relationship between the CBM and nipple for more subjects. Therefore, a more convenient method of using breast prostheses was used. Discussions are as follows.

5.2.3.2 Scanning of breast prostheses

From the experiences learnt from the finite element method for locating the centre of mass based on body-scanned images, it was believed that using tangible breast forms from which measurements could be a simpler and more convenient approach. Ideally, a silicon breast form duplicated from the subject's breasts should have been made. However, due to the limited resources in this postgraduate study, breast prostheses that were available in the University were used to approximate to the human breast shapes. The potential inaccuracy of this approach is acknowledged but at least it enabled the model concepts to be tested. The approach was to use the breast prostheses to derive a relationship between the position of the centre of the breast prosthesis' mass (CBM) and the nipple, which could then be used to extrapolate the motion of the CBM from the trajectory of nipple displacement in actual breasts.

Therefore, to locate the CBM and the nipple point of different breast sizes (Table 5.2), eleven commercially-available breast prostheses (Naturalwear byTrulife, Ireland) of different sizes were scanned using a NextEngine 3D laser scanner (Next Engine Inc., Santa Monica, California, America).

Table 5.2 Size specifications of 11 breast prostheses (unit: cm)

		Band size												
Cup size	B	⋮	⋮	60	65	70	75	80	85	90	95	100	105	110
	C	⋮	⋮	⋮	60	65	70	75	80	85	90	95	100	105
	D	⋮	⋮	⋮	⋮	⋮	65	70	75	80	85	90	95	100
	DD	⋮	⋮	⋮	⋮	⋮	⋮	⋮	70	75	80	85	90	95
		↓	↓	↓	↓	↓	↓	↓	↓	↓	↓	↓	↓	↓
		01	02	03	04	05	06	07	08	09	10	11	12	13

Source: http://recoveryelements.com/images/TrulifeSizingGuide.pdf

Triangular shaped breast prostheses of sizes ranging from 03 to 13 (Table 5.2) were used to represent the women's breasts, because they have been used for over ten years by the mastectomy patients who have lost one or both breasts in Hong Kong. The sizes used included the sizes for the subjects in this study (i.e. size 06 to 10, for breast sizes 75B to 85D), with additional three smaller sizes (03 to 05) and three larger sizes (11 to 13). The coordinates of the centre of the breast prosthesis' mass (CBM) were obtained using the Rapidform 3D data processing software (Rapidform 2006, INUS Technology, Inc.) with the following procedures.

Preparation: The NextEngine laser 3D scanner (NextEngine Inc. Santa Monica, California, America) was calibrated before scanning. Any five points were marked on the breast prosthesis for later alignment to build a geometrical model of the breast prosthesis. Then it was placed under the shelf of the scanner as shown in Figure 5.6.

Figure 5.6 NextEngine 3D scanning apparatus

Scanning: Different viewing angles of the breast prosthesis were captured by rotating the auto-positioning turntable. Figure 5.7 shows the scanning process and the scanned images from different viewing angles.

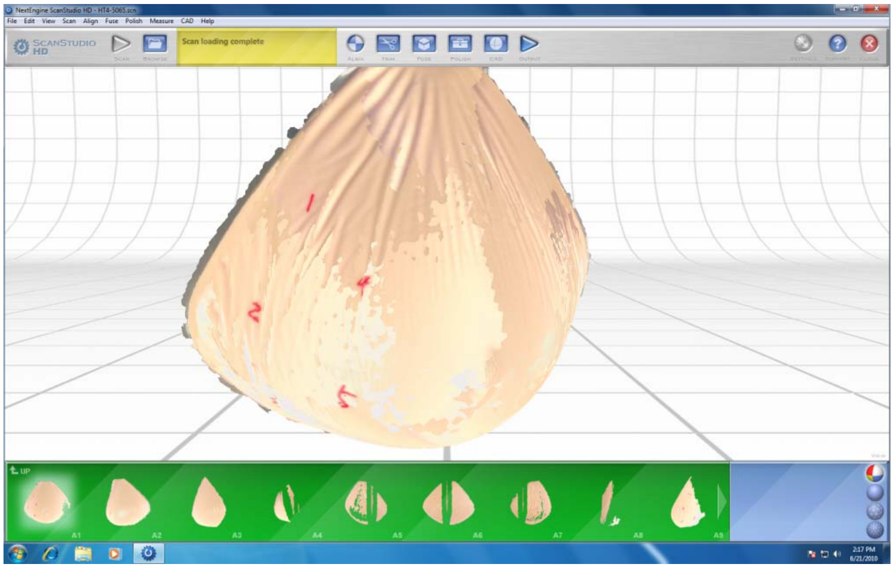

Figure 5.7 Scanned images of a breast prosthesis

Aligning: After aligning the marked points on any two scanned images of the breast prosthesis, the images were combined and rendered into a single integrated 3D model of the breast surface.

Fusing: The 3D surface was then “fused” to ensure a single smooth surface model with no overlapping.

Transforming: The 3D surface model was imported into the Rapidform software for computing the coordinates of the CBM.

Measuring: The locations of the CBM and the nipple point of the breast prosthesis were identified automatically by the Rapidform software.

The NextEngine 3D scanner was not recommended to be used to scan a live subject because the surface images of the torso and breasts were connected. When they were separated, the breast part would be like a shell not a solid.

5.2.3.3 Coordinates of the CBM and nipple point of the breast prosthesis

To derive the coordinates of the CBM relative to the nipple point, breast prostheses were used, and the coordinates were obtained in the following three steps.

Step 1: Calculating the breast origin "o" of the prosthesis in the GCS

As the breast prosthesis is left-right symmetrical and maintained in a static condition during scanning, the mid-point between the outermost and innermost points (BO-BI) was regarded as the breast origin "*o*" in the GCS:

$$x_o = \frac{x_{po} + x_{pi}}{2}, \; y_o = \frac{y_{po} + y_{pi}}{2} \text{ and } z_o = \frac{z_{po} + z_{pi}}{2}$$

where (x_o, y_o, z_o), (x_{po}, y_{po}, z_{po}) and (x_{pi}, y_{pi}, z_{pi}) are the coordinates of breast origin "*o*", and the Rapidform software system automatically calculated the coordinates of the most lateral point on the left breast (BO) and the most medial point on the left breast (BI) in the GCS.

Step 2: Transforming the coordinates from the GCS to the BCS

Since the breast prosthesis is static, the coordinates of the CBM (x_{bw}, y_{bw}, z_{bw}) and the breast prosthesis' nipple (x_{bp}, y_{bp}, z_{bp}) in the BCS are simply calculated as follows.

$$x_{bw} = x_{wo} - x_{po}, \; y_{bw} = y_{wo} - y_{po} \text{ and } z_{bw} = z_{wo} - z_{po}$$

$x_{bp} = x_{pl} - x_{po}$, $y_{bp} = y_{pl} - y_{po}$ and $z_{bp} = z_{pl} - z_{po}$

where (x_{wo}, y_{wo}, z_{wo}) and (x_{pl}, y_{pl}, z_{pl}) are the coordinates of the CBM and the breast prosthesis' nipple, respectively, in the GCS.

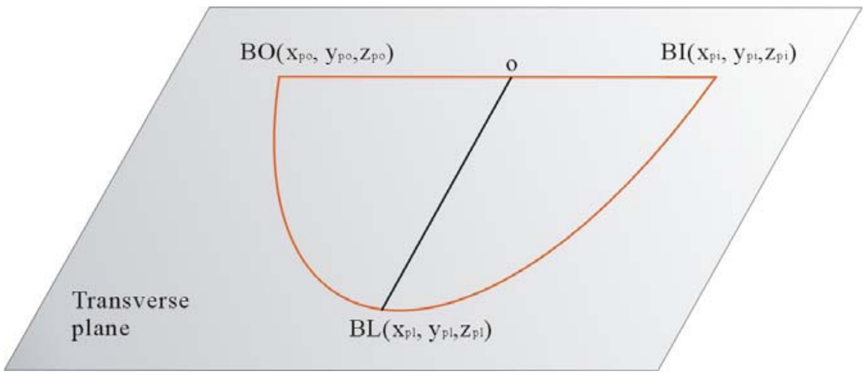

Figure 5.8 Transverse plane of BL, BO and BI

Step 3: Calculating the relationship between the coordinates of the CBM and those of the breast prostheses' nipple in the BCS

Table 5.3 Coordinates of the breast prostheses' nipple point (x_{bp}, y_{bp}, z_{bp}) and the CBM (x_{bw}, y_{bw}, z_{bw}) (unit: cm)

Breast prosthesis	x_{bp}	x_{bw}	y_{bp}	y_{bw}	z_{bp}	z_{bw}
1	4.4	1.7	-1.1	0.2	-1.0	-0.5
2	4.8	1.9	-1.5	-0.2	0.2	0.8
3	5.0	2.2	-1.8	-0.2	0.3	0.0
4	5.6	2.4	-2.0	-0.8	0.4	0.1
5	5.8	2.6	-2.0	-0.5	0.5	0.2
6	7.5	3.3	-2.2	-0.9	0.8	0.5
7	8.2	3.5	-3.0	-1.1	1.0	0.3
8	8.3	3.1	-3.5	-1.5	1.2	0.2
9	8.5	3.1	-3.5	-1.8	2.9	1.9
10	9.3	3.8	-3.9	-2.4	4.2	2.2
11	10.0	3.8	-4.3	-2.5	4.5	2.7

Table 5.3 shows the coordinates of the CBM (x_{bw}, y_{bw}, z_{bw}) and those of the

breast prostheses' nipple (x_{bp}, y_{bp}, z_{bp}) in the BCS.

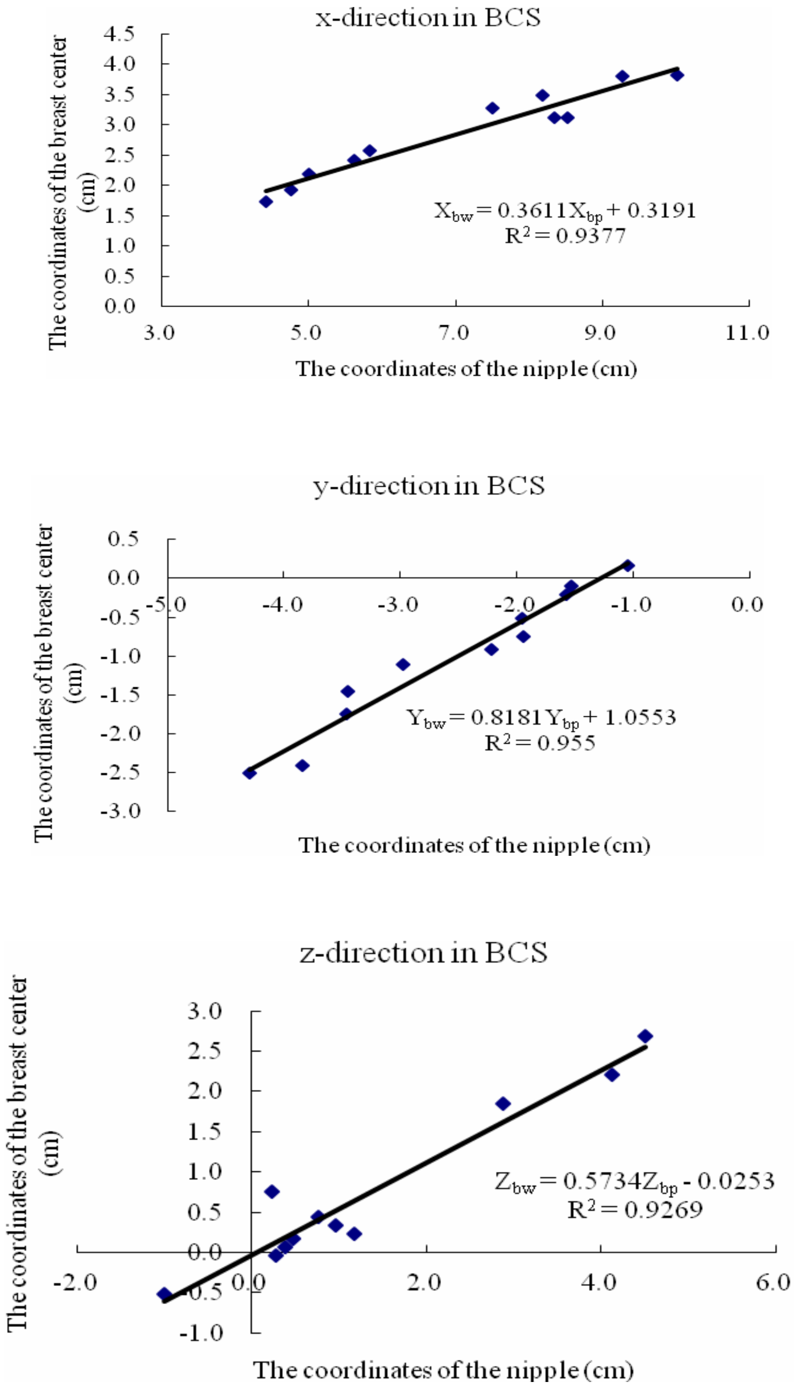

Figure 5.9 Relationships between the coordinates of the CBMs and nipple points of 11 breast prostheses

Figure 5.9 shows the 3D coordinates of the breast prosthesis' nipple point and the CBM. Their relationships are described by linear equations in three orthogonal directions.

$$x_{bw} = 0.3611x_{bp} + 0.3191,\ R^2 = 0.9377 \tag{5.12}$$

$$y_{bw} = 0.8181y_{bp} + 1.0553,\ R^2 = 0.955 \tag{5.13}$$

$$z_{bw} = 0.5734z_{bp} - 0.0253,\ R^2 = 0.9269 \tag{5.14}$$

where (x_{bp}, y_{bp}, z_{bp}) and (x_{bw}, y_{bw}, z_{bw}) are the coordinates of the breast prosthesis' nipple point and the CBM.

5.2.4 Free vibration of breast

As mentioned in Section 5.2.2 point b), in order to construct a 3D mechanical model and to derive the force acting on the breast, a free vibration test of a breast would be helpful to estimate the values of spring constants and damping coefficients of the breast. Therefore, in vivo experiments of free vibration of the breast were carried out under braless and sports bra conditions. The spring constant of the breast is mainly related to the oscillation frequencies and breast mass through the following equation.

$$k_b = (2\pi f_b)^2 \times m_b,$$

where k_b is the spring constant of the breast, f_b is the oscillation frequency of the breast and m_b is the breast mass.

A spherical retro-reflective marker with a diameter of 9.5 mm and a mass of 1.81 g was used in the experiment to measure the natural frequency of free vibration of the breast. The marker was attached at the left nipple of Subject A , whose breast size was 80B in a ptotic drooping tear shape, or on the left bra cup.

The subject was asked to stand still and look straight ahead. The left breast was gently raised by herself with her left palm and held stationary. Then her palm was quickly removed from the breast to allow it to freely vibrate due to the breast mass and inertia. The vibration motion was recorded by a six-camera Vicon system as described in Section 4.2.3, with a sampling frequency of 120 Hz. The experiment was repeated for three times under the same conditions. The procedures of data processing are as follows.

5.2.4.1 Data processing

a) Spring constants of the breasts

Under a braless condition

The following three steps were used to derive the spring constant of the breasts.

Step 1: Evaluating the oscillation frequency of the breasts

Figure 5.10 shows the waveforms of breast movement in a vertical direction. The waveforms were acquired from the damped natural oscillation in a braless condition.

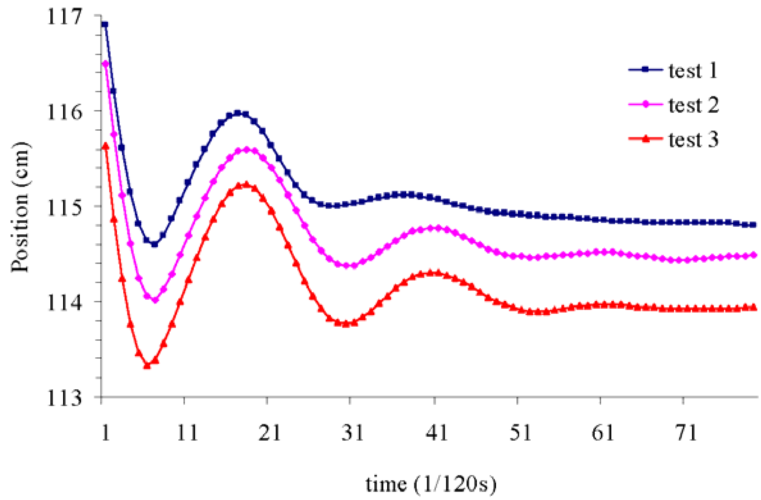

Figure 5.10 Three waveforms of breast displacement in a vertical direction

Frequency is defined as the number of cycles per unit time. It is the reciprocal of the oscillation period T as shown in Figure 5.11.

$$f_b = \frac{1}{T} \tag{5.15}$$

where f_b is the oscillation frequency of the nude breast (in Hz).

According to the average natural frequency of the breast as shown in Figure 5.11, $T = \frac{24}{120}(s) = \frac{1}{5}(s)$, the oscillation frequency of the breast is calculated to be 5 Hz under a braless condition.

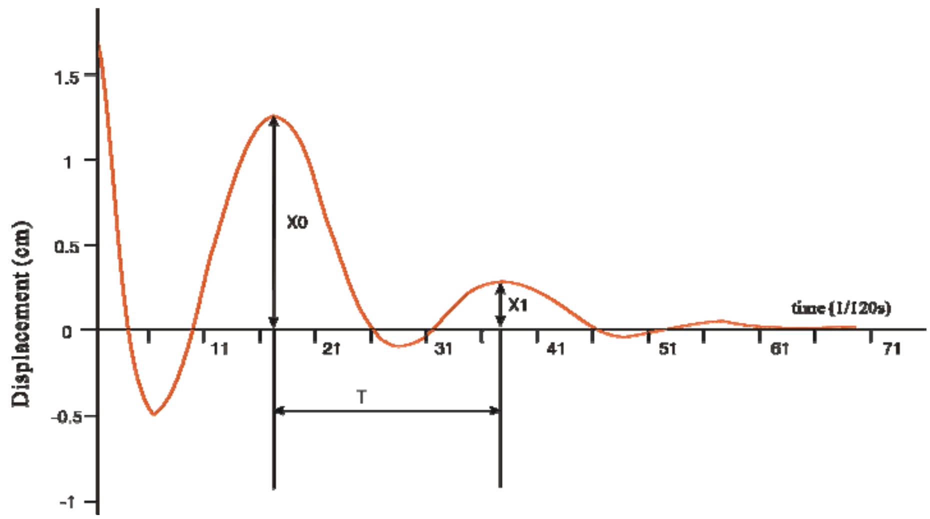

Figure 5.11 Single waveform of displacement in a vertical direction

Step 2: Calculating the angular frequency of the breasts

The angular frequency can be written as:

$$\omega_b = 2\pi f_b \tag{5.16}$$

where ω_b is the angular frequency of the nude breast measured in radians per second. This frequency can be regarded as that of the projected simple harmonic motion, which is the same as the angular velocity of a circular motion.

When dealing with small oscillations [106]:

$$\omega_b = \sqrt{\frac{k_b}{m_b}} \tag{5.17}$$

where k_b is the spring constant of the naked breast and m_b is the breast mass.

Step 3: Estimating the spring constant of the breasts

k_b can be calculated from Equations (5.16) and (5.17).

$$k_b = (2\pi f_b)^2 \times m_b \tag{5.18}$$

where the breast volume of Subject A is 311.5 cm^3 . The method of determining the breast volume was reported in Section 4.5.3.1, and the breast density suggested by literature was 1.017×10^{-3} kg/cm^3 [25].

So, $m_b = 0.3168$ *kg* and $k_b = 312.36$ N/m in a braless condition.

Under a sports bra condition

The spring constant is an important material property for the breasts within the breast mechanical model. Under different breast-supporting conditions, the spring constants are likely to be different, so it is necessary to do further experiments to study breast motion in a sports bra with different levels of support. Using the above-mentioned steps, the spring constants under a sports bra condition with nine different shoulder straps were determined as shown in Table 5.4.

Table 5.4 The oscillation frequencies f_{sb} and the spring constants k_{sb} of the breast with different shoulder straps

Shoulder strap	SS1	SS2	SS3	SS4	SS5	SS6	SS7	SS8	SS9
f_{sb} *(Hz)*	5.33	5.85	6.32	7.06	7.27	5.58	6.00	6.32	6.86
k_{sb} (N/m)	354.94	427.58	499.04	622.75	660.35	389.02	449.79	499.04	587.97

where f_{sb} and k_{sb} are the oscillation frequencies and spring constants of the breast under a sports bra condition, respectively.

A linear relationship between the strap modulus (at 40% extension) and the spring constants for the breast is shown in Figure 5.12.

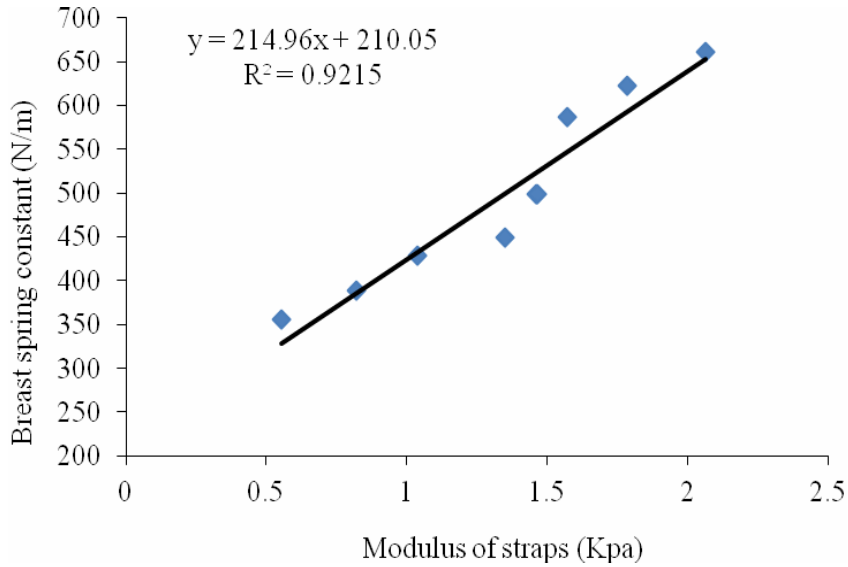

Figure 5.12 Linear relationship between the strap modulus and spring constant of the breast

The linear relationship can be written as follows:

$$k_{sb} = 214.96M_{ss} + 210.05\,,\ R^2 = 0.9215 \qquad (5.19)$$

where M_{ss} is the strap modulus (Table 4.13).

b) Damping coefficients of the breasts

Under a braless condition

The following three steps were used to evaluate the damping coefficients.

Step 1: Calculating the logarithmic decrement

The logarithmic decrement, δ, is used to derive the damping ratio of an under-damped system in a time domain [107]. δ is the natural *log* of the amplitudes of any two successive peaks.

$$\delta = \frac{1}{n} \ln \frac{x_0}{x_n} \tag{5.20}$$

where x_0 is the greatest amplitude and x_n is the amplitude of a peak that is *n* periods away. Any *n* can be used to calculate the logarithmic decrement (δ_b). When *n*=1,

$$\delta_b = \ln \frac{x_0}{x_1} \tag{5.21}$$

where δ_b is the logarithmic decrement in the braless condition, x_0 and x_1 can be attained from Figure 5.11.

Step 2: Measuring the damping ratio

The damping ratio is found from δ.

$$\zeta = \frac{\delta}{\sqrt{(2\pi)^2 + \delta^2}} \tag{5.22}$$

where ζ is the damping ratio

Hence, the damping ratio, ζ_b, in a braless condition is

$$\zeta_b = \frac{\delta_b}{\sqrt{(2\pi)^2 + \delta_b^{\,2}}} \tag{5.23}$$

ζ_b can also be expressed as

$$\zeta_b = \frac{c_b}{2\sqrt{m_b k_b}} \tag{5.24}$$

where c_b is the damping constant of the naked breast.

Step 3: Evaluating the damping constant

According to Equations (5.18) and (5.24), c_b can be written as

$$c_b = 4\pi f m_b \zeta_b\,. \tag{5.25}$$

Based on Equations (5.25), (5.23) and (5.21),

$$c_b = 4\pi f m_b \times \frac{\delta_b}{\sqrt{(2\pi)^2 + \delta_b^{\,2}}} = 4\pi f m_b \times \frac{\ln\frac{x_0}{x_1}}{\sqrt{(2\pi)^2 + (\ln\frac{x_0}{x_1})^2}}\,. \tag{5.26}$$

So, c_b can be calculated based on Equation (5.26) in which c_b = 3.9525 Ns/m.

Under sports bra condition

According to the results of the experiments in which Subject A wore a sports bra with different shoulder straps (Section 4.5.2), a relationship between the strap modulus and the damping constant was obtained, as shown in Figure 5.13.

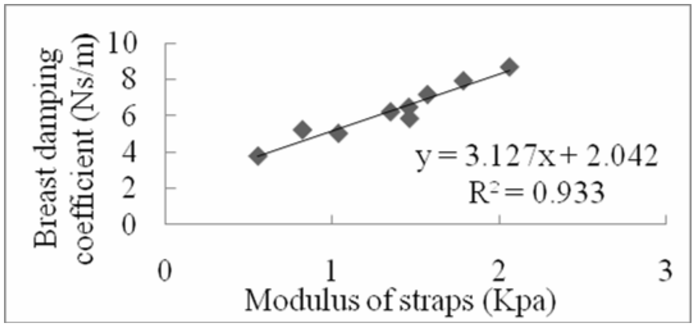

Figure 5.13 Linear relationship between strap moduli and damping coefficients

The linear relationship is

$$c_{sb} = 3.1278M_{ss} + 2.0421, R^2 = 0.9337 \tag{5.27}$$

where c_{sb} is the damping constants under a sports bra condition and M_{ss} is the strap modulus (Table 4.13), respectively.

5.3 Results

5.3.1 Motion curves of nipple displacement

As mentioned in Section 5.2.2 point c), the 3D motion data of the nipple displacement was required to derive the force acting on the breast. To predict the breast force in the breast mechanical model, it is first necessary to obtain characterized equations of 3D nipple displacement, velocity and acceleration. Therefore, the SYSTAT TableCurve 2D v5.01 software (Systat Software UK Ltd., London, UK) was used to fit the nonlinear curves of the 3D nipple displacement. Among over 100 possible equations, the best fitted curve (with $R^2 > 0.90$) of nipple displacement that was simple enough to permit ease of application was selected for each direction.

Under a braless condition

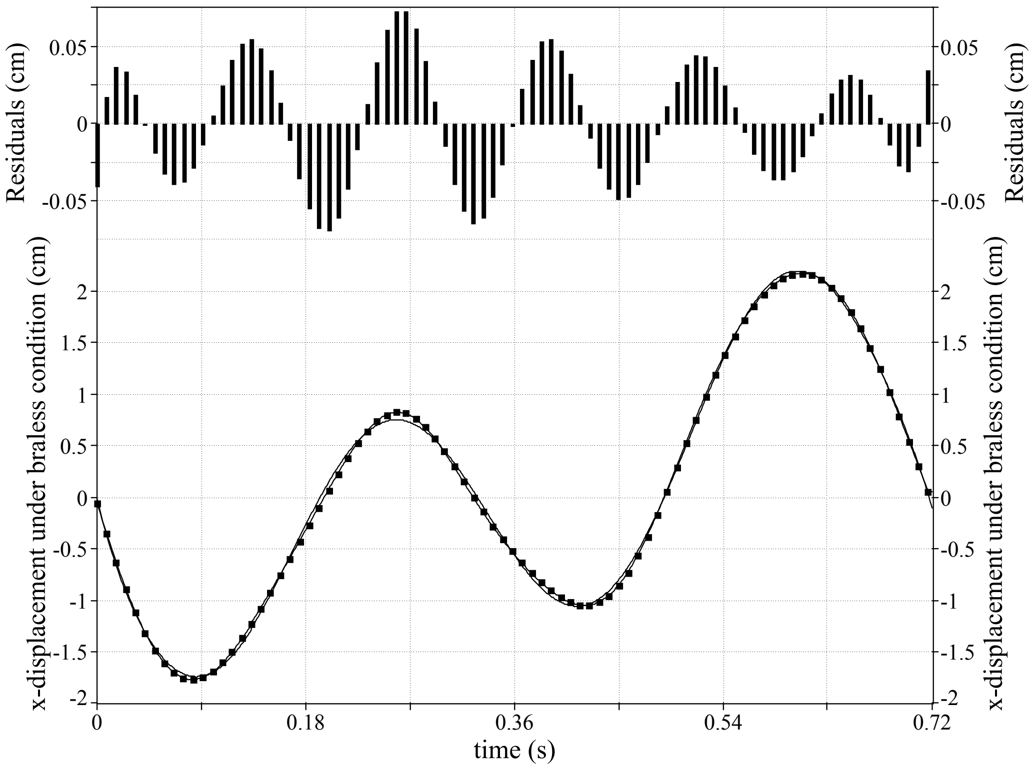

Figure 5.14 Fit graph and residuals of nipple x-displacement during Subject A's jogging under a braless condition.

(The dotted line is the actual data and the solid line is the fitted curve)

Figure 5.14 shows the fitted graph of nipple displacement x_1' with residuals in the x-direction, during a single jogging stride of Subject A under a braless condition. The equation is

$$x_1' = a_1 + b_1 t + c_1 t^2 + d_1 t^3 + e_1 t^4 + f_1 t^5 + g_1 t^6 + h_1 t^7 + i_1 t^8 + j_1 t^9 + k_1 t^{10}, \mathrm{R}^2 = 0.999 \tag{5.28}$$

The coefficients $a_1, b_1, \cdots, k_1$ are listed in Table 5.5, and t is the jogging time in second.

Table 5.5 Coefficients of the curve-fit equation of the *x*-, *y*- and *z*-displacement under a braless condition

x-displacement	*y*-displacement	*z*-displacement
a_1= -0.02	a_2= 0.62	a_3= 0.39
b_1= -46.73	b_2= -174.08	b_3= -118.04
c_1= 521.16	c_2= 3293.43	c_3= 1980.66
d_1= -5347.08	d_2= -29289.44	d_3= -20708.83
e_1= 53857.53	e_2= 166238.71	e_3= 132150.55
f_1= -303752.98	f_2= -644877.81	f_3= -463096.57
g_1= 923877.39	g_2= 1665283.30	g_3= 784746.54
h_1= -1571198.90	h_2= -2733431.50	h_3= -247996.39
i_1= 1478884.40	i_2= 2680896.30	i_3= -1140415.10
j_1= -701528.47	j_2= -1398951.30	j_3= 1610513
k_1= 123506.39	k_2= 287481.20	k_3= -666575.44

By substituting Equation 5.17 into Equation (5.12), the curve fit equation of the x-displacement x_1 of the CBM is given in Equation 5.18.

$$x_1 = 0.3611(a_1 + b_1 t + c_1 t^2 + d_1 t^3 + e_1 t^4 + f_1 t^5 + g_1 t^6 + h_1 t^7 + i_1 t^8 + j_1 t^9 + k_1 t^{10}) \tag{5.29}$$

To estimate the force on the breast, its acceleration is required in developing the breast mechanical model. From Equation (5.29), the velocity and acceleration of the CBM can be obtained by single and double derivatives, respectively, as follows.

$$\dot{x}_1 = 0.3611(b_1 + 2c_1 t + 3d_1 t^2 + 4e_1 t^3 + 5f_1 t^4 + 6g_1 t^5 + 7h_1 t^6 + 8i_1 t^7 + 9j_1 t^8 + 10k_1 t^9) \tag{5.30}$$

$$\ddot{x}_1 = 0.3611(2c_1 + 6d_1 t + 12e_1 t^2 + 20f_1 t^3 + 30g_1 t^4 + 42h_1 t^5 + 56i_1 t^6 + 72j_1 t^7 + 90k_1 t^8) \tag{5.31}$$

where x_1, $\dot{x}_1$ and $\ddot{x}_1$ are the CBM's *x*-displacement, *x*-velocity and *x*-acceleration during a single jogging stride of Subject A under a braless condition.

Similarly, the displacement, velocities and accelerations of the CBM in the *y*- and *z*-directions are shown in Table 5.6

Table 5.6 Equations of displacement, velocities and accelerations of the CBM of Subject A in a jogging stride under a braless condition

y-direction
$x_2' = a_2 + b_2 t + c_2 t^2 + d_2 t^3 + e_2 t^4 + f_2 t^5 + g_2 t^6 + h_2 t^7 + i_2 t^8 + j_2 t^9 + k_2 t^{10}$ (5.32)
$x_2 = 0.8181(a_2 + b_2 t + c_2 t^2 + d_2 t^3 + e_2 t^4 + f_2 t^5 + g_2 t^6 + h_2 t^7 + i_2 t^8 + j_2 t^9 + k_2 t^{10})$ (5.33)
$\dot{x}_2 = 0.8181(b_2 + 2c_2 t + 3d_2 t^2 + 4e_2 t^3 + 5f_2 t^4 + 6g_2 t^5 + 7h_2 t^6 + 8i_2 t^7 + 9j_2 t^8 + 10k_2 t^9)$ (5.34)
$\ddot{x}_2 = 0.8181(2c_2 + 6d_2 t + 12e_2 t^2 + 20f_2 t^3 + 30g_2 t^4 + 42h_2 t^5 + 56i_2 t^6 + 72j_2 t^7 + 90k_2 t^8)$ (5.35)
z-direction
$x_3' = a_3 + b_3 t + c_3 t^2 + d_3 t^3 + e_3 t^4 + f_3 t^5 + g_3 t^6 + h_3 t^7 + i_3 t^8 + j_3 t^9 + k_3 t^{10}$ (5.36)
$x_3 = 0.5734(a_3 + b_3 t + c_3 t^2 + d_3 t^3 + e_3 t^4 + f_3 t^5 + g_3 t^6 + h_3 t^7 + i_3 t^8 + j_3 t^9 + k_3 t^{10})$ (5.37)
$\dot{x}_3 = 0.5734(b_3 + 2c_3 t + 3d_3 t^2 + 4e_3 t^3 + 5f_3 t^4 + 6g_3 t^5 + 7h_3 t^6 + 8i_3 t^7 + 9j_3 t^8 + 10k_3 t^9)$ (5.38)
$\ddot{x}_3 = 0.5734(2c_3 + 6d_3 t + 12e_3 t^2 + 20f_3 t^3 + 30g_3 t^4 + 42h_3 t^5 + 56i_3 t^6 + 72j_3 t^7 + 90k_3 t^8)$ (5.39)
x_2' and x_3' are the nipple displacement, where the values of $a_2, b_2, \cdots, k_2$, $a_3, b_3, \cdots, k_3$ have been listed in Table 5.5. x_2, $\dot{x}_2$ and $\ddot{x}_2$, and x_3, $\dot{x}_3$ and $\ddot{x}_3$ are the CBM displacement, velocity and acceleration in the *y*- and *z*- directions, respectively.

Figure 5.15 and 5.16 show the nipple displacement and the fitted graph and the residuals, during a single jogging stride of Subject A under a braless condition, in the *y*-direction and *z*-direction, respectively.

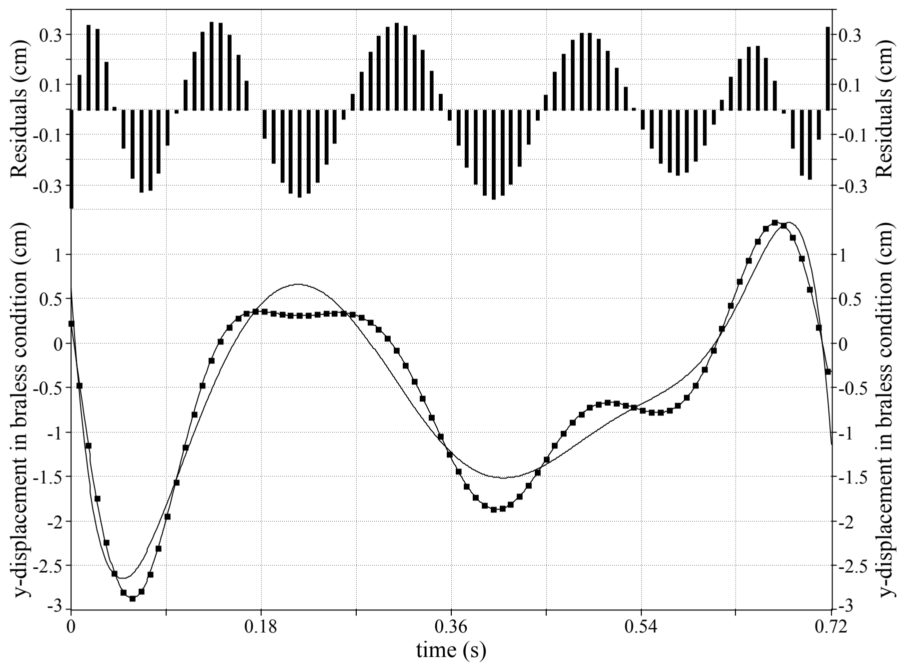

Figure 5.15 Fit graph and residuals of nipple *y*-displacement during Subject A's jogging under a braless condition

(The dotted line is the actual data and the solid line is the fitted curve)

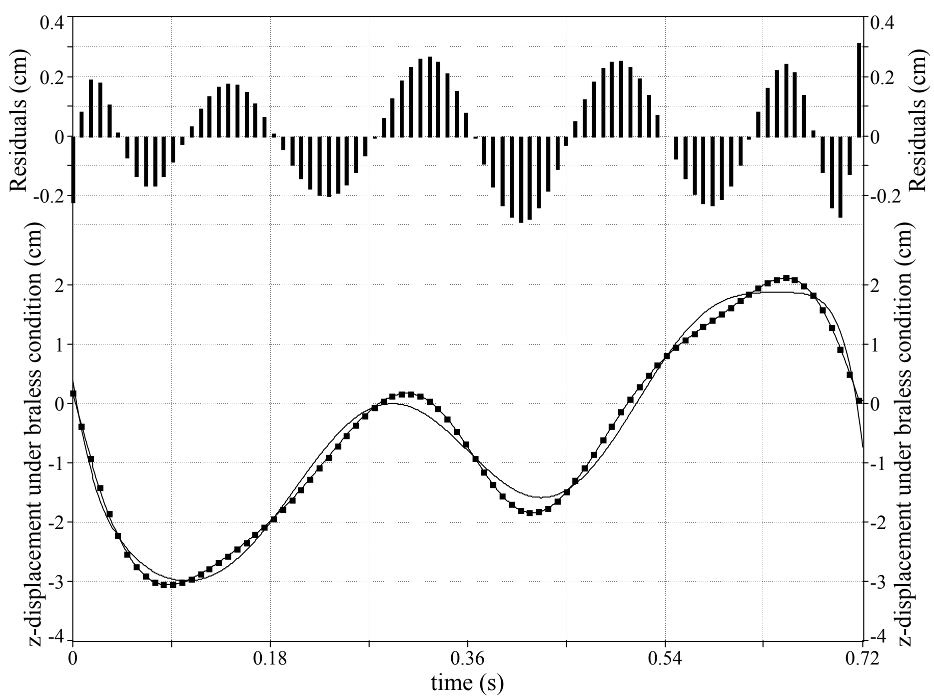

Figure 5.16 Fit graph and residuals of nipple *z*-displacement during Subject A's jogging under a braless condition.

(The dotted line is the actual data and the solid line is the fitted curve)

Under sports bra condition

Using the same logic and procedure, the equations for displacement, velocities and accelerations of the CBM of Subject A in a jogging stride under the sports bra condition are shown as Table 5.7.

Table 5.7 Equations of displacement, velocities and accelerations of the CBM of Subject A in a jogging stride under a sports bra condition

In the sports bra condition
x-direction $x_4' = a_4 + b_4 t + c_4 t^2 + d_4 t^3 + e_4 t^4 + f_4 t^5 + g_4 t^6 + h_4 t^7 + i_4 t^8 + j_4 t^9 + k_4 t^{10}$ (5.40) $x_4 = 0.3611(a_4 + b_4 t + c_4 t^2 + d_4 t^3 + e_4 t^4 + f_4 t^5 + g_4 t^6 + h_4 t^7 + i_4 t^8 + j_4 t^9 + k_4 t^{10})$ (5.41) $\dot{x}_4 = 0.3611(b_4 + 2c_4 t + 3d_4 t^2 + 4e_4 t^3 + 5f_4 t^4 + 6g_4 t^5 + 7h_4 t^6 + 8i_4 t^7 + 9j_4 t^8 + 10k_4 t^9)$ (5.42) $\ddot{x}_4 = 0.3611(2c_4 + 6d_4 t + 12e_4 t^2 + 20f_4 t^3 + 30g_4 t^4 + 42h_4 t^5 + 56i_4 t^6 + 72j_4 t^7 + 90k_4 t^8)$ (5.43)
y-direction $x_5' = a_5 + b_5 t + c_5 t^2 + d_5 t^3 + e_5 t^4 + f_5 t^5 + g_5 t^6 + h_5 t^7 + i_5 t^8 + j_5 t^9 + k_5 t^{10}, \mathrm{R}^2 = 0.9386$ (5.44) $x_5 = 0.8181(a_5 + b_5 t + c_5 t^2 + d_5 t^3 + e_5 t^4 + f_5 t^5 + g_5 t^6 + h_5 t^7 + i_5 t^8 + j_5 t^9 + k_5 t^{10})$ (5.45) $\dot{x}_5 = 0.8181(b_5 + 2c_5 t + 3d_5 t^2 + 4e_5 t^3 + 5f_5 t^4 + 6g_5 t^5 + 7h_5 t^6 + 8i_5 t^7 + 9j_5 t^8 + 10k_5 t^9)$ (5.46) $\ddot{x}_5 = 0.8181(2c_5 + 6d_5 t + 12e_5 t^2 + 20f_5 t^3 + 30g_5 t^4 + 42h_5 t^5 + 56i_5 t^6 + 72j_5 t^7 + 90k_5 t^8)$ (5.47)
z-direction $x_6' = a_6 + b_6 t + c_6 t^2 + d_3 t^3 + e_6 t^4 + f_6 t^5 + g_6 t^6 + h_6 t^7 + i_6 t^8 + j_6 t^9 + k_6 t^{10}, \mathrm{R}^2 = 0.9983$ (5.48) $x_6 = 0.5734(a_6 + b_6 t + c_6 t^2 + d_6 t^3 + e_6 t^4 + f_6 t^5 + g_6 t^6 + h_6 t^7 + i_6 t^8 + j_6 t^9 + k_6 t^{10})$ (5.49) $\dot{x}_6 = 0.5734(b_6 + 2c_6 t + 3d_6 t^2 + 4e_6 t^3 + 5f_6 t^4 + 6g_6 t^5 + 7h_6 t^6 + 8i_6 t^7 + 9j_6 t^8 + 10k_6 t^9)$ (5.50) $\ddot{x}_6 = 0.5734(2c_6 + 6d_6 t + 12e_6 t^2 + 20f_6 t^3 + 30g_6 t^4 + 42h_6 t^5 + 56i_6 t^6 + 72j_6 t^7 + 90k_6 t^8)$ (5.51)
x_4', x_5' and x_6' is the nipple displacement in the *x*-, *y*- and *z*-directions, respectively, where the values of $a_4, b_4, \cdots, k_4$, $a_5, b_5, \cdots, k_5$ $a_6, b_6, \cdots, k_6$ are listed in Table 5.8. x_4, $\dot{x}_4$ and $\ddot{x}_4$, x_5, $\dot{x}_5$ and $\ddot{x}_5$, and x_6, $\dot{x}_6$ and $\ddot{x}_6$ are the CBM displacement, velocity and acceleration in the *x*-, *y*- and *z*-directions, respectively.

Coefficients of the curve-fit equation of the *x*-, *y*- and *z*- displacement, velocities and accelerations of the CBM of Subject A in a jogging stride under the sports bra condition are shown in Table 5.8.

Table 5.8 Coefficients of the curve-fit equation of the *x*-, *y*- and *z*- displacement under a sports bra condition

x-displacement	*y*-displacement	*z*-displacement
a_4= -0.02	a_5= -0.03	a_6= 0.01
b_4=1.27	b_5=5.76	b_6= 0.27
c_4=-150.95	c_5=-112.17	c_6= 49.98
d_4=2595.18	d_5=414.56	d_6= -1043.41
e_4=-19147.89	e_5=7654.62	e_6= 9330.99
f_4=75500.16	f_5=-86418.19	f_6= -46868.31
g_4=-170868.52	g_5=386350.76	g_6= 142101.43
h_4=220699.11	h_5=-925463.08	h_6= -264072.13
i_4=-146838.84	i_5=1251257.40	i_6= 293560.25
j_4=32337.96	j_5=-902789.60	j_6= -179062.84
k_4=6303.86	k_5=271016	k_6= 46092.94

Table 5.9 shows the R^2 s of all the fitted equations of nipple displacement under braless and sports bra conditions for three directions. All R^2 s are more than 0.93 which reveals that the fitted equations can accurately describe the nipple displacement.

Table 5.9 Correlation coefficients R^2 s of all fitted equations of the nipple displacement under braless and sports bra conditions

Wearing condition	*x*-direction	*y*-direction	*z*-direction
Braless	R_1^2= 0.999	R_2^2= 0.948	R_3^2= 0.988
Sports bra	R_4^2=0.969	R_5^2=0.938	R_6^2= 0.998
where R_1, R_2, R_3 and R_4, R_5, R_6 are the correlation coefficients of the fitted equations of the nipple displacement in *x*-, *y*- and *z*- directions			

Figure 5.17 to 5.19 show the nipple displacement fitted graph, and the residuals in the *x*-, *y*- and *z*- directions, during for a single jogging stride of Subject A under a sports bra condition.

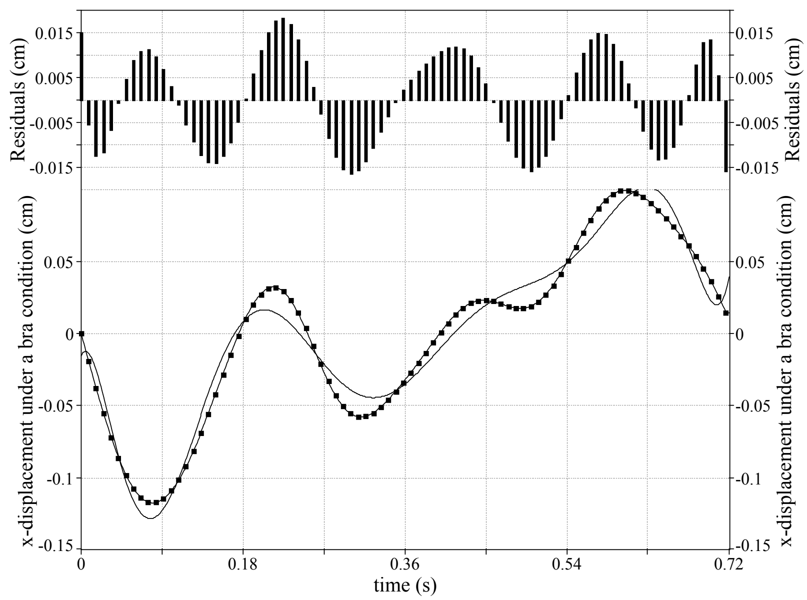

Figure 5.17 Fit graph and residuals of nipple *x*-displacement during Subject A's jogging under a sports bra condition.
(The dotted line is the actual data and the solid line is the fitted curve)

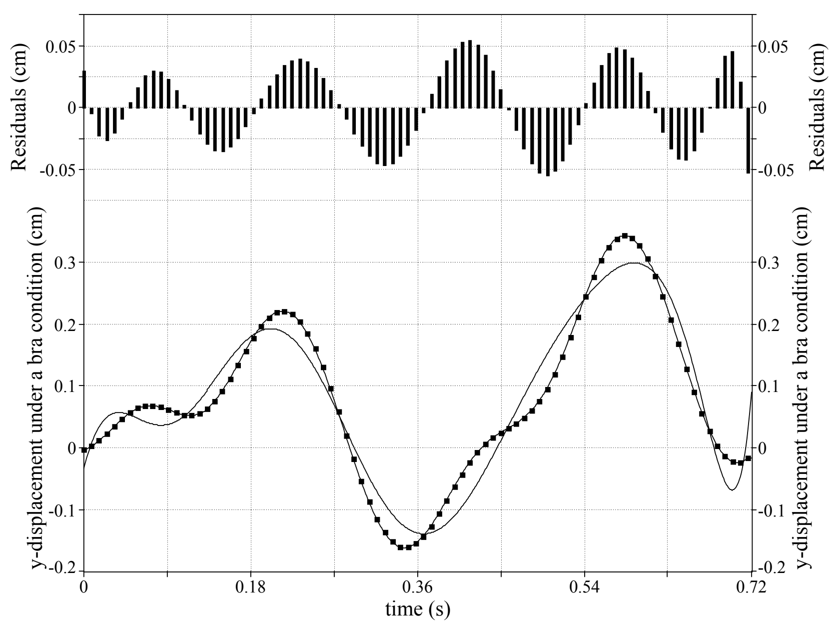

Figure 5.18 Fit graph and residuals of nipple *y*-displacement during Subject A's jogging under a sports bra condition.
(The dotted line is the actual data and the solid line is the fitted curve)

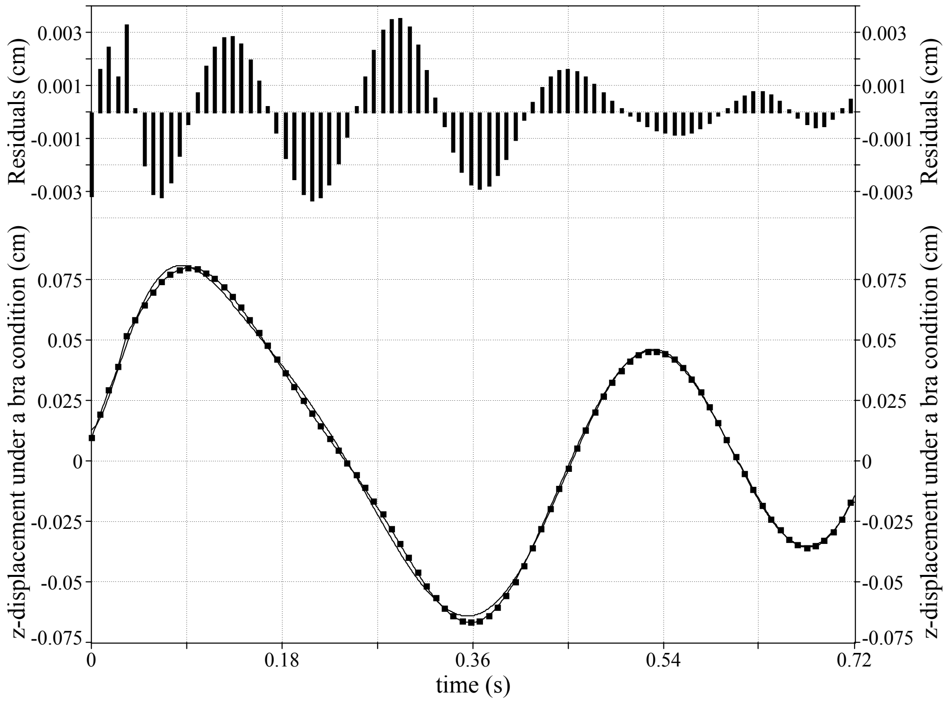

Figure 5.19 Fit graph and residuals of nipple z-displacement during Subject A's jogging under a sports bra condition.
(The dotted line is the actual data and the solid line is the fitted curve)

5.3.2 Calculations of breast force during jogging in braless and sports bra conditions

The equations for the force on the breasts under braless and sports bra conditions were previously derived in Section 5.2.5. These are shown in Table 5.10.

Table 5.10 Equations of the force on the breasts during jogging

Direction	Braless condition	Sports bra condition
x	$F_1 = m_b\ddot{x}_1 + c_b\dot{x}_1 + k_b x_1$ (5.52)	$F_4 = m_b\ddot{x}_4 + c_{sb}\dot{x}_4 + k_{sb}x_4$ (5.53)
y	$F_2 = m_b\ddot{x}_2 + c_b\dot{x}_2 + k_b x_2$ (5.54)	$F_5 = m_b\ddot{x}_5 + c_{sb}\dot{x}_5 + k_{sb}x_5$ (5.55)
z	$F_3 = m_b\ddot{x}_3 + c_b\dot{x}_3 + k_b x_3$ (5.56)	$F_6 = m_6\ddot{x}_6 + c_{sb}\dot{x}_6 + k_{sb}x_6$ (5.57)

where F_1, F_2, F_3 are the force in the *x*-, *y*- and *z*- directions, respectively, under braless conditions. F_4, F_5 *and* F_6 are the force in the *x*-, *y*- and *z*- directions, respectively, under the sports bra condition.

To determine the values of the force for Subject A, the following values previously derived in Sections 5.2.3.1 and 5.2.4.1 were used.

m_b = 0.3168 *kg*, k_b = 312.36 N/m, c_b = 3.9525 Ns/m, k_{sb} = 214.96 M_{ss} + 210.05 and c_{sb} = 3.1278 M_{ss} + 2.0424

Substituting these values into equations 5.52 to 5.57 the force on her breasts under braless and sports bra conditions can be calculated, based on the CBM displacement, velocities and accelerations.

$$F_1 = 0.3168\ddot{x}_1 + 3.9525\dot{x}_1 + 312.36x_1 \tag{5.58}$$

$$F_2 = 0.3168\ddot{x}_2 + 3.9525\dot{x}_2 + 312.36x_2 \tag{5.59}$$

$$F_3 = 0.3168\ddot{x}_3 + 3.9525\dot{x}_3 + 312.36x_3 \tag{5.60}$$

$$F_4 = 0.3168\ddot{x}_4 + (3.1278M_{ss} + 2.0421)\dot{x}_4 + (214.96M_{ss} + 210.05)x_4 \tag{5.61}$$

$$F_5 = 0.3168\ddot{x}_5 + (3.1278M_{ss} + 2.0421)\dot{x}_5 + (214.96M_{ss} + 210.05)x_5 \tag{5.62}$$

$$F_6 = 0.3168\ddot{x}_6 + (3.1278M_{ss} + 2.0421)\dot{x}_6 + (214.96M_{ss} + 210.05)x_6 \tag{5.63}$$

Figures 5.20 and 5.21 show the force on the breasts in a single jogging stride of Subject A under braless and sports bra conditions, respectively.

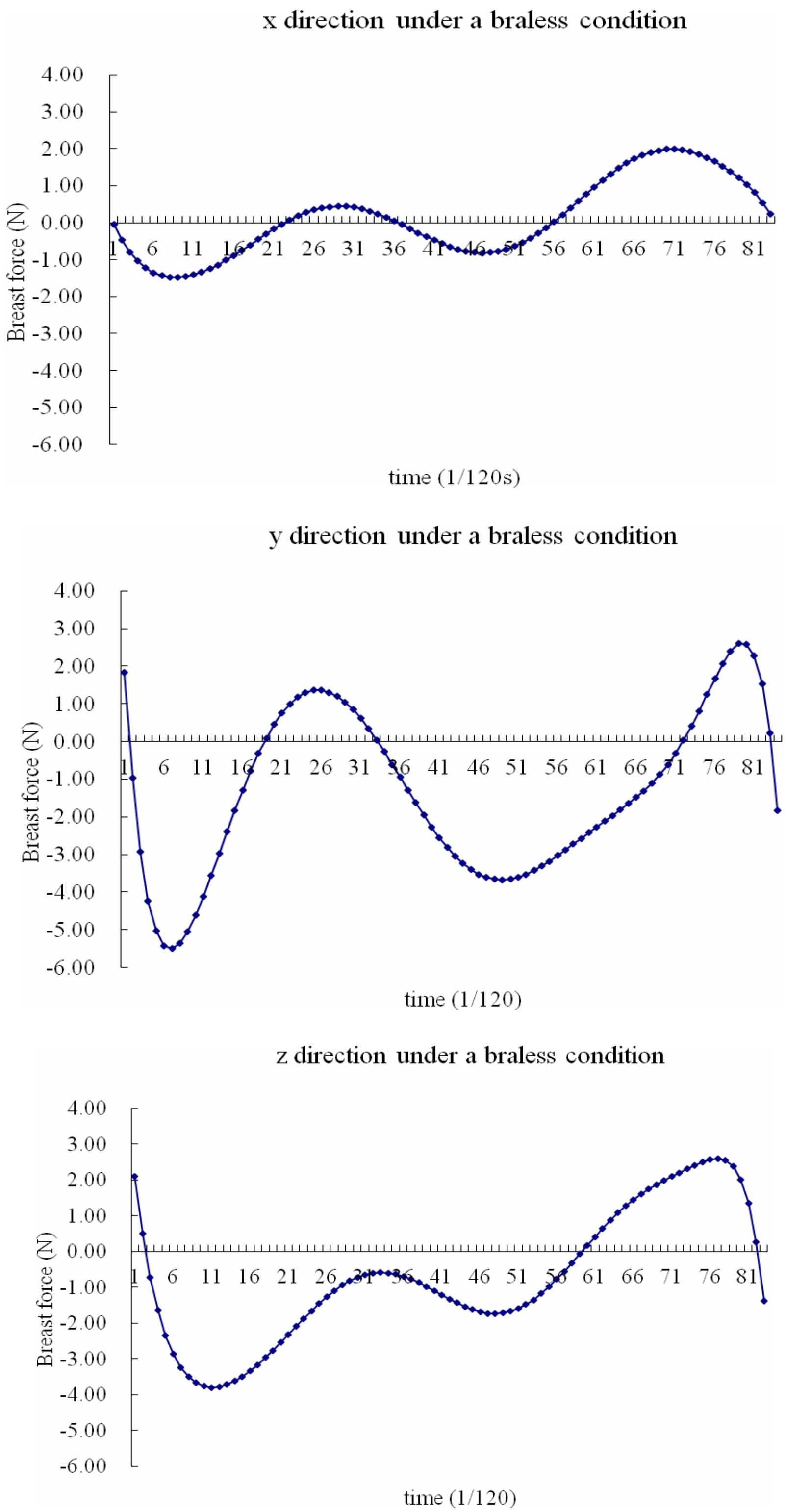

Figure 5.20 Force on breasts for a single jogging stride of Subject A under a braless condition

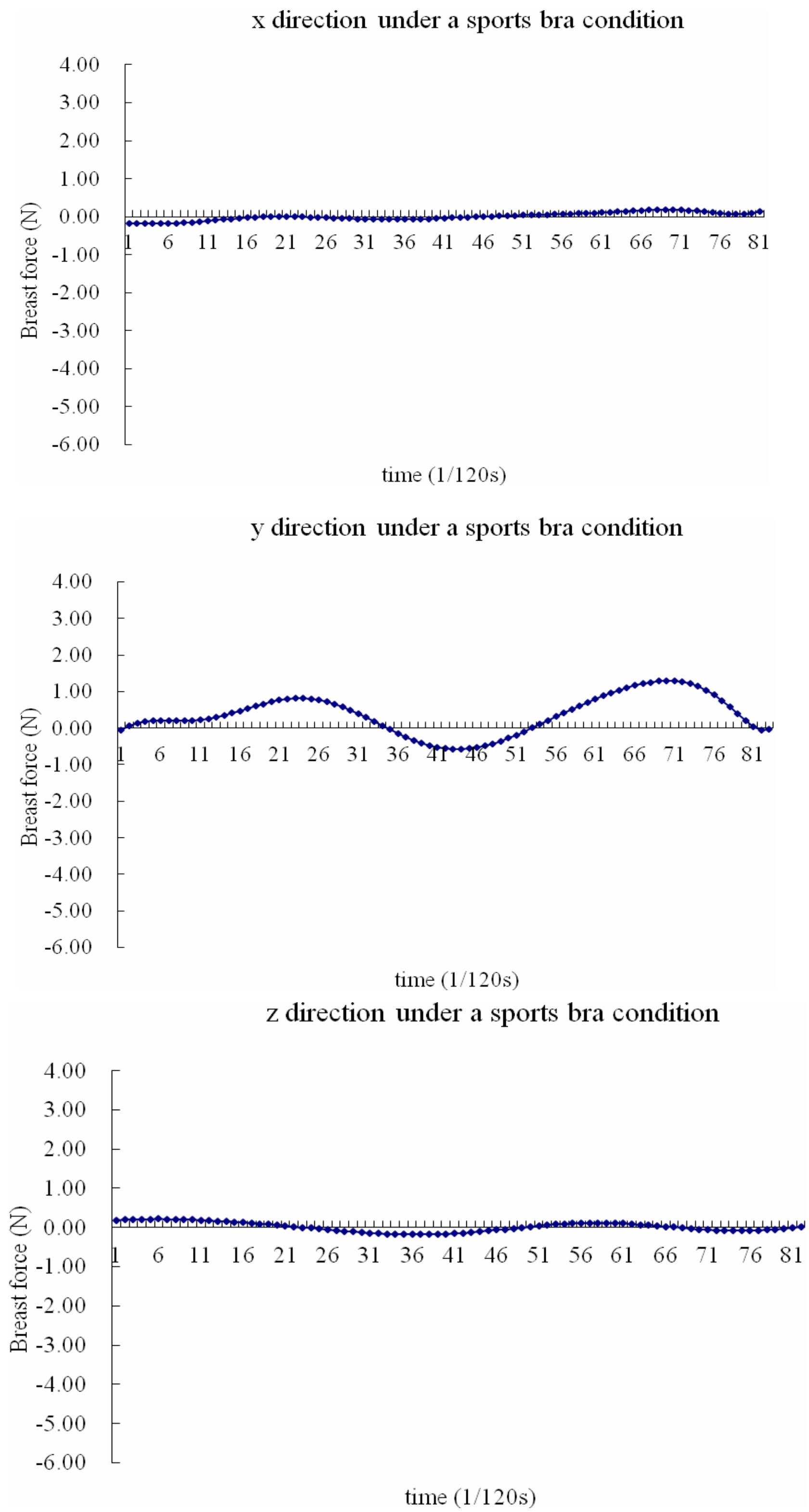

Figure 5.21 Force on breasts for a single jogging stride of Subject A under a sports bra condition

5.3.3 Predicted force involved during jogging under a braless condition

As shown in Figure 5.20, the predicted breast force was the largest and rapidly changing in the *y*-direction during the entire jogging stride under a braless condition. There are several types of possible force exerted on the breast in the *y*-direction, including the breast weight, the air resistance to the breast movement, the reaction force from the ground, the vibration caused by the inertia of breast mass, the contraction of pectoral muscles, and the tension of ligament and skin.

The predicted maximum breast forces (2.3 N superior and 5.5 N inferior) for this specific subject with a breast mass of 316.8g were close to the lower range of breast force reported by Gefena and Dilmoney [21] who found that the approximated values of internal vertical force in the pectoralis fascia of the breast tissues ranged 2.3 - 10.2 N, assuming a breast mass of 500 - 1000 g during jogging at a speed of 7 km/h with a maximum vertical trunk acceleration of 0.8 g where g = 9.81 m/s^2. This provides encouraging evidence to support the validity of the model and the concepts used to derive data for the model. However, to further validate the model more fully further experiments will need to be conducted in future work.

In the *z*-direction, the force mainly comes from the medial-lateral thoracic movement brought by arm swing, and the contraction of pectoral muscles. The breast force was the smallest in the *x*-direction, because the force only involved the reaction force from the thorax and air resistance.

5.3.4 Predicted force involved during jogging in a sports bra

When jogging with a bra support, the predicted forces on the breast were well balanced in all directions, except that there was still approximately 1 N force in the vertical direction during jogging, as shown in Figure 5.21. This is mainly affected by breast weight and the effectiveness of the bra in controlling the upward movement. Therefore, it would be interesting to consider the force involved particularly in the vertical direction, with different levels of bra support, using different properties of shoulder straps.

5.4 Breast mechanical model with different shoulder straps

5.4.1 Different widths of shoulder straps

Previous study has shown that for situations where the load does not exceed the elastic limit of the shoulder strap, its extension was directly proportional to the load applied [108]. Therefore, the shoulder straps should behave like springs.

Considering two shoulder straps with the same material properties, the width of strap *b* is twice that of strap *a*. The strap *a* is regarded as a single spring, and strap *b* as a twin spring, as shown in Figure 5.22. The spring constant (k_{eq}) of strap *b* becomes

$$k_{eq} = k_1 + k_2 \tag{5.64}$$

where k_1 and k_2 are the spring constants of the two parallel springs respectively.

Assuming that the spring constants are proportional to the width of the shoulder straps, the spring constants k_1 and k_2 of strap *b* are equal to the spring constant (k) of strap *a* , i.e. k_{eq} = 2k.

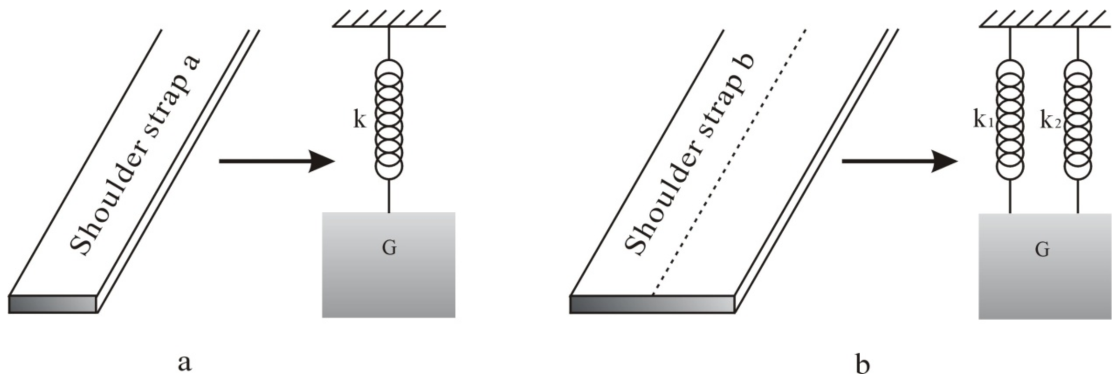

Figure 5.22 Two shoulder straps with different widths

It follows that if the two straps support the same force (f), the displacement (x_1) of strap *a*, which is the change in length from its equilibrium position, will be twice that (x_2) of shoulder strap *b*. According to Hooke's law,

$$f = kx_1 \tag{5.65}$$

$$f = k_{eq}x_2 = 2kx_2 \tag{5.66}$$

So $x_1 = \dfrac{f}{k}$ and $x_2 = \dfrac{f}{2k}$, i.e. $x_1 = 2x_2$

In supporting the same force, the breast displacement decreases when the width of the shoulder strap increases. Therefore, a wider shoulder strap is more effective in controlling breast displacement than a narrow shoulder strap. This implies that sports bras with wider straps can reduce the force on the breasts during activities, all else being constant.

5.4.2 Different styles of shoulder straps

The styles of the shoulder straps can be in fixed length or adjustable lengths, plain or bound. Table 5.11 shows the force equations for different styles of shoulder straps, based on

Hooke's law.

Table 5.11 Force and displacement analysis of shoulder straps

<table>
<tr><th>Strap type</th><th>The cross section of shoulder straps</th><th>Model</th><th>Parameter name</th><th>Parameter calculation</th><th>Style</th></tr>
<tr><td rowspan="6">
Type 1
Fixed</td><td rowspan="3">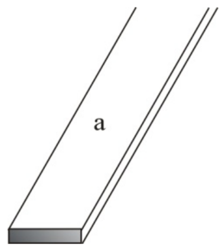
Plain style</td><td rowspan="3">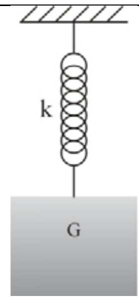</td><td>Spring constant</td><td>k</td><td rowspan="3">Style 1</td></tr>
<tr><td>Displacement</td><td>x</td></tr>
<tr><td>Force</td><td>$F = kx$</td></tr>
<tr><td rowspan="3">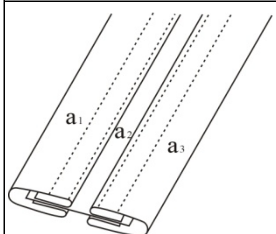
Bound style</td><td rowspan="3">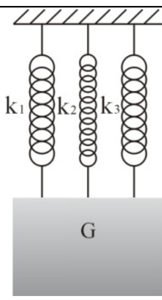</td><td>Equivalent spring constant</td><td>$k_{eq} = k_1 + k_2 + k_3$
k_{eq} is equivalent spring constant</td><td rowspan="3">Style 2</td></tr>
<tr><td>Displacement</td><td>$x_1 = x_2 = x_3 = x$</td></tr>
<tr><td>Force</td><td>$F = (k_1 + k_2 + k_3)x$</td></tr>
<tr><td rowspan="3">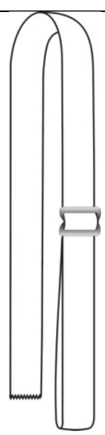
Type 2
Adjustable</td><td rowspan="3">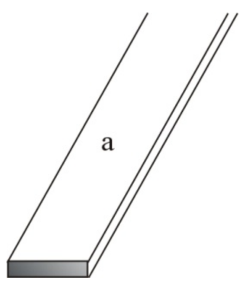
Plain style</td><td rowspan="3">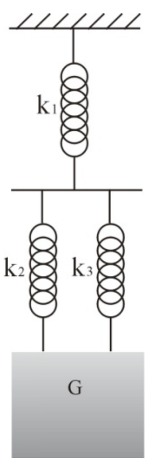</td><td>Equivalent spring constant</td><td>$k_{eq} = \frac{2}{3}k$
$(k_1 = k_2 = k_3 = k)$</td><td rowspan="3">Style 3</td></tr>
<tr><td>Displacement</td><td>$x = \frac{3}{2}x_1$
$(x_2 = x_3 = \frac{1}{2}x_1)$</td></tr>
<tr><td>Force</td><td>$F = \frac{2}{3}kx$</td></tr>
</table>

If the three styles of shoulder straps are made of the same material with the same width and supporting the same force (F), the displacement of the shoulder straps is shown in Table 5.12.

Table 5.12 Displacement of the shoulder straps

Style	Style 1	Style 2	Style 3
Displacement	$\frac{F}{k}$	$\frac{F}{k_1+k_2+k_3}$	$\frac{3F}{2k}$

The spring constant ($k_1+k_2+k_3$) for Style 2 should be more than that of Style 1 (k) due to the two-folded bound edges of the material in Style 2 that was formed by five layers of material (Table 5.12.), whereas the spring constant for Style 3 ($2k$) is larger than that of Style 1 (k). Consequently, the displacement of Style 3 should be the smallest and Style 2 should be the largest when the same force is supported. Based on these findings, Style 3 would be the most effective in controlling breast displacement, followed by Style 2. This implies that the force on breasts would be the smallest when wearing a sports bra with a bound shoulder strap in fixed length during activities.

5.4.3 Different positions of shoulder straps

The positions of the shoulder straps on the shoulder are located between the side neck point and shoulder point. In this section, consideration will be given to the force exerted on the breasts, and the moments that act on the breasts when the shoulder straps are in different positions on the shoulders.

5.4.3.1 Straps in a natural position on the shoulder

The ranges of positions and angles of shoulder straps on the shoulders are determined by the body form, whereas the position of the centre of breast's gravity (CBG) is related to the breast shape and properties. The location of the shoulder strap on the shoulder can affect the force and the moment on the breasts.

In the BCS, if the direction of the force on a shoulder strap and the coordinate of the CBG are known, the force and moment on the breast associated with the shoulder strap can be calculated as follows.

As shown in Figure 5.23, The force F that acts on the shoulder strap is decomposed into three force $F_{(x)}, F_{(y)}$ and $F_{(z)}$ along the *x, y* and *z* axes, respectively, and can be calculated by Equation (5.67).

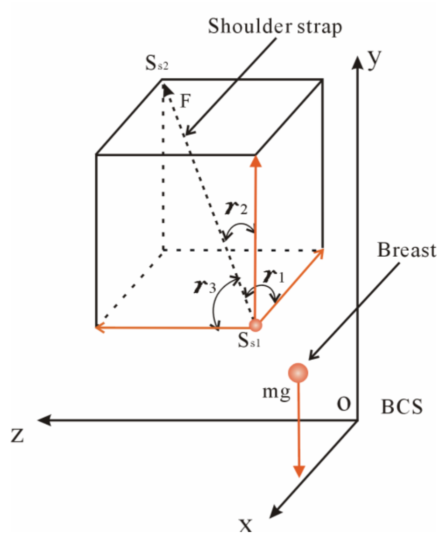

Figure 5.23 Force F that acts on the shoulder strap
(S_{s1} and S_{s2} are on the shoulder strap, mg is the breast weight)

$$\begin{cases} F_{(x)} = F\cos\gamma_1 \\ F_{(y)} = F\cos\gamma_2 \\ F_{(z)} = F\cos\gamma_3 \end{cases} \tag{5.67}$$

where the angles γ_1, γ_2 and γ_3 are made by $F_{(x)}, F_{(y)}$ and $F_{(z)}$ along the *x, y* and *z* axes, respectively.

Thus, the moments of F about the CBG can be obtained by Equation (5.68):

$$\begin{cases} M_{(x)}(F) = (y_{S1} - y_M)F_{(z)} - (z_{S1} - z_M)F_{(y)} \\ M_{(y)}(F) = (z_{S1} - z_M)F_{(x)} - (x_{S1} - x_M)F_{(z)} \\ M_{(z)}(F) = (x_{S1} - x_M)F_{(y)} - (y_{S1} - y_M)F_{(x)} \end{cases} \tag{5.68}$$

where $M_{(x)}(F), M_{(y)}(F)$ and $M_{(z)}(F)$ are the moments of F about the CBG along the *x*-, *y*- and *z*- axes, and (x_{S1}, y_{S1}, z_{S1}) and (x_M, y_M, z_M) are the coordinates of point *S* (the point of F action) and the CBG (M*)* in the BCS, respectively.

Equation (5.69) can be re-written from Equations (5.67) and(5.68):

$$\begin{cases} M_{(x)}(F) = (y_{S1} - y_M)F\cos\gamma_3 - (z_{S1} - z_M)F\cos\gamma_2 \\ M_{(y)}(F) = (z_{S1} - z_M)F\cos\gamma_1 - (x_{S1} - x_M)F\cos\gamma_3 \\ M_{(z)}(F) = (x_{S1} - x_M)F\cos\gamma_2 - (y_{S1} - y_M)F\cos\gamma_1 \end{cases} \tag{5.69}$$

The point of application of F is the end point (S_{s1}) of the shoulder strap; and the direction of the force F_S is along the strap direction ($\overrightarrow{S_{s1}S_{s2}}$).

$$\begin{cases} \cos\gamma_1 = \dfrac{x_{s2} - x_{s1}}{\sqrt{(x_{s2} - x_{s1})^2 + (y_{s2} - y_{s1})^2 + (z_{s2} - z_{s1})^2}} \\ \cos\gamma_2 = \dfrac{y_{s2} - y_{s1}}{\sqrt{(x_{s2} - x_{s1})^2 + (y_{s2} - y_{s1})^2 + (z_{s2} - z_{s1})^2}} \\ \cos\gamma_3 = \dfrac{z_{s2} - z_{s1}}{\sqrt{(x_{s2} - x_{s1})^2 + (y_{s2} - y_{s1})^2 + (z_{s2} - z_{s1})^2}} \end{cases} \tag{5.70}$$

where (x_{s1}, y_{s1}, z_{s1}) and (x_{s2}, y_{s2}, z_{s2}) are the coordinates of points S_{s1} & S_{s2} respectively.

Hence, the force and moment on the breasts caused by the shoulder strap can be calculated by Equations (5.67) to (5.69).

5.4.3.2 Straps in other positions on shoulder

To further examine the changes of force on the breasts and the moment of F about the breasts in different situations, the following three different positions of the straps on shoulder (Figure 5.24) were studied.

Natural position (P_1): The shoulder strap is located in plane π_1, direction of breast gravitational force and the shoulder strap loading direction. Plane π_1 is parallel to the mid-sagittal plane π_0 of the body as shown in Figure 5.24 a;

Halter position 2 (P_2): The shoulder strap is positioned between P_1 and the neck point on the left side, and located on plane π_2 as shown in Figure 5.24 b.

Wide shoulder position 3 (P_3): The shoulder strap is situated between P_1 and the left shoulder point, and located on plane π_3 as shown in Figure 5.24 c.

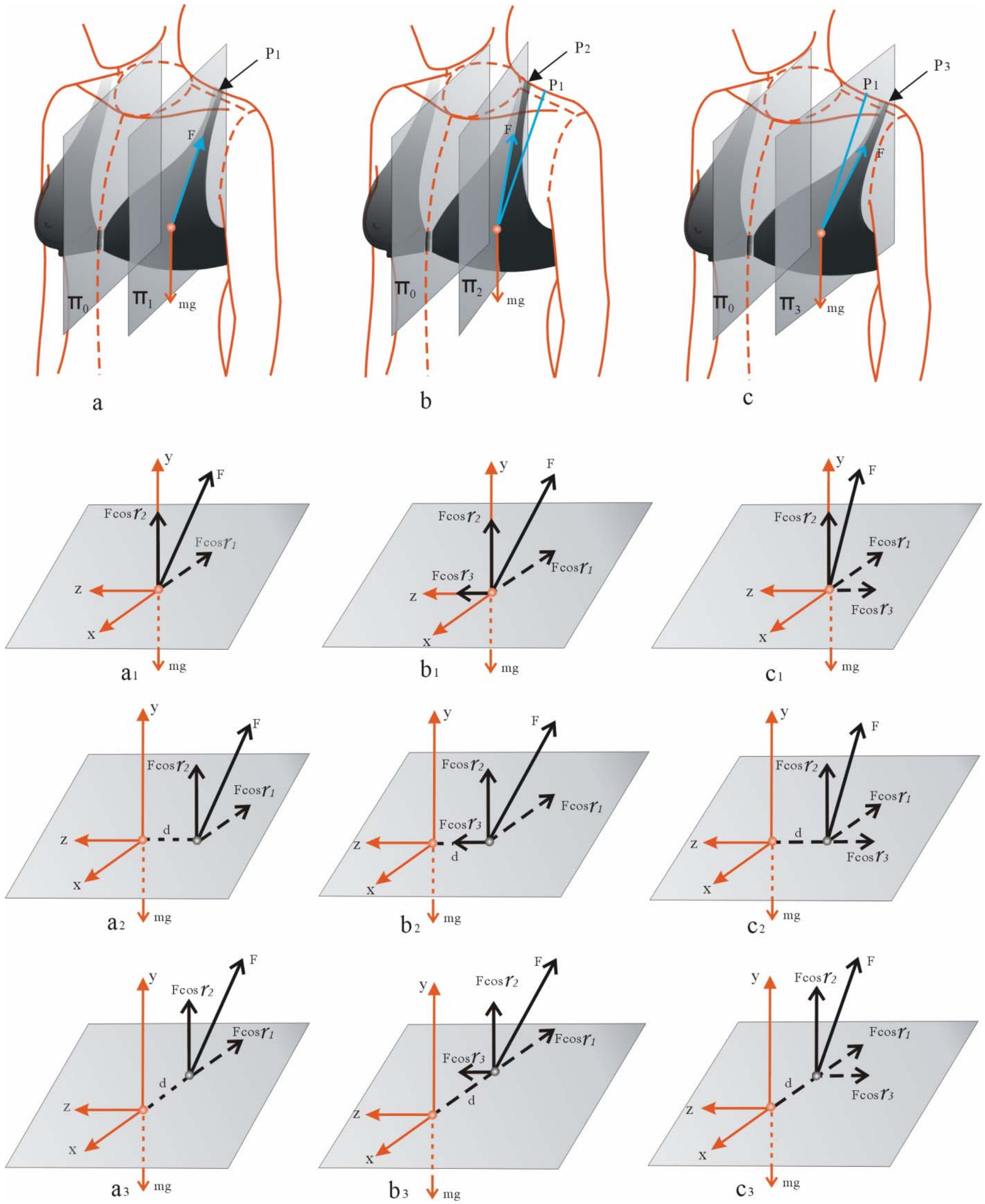

Figure 5.24 Force analysis of shoulder straps

The moments of F about the CBG along the *x-, y-* and *z-* axes at these three strap positions are in:

Case a) the CBG as shown in Figure 5.24 a_1, b_1 and c_1,

Case b) the *z*-axis that passes through the CBG in Figure 5.24 a_2, b_2 and c_2, and

Case c) the *x*-axis that passes through the CBG in Figure 5.24 a_3, b_3 and c_3.

According to Equation (5.67), F is divided into three components, as shown in Figure 5.24.

Table 5.13 summaries the force of the shoulder straps located at the three positions along the *x*-, *y*- and *z*-axes.

Table 5.13 Tensile force on the shoulder strap along the three axes

Position	*x*-axis	*y*-axis	*z*-axis
Position 1 (P_1) a_1, a_2, a_3	$-F\cos\gamma_1$	$F\cos\gamma_2$	0
Position 2 (P_2) b_1, b_2, b_3	$-F\cos\gamma_1$	$F\cos\gamma_2$	$F\cos\gamma_3$
Position 3 (P_3) c_1, c_2, c_3	$-F\cos\gamma_1$	$F\cos\gamma_2$	$-F\cos\gamma_3$

Table 5.13 shows that the shoulder straps exert a force of $-F\cos\gamma_1$ and $F\cos\gamma_2$ along the –*x*-axis and +*y*-axis, hence, they can control the anterior and posterior breast movement by supporting the breast weight and reduce the force exerted onto the breasts.

In the case of halter style with straps on P_2, the breast movement can be controlled and the lateral force exerted onto the breasts is reduced as $F\cos\gamma_3$ that is shown in Table 5.13 and

Figure 5.24 (b).

In the style of wide shoulder with straps on P_3 as shown in Figure 5.24 (c), the restraining component of $-F\cos\gamma_3$ makes the strap slip off the shoulder more easily.

When F does not pass through the CBG, the moments of F about the CBG will be produced. Table 5.14 shows the moments of F along the three axes.

Table 5.14 Moments of *F* on the CBG in the three axes

Figure	*x*-axis	*y*-axis	*z*-axis
Figure 5.24 a_1, b_1, c_1	0	0	0
Figure 5.24 a_2	$d\times F\cos\gamma_1$	$d\times F\cos\gamma_2$	0
Figure 5.24 a_3	0	$d\times F\cos\gamma_2$	0
Figure 5.24 b_2, c_2	$d\times F\cos\gamma_1$	$d\times F\cos\gamma_2$	0
Figure 5.24 b_3, c_3	0	$d\times F\cos\gamma_2$	$d\times F\cos\gamma_3$

Note: where d is the distance from the CBG to the intersection point of the force F and the *x-z* plane

In Figure 5.24 a_1, b_1, and c_1, there are no moments acting on the breast, whilst the other conditions have moments that act on the breast along different directions. In a static state, this movement is balanced out by the deformation of the bra cups. However, in a dynamic state, if the force is not in equilibrium, it will cause breast distortions that may lead to discomfort or pain. Therefore, in designing the positions of the shoulder straps, it is necessary to ensure that the shoulder strap produces minimum moments on the breast to ensure wearing comfort.

5.5 Conclusions

In this chapter, 3D mechanical models have been developed to evaluate the force exerted on breasts in *x*-, *y*- and *z*- directions during jogging. Confidence in the validity of the model was derived from the similarity between the predicted maximum breast force and the values reported previously by Gefena and Dilmoney [21]. However, the model will need to be validated more fully in further experiments that will need to be conducted in future work.

The variability of force during jogging in a braless condition predicted by the model was the largest in the *y*-direction, followed by the *z*-direction.

The present models can provide a convenient and simple approach to predict the force exerted onto breasts during jogging with or without sports bra. The concept used to construct the models can be applied to other sports activities.

The theoretical analysis predicted that, when the shoulder straps supported the same force, wider shoulder straps were more effective in reducing the breast force than the narrow ones. This explains why designers often use 1.6 cm to 3 cm wide shoulder straps for the sports bras, but only 1 cm to 1.3 cm for the fashion bras.

The force exerted onto the breasts was also related to the styles of shoulder straps and the positions on the shoulder. In designing the positions of shoulder straps, it is better to ensure that the shoulder strap produces minimum force moments on the breast for preventing breast discomfort.

The spring constants and damping constants of the breast were based on one subject, to demonstrate how the new method may be used to predict the force exerted on the breast.

The results may not be extrapolated to the general female population. The relationship between the coordinates of the CBM and that of the nipple was difficult to establish with real breasts, so an extrapolation procedure based on the use of breast prostheses was proposed. The breast was assumed to be a homogeneous soft object like breast prosthesis, and the movement of the CBM were used to represent those of the whole breast.

In future work, finite element models may be developed to simulate the breast force more discretely. Having said that, the concepts proposed in this more simplistic approach have provided a useful theoretical basis on the force on breasts and the associated design of bras can be better understood and that may be further developed as an alternative to finite element modelling that is inherently more difficult.

Chapter 6 Summary, conclusions and recommendations for future work

6.1 Summary and Conclusions

Reducing breast movement during exercises is the key function of sports bras, particularly for Chinese women to minimise breast bouncing and avoid embarrassment. The engineering design of supportive sports bras requires knowledge covering textile science and biomechanics related to breast motion.

Previous studies have primarily reported vertical breast displacement in the coronal plane [3-6,10-20,23,50] when female subjects performed activities under braless or different sports bra conditions. As mentioned in Chapter 2, different unreliable or unclear reference systems were used. Heretofore, none of the previous work has developed and published a standardised, valid and reliable local coordinate system for 3D biomechanical analysis of breast movement relative to the body. Besides, published research on the textile factors influencing the effectiveness of sports bra is very limited, and there is no previously published literature to explain the force exerted by a bra on the breasts in three dimensions.

To fill these knowledge gaps, this study aimed to propose a reliable method for 3D analysis of breast motion under different bra-supported conditions, and to determine the design requirements of more supportive sports bras to reduce breast movement during different activities.

The intention in the study has been to answer the following set of research questions:

Q.1 How can the relative breast movement be measured more accurately and comprehensively?

Q.2 How do breasts move three-dimensionally during different activities under braless and sports bra conditions?

Q.3 Which features of sports bras are effective in controlling breast movement and which are not?

Q.4 How do breast volume and the properties of shoulder straps affect breast movement?

Q.5 Can a breast model be developed to simulate breast movement and predict the force acting on breasts during jogging to provide a theoretical basis for the design of sports bras?

To answer the research questions, the following research objectives were set:

a) to develop a 3D local coordinate system to evaluate breast displacement and trajectory relative to the thorax;
b) to investigate 3D breast movement in different support conditions during various activities;
c) to evaluate the effectiveness of different bra features on the reduction of breast movement;
d) to analyse the effects of breast volume and material properties of shoulder straps on the breast displacement; and
e) to build breast mechanical models to analyse breast forces during jogging.

The major achievements and interesting findings for each objective are summarized as follows.

6.1.1 Development of 3D breast coordinate system

As described in Chapter 3, a stable and valid Breast Coordinate System (BCS) has been proposed and validated to enable reliable and accurate measurements of 3D breast movement relative to the thorax. It has overcome the limitations of previous work that only reported breast (mainly nipple) movement under unreliable or unclear reference systems. This study proposed a method to define a stable and easy to define reference system on the thoracic cage, and a physically-meaningful breast local origin to accurately measure the 3D breast motion. This provided a basis for subsequently exploring breast movement trajectories, and for evaluating the effectiveness of different sports bras in reducing breast displacement in Chapter 4.

6.1.2 3D breast movement under different bra conditions during various activities

Breast displacement of six breast points

Chapter 4 demonstrated the first ever studies of 3D breast movement trajectories (BMTs) relative to the thorax in the BCS, at different six breast points during walking, jogging and stepping in both braless and sports bra conditions. The BMT of the nipple appeared to be chaotic, but the M6 and other markers uniformly resembled a “butterfly” shape. All six breast points had two substantial anterior-posterior and superior-inferior movements in every jogging stride. The superior displacement of the nude breasts was much larger than the inferior one, while the anterior movement is slightly less than the posterior, and the lateral displacement is also smaller than the medial. The largest displacement occurs at the nipple and the smallest at the top breast region. The displacement of all breast points was controlled within a range of $\pm$ 0.3 cm in all directions. The finding was similar to a previous study for Japanese women [10], except that the top breast region was less controlled, compared to other areas of the breast in the anterior, superior and medial directions.

In the braless condition, the least breast displacement was in the top breast region in the vertical direction during walking, which is consistent with a previous study in Japan. The maximum nude breast displacement was mostly found at the outer breast and nipple, especially during stepping up and down in the vertical direction.

In the sports bra conditions, the minimum displacement was in the region of inner breast and lower breast, especially in the *z*-direction during walking, due to the rigid materials of the centre gore and lower cup. The maximum displacement was in the upper breast region, probably because there was a gap between the body and the neckline of the bra during activities.

Breast displacement of nipple

In comparison with the previous literature, the corresponding data of relative nipple displacement during braless jogging at 7 km/h have showed that the findings in this study (1.5 cm anterior-posterior, 1.4 cm vertical, and 0.8 cm medial-lateral) were smaller than that for D-cup women as reported by Scurr et al. [61]. In the sports bra conditions, the mean nipple displacement during jogging was 0.2 cm - 0.7 cm in three dimensions, again smaller than the previous findings (1.4 cm - 2.0 cm). The difference was considered reasonable because smaller-breasted B-cup and C-cup women were participating in this study. These new findings have added to a body of knowledge in a field that has very limited research on Chinese women's breast motion.

Paired t-tests showed that the displacement at the nipple were significantly different from other breast points, so the displacement of various breast points were useful to provide comprehensive data for designing sports bras to fully control different breast regions. The maximum nude breast displacement was found to occur at the nipple during activities, especially in the vertical direction.

6.1.3 Effectiveness of different bra features on the reduction of breast movement

Chapter 4 also demonstrated the value of the comprehensive measurement of breast movement to more fully evaluate the effectiveness of different bra designs in reducing breast displacement. It was found that the more effective bras for Chinese women with B- and C-cup sizes had common features such as compression type, short vest style, high neckline, rigid cup seams, side slings, racer back panel, bound neckline with slight elasticity, no centre gore, no cradle, no wire, no pad, and non-adjustable wide straps .

The bra samples tested were most effective in controlling breast movement in the medial-lateral direction, but less effective in the anterior-posterior direction, so it is recommended that more attention should be paid to the design of a bra's centre front, the plasticity of cup fabric and the location of cup seams and the neckline. To improve the effectiveness of sports bras in supporting the top part of the breast, the neckline height should be well fitted to the upper breast boundary even during exercise.

It was found that the shoulder strap elongation percentage was significantly and strongly correlated with the reduction of breast displacement (RBD) because more extensible straps stayed better with the body than inextensible straps. This brought a further examination of different shoulder straps in Experiment 2, as reported in the following section.

6.1.4 Effects of breast volume and shoulder straps on the bra displacement

In Experiment 2, eleven subjects of different breast volumes participated in jogging motion studies in a braless conditon and in a sports bra condition, varying with 10 shoulder straps of different properties. Chapter 4 has reported that that the bra movement significantly increased with increasing breast volume, but less significantly in the *x*- and *z*- directions. The modulus of the shoulder straps at 25% extension had an inverse relationship with vertical bra displacement, for large breast volumes in excess of 309 cm^3. However, the displacement for smaller breasts did not show a significant change with different shoulder straps. Less vertical bra displacement was observed with a higher modulus of shoulder straps. Therefore, designers of sports bras are recommended to use stronger shoulder straps for larger-breasted women. In the light of this, it was proposed to derive mechanical models to analyse the mechanics of different combinations of shoulder straps, as presented in Chapter 5.

6.1.5 Breast mechanical models to analyse the breast force during jogging

In Chapter 5, a theoretical breast mechanical model was developed, based on an assumption that the breast is a homogenous object that may be represented by a system comprising a mass, springs and dampers. Although the coordinates of the centre of breast mass were difficult to establish with live subjects, an extrapolation procedure based on the uses of breast prostheses was devised.

The orthogonal force exerted on the breasts during jogging with or without sports bra was derived from a set of polynomial equations characterising nipple acceleration against time. The predicted results of maximum breast force were consistent with the values reported by

Gefena and Dilmoney [21]. Variability of the predicted force during braless jogging was the largest in the *y*-direction, followed by the *z*-direction.

The model predicted that wider shoulder straps were more effective in reducing the breast force than the narrow ones. The force was also related to the styles of shoulder straps and the position on the shoulder, so it is suggested that the position of shoulder straps should be designed to minimise the force moments on the breast.

6.2 Limitations and future work

In this study, passive markers were selected to monitor breast motion because they were wireless, so as to avoid deformation on the breast. However, relative breast movement within the bra might occur during activities. Active markers placed directly on the breast skin under the bra could be an alternative for future studies, and will be useful in quantifying the bra fit problems.

The breast mechanical models assumed that the breast was a homogeneous object and the movement of the centre of the breast mass could represent that of the whole breast. To locate the centre of the breast mass, eleven prostheses of different sizes were used. Finite element analysis of scanned images of human breasts should be accurate, but the preliminary study found that it was too time-consuming and unrealistic to be completed in this study. Future research, if budget allows, should use Magnetic resonance imaging to obtain the detailed data on the structure of real breasts for more accurate breast modelling.

Based on the power analysis, this study was limited to only 11 Chinese women aged from 24 to 40 years of age, with breast sizes from 75 B to 85D in the Metric system, and the jogging speed was set at a slow speed of 7km/h. This resulted in smaller breast displacement than those reported in the previous studies that were mainly for British and Australian women of size D in average. Future studies should recruit more subjects of cup size D, so the comparisons with the western studies will be more relevant.

Seven bra samples of different design features and measurements were examined to identify the successful components of effective sports bras in this study, and 10 shoulder straps were tested to study their effects on breast displacement. For future studies, a more detailed investigation on the effects of each parameter used in bra design such as the cup and neckline can be studied systematically in experiments, to understand the integrative effectiveness of each component within the sports bras.

Future more comprehensive work should cover different races, different ages of human subjects with difference breast sizes. More types of exercises such as dancing, high jump and ball games should be analysed because their patterns and amplitudes of breast movement may be very different to determine whether the design of bras should be customised to specific activities.

In future work, finite element models may be developed to simulate the breast force more discretely. Having said that, the concepts proposed in this more simplistic approach have provided a useful theoretical basis on which the force on breasts and the associated design of bras can be better understood and that may be further developed as an alternative to finite element modelling that is inherently more difficult.

6.3 Final conclusion

A new, valid and reliable breast coordinate system and a theoretical model have been developed, together with a methodology for more comprehensive measurement of 3D breast motion. These provided new techniques to evaluate and compare the effectiveness of sports bras, so as to improve their designs for more comprehensive breast support during activities such as jogging.

Appendix 1

Load-extension behaviour of straps 2 to 9 in the third cycle of loading and unloading

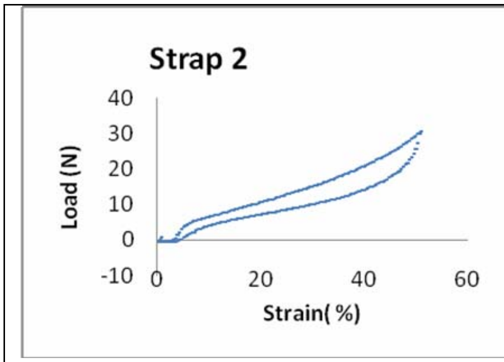

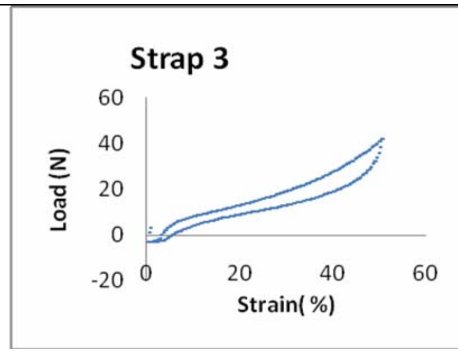

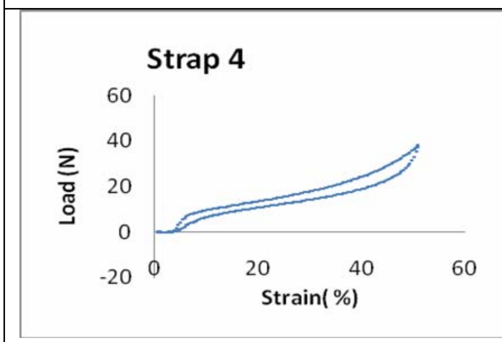

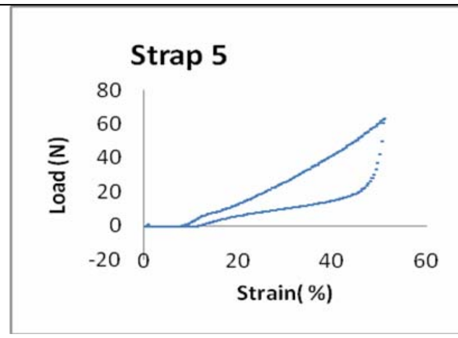

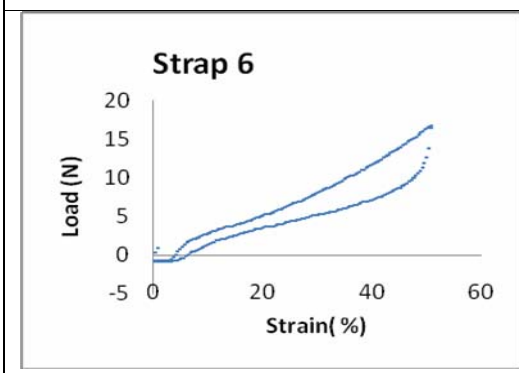

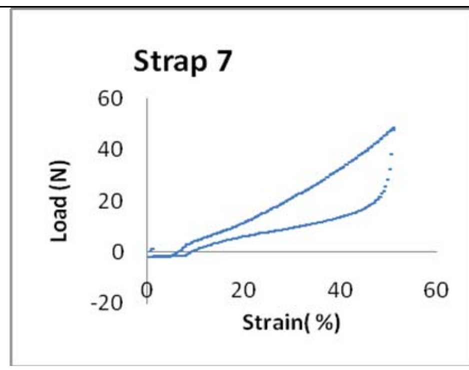

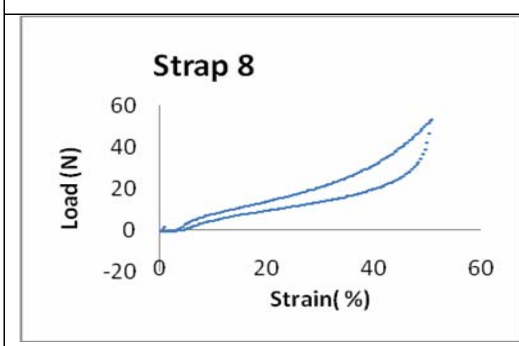

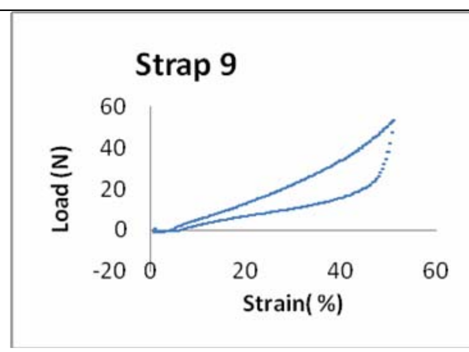

Appendix 2

INFORMATION SHEET

Breast Motion Study 1

You are invited to participate in a study conducted by the Institute of Textiles and Clothing in The Hong Kong Polytechnic University. This study aims to examine the effectiveness of the sports bras in controlling breast movements under seven different wearing conditions. You are asked to perform three different activities: walking on a treadmill at 3 km/h, running at 7 km/h, and stepping up and down on a platform that was 24 cm high. This experiment takes about two hours.

All information related to you will remain confidential, and will be identifiable by codes only known to the researcher. All data collected will be used solely for this study. You have every right to withdraw from the study before or during the research without penalty of any kind. If you have any complaints about the conduct of this research study, please do not hesitate to contact Mr. Eric Chan, Secretary of the Human Subjects Ethics Sub-Committee of The Hong Kong Polytechnic University in person or in writing (c/o Human Resources Office of the University). If you would like more information about this study, please contact Dr. Winnie Yu at telephone number 2766 6525.

Thank you for your interest in participating in this study.

Dr. Winnie Yu

Principal Investigator / Chief Investigator

Appendix 3

THE HONG KONG
POLYTECHNIC UNIVERSITY
香港理工大學

有 關 資 料

乳房運動研究 1

你好，我們謹代表香港理工大學紡織及製衣學系誠邀你參與一項研究計劃。這項研究的目的在於評估运动文胸控制乳房运动的效果。你會被邀請參加一項試穿計劃，試穿七種不同種類的運動文胸，同時你需在跑步機上步行和跑步， 在木制的盒子上踏步。這項研究大約需两小時。

所有有關你的個人資料將會被保密處理，並只有研究人員才能理解的編碼保存，而所得的數據也只會作研究用途。你有絕對的權利在研究開始前或進行時要求退出，退出研究後你絕不會受到任何懲罰。如果閣下對這項研究有任何投訴或意見，歡迎以書面或親身與香港理工大學人事倫理委員會秘書陳先生聯絡（請郵寄至以下地址轉交：香港理工大學人力資源辦公室）。如果閣下希望獲得更多有關這項研究計劃的資料，歡迎於辦公時間內與余詠文博士（電話：2766 6525）聯絡。

多謝閣下的參與！

余詠文博士

研究主管／首席研究員

Appendix 4

THE HONG KONG POLYTECHNIC UNIVERSITY
香港理工大學

Breast Motion Study 1

I ______________________hereby consent to participate in the captioned research conducted by the Institute of Textiles and Clothing, The Hong Kong Polytechnic University.

I understand that information obtained from this research may be used in future research and published. However, my right to privacy will be retained, i.e. my personal details will not be revealed.

The procedure as set out in the attached information sheet has been fully explained. I understand the benefit and risks involved. My participation in the project is voluntary.

I acknowledge that I have the right to question any part of the procedure and can withdraw from the study at any time without penalty of any kind.

Name of participant ____

Signature of participant ____

Name of researcher ____

Signature of researcher ____

Date ____

Appendix 5

THE HONG KONG
POLYTECHNIC UNIVERSITY
香港理工大學

CONSENT TO PARTICIPATE IN RESEARCH

參 與 研 究 同 意 書

乳房運動研究 1

本人________________________同意參加這項由香港理工大學紡織及製衣學系余詠文博士負責執行的研究項目。

本人明白由這項研究所獲得的資料可能會被應用於未來的研究或學術交流，然而本人的個人資料將不會被洩漏，以確保本人的個人隱私。

本人已對所附資料的有關研究步驟有充分的理解，並清楚明白在研究過程中可能會出現風險，但本人是自願參與這項研究。

本人理解在研究過程中有權提出問題，並在任何時候決定退出研究，而不會受到任何不正常的對待或被追究責任。

參加者姓名：____________________

參加者簽署：____________________

研究人員姓名：____________________

研究人員簽署：____________________

日期：____________________

Appendix 6

THE HONG KONG POLYTECHNIC UNIVERSITY
香港理工大學

INFORMATION SHEET

Breast Motion Study 2

You are invited to participate in a study conducted by the Institute of Textiles and Clothing in The Hong Kong Polytechnic University. This study aims to examine the effectiveness of the sports bra with 10 different shoulder straps in controlling breast movements during jogging. Your breast volume will be measured by a [TC]^2 NX-16 3D full-body non-contact body scanner. This experiment takes about two hours.

All information related to you will remain confidential, and will be identifiable by codes only known to the researcher. All data collected will be used solely for this study. You have every right to withdraw from the study before or during the research without penalty of any kind. If you have any complaints about the conduct of this research study, please do not hesitate to contact Mr. Eric Chan, Secretary of the Human Subjects Ethics Sub-Committee of The Hong Kong Polytechnic University in person or in writing (c/o Human Resources Office of the University). If you would like more information about this study, please contact Dr. Winnie Yu at telephone number 2766 6525.

Thank you for your interest in participating in this study.

Dr. Winnie Yu

Principal Investigator / Chief Investigator

Appendix 7

THE HONG KONG
POLYTECHNIC UNIVERSITY
香港理工大學

有 關 資 料

乳房運動研究 2

你好，我們謹代表香港理工大學紡織及製衣學系誠邀你參與一項研究計劃。這項研究的目的在於評估运动文胸控制乳房运动的效果及其产生的压力。你會被邀請參加一項試穿計劃，試穿一件運動文胸替換十種不同的肩帶，同時你需在跑步機上跑步。這項研究大約需两小時。

所有有關你的個人資料將會被保密處理，只有研究人員才能理解的編碼保存，而所得的數據也只會作研究用途。你有絕對的權利在研究開始前或進行時要求退出，退出研究後你絕不會受到任何懲罰。如果閣下對這項研究有任何投訴或意見，歡迎以書面或親身與香港理工大學人事倫理委員會秘書陳先生聯絡（請郵寄至以下地址轉交：香港理工大學人力資源辦公室）。如果閣下希望獲得更多有關這項研究計劃的資料，歡迎於辦公時間內與余詠文博士（電話：2766 6525）聯絡。

多謝閣下的參與！

余詠文博士

研究主管／首席研究員

Appendix 8

THE HONG KONG
POLYTECHNIC UNIVERSITY
香港理工大學

CONSENT TO PARTICIPATE IN RESEARCH

Breast Motion Study 2

I ______________________hereby consent to participate in the captioned research conducted by the Institute of Textiles and Clothing, The Hong Kong Polytechnic University.

I understand that information obtained from this research may be used in future research and published. However, my right to privacy will be retained, i.e. my personal details will not be revealed.

The procedure as set out in the attached information sheet has been fully explained. I understand the benefit and risks involved. My participation in the project is voluntary.

I acknowledge that I have the right to question any part of the procedure and can withdraw from the study at any time without penalty of any kind.

Name of participant ____

Signature of participant ____

Name of researcher ____

Signature of researcher ____

Date ____

Appendix 9

THE HONG KONG
POLYTECHNIC UNIVERSITY
香港理工大學

參 與 研 究 同 意 書

乳房運動研究 2

本人_________________________同意參加這項由香港理工大學紡織及製衣學系余詠文博士負責執行的研究項目。

本人明白由這項研究所獲得的資料可能會被應用於未來的研究或學術交流，然而本人的個人資料將不會被洩漏，以確保本人的個人隱私。

本人已對所附資料的有關研究步驟有充分的理解，並清楚明白在研究過程中可能會出現風險，但本人是自願參與這項研究。

本人理解在研究過程中有權提出問題，並在任何時候決定退出研究，而不會受到任何不正常的對待或被追究責任。

參加者姓名：______________________________

參加者簽署：______________________________

研究人員姓名：______________________________

研究人員簽署：______________________________

日期：______________________________

References

1 Zhao, Y. B. *Ru fang bao jian yu ji bing fang zhi*. (Si Chuan Publishing House of Science & Technology, 2001).

2 Qiao, Q. & Sun, J. M. *Ru fang zheng xing mei rong wai ke xue*. (Zheng Zhou University Press, 2004).

3 Haycock, C. E., Shierman, G. & Gillette, J. The female athlete--does her anatomy pose prombles? *American Medical Association 19th Conference on the Medical Aspects of Sports, Monroe, WI: AMA Press*, 1-8 (1978).

4 Mason, B. R., Page, K. A. & Fallon, K. An analysis of movement and discomfort of the female breast during exercise and the effects of breast support in three cases. *Journal of Science and Medicine in Sport* **2**, 134-144 (1999).

5 Okabe, K. & Kurokawa, T. Vibration and dislocation of the breast when wearing brassieres during running. *Journal of Home Economics of Japan* **56**, 379-388 (2005).

6 White, J. L., Scurr, J. C. & Smith, N. A. The effect of breast support on kinetics during overground running performance. *Ergonomics* **52**, 492-498 (2009).

7 Hadi, M. S. A. A. Sports brassiere: Is It a Solution for Mastalgia? *The Breast Journal* **6**, 407-409 (2000).

8 Bowles, K.-A., Steele, J. R. & Chaunchaiyakul, R. Do Current Sports Brassiere Designs Impede Respiratory Function? *Official Journal of the American College of Sports Medicine* **37**, 1633-1640 (2005).

9 Page, K.-A. & Steele, J. R. Breast Motion and Sports Brassiere Design Implications for Future Research. *Sports Med* **27 (4)**, 205-211 (1999).

10 Okabe, K. & Kurokawa, T. Analysis of Breast Vibration While Exercising and Its Reflection to Vibration Proof Desing of Sports Brassiere. *Descente Sports Science* **23**, 180-188 (2002).

11 Okabe, K. & Kurokawa, T. Vibration Characteristics of Breasts during Exercise with and without a Brassiere. *Journal of Home Economics of Japan* **54**, 731-738 (2003).

12 Kazuyo, O. & Takao, K. Characteristics of Three-Dimensional Displacement of the Breasts Wearing Different Kind of Brassieres in Young Japanese Women. *Journal of the Japan Research Association for Textile End-Uses* **45**, 416-424 (2004).

13 Okabe, K. & Kurokawa, T. A Study of the Relationships between Breast Vibration, Clothing Pressure and Dislocation under Running Condition for Designing Sports Brassiere. *Descente Sports Science* **27**, 75-85 (2006).

14 Starr, C., Branson, D., Shehab, R., Farr, C., Ownbey, S., Biomechanical analysis of a prototype sports bra. *Journal of Textile and Apparel*, *Technology and Management* **4**, 1-14 (2005).

15 Fuseya, S. & Matsumoto, C. Three dimentional study on the vibration of breasts with brassieres. *Wayo Joshi Daigaku Kiyo. Kaseikeihen* **46**, 1-12 (2006).

16 Campbell, T. E., Munro, B. J., Wallace, G. G. & Steele, J. R. Can fabric sensors monitor breast motion? *Journal of Biomechanics* **40**, 3056-3059 (2007).

17 McGhee, D. E., Steele, J. R. & Power, B. M. Does deep water running reduce exercise-induced breast discomfort? *British Journal of Sports Medicine* **41**, 879-883 (2007).

18 McGhee, D. E. & Steele, J. R. Breast elevation and compression decrease exercise-induced breast discomfort. *Medicine and Science in Sports and Exercise* **42**, 1333-1338 (2010).

19 Haake, S. & Scurr, J. A dynamic model of the breast during exercise *Sports Engineering* **12**, 189-197 (2010).

20 Scurr, J. C., White, J. L. & Hedger, W. The effect of breast support on the kinematics of the breast during the running gait cycle. *Journal of Sports Sciences* **28**, 1103-1109 (2010).

21 Gefen, A. & Dilmoney, B. Mechanics of the normal woman's breast. *Technology and health care* **15**, 259-271 (2007).

22 Gefen, A. & Dilmoney, B. Mechanics of the normal woman's breast. *Technology and health care : official journal of the European Society for Engineering and Medicine* **15**, 259-271 (2007).

23 Gehlsen, G. & Stoner, L. J. The female breast in sports and exercise. *Medicine & Science in Sports & Exercise* **24**, 13-22 (1987).

24 Borgen, P. I. & Hill, A. *Breast Diseases*. (Georgetown, TX Landes Bioscience, Inc., 2000).

25 Katch, V. L. *et al.* Contribution of breast volume and weight to body fat distribution in females. *American Journal of Physical Anthropology* **53**, 93-100 (1980).

26 Hall, J. A. & Knaus, J. V. *An atlas of breast disease*. 15-19 (New York Informa Healthcare, 2003).

27 Calvo, F. & Magdelenat, H. *Breast Cancer Advances in Biology and Therapeutics* (John Libbery and Company LtD, 1996).

28 Joseph F. Hair, J., Anderson, R. E., Tatham, R. L. & Black, W. C. *Multivariate data analysis* (Upper Saddle River, N.J. : Prentice Hall, 1998).

29 Sloane, E. *Biology of women*. (Albany, N.Y. : Delmar Thomson Learning, 2002).

30 Stoppard, M. *The breast book* (London : Dorling Kindersley, 1996).

31 Haycock, C. E. Breast support and protection in the female athlete. *In American Alliance for Health, Physical Education,Recreation, and Dance Consortium Symposium Paper* **1**, 50-53 (1978).

32 Haycock, C. E. How I Manage Breast Problems in Athletes. *Physician and Sportsmedicine* **15**, 89-95 (1987).

33 Bowles, K. A., Steele, J. R. & Munro, B. What are the breast support choices of Australian women during physical activity? *British Journal of Sports Medicine* **42**, 670-673 (2008).

34 Zadpoor, A. A., Nikooyan, A. A. & Arshi, A. R. A model-based parametric study of impact force during running *Journal of Biomechanics* **40**, 2012-2021 (2007).

35 Nigg, B. M. & Liu, W. The effect of muscle stiffness and damping on simulated impact force peaks during running. *Journal of Biomechanics* **32**, 849-856 (1999).

36 Vance, J., Hreljac, A. & Hamill, J. Relationship between shock attenuation and stride length during running at different velocities. *European Journal of Applied Physiology* **87**, 403-408 (2002).

37 Bobbert, M. F., Yeadon, M. R. & Nigg, B. M. Mechanical analysis of the landing phase in heel toe running. *Journal of Biomechanics* **25**, 223-234 (1992).

38 Christina, K. A., White, S. C. & Gilchrist, L. A. Effect of localized muscle fatigue on vertical ground reaction forces and ankle joint motion during running. *Human Movement Science* **20**, 257-276 (2001).

39 Zhang, Y. Z. *Xin Bian Zhong Yi Fu Ke Xue*. (Shang Hai Publishing House of Science & Technology, 2001).

40 Yu, W., Fan, J., Harlock, S. C. & Ng, S.P.. Innovation and technology of women's intimate apparel. 171-172 (2006).

41 Stamford, B. Sports bras and briefs: Choosing good athletic support. *The Physician and Sportsmedicine* **24**, 99-100 (1996).

42 Shishoo, R. *Textiles in sport*. (Cambridge : Woodhead Pub., 2005).

43 Zhou, J., Yu, W., Ng, S.-p. & Hale, J. *1st International Symposium of Textile Bioengineering and Informatics,* Hong Kong, (2008).

44 McGhee, D., Steele, J. , Munro, B. *Sports Bra Fitness Booklet*. Wollongong: Breast Research Australia, 11-12 (2008).

45 Greydanus, D. E., Patel, D. R. & Baxter, T. L. The breast and sports: issues for the clinician. *Adolescent Medicine* **9**, 533-550 (1998).

46 Haycock, C. E. Supportive bras for jogging. *Medical Aspects of Human Sexuality* **14**, 6 (1980).

47 Shivitz, N. L. *Adaptation of Vertical Ground Reaction Force due to Changes in Breast Support in Running* Master of Science thesis, Oregon State University, (2001).

48 Joanne, B.-D. Sports Bras: Everything you need to know from A to D. *Womens Sports Fitness*, 31-33, 48-49 (1986).

49 Lorentzen, D. & Lawson, L. Selected sports bras: a biomechanical analysis of breast motion while jogging. *Physician and Sportsmedicine* **15**, 128-139 (1987).

50 Gehlsen, G. & Albohm, M. Evaluation of sports bras. *Physician and Sportsmedicine* **8**, 88-97 (1980).

51 Schuster, K. Equipment update: Jogging bras hit the streets. *Physician and Sportsmedicine* **7**, 125-128 (1979).

52 Hunter, L. Y. & Torgan, C. The bra controversy: Are sports bras a necessity? *The Physician and Sportsmedicine* **10**, 75-76 (1982).

53 Lawson, L. & Lorentzen, D. Selected Sports Bras: Comparisons of Comfort and Support. *Clothing and Textiles Research Journal* **8**, 55-60 (1990).

54 McGhee, D. & Steele, J. Breast elevation and compression decrease exercise-induced breast discomfort. *Medicine & Sciences in Sports & Exercise* **42**, 1333-1338 (2010).

55 Gehlsen, G. & Albohm, M. Evaluation of sports bras. *The Physician and Sportsmedicine* **8**, 88-97 (1980).

56 Lorentzen, D. & Lawson, L. Selected sports bras: a biomechanical analysis of breast motion while jogging. *The Physician and Sportsmedicine* **15**, 128-139 (1987).

57 Scurr, J., White, J. & Hedger, W. Breast displacement in three dimensions during the walking and running gait cycles. *Journal of Applied Biomechanics* **25**, 322-329 (2009).

58 Okabe, K. & Kurokawa, T. Relationship between wearing comfort and clothing pressure for designing comfortable brassieres. *Bulletin of Japanese Society for Science of Design* **51**, 31-38 (2004).

59 Zheng, R. *Breast sizing and development od 3D seamless bra* Ph.D thesis, The Hong Kong Polytechnic University, (2006).

60 Scurr, J., Galbraith, H., Hedger, W. & White, C. Qualitative analysis of 3D breast displacement during treadmill activity, *12th Annual Congress of the ECSS* 11-14 (2007).

61 Scurr, J. C., White, J. L. & Hedger, W. Supported and unsupported breast displacement in three dimensions across treadmill activity levels. *Journal of Sports Sciences* **29**, 55-61 (2011).

62 Himmelsbach, J. A., Valient, G. A., Lawson, L. & Eden, K. B. Peak breast accelerations when running different sports bras. *Medicine & Science in Sports & Exercise* **24(Suppl)**, S187 (1992).

63 Conti, G., Cristofolini, L., Juszczyk, M., Leardini, A. & Viceconti, M. Comparison of three standard anatomical reference frames for the tibia-fibula complex. *Journal of Biomechanics* **41**, 3384-3389 (2008).

64 Veeger, H. E. J., Helm, F. C. T. v. d., Chadwick, E. K. J. & Magermans, D. Toward standardized procedures for recording and describing 3-D shoulder movements. *Behavior Research Methods, Instruments, & Computers* **35**, 440-446 (2003).

65 Selvik, G. Roentgen stereophotogrammetry. A method for the study of the kinematics of the skeletal system. *Acta Orthop Scand* **60**, 1-51 (1989).

66 Winter, D. A. *Biomechanics and motor control of human movement*. (Hoboken,

N.J.: John Wiley & Sons, 2005).

67 Sha, D. H., Mullineaux, D. R. & Clayton, H. M. Three-dimensional analysis of patterns of skin displacement over the equine radius. *Equine veterinary journal* **36**, 665-670 (2004).

68 Helm, F. C. T. v. d. A standardized protocol for motion recordings of the shoulder. *Proceedings of the First Conference of the ISG,* 7-12 (1998).

69 Stokes, V. P., Andersson, C. & Forssberg, H. Rotational and translational movement features of the pelvis and thorax during adult human locomotion. *Journal of Biomechanics* **22**, 43-50 (1989).

70 Sahara, W., Sugamoto, K., Murai, M. & Yoshikawa, H. Three-dimensional clavicular and acromioclavicular rotations during arm abduction using vertically open MRI. *Journal of Orthopaedic Research* **25**, 1243-1249 (2007).

71 Graichen, H., Stammberger, T & Bonel, H. Magnetic resonance-based motion analysis of the shoulder during elevation. *Clinical Orthopaedics and Related Research* **370**, 154-163 (2000).

72 Bourne, D. A., Choo, A. M. T., Regan, W. D., MacIntyre, D. L. & Oxland, T. R. Three-dimensional rotation of the scapula during functional movements: An in vivo study in healthy volunteers. *Journal of Shoulder and Elbow Surgery* **16**, 150-162 (2007).

73 Li, Y., Zhang, X. & Yeung, K. W. A 3D biomechanical model for numerical simulation of dynamic mechanical interactions of bra and breast during wear. *SEN'I GAKKAISHI ,* **59,** 12-21 (2003).

74 Perez del Palomar, A., Calvo, B., Herrero, J., Lopez, J. & Doblare, M. A finite element model to accurately predict real deformations of the breast. *Medical Engineering & Physics* **30**, 1089-1097 (2008).

75 Azar, F. S., Metaxas, D. N. & Schnall, M. D. A deformable finite element model of the breast for predicting mechanical deformations under external perturbations *Academic Radiology,* **8,** 965-975 (2001).

76 Ruiter, N. *et al.* Automatic image matching for breast cancer diagnostics by a 3D deformation of the mamma. *Biomedizinische Technik,* **47**, 644-647 (2002).

77 Schnabel, J. A. *et al.* Validation of nonrigid image registration using finite-element methods: application to breast MR images. *IEEE Transactions on Medical Imaging* **22**, 238-247 (2003).

78 Washington, C. W. & Miga, M. I. Modelity Independent Elastography (MIE): A New Approach to Elasticity Imaging. *IEEE Transactions on Medical Imaging* **23**, 1117-1128 (2004).

79 Rajagopal, R., Lee, A., Chung, J. H. & Warren, R. Creating individual-specific biomechanical models of the breast for medical image analysis. *Academic Radiology* **15**, 1425-1436 (2008).

80 Bakic, P. R. *Breast tissue description and modeling in mammography* PhD thesis,

Lehigh University, (2000).

81 Wu, G. & P.R., C. ISB recommendations for standardization in the reporting of kinematic data. *Journal of Biomechanics* **28**, 1257-1261 (1995).

82 Helm, F. C. T. v. d. & Pronk, G. M. Three-dimensional recording and description of motions of the shoulder mechanism. *Journal of Biomechanical Engineering* **117**, 27-40 (1995).

83 Wu, G. *et al.* ISB recommendation on definitions of joint coordinate systems of various joints for the reporting of human joint motion--Part II: shoulder, elbow, wrist and hand. *Journal of Biomechanics* **38**, 981-992 (2005).

84 Cappozzo, A., Cappello, A., Croce, U. D. & Pensalfini, F. Surface-marker cluster design criteria for 3-D bone movement reconstruction. *IEEE transactions on bio-medical engineering* **44**, 1165-1174 (1997).

85 Yu, W. *Achieving comfort in intimate apparel, Chapter 17, In "Improving Comfort in Clothing"*. (Woodhead Publishing: Cambridge, 2011).

86 Chow, D. H. K., Leung, K. T. Y. & Holmes, A. D. Changes in spinal curvature and proprioception of schoolboys carrying different weights of backpack *Ergonomics* **50**, 2148-2156 (2007).

87 Eden, K. B., Valiant, G. A., lawson, L. J. & Himmelsbach, J. Three dimensional kinematic evaluation of sport bra design. *Medicine and Science in Sports and Exercise* **24(Suppl)**, S187 (1992).

88 Scurr, J., White, J. & Hedger, W. Three-dimensional displacement, velocity and acceleration of the breast during a running gait cycle. *Medicine & Science in Sports & Exercise* **40**, S221 (2008).

89 Zhou, J., Yu, W. & Ng, S. P. Method of Studying Breast Motion in Sports Bras: a review. *Textile Research Journal* **81***,* 1234-1248 (2011).

90 Song, G. *Improving Comfort in Clothing*. (Woodhead Publishing, 2011).

91 Zheng, R. *Breast sizing and development of 3D seamless bra* PHD thesis, The Hong Kong Polytechnic University, (2006).

92 Vicon. *The Vicon Manual*. Vicon industries inc (2002).

93 LI, J. W. *The effects of menstrual cycle, site and individual variation on breast elasticity and thickness* MPhil thesis, The Hong Kong Polytechnic University, (2009).

94 Dixon, A. M. *Breast ultrasound: how, why and when*. (New York: Churchill Livingstone Elsevier, 2008).

95 Ulger, H., Erdogan, N., Kumanlioglu, S. & Unur, E. Effect of age, breast size, menopausal and hormonal status on mammographic skin thickness. *Skin Research and Technology* **9**, 284-289 (2003).

96 Snell, R. S. *Clinical anatomy by regions*. (Lippincott Williams and Wilkins, 2008).

97 Haycock, C., Shierman, G. & Gillette, J. The female athlete – does her anatomy

pose problems? *Proceedings of the 19th National Conference on the Medical Aspects of Sports,* 1977, San Francisco. Monroe, Wisconsin: American Medical Association, 1–8.(1978).

98 Ni, G.-p. & Wang, S.-h. *Shi yong lin chuang ru xian bing xue*. China Medical Science Press (2002).

99 Leea, H.-Y., Honga, K. & Kim, E. A. Measurement protocol of women's nude breasts using a 3Dscanning technique. *Applied Ergonomics* **35** 353-359 (2004).

100 Lerman, J. Study design in clinical research sample size estimation and power analysis. *Canadian Journal of Anesthesia* **43**, 184-191 (1996).

101 [TC] 2 NX-16 3D full-body non-contact body scan guide.

102 Qiao, Q., Zhou, G. & Ling, Y. C. Breast volume measurement in young Chinese women and clinical applications. *Aesthetic Plastic Surgery Electronic Resource* **21**, 362-368 (1997).

103 Yang, W. Y. & Qiang, W. *Mechanical behavior of materials*. Beijing: Chemical Industry Press (2009).

104 Bishop, R. E. D. *The mechanics of vibration*. Cambridge University Press (1979).

105 Tanner, C., Schnabel, J. A., Hill, D. L. G. & Hawkes, D. J. Factors influencing the accuracy of biomechanical breast models. *Medical Physics* **33**, 1758-1769 (2006).

106 Serway, R. A. & Jewett, J. W. *Principles of physics*. 375, 376, 385, 397 Saunders College Pub (2006).

107 Nise, N. S. *Control system engineering*. 5th edn, New Jersey: Wiley (2008).

108 Ewen, D., Schurter, N. & Gundersen, P. E. *Applied physics*. 9th ed., New Jersey: Pearson Prentice Hall (2009).